



University
of Glasgow

Dalziel, Catherine Ellen (2014) *The molecular basis of adjuvant activity of pneumolysin*. PhD thesis.

<http://theses.gla.ac.uk/5405/>

Copyright and moral rights for this work are retained by the author

A copy can be downloaded for personal non-commercial research or study, without prior permission or charge

This work cannot be reproduced or quoted extensively from without first obtaining permission in writing from the author

The content must not be changed in any way or sold commercially in any format or medium without the formal permission of the author

When referring to this work, full bibliographic details including the author, title, awarding institution and date of the thesis must be given

Enlighten:Theses
<http://theses.gla.ac.uk/>
theses@gla.ac.uk



University
of Glasgow | Institute of Infection,
Immunity & Inflammation

The Molecular Basis of Adjuvant Activity of Pneumolysin

**A thesis submitted to the University of Glasgow for the degree of
Doctor of Philosophy**

by

Catherine Ellen Dalziel

Submitted November 2013

Institute of Infection, Immunity and Inflammation
College of Medical Veterinary and Life Sciences
Glasgow Biomedical Research Centre
120 University Place
Glasgow
G12 8TA

Acknowledgements

Firstly, I would like to thank Professor Tim Mitchell for this opportunity and for the invaluable advice and support he has given me throughout this project.

There are many members of the Mitchell group that I'd like to thank for making this an enjoyable experience including all of the Mitchell group members who have supported me through this project and made this experience enjoyable, in particular Carol, Ashleigh, Jenny, Ryan, Jiang, Matt, Kashif, Sultan, Kirsty and Friedi. I'd also like to thank Denise Candlish and June Irvine for their ability to solve any problem, of which there were many! I'd like to give special thanks to Andrea Mitchell for her support, particularly in this last year of my PhD, without her advice, hard work and emotional support during the lab's transition to the University of Birmingham my final year would have been incredibly difficult.

I'm incredibly grateful for the support and encouragement of my family and friends over the past four years. Finally, I'd like to thank my partner Tom for his patience and understanding over this past year and for the endless supplies of tea and toast while I was writing this thesis.

Author's declaration

This thesis is the original work of the author unless otherwise stated.

Catherine Ellen Dalziel

November 2013

Abstract

Streptococcus pneumoniae is a major human pathogen and causes a significant burden of disease in both developed and developing countries. Currently, two pneumococcal vaccines are available, a polysaccharide conjugate vaccine for children <2 years of age and an adult polysaccharide vaccine for 'at risk' groups such as the elderly and immunocompromised. Unfortunately, due to the vast variation and highly recombinant nature of the pneumococcus vaccine escape through serotype replacement is significantly decreasing the efficacy of pneumococcal vaccines globally. New cost-effective and protective pneumococcal vaccines are urgently required.

Pneumolysin (PLY) is a 53Kd cholesterol-dependent cytolysin that is largely conserved in all strains of *Streptococcus pneumoniae*, making it an ideal candidate for inclusion in a broad spectrum vaccine. It has been shown that PLY is not only a protective immunogen but also has potent adjuvant properties and stimulates both IgG and IgA antibody responses to antigens genetically coupled to the toxin (Douce et al., 2010). Both systemic and mucosal responses are induced when PLY is used as an adjuvant which may prevent colonization and therefore provide non-serotype specific herd immunity to *Streptococcus pneumoniae*. The cytolytic activity of PLY prevents its inclusion in a human vaccine; a non-lytic deletion mutant $\Delta 6$ PLY was created for this purpose which retains adjuvanticity, albeit slightly reduced. These properties of PLY formed the basis of this PhD project; the aim of this study was to elucidate the mechanism(s) of PLY/ $\Delta 6$ PLY adjuvanticity, it will be essential to have a basic model of adjuvant activity before PLY-based vaccines can be advanced to human clinical trials.

This project used a combination of high-throughput methods such as protein pull-downs and gene expression profiling to examine the abilities of PLY, $\Delta 6$ PLY and the truncation mutants D123PLY and D4PLY to bind to and be internalized by host cells and to differentially regulate gene expression. These studies highlighted specific and direct interactions between PLY variants and the host cytoskeleton that could mediate antigen/PLY uptake; they also revealed a

pattern of gene expression that is similar to those of other adjuvants and could provide the basis for a model of adjuvanticity.

Finally, through the use of reporter cell lines and transgenic TLR4^{-/-} BMDM, the relationship between PLY and TLR4 has been further defined. A novel method for preparing vehicle controls provided evidence that the ligation of TLR4 in this system is PLY-dependent and is not an artefact caused by contaminating TLR ligands such as LPS. Once this was established it was possible to further investigate the role of TLR4 in the adjuvant activity of PLY, in particular the PLY-dependent production of IL-1 β . Through these studies a surprising role for TLR4 in *in vitro* PLY-dependent cytokine production was discovered.

Additionally, it was found that complement has an essential role in the PLY-dependent production of IL-1 β . The role(s) of complement and IL-1 β in the adjuvant activity were further investigated using an *in vivo* immunization model and the biological basis for the difference in adjuvant activity of PLY and Δ 6PLY was defined.

Table of Contents

The Molecular Basis of Adjuvant Activity of Pneumolysin	1
Acknowledgements.....	2
Author's declaration	3
Abstract	4
Table of Contents	6
List of Tables.....	11
List of Figures.....	12
List of Abbreviations	16
1. Introduction.....	19
1.1 <i>Streptococcus pneumoniae</i> background.....	20
1.2 Pneumococcal Disease Burden: Prevention and Treatment.....	21
1.2.1 Disease burden.....	21
1.2.2 Treatment of pneumococcal disease and antibiotic resistance	22
1.2.3 Pneumococcal vaccines: Coverage, effectiveness and limitations ..	22
1.3 Immunity to <i>Streptococcus pneumoniae</i>	24
1.3.1 Innate Immunity to the pneumococcus.....	24
1.3.2 Humoral immunity to the pneumococcus	25
1.3.3 Cell mediated immunity to the pneumococcus	27
1.3.4 Mucosal immunization	28
1.3.5 Novel pneumococcal vaccines/ PATH project.....	29
1.3.6 The future of pneumococcal vaccination	34
1.4 Pneumolysin as a Virulence Factor and Vaccine Antigen	34
1.5 Vaccine Adjuvants and their Mode(s) of Action	39
1.6 Pneumolysin as a Novel Vaccine Adjuvant.....	40
1.6.1 Interaction with Pattern Recognition Receptors (PRR)	41
1.6.2 Activation of the classical complement pathway	44
1.6.3 Upregulation of genes.....	45
1.6.4 Known cytokine and chemokine responses to PLY.....	46
1.6.5 Interaction with the cell cytoskeleton, a mechanism for antigen uptake?.....	46
1.6.6 The neutrophil response to pneumolysin.....	47
1.7 Aims of this study.....	48
2. Materials and Methods.....	50
2.1 Materials.....	50
2.1.1 Chemicals.....	50
2.1.2 Enzymes.....	50
2.1.3 Protein purification supplies.....	50
2.1.4 Antibiotics	50
2.2 Bacterial strains and vectors.....	51
2.2.1 Storage and growth conditions	51
2.2.2 Bacterial strains	52
2.2.3 Vectors	52
2.2.3.1 pET33b	52
2.2.3.2 pFN18A HaloTag® Flexi® Vector.....	52
2.2.4 Electrocompetent cells	53
2.3 Molecular cloning.....	54
2.3.1 Oligonucleotides	54
2.3.2 Polymerase chain reaction (PCR).....	56

2.3.2.1	Typical PCR conditions using GoTaq standard fidelity DNA polymerase	56
2.3.2.2	Typical PCR conditions using <i>PfuUltra II</i> fusion HS high fidelity DNA polymerase	57
2.3.3	Agarose gel electrophoresis	58
2.3.4	Plasmid purification	58
2.3.5	Restriction digest	58
2.3.6	Gel extraction and PCR product purification	58
2.3.7	Ligation	58
2.3.8	Bacterial transformation	59
2.4	Construction of plasmids	59
2.4.1	pET33bPLY: PLY derivatives and eGFP.	59
2.4.1.1	pET33b- Δ 6D123	61
2.4.1.2	pET33b-eGFP Δ 6D123PLY	63
2.4.2	pFN18A: PLY derivatives and eGFP.	64
2.5	Protein expression and purification.....	65
2.5.1	Protein expression in <i>E. coli</i> BL21 (DE3)	65
2.5.2	Lysate preparation	66
2.5.3	Purification of His-tagged Proteins	66
2.5.3.1	Nickel-affinity chromatography (NAC).....	66
2.5.3.2	Anion-exchange chromatography (AEC)	67
2.5.4	Purification/Isolation of HaloTagged Proteins	69
2.6	Analysis of Isolated proteins	69
2.6.1	SDS-PAGE and western blotting	69
2.6.2	Haemolytic assay	70
2.6.3	Determination of protein concentration	72
2.6.3.1	Lysates	72
2.6.3.2	HaloTagged Proteins	73
2.6.3.3	Purified proteins	73
2.6.4	Separation of His-tagged protein from solvent using nickel magnetic beads.....	73
2.6.5	Determination of LPS concentration in purified protein preparations	74
2.7	Tissue culture techniques	74
2.7.1	Generation and analysis of bone marrow derived macrophages (BMDM).....	74
2.7.1.1	Preparation of L929 conditioned culture medium	74
2.7.1.2	Isolation and differentiation of BMDM	74
2.7.1.3	Analysis of BMDM culture phenotype by flow cytometry	75
2.7.2	Cell line information and culture requirements	77
2.7.3	Resuscitation of frozen cell lines.....	77
2.7.4	Routine sub-culturing techniques	78
2.7.5	Storage of cell line aliquots in liquid nitrogen	78
2.8	Microscopy.....	78
2.8.1	Analysis of PLY interactions with RAW 264.7 macrophages	78
2.8.1.1	Staining with CellMask deep red plasma membrane stain and Halo TMR-direct ligand	78
2.8.1.2	Staining with rhodamine phalloidin and eGFP tagged PLY variants.....	79
2.8.2	Image analysis.....	79
2.9	<i>In Vitro</i> analysis of recombinant PLY and its derivatives	80
2.9.1	Analysis of PLY cytotoxicity	80

2.9.1.1	Lactate Dehydrogenase Release	80
2.9.1.2	Analysis of Apoptosis	80
2.9.2	Treatment of mammalian cells with PLY and its derivatives	80
2.9.3	Analysis of cytokine expression.....	81
2.9.4	Analysis of gene expression by RT ² qPCR.....	81
2.9.4.1	Isolation of RNA from PLY treated mammalian cells	81
2.9.4.2	Analysis of RNA quality and concentration.....	81
2.9.4.3	cDNA synthesis	82
2.9.4.4	Real-Time PCR using RT ² qPCR primer assays or RT ² qPCR profiler assays and RT ² SYBR green mastermixes.....	82
2.9.5	QUANTI-Blue™ assay for detection of SEAP secreted by reporter cell lines.....	82
2.9.6	Analysis of protein-protein interaction by pull-down using HaloTagged proteins.....	83
2.9.7	Analysis of Actin Binding by ELISA.....	84
2.9.7.1	Preparation of actin solution	84
2.9.7.2	Actin binding ELISA	84
2.10	<i>In Vivo</i> analysis of recombinant PLY and its derivatives	84
2.10.1	Intranasal vaccination	85
2.10.2	Analysis of Antibody Response in Immunized Mice	86
2.10.2.1	Analysis of immunoglobulin G presence in serum.....	86
2.10.2.2	Analysis of IgA presence in nasal washes.....	87
2.10.2.3	Determining IgG clonotype generated in response to PLY-fusion vaccines.....	87
2.10.3	Preparation of whole mouse serum and preservation of complement activity.....	88
2.11	Statistical analysis	89
3.	Functional Analysis of Recombinant Pneumolysin and its Derivatives	91
3.1	Analysis of Cytolytic Activity in Purified Recombinant PLY and its Derivates	92
3.1.1	Haemolytic Activity	92
3.1.2	Cytotoxic Activity/Lysis	94
3.2	Analysis of LPS Content and Preparation of Vehicle Controls.....	98
3.2.1	LPS testing.....	99
3.2.2	Preparation of vehicle controls.....	99
3.3	Is PLY a TLR4 ligand?.....	104
3.4	Cytokine expression in PLY treated BMDM.....	109
3.4.1	The IL-1 β hypothesis	109
3.4.2	KC expression in response to PLY and the role of TLR4.....	112
3.5	Discussion.....	113
4.	Investigating Direct Interactions between PLY and Mammalian Cell Receptors and Cytoskeleton	119
4.1	Analysis of Binding of PLY and its Derivatives to Mammalian Cells by Confocal Fluorescence Microscopy	119
4.1.1	Analysis of PLY binding using HaloTag technology.....	122
4.1.2	Analysis of Δ 6PLY binding using HaloTag technology.....	123
4.1.3	Analysis of D123PLY binding using HaloTag technology.....	125
4.1.4	Analysis of D4PLY binding using HaloTag technology.....	127
4.1.5	Analysis of eGFP (control) binding using HaloTag technology	129
4.2	Investigating PLY-Host Interactions by Protein Pull-down.....	131
4.2.1	Analysis of Pull-down efficiency by western blot and SDS-PAGE ...	133
4.2.2	Separation and extraction of Pull-down proteins by SDS-PAGE.....	136

4.2.3	Mass Spectrometry results.....	140
4.3	Interactions between PLY and the Actin Cytoskeleton	142
4.3.1	Visualising interactions between eGFP and the actin cytoskeleton using purified eGFP	142
4.3.2	Visualising interactions between PLY and the actin cytoskeleton using eGFP-tagged PLY	143
4.3.3	Visualising interactions between $\Delta 6$ PLY and the actin cytoskeleton using eGFP-tagged $\Delta 6$ PLY	145
4.3.4	Visualising interactions between D123PLY and the actin cytoskeleton using eGFP-tagged D123PLY	147
4.3.5	Visualising interactions between D4PLY and the actin cytoskeleton using eGFP-tagged D4PLY	149
4.3.6	Analysis of colocalization by thresholded Pearson's correlation coefficient (PCC)	151
4.3.7	Quantifying binding affinity between PLY and actin by ELISA	152
4.4	Discussion	153
5.	The Role of TLR4, Complement and IL-1 β in the Adjuvant Activity of Pneumolysin	160
5.1	The production of IL-1 β in PLY Treated BMDM is Dependent on Pore Formation and NLRP3 Activation	161
5.2	The Role of Complement in IL-1 β Production in PLY Treated BMDM....	162
5.3	Cytokine Production in PLY Treated Transgenic BMDM	165
5.3.1	C3-/- BMDM.....	166
5.3.2	TLR4-/- BMDM and VIPER treated BMDM	168
5.4	The Role of Complement and IL-1 β in PLY Adjuvant Activity	172
5.4.1	The Role of Complement in Adjuvant Activity	172
5.4.2	The Role of IL-1 β in Adjuvant Activity.....	172
5.5	Analysis of IgG Subclasses Produced in Response to e-PLY and e- $\Delta 6$ PLY Immunization in NLRP3-/- and BALB/c Mice	177
5.6	Discussion	180
6.	Effect of Fusion Antigens on Immunization Outcome.....	186
6.1	IgG subclasses induced by Immunization with PsaA fusion vaccines	187
6.2	IgG subclasses induced by Immunization with PspA fusion vaccines....	189
6.3	IgG subclasses induced by Immunization with PspC fusion vaccines....	190
6.4	IgG subclasses induced by Immunization with PhtD fusion vaccines....	193
6.5	IgG subclasses induced by Immunization with a 10x mix of PsaA/PspA/PspC/PhtD - $\Delta 6$ PLY fusion vaccines	195
6.6	Discussion	200
7.	Final Discussion.....	203
7.1	The Interaction of PLY with Toll-like Receptors	203
7.2	The Production of KC, IL-6 and IL-1 β and Their Potential Role(s) in the Adjuvant Activity of PLY	203
7.2.1	IL-1 beta	204
7.2.2	IL-6.....	205
7.2.3	KC	206
7.2.4	The Role of Complement in Cytokine Production and Adjuvant Activity.....	206
7.3	Binding of PLY Variants to Host Cells and Interactions with the Cell Cytoskeleton.....	207
7.4	Characteristics of Final Immune Phenotype following Immunization with PLY/ $\Delta 6$ PLY Fusion Vaccines	208
7.5	Gene expression analysis	209

7.6	Future work	213
7.7	Conferences/presentations	214
	Appendices	217
	Appendix 1 - Buffer recipes	217
	Appendix 2 - Table of Properties of PLY and its Derivatives (mol. weight etc.)	219
	Appendix 3 - Concentration of HaloTagged proteins in Halo lysates	219
	Appendix 4 - Sequence alignment of Tubulin β -5 chain from <i>Bos taurus</i> and <i>Mus musculus</i>	220
	Appendix 5 - Analysis of BMDM Gene Expression in Response to Treatment with PLY and its Derivatives	220
	List of References	226

List of Tables

Table 1-1 Novel Pneumococcal Vaccines: Composition and Efficacy	30
Table 2-1 List of antibiotics, preparation guidelines and storage conditions. ...	51
Table 2-2 List of antibiotics for tissue culture, preparation guidelines and storage conditions.....	51
Table 2-3 Bacterial strain information.	52
Table 2-4 Oligonucleotide primers.....	54
Table 2-5 GoTaq PCR mix	56
Table 2-6 GoTaq PCR cycling conditions	56
Table 2-7 <i>PfuUltra II</i> PCR mix	57
Table 2-8 <i>PfuUltra II</i> PCR cycling conditions	57
Table 2-9 pET33b constructs available for use.....	61
Table 2-10 Table of primers and DNA templates used to clone PLY and its derivatives into pFN18A.	65
Table 2-11 Preparation of Protein standards for Bradford Assay.....	72
Table 2-12 Description of Cell line Origins, Characteristics and Growth Requirements	77
Table 2-13 Immunization schedule.	85
Table 2-14 Table of transgenic animals and their genetic backgrounds	86
Table 2-15 Subclasses ELISA Secondary Antibody Layout.....	88
Table 3-1 Abbreviations and Definitions of PLY variants used in this Project....	92
Table 3-2 Calculated Haemolytic Activity of Lytic PLY Variants	94
Table 3-3 LPS Concentration in Purified Recombinant PLY and its Derivatives. .	99
Table 3-4 Protein Concentration of Controls Created using Ni-magnetic Beads	100
Table 3-5 Ranked Order of Cell Sensitivity to PLY-mediated Lysis.....	115
Table 4-1 Fractions Analyzed Following Protein Pull-down Protocol	133
Table 4-2 Proteins identified my MS/MS mass spectrometry.....	140
Table 4-3 PCC values for PLY variants and actin	152
Table 5-1 Role of Cytokines in Regulating Ig Isotype Expression (recreated from Immunobiology, 6 th edition, Janeway et al.).....	178
Table 5-2 Description of IgG Subsets and their Functions.....	178
Table 7-1 Regulation of adjuvant core response genes following PLY treatment	210
Table 7-2 Regulation of Adjuvant Core Response genes Following PLY treatment.	211

List of Figures

Figure 1-1 Schematic of PATH experimental procedure.	32
Figure 1-2 Domain structure of pneumolysin.	35
Figure 1-3 Process of pore formation.	36
Figure 1-4 Diagram of LPS/TLR4 complex	44
Figure 2-1 Diagram of pFN18A cloning site.	53
Figure 2-2 Mutation and truncation of pneumolysin.	60
Figure 2-3 DNA insert $\Delta 6D123PLY$	62
Figure 2-4 Colony screening PCR.	63
Figure 2-5 Example purification of $\Delta 6D123PLY$ by NAC.	67
Figure 2-6 Example purification of $\Delta 6D123PLY$ by AEC.	68
Figure 2-7 Analysis of purified protein by SDS-PAGE and western blotting.	70
Figure 2-8 Example haemolytic assay.	71
Figure 2-9 Analysis of BMDM culture phenotype by flow cytometry.	76
Figure 3-1 Analysis of haemolytic activity of PLY variants.	93
Figure 3-2 Analysis of cytolytic activity of PLY against L929 and RAW264.7 macrophages.	95
Figure 3-3 LDH release in PLY treated bone marrow derived macrophages at 3(A), 6(B), 12(C) and 24(D) hours.	97
Figure 3-4 Apoptosis in BMDM treated with PLY, $\Delta 6PLY$, D123PLY, D4PLY.	98
Figure 3-5 Analysis of vehicle controls and eluted proteins following Ni-magnetic bead treatment of PLY and $\Delta 6PLY$	101
Figure 3-6 Haemolytic assay of purified PLY, Ni-cleaned PLY vehicle and eluted PLY.	102
Figure 3-7 Analysis of haemolytic activity of PLY, PLY vehicle and eluted PLY following Ni-magnetic bead treatment.	103
Figure 3-8 SDS-PAGE analysis of purified PLY derivatives.	104
Figure 3-9 SEAP production in THP1-blue CD14 reporter cells following treatment with PLY variants.	106
Figure 3-10 SEAP production in HEK293/SEAP/TLR5 reporter cells following treatment with PLY variants.	107
Figure 3-11 SEAP production in HEK293/SEAP/TLR4/MD2 reporter cells following treatment with PLY variants.	108
Figure 3-12 The IL-1 β hypothesis.	110
Figure 3-13 IL-1 β production in BMDM treated with PLY or $\Delta 6PLY$	111
Figure 3-14 Putative model of PLY-dependent IL-1 beta production, version 1.	112
Figure 3-15 KC production in (A - MF1) or (B - TLR4-/-) BMDM treated with either PLY, $\Delta 6PLY$, D123PLY or D4PLY.	113
Figure 4-1 Analysis of h-PLY binding to RAW264.7 cells at different incubation times.	121
Figure 4-2 2D merged image of h-PLY treated RAW 264.7 cells stained with CellMask Deep-red plasma membrane stain and HaloTag TMR-direct ligand. ...	122
Figure 4-3 3D image of h-PLY treated RAW 264.7 cells stained with Deep-red plasma membrane stain and Halo TMR-direct ligand.	123
Figure 4-4 2D merged image of h- $\Delta 6PLY$ treated RAW 264.7 cells stained with CellMask Deep Red plasma membrane stain and HaloTag TMR-direct ligand.	124
Figure 4-5 3D image of h- $\Delta 6PLY$ treated RAW 264.7 cells stained with Deep-red plasma membrane stain and Halo TMR-direct ligand.	125

Figure 4-6 2D merged image of h-D123PLY treated RAW 264.7 cells stained with CellMask Deep Red plasma membrane stain and HaloTag TMR-direct ligand....	126
Figure 4-7 3D image of h-D123PLY treated RAW 264.7 cells stained with Deep-red plasma membrane stain and Halo TMR-direct ligand.	127
Figure 4-8 2D merged image of h-D4PLY treated RAW 264.7 cells stained with CellMask Deep Red plasma membrane stain and HaloTag TMR-direct ligand....	128
Figure 4-9 3D image of h-D4PLY treated RAW 264.7 cells stained with Deep-red plasma membrane stain and Halo TMR-direct ligand.	129
Figure 4-10 2D merged image of h-eGFP treated RAW 264.7 cells stained with CellMask Deep Red plasma membrane stain and HaloTag TMR-direct ligand....	130
Figure 4-11 Schematic of a modified Halo-tag pull-down protocol.	132
Figure 4-12 Analysis of pull-down efficiency by silver staining and western blot.	135
Figure 4-13 Analysis of pull-down efficiency by silver staining and western blot.	136
Figure 4-14 Separation and excision of proteins from h-PLY and h- Δ 6PLY pull-down.....	138
Figure 4-15 Separation and excision of proteins from h-D123PLY and h-D4PLY pull-down.	139
Figure 4-16 2D merged image of eGFP treated RAW 264.7 cells stained with rhodamine phalloidin.	143
Figure 4-17 2D merged image of e-PLY treated RAW 264.7 cells stained with rhodamine phalloidin.	144
Figure 4-18 3D image of e-PLY treated RAW 264.7 cells stained with rhodamine phalloidin.	145
Figure 4-19 2D merged image of e- Δ 6PLY treated RAW 264.7 cells stained with rhodamine phalloidin.	146
Figure 4-20 3D image of e- Δ 6PLY treated RAW 264.7 cells stained with rhodamine phalloidin.	147
Figure 4-21 2D merged image of e-D123PLY treated RAW 264.7 cells stained with rhodamine phalloidin.	148
Figure 4-22 3D image of e-D123PLY treated RAW 264.7 cells stained with rhodamine phalloidin.	149
Figure 4-23 2D merged image of e-D4PLY treated RAW 264.7 cells stained with rhodamine phalloidin.	150
Figure 4-24 3D image of e-D4PLY treated RAW 264.7 cells stained with rhodamine phalloidin.	151
Figure 4-25 Actin Binding ELISA.	153
Figure 4-26 Electron microscopy image of pore formation.....	155
Figure 5-1 IL-1 beta and KC production in NLRP3 ^{-/-} BMDM treated with PLY and Δ 6PLY.....	161
Figure 5-2 IL-1 β production in BMDM treated with PLY plus sera.	163
Figure 5-3 IL-1 β production in BMDM treated with PLY in the presence or absence of complement.....	164
Figure 5-4 Putative model of PLY-dependent IL-1 beta production, version 2. .	165
Figure 5-5 IL-1 β production in C3 ^{-/-} BMDM.	166
Figure 5-6 KC production in (A) C3 ^{-/-} and (B) MF1 BMDM.	167
Figure 5-7 IL-1 β production in TLR4 ^{-/-} BMDM.	168
Figure 5-8 IL-1 β production in VIPER treated BMDM.....	169
Figure 5-9 Putative model of PLY-dependent IL-1 beta production, version 3. .	170
Figure 5-10 Putative model of PLY-dependent IL-1 beta production, version 4. .	171
Figure 5-11 IL-1 beta Hypothesis - expanded.....	173

Figure 5-12 Anti-eGFP IgG titres in NLRP3 ^{-/-} (A) and BALB/c (B) mice immunized with e-Δ6PLY or e-PLY.	174
Figure 5-13 Anti-eGFP IgG titres in NLRP3 ^{-/-} (A) and BALB/c (B) mice immunized with e-Δ6PLY or e-PLY.	175
Figure 5-14 Anti-eGFP IgA titres in NLRP3 ^{-/-} and BALB/c mice immunized with e-Δ6PLY.	176
Figure 5-15 Analysis of anti-eGFP IgG subsets.....	179
Figure 5-5-16 Final putative model of PLY-dependent IL-1β production.	181
Figure 5-17 Diagram of the classical complement cascade.	183
Figure 6-1 PATH 1.	187
Figure 6-2 PATH 2.	188
Figure 6-3 PATH 3.	189
Figure 6-4 PATH 4.	190
Figure 6-5 PATH 5.	191
Figure 6-6 PATH 6.	192
Figure 6-7 PATH 7.	193
Figure 6-8 PATH 8.	194
Figure 6-9 PATH 9.	198
Figure 6-10 PATH 10.	200

List of Abbreviations

%	Percentage
Δ	Deletion
°C	Degrees Celsius
μg	Microgram
μl	Microlitre
μM	Micromolar
APC	Antigen presenting cell
APS	Ammonium persulphate
BALF	Bronchiolar lavage fluid
BMDC	Bone marrow derived dendritic cells
BMDM	Bone marrow derived macrophages
BSA	Bovine serum albumin
CDC	Cholesterol-dependent cytolysin
Conc.	Concentration
DIC	Differential interference contrast
DNA	Deoxyribonucleic acid
dNTP	Deoxyribonucleotide triphosphate
DTaP	Diphtheria, Tetanus, acellular pertussis vaccine
DTT	Dithiothreitol
EDTA	Ethylendiaminetetraacetic acid
ELISA	Enzyme-linked immunosorbant assay
Fc	Fragment crystallisable
eGFP	Enhanced green fluorescent protein
G	Grams
HRP	Horse radish peroxidase
HU	Haemolytic units
IFN	Interferon
IgA	Immunoglobulin A
IgG	Immunoglobulin G
IL-	Interleukin
I.N.	Intranasal
IPD	Invasive pneumococcal disease

IPTG	Isopropyl B-D-1-thiogalactopyranoside
kDa	Kilo Daltons
L	Litre
LB	Luria-Bertani/Lysogeny Broth
LBP	LPS-binding protein
LDH	Lactate dehydrogenase
LPS	Lipopolysaccharide
MCSF	Monocyte colony stimulating factor
mg	Microgram
ml	Microlitre
nm	nanometre
nM	Nanomolar
NFκB	Nuclear factor kappa-light-chain-enhancer of activated B cells
NLR	Nod-like receptor
NLRP3	Nod-like family receptor, pyrin domain containing 3
OD	Optical density
O/N	Overnight
OPA	Opsonophagocytosis assay
PATH	Programme for Appropriate Technology in Health
PAMP	Pathogen associated molecular pattern
PBS	Phosphate buffered saline
PCC	Pearson's correlation coefficient
PCR	Polymerase chain reaction
PCV	Pneumococcal conjugate vaccine
PhtD	Pneumococcal histidine triad protein D
pmol	Picomoles
PMNL	Polymorphonuclear leukocytes
PRR	Pattern recognition receptor
PsaA	Pneumococcal surface adhesin A
PspA	Pneumococcal surface protein A
PspC	Pneumococcal surface protein C
RIN	RNA integrity number
RNA	Ribonucleic acid
S.C.	Subcutaneous
SDS-PAGE	Sodium dodecyl sulphate - polyacrylamide gel electrophoresis

SEAP	Secreted embryonic alkaline phosphatase
TGFB	Transforming growth factor beta
TLR	Toll-like receptor
TNF	Tumour necrosis factor

1. Introduction

Streptococcus pneumoniae is an important human pathogen, it causes a range of diseases but the most common are otitis media, pneumonia, septicaemia and meningitis. Pneumococcal disease burden is a concern in both developed and developing countries, particularly in children under the age of 5 and adults over the age of 60 and as such vaccination is recommended for individuals in these higher risk categories. Currently used vaccines include the single dose 23-valent polysaccharide vaccine which confers protection against the most prevalent of the 90 different serotypes. However, this vaccine is ineffective in children under the age of 2 (who cannot produce strong T-cell-independent responses) (Pollard et al., 2009). To combat this, a pneumococcal conjugate vaccine is available for all children aged 2-23 months, this vaccine is given in 4 doses and confers strong protection against the most invasive serotypes, however it does not give a broad spectrum of protection. The available pneumococcal vaccines have limited effectiveness, they are not effective on a global scale due to varying serotype prevalence and they may promote serotype replacement. Modern vaccine research to prevent and control *S. pneumoniae* infections aims to address the limitations of both vaccines by providing species wide protection through conserved pneumococcal virulence factors; ideally this vaccine would also prevent nasopharyngeal colonization so as to confer non-serotype specific herd immunity to a sufficiently immunized population. The work presented in this thesis aimed to elucidate the mechanism of action of one such novel pneumococcal vaccine, designed and constructed within the Mitchell group. The basis for this vaccine is pneumolysin (PLY), a cholesterol-dependent cytolysin (CDC) and highly conserved pneumococcal virulence factor. It was found that PLY is both an immunogen and adjuvant in its own right and that genetic fusion of other conserved pneumococcal virulence factors to the toxin created an effective and protective pneumococcal vaccine. This was also true where a non-lytic deletion mutant of PLY ($\Delta 6$ PLY) was used as the protein carrier and adjuvant. A particular aim of this study was to discover the mechanisms of adjuvant activity that were dependent/independent of pore formation.

1.1 *Streptococcus pneumoniae* background

Streptococcus pneumoniae, first discovered in 1881, is a gram positive facultative anaerobe; it is coccoid in shape and typically grows in pairs or chains resulting in its original name “the diplococcus” (Pasteur, 1881; Sternberg, 1881). It is both a commensal organism of the human nasopharynx (it is conservatively estimated that 20-40% of healthy children and 5-10% of healthy adults are carriers) and an opportunistic pathogen. Armed with a number of virulence factors, the most widely studied and targeted for immunization is the capsule; there are over 90 known capsular serotypes of *S. pneumoniae*, the Danish nomenclature system which classifies serotypes according to their structural and antigenic characteristics is the adopted standard. Although there are virulent unencapsulated variants of *S. pneumoniae* these are less commonly isolated and are associated with specialized disease e.g. conjunctivitis (Marimon et al., 2013), encapsulated pneumococci are far more frequently identified in both disease and carriage and in animal models tend to be more virulent than isogenic unencapsulated pneumococci. The pneumococcal capsule promotes survival of the bacterium in multiple ways; firstly, the capsule helps to prevent mechanical removal by mucus (Nelson et al., 2007), it also confers resistance to antibody deposition and complement mediated lysis and inhibits phagocytosis by host cells (Hyams et al., 2010). There is a relationship between capsular thickness and survival in certain anatomical location e.g. blood. The pneumococcus has a variety of other surface associated virulence factors involved in adhesion, complement resistance and scavenging (AlonsoDeVelasco et al., 1995; Mitchell & Mitchell, 2010), the virulence factors PspA, PspC, PsaA, PhtD and PLY which were chosen as novel antigenic targets are described further in chapter 6 and sections 1.3 and 1.6.

There is vast genetic variation within the species, in addition to the 90 known capsular types over 4000 multi-locus sequence types (MLST) have been identified (spneumoniae.mlst.net). In addition, *S. pneumoniae* is naturally recombinant and able to acquire additional virulence factors and indeed swap capsules-types during mixed colonization. This is a particularly relevant characteristic when constructing new pneumococcal vaccines, as antigenic targets should be highly conserved indicating their importance in pneumococcal survival and/or spread.

1.2 Pneumococcal Disease Burden: Prevention and Treatment

As mentioned previously *S. pneumoniae* is capable of causing otitis media, pneumoniae, septicaemia and meningitis, it can also cause conjunctivitis, empyema, endocarditis and others (though more rarely) (Carvalho et al., 2003; Facklam et al., 2003; Musher et al., 1992). Pneumococcal disease is not usually associated with sustained carriage, it is thought to arise when the host is colonized by a new serotype by transmission via respiratory droplets (Gray et al., 1980). Aside from the 'at risk' age groups previously mentioned other risk factors for pneumococcal disease include HIV, asplenia, complement deficiency and smoking (active or passive) (Ram et al., 2010). Increased susceptibility to pneumococcal disease is also associated with ethnicity, among other races Alaskan Inuit and Australian aborigines are at risk with a specific predisposition to severe otitis media (Wenger et al., 2010). Otitis media in Australian aboriginal children is unusual as it can often be asymptomatic and is subsequently not diagnosed until tympanic rupture occurs (Mackenzie et al., 2009)

1.2.1 Disease burden

All cause pneumonia (of which the pneumococcus is the greatest contributor) currently kills more children under the age of 5 than measles, malaria and HIV combined, the World Health Organization's latest figures state that in 2000 there were approximately 14.5 million cases of serious pneumococcal disease, resulting in the deaths of approximately 826,000 children under the age of 5. The highest burden of disease is found in Africa and Southeast Asia, areas where there are not efficient or affordable vaccination programmes (O'Brien et al., 2009; Scott, 2007). There is also the consideration of cost and mortality, for instance, pneumococcal meningitis is rare but has a high mortality rate (~37%) (Gouveia et al., 2011) whereas pneumococcal otitis media has a very low

mortality rate but is common in children under the age of 2 and puts considerable financial burden on healthcare systems.

1.2.2 Treatment of pneumococcal disease and antibiotic resistance

As with many other bacterial pathogens there is increasing incidence of antibiotic-resistant pneumococci. Particularly, there is increasing resistance (and in some cases multi-resistance) to β -lactams, macrolides and fluoroquinolones such as penicillin, erythromycin and ciprofloxacin (Doern, 2001). This is a global issue and although the introduction of pneumococcal vaccines and regulation of antibiotic prescription have reduced the incidence of new resistant strains (Liñare et al., 2010) it is imperative that new antimicrobials are developed in conjunction with sensible prescription policies; a non-serotype specific vaccine that provides broad protection against all pneumococcal strains would also be an effective intervention. It has been suggested that antibodies to pneumococcal capsular polysaccharide that are non-opsonic can increase genetic exchange (Yano et al., 2011), it could be important to consider this when designing future pneumococcal polysaccharide vaccines as a means of reducing capsule switching and antibiotic resistance.

1.2.3 Pneumococcal vaccines: Coverage, effectiveness and limitations

Currently used vaccines target pneumococcal capsular polysaccharide and include the single dose 23-valent polysaccharide vaccine Pneumovax 23 (PPV-23) which confers protection against the most prevalent of the 90 different serotypes (1, 2, 3, 4, 5, 6B, 7F, 8, 9N, 9V, 10A, 11A, 12F, 14, 15B, 17F, 18C, 19F, 19A, 20, 22F, 23F and 33F.); however this vaccine is ineffective in children under the age of 2 (who cannot produce strong T-cell independent responses). To combat this, a pneumococcal conjugate vaccine PCV13 is available for all

children aged 2-23 months, this vaccine is given in 4 doses and confers strong protection against 13 pneumococcal serotypes (1, 3, 4, 5, 6A, 6B, 7F, 9V, 14, 18C, 19A, 19F and 23F). Both vaccines have been shown to provide effective protection against invasive pneumococcal disease.

Considering there are over 90 known serotypes of *S. pneumoniae* it is obvious that the current vaccines do not give a broad spectrum of protection. Serotypes associated with disease tend to vary geographically; therefore the serotypes included within these vaccines may not be appropriate in some countries. The phenomenon of serotype replacement describes the increasing incidence of disease caused by serotypes not included in either pneumococcal vaccine following their introduction (Weinberger et al., 2011; Hicks et al., 2007). This phenomenon is now widely recognised and affects virtually all populations immunized against *S. pneumoniae*; in one case serotype replacement has made immunization with the current vaccines completely ineffective at controlling pneumococcal infections within the population (Wenger et al., 2010). The available pneumococcal vaccines have limited efficacy in preventing pneumonia and otitis media (Huss et al., 2009), in addition, the initial reductions seen in incidence of pneumococcal pneumonia following introduction of either vaccine quickly begin to diminish; this is likely due to serotypes not included in the vaccines.

Aside from serotype replacement there are conflicting reports of the efficacy of pneumococcal conjugate vaccines. The majority of analyses focus on PCV-7 since PCV-13 has not yet been introduced into all vaccine schedules and has only been available for 3 years. Colonization in children immunized with PCV-7 is not completely controlled; children immunized with PCV-7 are less likely to be colonized with vaccine serotypes but are more likely to be colonized by non-vaccine serotypes (O'Brien et al., 2007). A meta-analysis of clinical trial data has shown that PCV-7 has 55-57% efficacy in preventing acute otitis media and 89% efficacy in preventing invasive disease, yet efficacy for preventing clinical and radiograph-confirmed pneumonia was only 5-7% and 29-32%, respectively (Pavia et al., 2009).

Pneumovax, the 23-valent pneumococcal polysaccharide vaccine is considered effective in preventing IPD, however, a meta-analysis of immunized over 65 year olds demonstrated that Pneumovax is ineffective at preventing pneumococcal

pneumonia (Huss et al., 2009). In 2011 the Joint Council on Vaccines and Immunization (JCVI) concluded that there was insufficient evidence to suggest that Pneumovax had any effect in preventing IPD in the over 65 group (in England) and the continuation of the immunization programme is under review (JCVI, 2011). It was suggested that any perceived protection in this group is likely due to immunization of children with PCV-7/-13 preventing transmission. In addition, within this age group pneumococcal pneumonia is often secondary to Influenza infection, therefore high uptake and efficacy of the Influenza immunization programme could also protect against pneumococcal disease (Mina et al., 2013).

Purification and/or conjugation of capsular polysaccharides is a lengthy and expensive process; a typical dose of PCV-13 costs around \$5, while this may be cost-effective in high-income countries the cost of four doses for each child makes immunization difficult in lower income countries, particularly where there is no state help. The GAVI alliance in combination with the Bill and Melinda Gates foundation are providing pneumococcal vaccines and financial aid in 25 eligible countries to reduce the inequality of pneumococcal disease prevention.

1.3 Immunity to *Streptococcus pneumoniae*

Novel pneumococcal vaccine research seeks to provide non-serotype specific immunity to avoid the increasingly recognised issue of serotype replacement. Additionally, a better understanding of the immune phenotype that is required to effectively clear pneumococcal infection allows vaccines to be chosen that induce this type of response.

1.3.1 Innate Immunity to the pneumococcus

Early innate immune responses to the pneumococcus involve the influx of inflammatory leukocytes such as neutrophils and macrophages, this is an essential protective response (Herbold et al., 2010; Sun et al., 2011). In addition the pneumococcus is thought to interact with a number of pattern

recognition receptors (PRR), particularly TLR2 and the intracellular receptor NOD2, recognition by both of these receptors induces the production of TNF α , IL-6, CCL2 and IL-1 β (Opitz et al., 2004; Paterson & Mitchell, 2006). In addition a type-I IFN response is induced by the pneumococcus, the role of IFN in pneumococcal infection has not yet been fully elucidated, neither has the mechanism of induction of this response (Koppe et al., 2011). Finally, TLR4 has been shown to be protective during pneumococcal infection, furthermore its role is PLY-dependent (Malley et al., 2003). A clear binding mechanism has not yet been identified, neither has a role for TLR4 in the humoral or cell-mediated immune responses to PLY. This role/mechanism was a particular focus of the work presented in this thesis.

1.3.2 Humoral immunity to the pneumococcus

Currently, the efficacy of pneumococcal vaccines is predicted and quality controlled by assessing the opsonic activity of antibodies generated in mouse models of immunization. Typically, an opsonic titre of 1:8 is considered the minimum activity permitted and equates to an efficacious IgG concentration of 0.2 to 0.35 μ g/ml in immunized infants. A standard assessment of opsonophagocytic activity between diagnostic centres exists, the Romero-Steiner assay is considered the 'Gold standard' opsonophagocytosis assay (OPA) (Fleck & Nahm, 2005; Romero-Steiner et al., 1997; Romero-Steiner et al., 2006). Therefore, it is clear that anti-pneumococcal antibodies are considered vital for protection against the pneumococcus.

S. pneumoniae is resistant to phagocytosis unless opsonised by complement, this can be achieved either through the alternative complement pathway, or, by targeted activation of the classical complement pathway by specific anti-pneumococcal antibodies. It is through this mechanism that anti-pneumococcal antibodies mediate protection, in particular IgG subsets IgG2a and IgG2b confer the highest phagocytic activity (Lefeber et al., 2003). As detailed in section 1.2.3, non-opsonising antibodies are inefficient at conferring protection against *S. pneumoniae* and can have negative effects, increasing recombination events (Yano et al., 2011).

Humoral immunity is a particularly relevant topic with respect to children; typically children are incapable of producing T-cell independent antibody responses until between 2 and 5 years of age (necessitating conjugate vaccines) (Lane, 1996). Children have high rates of carriage and although infection is more common than in healthy adults some level of protection is afforded through both maternal antibodies and generation of antibodies to pneumococcal proteins. Understanding the dynamics of colonization, passive immunity and maturation of active immune responses may help identify more suitable antigens for non-serotype specific vaccines. One longitudinal study correlated levels of IgM, IgG and IgA against 17 pneumococcal vaccine antigen candidates simultaneously with nasopharyngeal colonization in infants from 1.5 to 24 months of age (Lebon et al., 2011). This study was performed before the introduction of PCV-7 and also monitored incidence of respiratory tract infection (RTI) in subjects, it was found that maternal antibodies did not prevent colonization, in fact higher maternal anti-pneumococcal antibody levels correlated with higher levels of colonization. Colonization itself induced protective antibodies against some virulence factors, levels of IgG increased over time as expected but while this increase in specific antibody was associated with decreased RTI it did not prevent colonization. It is well known that colonization of adults can stimulate production of anti-capsular antibodies (Musher et al., 1997). In a longitudinal study of unvaccinated adults nasopharyngeal carriage was associated with serotype specific antibody production; however, this did not prevent further colonization, similarly antibodies generated toward PLY and PsaA were modestly increased following carriage but did not prevent future colonization against any serotype (Goldblatt et al., 2005). Protection against disease was not measured. These studies raise interesting questions about the goals of current immunization strategies where prevention of colonization is central to perceived efficacy; this study demonstrates that invasive disease can be prevented while allowing colonization, however, this would not provide herd immunity. A vaccine that mimics natural immunity and allows colonization while preventing invasive disease would also eliminate concerns about potentially harmful colonizers that would fill the niche left by *S. pneumoniae* should a non-serotype specific vaccine that prevents colonization be introduced.

Natural antibodies exist in the naive host and typically have an IgM isotype (Baumgarth et al., 2005). The role of natural antibodies in preventing and clearing pneumococcal infections is of important consideration as it may give insight into the most desirable antibody response following immunization. These antibodies form part of the host's innate defence and are produced by B-1 cells. B-1 cells are an unconventional B cell subset in that they can produce specific antibody in a T-cell-independent manner. B-1 cells are further subdivided into B-1a and B-1b cells according to their expression of the surface marker CD5 (positive and negative, respectively). The role of these unusual B cells in immunity to the pneumococcus has been investigated in mice genetically lacking either subset (Haas et al., 2005); it has been shown that natural antibodies against pneumococcal polysaccharide (PPS) are produced by the B-1a subset, B-1b cells produce antibodies directed against PPS following immunization. Mice lacking B-1b cell but retaining B-1a cells have no increased susceptibility to infection but immune memory to PPS following immunization is short-lived. In contrast mice lacking B-1a cells but retaining B-1b are more susceptible to infection but have more efficient and long-lasting humoral immunity.

1.3.3 Cell mediated immunity to the pneumococcus

Several studies have demonstrated the importance of CD4⁺ T cell in mediating protection from and clearance of the pneumococcus, specifically Th17 cells. In a CD4⁺ T cell deficient model, mice were significantly more susceptible to pneumococcal pneumonia and bacteraemia than those with intact T cell responses (Kadioglu et al., 2004). Furthermore, CD4⁺ T cells have also been shown to be involved in acquired immune responses to pneumococci that prevent colonization and can be elicited by intranasal immunization with pneumococcal proteins (Basset et al., 2007) or capsular polysaccharide (Malley et al., 2006) in immunoglobulin deficient mouse models. The protective T-cell subset identified in response to pneumococcal infection or immunization is Th17, a phenotype recognized as protective against extracellular bacterial or fungal infections. The cytokine IL-17A is signature cytokine of the Th17 T cell phenotype and has been shown to have an essential role in clearing

pneumococcal colonization (Lu et al., 2008; Malley et al., 2006). The production of IL-17A by Th17 cells is thought to enhance pneumococcal clearance via the recruitment of inflammatory leukocytes such as monocytes/macrophages and neutrophils which have roles in both early and late responses, respectively (Zhang et al., 2009). Interestingly, neutrophils are also producers of IL-17; although there is huge early neutrophil migration into the pneumococcal lung this does not seem to be effective until later stages of infection. It may be that infiltrating neutrophils do not act in a classical manner during early infection and instead the lesser recognised functions of neutrophils such as antigen presentation are utilized (Culshaw et al., 2008; Matthias et al., 2013). The production of IL-17 by recruited neutrophils may also serve to enhance the influx of other inflammatory leukocytes, creating a positive feedback-loop. The discovery that Th17-mediated responses are essential in preventing pneumococcal colonization led to high-throughput identification studies to find Th17 inducing pneumococcal antigens for novel pneumococcal vaccines (Moffitt et al., 2012).

1.3.4 Mucosal immunization

Mucosal immunization has many advantages over traditional subcutaneous and intramuscular immunization, it requires no needles and therefore is cheaper to administer as well as safer (reduced risk of needle being re-used and therefore risk of associated infections such as HIV). The primary aim/advantage in mucosal immunization is to induce protective immunity against pathogens that enter the body at these sites, specifically through the induction of IgA (Neutra & Kozlowski, 2006). In addition, the phenomenon of ‘common mucosal immunity’ results in immunity at all mucosal sites following immunization at one e.g. intranasal immunization would also induce immunity at peripheral sites such as the gut and genital mucosa (McDermott & Bienenstock, 1979). However, there have been difficulties in perfecting this mode of immunization, mainly the difficulty of inducing protective immune responses and avoiding tolerance induction (Neutra & Kozlowski, 2006). Interestingly this has been less of an issue with intranasal pneumococcal vaccines, several novel intranasal pneumococcal

vaccines have been developed using murine models and are well tolerated and induce protective immunity, some of which are discussed in section 1.3.5. It is important to note the anatomical difference between humans and mice which may cause difficulty in translating experimental intranasal vaccines into real human interventions, while the nasal-associated lymphoid tissue (NALT) of mice is a disorganised structure on the soft palate, humans have Waldeyer's ring - an organised collection of lymphoid tissues (the palatine, lingual and nasopharyngeal tonsils).

1.3.5 Novel pneumococcal vaccines/ PATH project

In the quest for more effective pneumococcal vaccines a number of different approaches have been taken to create novel pneumococcal vaccines. Novel pneumococcal vaccines can be roughly split into three categories - vaccines based on conserved pneumococcal surface proteins, conjugate vaccines using pneumococcal polysaccharide conjugated to a pneumococcal protein carrier and vaccines that use novel adjuvants. In some cases all three approaches have been combined, a selection of these is summarized in table 1-1. One such approach carried out by the Mitchell group was funded by the Programme for Appropriate Technology in Health (PATH), referred to as 'the PATH project' throughout this thesis.

Table 1-1 Novel Pneumococcal Vaccines: Composition and Efficacy

Antigenic composition of vaccine	Adjuvant	Protection?		Reference
		Carriage	Disease	
eGFP or PsaA genetically conjugated to PLY or $\Delta 6$ PLY	PLY/ $\Delta 6$ PLY	Yes	No	(Douce et al., 2010)
PlyD1 (toxoided version of PLY)	Alhydrogel	N/A	N/A	(Kamtchoua et al., 2013)
PdB (toxoided version of PLY)	Aluminium phosphate	N/A	Yes	(Alexander et al., 1994)
PspA, PspC, PdT (toxoided version of PLY)	Cholera toxin (CT)	Yes	N/A	(Basset et al., 2007)
PspA, PspC	none	N/A	Yes	(Ferreira et al., 2009)
PspA, PdT (toxoided version of PLY)	Aluminium hydroxide	N/A	Yes	(Goulart et al., 2013)
PsaA, PdT, pneumococcal cell wall polysaccharide	Aluminium hydroxide	No	Yes	(Lu et al., 2009)
PcsB, StkP, PsaA, PspA	IC31 (novel adjuvant and TLR9 ligand)	N/A	Yes	(Olafsdottir et al., 2012)
PspA	Flt3 ligand (novel adjuvant)	N/A	Yes	(Kataoka et al., 2011)

The study published by Douce et al., 2010 describes some of the initial results from the PATH project; although this example does not show protection against disease other formulations from the PATH project did show protection (unpublished data). The study published by Douce et al. also demonstrated that PLY and the non-pore forming mutant delta 6 PLY ($\Delta 6$ PLY) possess adjuvant activity as antibodies were raised against both PspA and the model adjuvant eGFP when genetically conjugated to PLY/ $\Delta 6$ PLY in the absence of an additional adjuvant.

The PATH vaccines are based on highly conserved pneumococcal protein antigens PsaA, PspA, PspC and PhtD genetically conjugated to either PLY or $\Delta 6$ PLY and administered either intranasally or subcutaneously. This resulted in 10 PATH experiments, where odd numbers indicate immunization via the intranasal route and even numbers the subcutaneous route (figure 1-1).

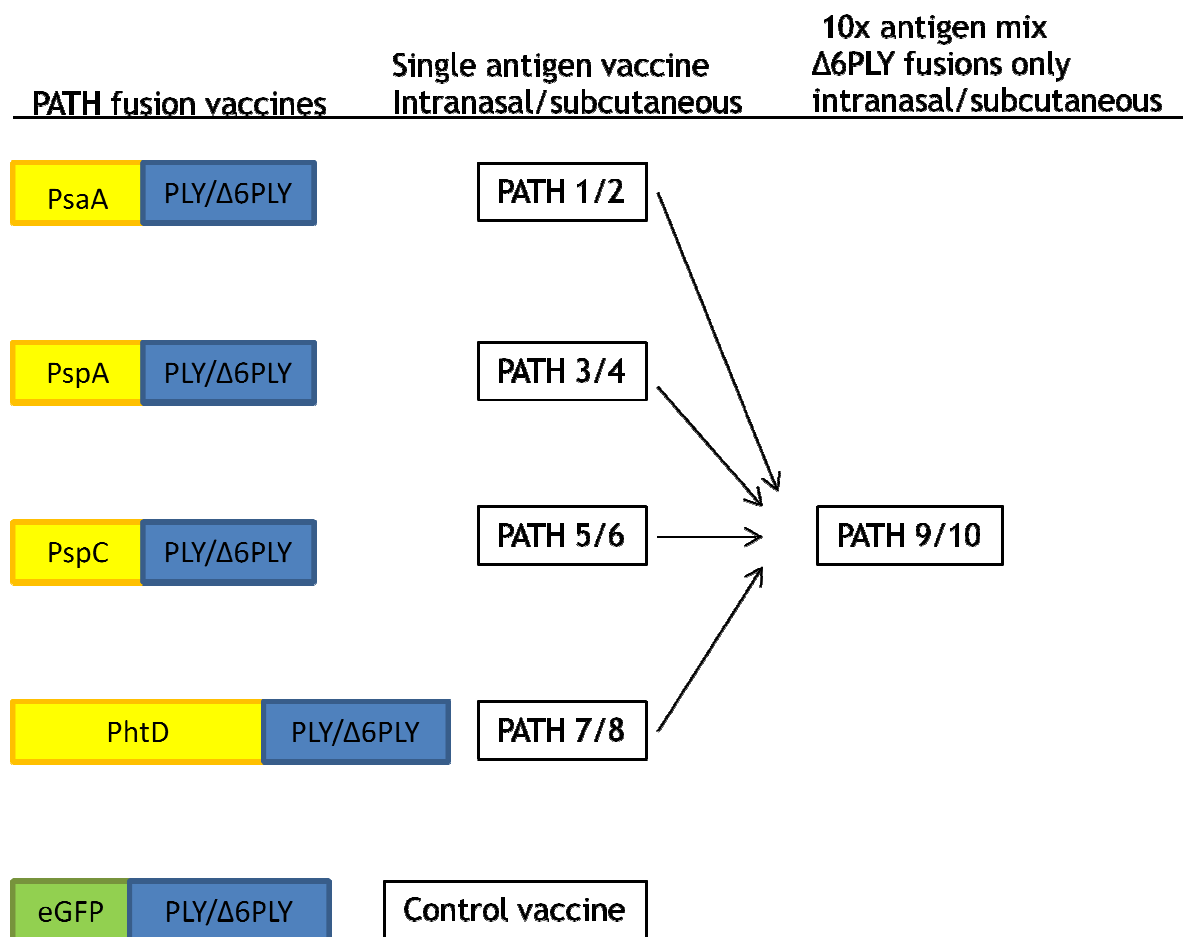


Figure 1-1 Schematic of PATH experimental procedure.

The PATH project consisted of the experimental adjuvant PLY/ Δ 6PLY genetically conjugated to PsaA (PATH 1/2), PspA (PATH 3/4), PspC (PATH 5/6), PhtD (PATH 7/8) and a mix of all 4 Δ 6PLY conjugates given at a higher dose (10X) (PATH 9/10). The vaccines were administered either intranasally (odd numbers) or subcutaneously (even numbers) following the schedule detailed in table 2-13. A control vaccine using the model antigen eGFP was also investigated (Douce et al., 2010).

The pneumococcal antigens for the PATH project were chosen because they are highly conserved and are important pneumococcal virulence factors. PsaA is a sub-capsular lipoprotein and forms part of a Mn⁺ transporter of *S. pneumoniae* (Johnston et al., 2004), it is an adhesin and has a vital role in pneumococcal survival and growth and is particularly important in pneumococcal resistance to oxidative stress (Tseng et al., 2002). PsaA is highly conserved and has been shown to confer protective immunity in a fusion vaccine consisting of PsaA, pneumococcal cell wall polysaccharide and a non-toxic PLY derivative (PdT) (Lu et al., 2009). PspA is a protein exposed on the surface of the pneumococcus, its primary function is to inhibit the activation of host complement by binding and

thereby inhibiting the action of Factor B, pneumococcal strains lacking PspA are rapidly cleared from blood in murine challenge experiments (Tu et al., 1999). Monoclonal antibodies directed against PspA are highly efficient in preventing fatal pneumococcal infection in mice (McDaniel et al., 1991), fusion vaccines based on PspA coupled to the non-toxic PLY derivatives PdT and PdB were found to confer similarly protective immune responses in immunized mice (Goulart et al., 2013). PspC (also called choline-binding protein A, CbpA) is another important surface protein of *S. pneumoniae*. PspC contains proline-rich and choline-binding domains that are identical to those of PspA and as such there is significant cross-reactivity in antibodies to these proteins (Brooks-Walter et al., 1999). Like PspA, PspC acts as a virulence factor by protecting the pneumococcus from the host complement system, it does so by binding complement Factor H conferring resistance to complement-mediated opsonophagocytosis (Dave et al., 2004; Kerr et al., 2006). The contribution of PspC to pneumococcal virulence has been shown to be strain-dependent (Kerr et al., 2006) and previous PspC-based vaccines have failed to protect mice against invasive disease (Ferreira et al., 2009). However, PspC is highly conserved within the species (75%) (Dave et al., 2001) and its cross-reactivity with PspA makes it a useful candidate in broad spectrum vaccines that hope to limit vaccine escape. PhtD is a member of the polyhistidine triad (Pht) family of proteins; it is associated with the surface of the pneumococcus and is an important virulence factor, aiding adherence to the surface of host cells and scavenging zinc ions (Khan & Pichichero, 2012; Plumptre et al., 2013). Anti-PhtD antibodies present in healthy human serum have been shown to decrease pneumococcal adherence to host cells suggesting PhtD is a good vaccine candidate (Khan & Pichichero, 2012).

Serum samples taken from each PATH experiment were available as research materials and were used by the author to determine the influence of conjugate antigens on the IgG subclass of raised specific antibodies, presented in chapter 6.

1.3.6 The future of pneumococcal vaccination

Pneumococcal clearance and survival has been demonstrated to require both antibody and cell-mediated immunity, specifically, antibody mediated complement opsonisation and a Th17 response. It would seem that Th17 is important in preventing/clearing colonization and early lung infection whereas antibody mediated protection is essential in protection from invasive disease such as bacteraemia (Cohen et al., 2011; McCool & Weiser, 2004). Any effective future vaccine(s) should elicit both humoral and cell-mediated protection. In the case of either mode of immunity, choice of antigen is critical in determining success.

Modern vaccine research into *S. pneumoniae* aims to address the limitations of both vaccines by providing species wide protection through conserved constituents of the pneumococcal cell wall; ideally this vaccine would also prevent nasopharyngeal colonization so as to confer non-serotype specific herd immunity to a sufficiently immunized population.

1.4 Pneumolysin as a Virulence Factor and Vaccine Antigen

Pneumolysin is a member of the cholesterol-dependent cytolysin (CDC) family of virulence factors that bind to and form pores in cholesterol-containing membranes. This family is characterized by a conserved amino acid sequence (ECTGLAWEWWR) termed the undecapeptide that is located in the C-terminal domain 4 and is critical for the structural changes that occur during pore formation (Dowd & Tweten, 2012). The cholesterol recognition/binding motif (CRM) is located near this conserved sequence and consists of two amino acids (threonine and leucine) that are conserved in all CDCs (Farrand et al., 2010). Cholesterol-dependent cytolysins are possessed by over 20 genera of gram positive bacteria including *Listeria*, *Bacillus*, *Clostridium* and *Streptococcus*. There are 14 known PLY alleles (Jefferies et al., 2007) and PLY is unique in being the only CDC lacking a secretion signal sequence (all other CDC depend on type II secretion systems) (Price et al., 2012). CDCs act as virulence factors by causing

cytolysis in host cells through binding to cholesterol in the host cell membranes, forming large oligomers and inserting into the host cell resulting in the formation of pores (Tveten, 2005a). The membrane disruption caused by CDCs, results in a series of pro-inflammatory responses by the host, these are detailed with reference to PLY later in this section.

In the absence of reliable crystallography data for PLY a putative structure has been suggested based on a best fit model using perfringolysin (PFO) as a template (Tilley et al., 2005); PLY consists of four distinct functional domains, in reality PLY consists of two separable domains as the polypeptide backbone weaves in and out of domains 1-3 making them impossible to purify individually. The proposed structure of PLY is shown in figure 1-2.

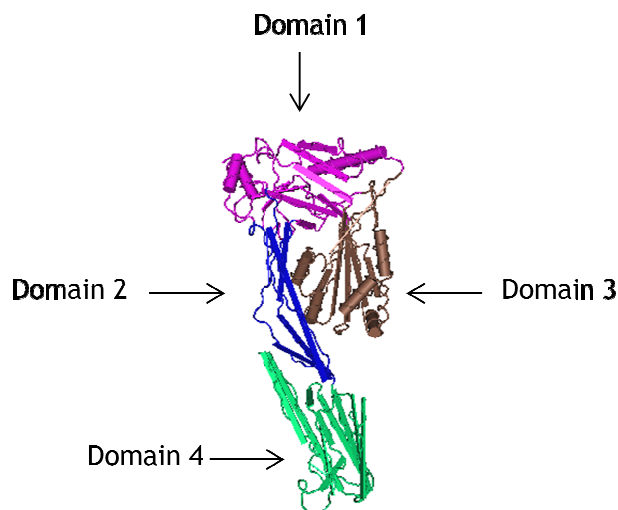


Figure 1-2 Domain structure of pneumolysin.

This worm and tube model shows the proposed structure of pneumolysin (not solved) based on the crystal structure of perfringolysin O (PFO). Structural data was retrieved from NCBI's Entrez structure database. Individual domains were highlighted using NCBI's visualisation programme for biomolecular structures; Cn3D (Wang et al., 2000).

During pore formation pneumolysin anchors to the cell membrane via domain four-cholesterol interactions (Baba et al., 2001); there is still some controversy over whether pneumolysin always oligomerizes on the cell membrane before insertion or whether individual monomers insert into the membrane and oligomerize *in situ*. Following oligomer complex formation a conformational change occurs in pneumolysin structure; first, two α -helical bundles in domain three change into two β -hairpin structures capable of piercing the membrane, then domain two collapses reducing the height of the overall complex by around

40Å. The collapse of the pore complex drives the β -hairpins formed by domain three into the membrane, piercing it to form a strikingly large pore. The pores formed can be up to 350Å in diameter with each pore containing as many as 50 PLY monomers (Nöllmann et al., 2004). This process is summarised in figure 1-3.

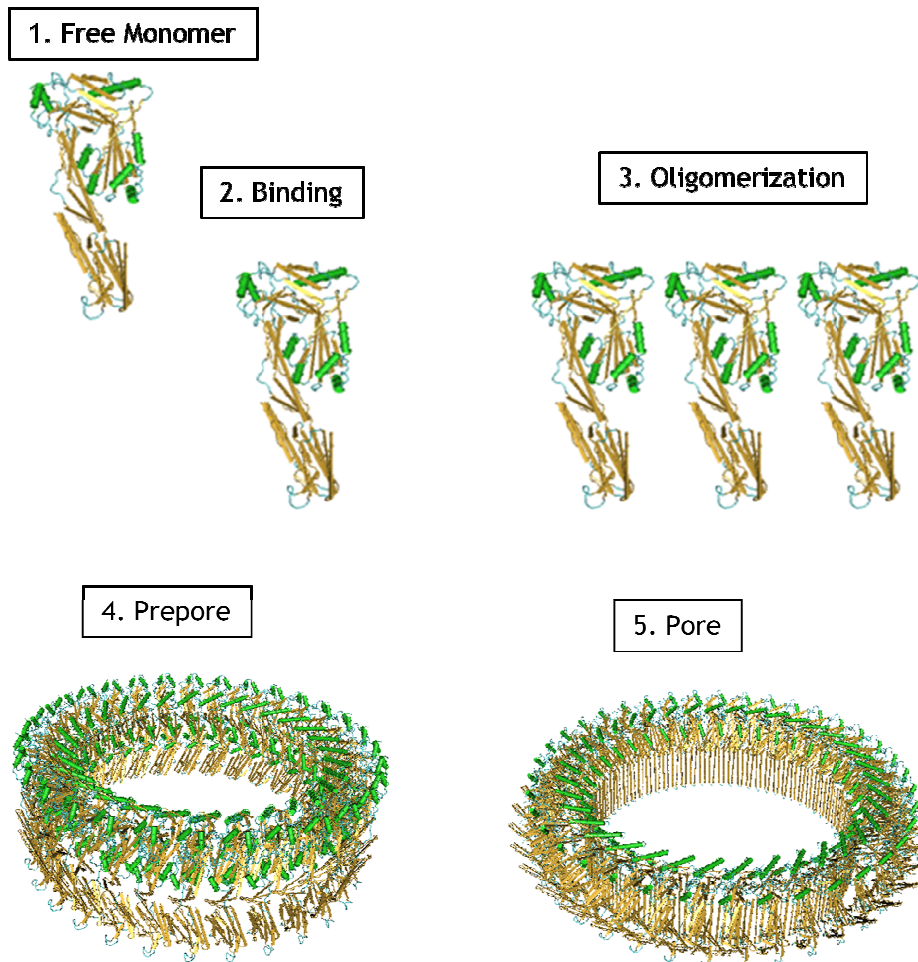


Figure 1-3 Process of pore formation.

The worm and tube models of PLY monomers, prepore and pore are based on the crystal structure of perfringolysin O (PFO). Structural data was retrieved from NCBI's Entrez structure database. Secondary structure highlighted (helix = green, strand = yellow, coil = blue) using NCBI's visualisation programme for biomolecular structures; Cn3D (Wang et al., 2000). The process of pore formation is described in section 1.4.

The formation of pores by pneumolysin frequently results in host cell death as membrane integrity is destroyed. The properties of PLY that allow it to act as a virulence factor are a combination of direct cytotoxicity through pore formation, subsequent disruption of cell structure and function, enhancement of proinflammatory mediator production and recruitment of leukocytes that further exacerbate inflammatory conditions. The induction of a proinflammatory response may seem counterintuitive, and indeed a delicate balance exists

between inducing inflammation that aids bacterial spread by subverting the immune response and eliciting host immunity that is detrimental to bacterial survival (Marriott et al. 2008); although the exact mechanism of PLY release is a contentious issue it is known to occur following autolysis of the pneumococcus; this may result in PLY release at sites where the pneumococcal population is contracting thereby directing immune responses away from the active infection. Additionally, as will be discussed in the final chapters of this thesis, the adjuvant activity of PLY is unusual in that it preferentially directs immune responses against antigens other than itself.

Pneumolysin facilitates the direct extension of the pneumococcus from the nasopharynx to the eyes, ears and lungs and subsequent spread to the blood and brain. Although inflammation caused by the proinflammatory reaction to PLY may cause loss of integrity and barrier function in epithelial and endothelial layers, PLY itself can directly disrupt barrier function by causing gross changes in the ultrastructure of epithelial and endothelial barriers. Damage to endothelial cells in a model of pneumococcal infection has been shown to precede the infiltration of leukocytes in a PLY-dependent manner (Rubins et al., 1992). In a model of the human respiratory mucosa, isogenic PLY positive and negative pneumococci rapidly adhere to mucus and both caused significant damage to the ultrastructure of the epithelium over 48hrs; damage includes extrusion of cells and cells debris. Pneumococci did not adhere directly to ciliated cells, however, PLY positive pneumococci caused significant damage to the ciliated epithelium; reduced ciliary beat or ciliary stasis and disorganization of cilia was observed (Rayner et al., 1995). These cellular changes could allow a model of bacterial spread where pneumococci travel from the nasopharynx into the lungs unimpeded by the mucocilliary elevator due to reduced function of the ciliated epithelium. The damage to ciliated cells during infection not only aids the spread of infection but can cause permanent damage to the host; an example of such damage is the sensorineural hearing loss that can sometimes accompany pneumococcal otitis media. PLY is responsible for loss of hearing due to damage caused to cochlear hair cells, the damage can be severe ranging from stereocilia disorganization as seen on ciliated epithelial cells, to total cell loss mediated by calcium influx. In addition, PLY can induce the separation of epithelial tight junctions and increased pneumococcal adherence is seen on the edges of

separated cells (Rayner et al., 1995). Once in the lungs reduced membrane integrity could allow extravasation from the lungs into the blood and from there to other to other anatomical sites such as the blood brain barrier (BBB). In a model of the blood brain barrier using Human Brain Microvascular Endothelial Cells (HBMEC), rapid PLY-dependent rounding and detachment of HBMEC was observed (Zysk et al., 2001). This is a similar cellular response to that seen in the model of respiratory endothelium and suggests pneumococci cross the respiratory endothelium and blood brain barrier using a similar mechanism that is at least partially PLY-dependent. As seen in other ciliated cells PLY has the ability to slow ciliary beat in ependymal cells of the rat brain, this was shown with both purified PLY and penicillin-lysed pneumococci (Hirst et al., 2004). In addition ciliary sloughing and cytoplasmic extrusions were noted following PLY treatment of ciliated ependymal cells, these effects of PLY could be blocked with anti-PLY antibodies (Hirst et al., 2004). The proinflammatory responses induced by PLY will be further discussed in the context of PLY as an adjuvant in section 1.6.

As discussed previously, incorporating PLY into pneumococcal vaccines has shown to it to be a protective antigen (table 1-1). Anti-PLY antibodies are produced in response to carriage, however, their role in natural immunity is questionable as anti-capsular antibody is a more effective indicator of protection (Goldblatt et al., 2005). Although anti-PLY responses following infection may not be strong or protective this does not preclude the efficacy of PLY as a vaccine antigen, for instance, the DTaP vaccine induces highly effective protection against the effects of Diphtheria and Tetanus toxins even though infection with *Corynebacterium diphtheriae* or *Clostridium tetani* does not induce antibody responses against these toxins (Casadevall & Pirofski, 2003). In addition to being an adjuvant and immunogen PLY is an ideal conjugate as it replaces current protein carriers and avoids the issue of anti-carrier antibodies within the current vaccine schedule.

1.5 Vaccine Adjuvants and their Mode(s) of Action

It is well known that in the case of subunit vaccines increasing purity results in decreasing immunogenicity, it therefore necessary to use an adjuvant. An adjuvant is defined as a substance which acts non-specifically to enhance the specific immune response to the target antigen(s). This definition may be outdated in that it is now widely accepted that initial interactions between pathogen and/or adjuvant and the host's innate immune system shape the final outcome of the immune response in a very specific manner (Iwasaki & Medzhitov, 2010). Historically, the field of adjuvant design has been empirical rather than rational; modern adjuvant design aims to produce adjuvants which are specifically tailored to elicit the most appropriate immune response to the target pathogen. However, given that that mechanism of adjuvanticity for Alum (the most widely used adjuvant) is still poorly understood this is fraught with difficulties. In addition, in all adjuvants there is a delicate balance between adjuvanticity and toxicity, and while many substances have adjuvant activity from mineral oils, mineral compounds and LPS to tapioca and breadcrumbs this does not translate to many adjuvants that are safe and sensible for inclusion in human vaccines (Gupta et al., 1993; Vogel et al., 1926).

Until recently the only adjuvants licensed for use in human vaccines were aluminium salts; however, they are known to induce Th2 type responses and are incapable of stimulating cytotoxic T cells making them unsuitable for many vaccines, there are now several new adjuvants available for use. Alum has been in use for around 80 years as a vaccine adjuvant and is included in the current DTaP (diphtheria, tetanus and acellular pertussis), pneumococcal conjugate, and hepatitis A and B vaccines to name a few. However, its mode of action is still not completely understood. Until very recently it was thought that alum-adsorption created an antigen depot, leading to slow release of antigen and allowing time for strong immune responses to develop, however it has recently been shown by removal of the injection site that this is not true (Hutchison et al., 2012). Additionally, the ability of Alum to activate the NLRP3 inflammasome and induce IL-1 β has been widely studied and attributed to phagosomal destabilization (Kuroda et al., 2011), it was thought that alum could somehow synergize with TLR agonists to induce pro-IL-1 β production (De

Gregorio et al., 2008). However, in some studies it has been shown that NLRP3 activation and IL-1 β production not an essential feature of alum adjuvanticity (Franchi & Núñez, 2008). There are still other biological activities of alum that could lead to a definitive mechanism, for example its ability to activate complement (Güven et al., 2013).

MF59 is an emulsion based vaccine adjuvant used in the Influenza vaccine Fludac®, it is remarkably potent and safe adjuvant. MF59 does not create a depot effect, however, similarly to alum it increases recruitment of inflammatory leukocytes such as monocytes and neutrophils to the injection site and causes enhanced antigen uptake (O'Hagan et al., 2012). In both cases this is thought to be due to induced secretion of the chemokines CCL2, CCL3, CCL4 and CXCL8.

AS03 and AS04 (Adjuvant System) were both created by GlaxoSmithKline and are currently in use in GSK vaccines Pandemrix (A/H5N1 Influenza) and Cervarix (Human Papilloma virus). AS03 is Squalene based and AS04 is a mix of aluminium hydroxide and monophosphoryl lipid A (MPL). AS04 is thought to induce a transient local immune response consisting of upregulation of IL-6, TNF α , CCL2 and CCL3 and influx of monocytes causing increased antigen presentation. It is thought some of these responses may be mediated by MPL binding to TLR4 (Didierlaurent et al., 2009). The mechanism of action for AS03 is still poorly understood, however, both AS03 and AS04 are capable of inducing cellular immunity which may lead to effective vaccines against intracellular infections such as malaria, HIV and tuberculosis (Baldwin et al., 2012)

A comparison of gene regulation in response to modern adjuvants demonstrated a shared pattern of gene regulation and could be a step towards understanding key features of adjuvanticity (Awate et al., 2012).

1.6 Pneumolysin as a Novel Vaccine Adjuvant

The mechanism(s) of action of currently licensed adjuvants are still not completely understood, however, through compare and contrast analysis of the adjuvants available certain patterns of activation are becoming discernible; for instance the upregulation of chemokines such as CCL2, CCL3, CCL4 and IL-8,

cytokines such as IL-6, IL-1 β , TNF α and IFN and complement activation. Although there are specific nuances to the response profile each adjuvant produces (leading to differences in the final immune phenotype), generally speaking adjuvants function by increasing influx and activation of proinflammatory leukocytes, increasing antigen uptake and presentation in the context of MHC while simultaneously upregulating costimulatory molecules (CD80 and CD86). The 'nuances' of each adjuvant response profile influence the phenotype of the subsequent adaptive immune response. PLY is a pleiotropic protein and the interactions with/responses of the immune system to PLY detailed below are a selection of responses that could potentially be involved in its mechanism of adjuvant activity. These have primarily been investigated in the context of infection biology, it is the aim of this project to determine which if any of these features of PLY toxicity are involved in adjuvant activity.

1.6.1 Interaction with Pattern Recognition Receptors (PRR)

Since pneumolysin is a cytolytic toxin it can be reasonably assumed that it will interact with host intracellular receptors. The Nod (nucleotide-oligomerization domain) like receptors (NLR) are a family of intracellular pattern recognition receptors (PRR), they are composed of a central NACHT domain which undergoes conformational change during PAMP (pathogen associated molecular pattern) recognition, a leucine rich repeat at the C-terminal and a protein-protein interaction domain at the N-terminal which is required to amplify the signal. The family consists of around 20 members not all of which have a defined ligand. It has been shown that the NLR Nod2 which recognises muramyl dipeptide plays a role in defence against *S. pneumoniae*, however there does not seem to be any NLR that can directly recognize pneumolysin. It is more likely that pneumolysin activates intracellular receptors by the endogenous danger signals it produces such as calcium influx and potassium efflux. During the course of this project several papers have been published establishing the activation of the NLRP3 inflammasome by PLY and investigating its role in the immune response to PLY. NLRP3 is able to sense potassium efflux and uric acid, it then forms the NLRP3 inflammasome by binding to two adaptor proteins ASC and CARDINAL, these

adaptor proteins are each capable of binding caspase-1. After the assembly of the NLRP3 inflammasome caspase-1 is activated and is able to cleave pro-IL-1 β into its active form. NLRP3 is also thought to promote the differentiation of Th17 cells through the induction of IL-23 production. IL-1 β has a variety of cellular functions including the induction of inflammation and fever, cellular proliferation and differentiation. The activation of NLRP3 is considered the second signal in the pathway towards IL-1 β secretion, the first signal is considered to be TLR4 stimulation which results in the upregulation of pro-IL-1 β via the NF κ B pathway. TLR4 has been shown to be protective if not essential in protection from and clearance of pneumococcal disease, and PLY has been demonstrated to be a TLR4 ligand, however, this is a contentious issue as a mechanism (or PLY domain/amino acid sequence) for PLY binding to TLR4 has not been established any many in the field believe that contaminating LPS may be the source of this relationship. Lipopolysaccharide (LPS) is the most extensively studied ligand of TLR4, a toll-like receptor family member capable of forming homodimers, TLR4 cannot bind LPS directly, it relies on MD-2 to bind to a complex of LPS, lipopolysaccharide binding protein (LBP) and CD14 (a coreceptor that transfers LPS:LBP to the TLR4/MD-2 complex) (figure 1-4) (Lu et al., 2008). Malley et al. have shown that a TLR4 mutant lacking MD-2 (C3H/HEJ mouse strain) which cannot recognize LPS is still involved in the production of inflammatory cytokines in response to pneumolysin (Malley et al., 2003). Macrophages from the C3H/HEJ strain treated with PLY are hyporesponsive and produce less TNF α and IL-6 compared to macrophages from the control mouse strain (C3H/HeOuJ). To rule out contaminating LPS macrophages were also treated with heat treated PLY; as LPS is heat-stable it would be unaffected by this treatment and any LPS-dependent cytokine production would remain. It was also found in this study that C3H/HEJ mice are more susceptible to colonisation with the bioluminescent *S. pneumoniae* strain A66.1 Xen 10, indicating a protective role for TLR4 in pneumococcal colonisation. This study did not include challenge with a PLY negative isogenic strain, this would have given stronger evidence of the role of PLY interactions with TLR4 and protection from colonisation. In a study of PLY-mediated apoptosis TLR4 was shown to be involved (Srivastava et al., 2005), RAW264.7 macrophages treated with PLY and a TLR4 inhibitor (B1287) were less susceptible to apoptosis as were macrophages derived from C3H/HEJ mice, conversely HEK293 cells transfected to express

TLR4 had increased apoptosis in response to PLY. In addition, an ELISA based solid phase binding assay was used to demonstrate that PLY can bind directly to purified TLR4 (but not TLR2), heat treatment of PLY abrogated this property. If it is the case that pneumolysin is capable of interactions with TLR4 then it could provide the first signal required for IL-1 β production. Although the role of TLR4 in the pneumolysin response is still poorly defined a synergistic relationship between pneumolysin and other TLR ligands has been demonstrated in DCs (McNeela et al., 2010). This study also used the C3H/HEJ mouse strain to demonstrate that PLY could induce production of IL-5, IL-10, IL-17 and IFN γ in splenocytes independently of TLR4. It was shown that production of IL-1 α and IL-1 β by DC in response to TLR ligands Pam3Cysk4 (TLR1/2), LPS (TLR4), Zymosan (TLR2), Muramyl dipeptide (TLR2) and CpG (TLR9) was significantly increased in the presence of PLY indicating a synergistic response. Interestingly, TLR4 binding has also been described in other CDCs. In a study of the apoptotic response to *Bacillus anthracis* apoptosis was found to be TLR4-dependent, further analysis of *B. anthracis* culture supernatants found the CDC anthrolysin O (ALO) to be responsible (Park et al., 2004). Further study using recombinant ALO to treat BMDM from C3H/HEJ mice demonstrated that in the absence of functional TLR4 the TNF α and IL-6 gene expression response was abrogated. The same response was found using the CDCs listeriolysin (LLO), perfringolysin O (PFO) and suiolysin (SLO) and could indicate that TLR4 binding is another conserved function of cholesterol-dependent cytolysins. The primary criticism of these studies is the widespread use of the C3H/HEJ mouse strain as it relies on the assumption that if PLY is a TLR4 ligand it will bind by the same mechanism as LPS, using MD2 as a coreceptor. While the direct binding assay (Srivastava et al., 2005) provides strong evidence of TLR4 binding, evidence of function (such as cytokine production) in a true model of TLR4 absence (such as the *tlr4*^{-/-} mouse strain used in this study) would provide stronger evidence of TLR4 binding.

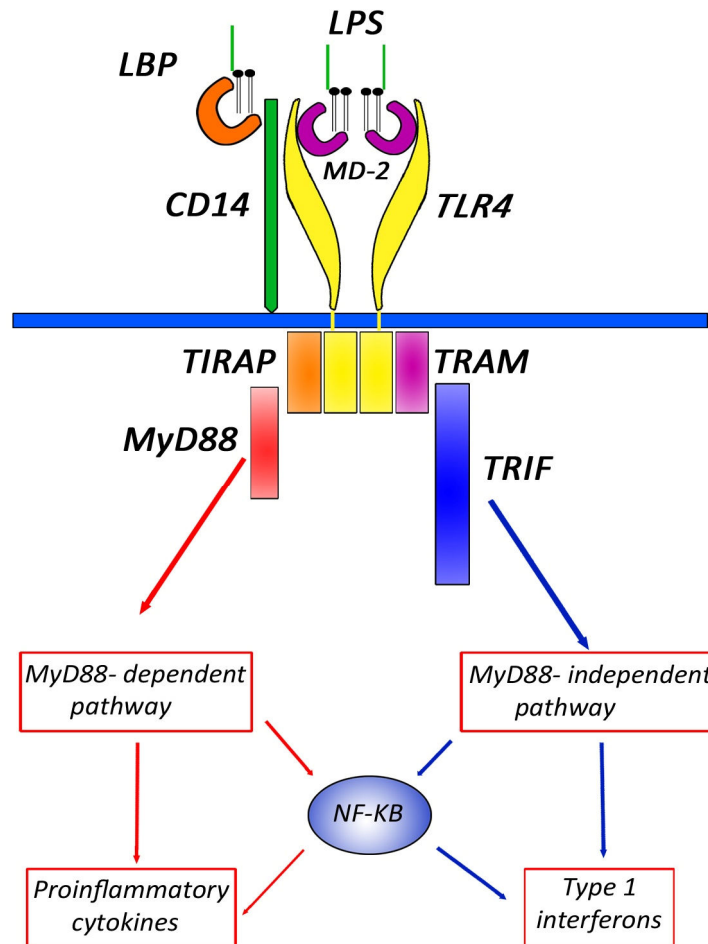


Figure 1-4 Diagram of LPS/TLR4 complex .

This diagram was reproduced from (Lu et al. 2008).

1.6.2 Activation of the classical complement pathway

The classical complement pathway is usually activated by the aggregation of antibodies on a target pathogen; it results in specific targeting of complement components to the pathogen surface resulting in opsonisation or the formation of the membrane attack complex (MAC) which results in cytolysis of the target. *Streptococcus pneumoniae* is resistant to the formation of membrane attack complexes (MAC) by complement, also, C3b deposition is inhibited by the pneumococcal polysaccharide capsule which provides some protection against phagocytosis (Jarva, 2003). However, activation of both the classical and alternative complement pathways is essential for pneumococcal clearance, it is thought these pathways initiate and determine the magnitude of C3b deposition, respectively (Yuste et al., 2005). In addition complement activation is thought to impede bacterial spread and is vital in preventing septicaemia by controlling

spread of the pneumococcus from the lungs into the bloodstream (Kerr et al., 2005; Yuste et al., 2005). Pneumolysin plays a central role in protecting the pneumococcus from complement attack and aiding its spread to other tissues/organs. PLY has been shown to activate the classical complement pathway, this occurs even in the absence of anti-PLY antibodies (Mitchell et al., 1991). During active pneumococcal infection patients often exhibit reduced serum complement levels, it is thought that this is caused by activation of complement by PLY resulting in depletion of complement components. PLY-treated serum has reduced opsonic activity, indicating exhaustion of complement components, this mechanism could aid bacterial survival and spread by reducing phagocytosis of bacteria (Alcantara et al., 2001; Giebink et al., 1980).

The complement activating ability of pneumolysin was previously thought to be due to sequence homology in the fourth domain to human CRP (C-reactive protein) but it is now known to be due to structural homology to the Fc region of IgG. The complement activating ability of pneumolysin has been shown to be dependent on amino acids Tyr₃₈₄ and Asp₃₈₅, amino acid substitutions at these positions through site-directed mutagenesis causes significant reduction or abolishment of complement activation, respectively (Mitchell et al., 1991). In both of these mutants the ability to bind the Fc portion of IgG was almost absent, suggesting that PLY activates complement through the non-specific aggregation of IgG.

1.6.3 Upregulation of genes

Only one study has investigated PLY-dependent gene regulation, this study examined differential gene regulation in the THP-1 cell line treated with isogenic PLY positive and negative pneumococci (strain D39) (Rogers et al., 2003). 148 genes were found to be differentially regulated in the presence of PLY, of interest were the caspases 4 and 6 (involved in apoptosis), MIP-1 β (monocyte chemoattractant), IL-8 (neutrophils chemoattractant), IL-2R β and CD68 (expressed on monocytes/macrophages with a role in phagocytosis). The aim of this study was to understand PLY-dependent gene regulation in the context of infection; this is reflected in the lists of genes differentially regulated

in this publication. It is of particular interest to study PLY-dependent gene regulation and interpret the results with focus on adjuvanticity.

1.6.4 Known cytokine and chemokine responses to PLY

The production of cytokines and chemokines in response to PLY has been extensively studied, particularly with reference to leukocyte chemotaxis. When PLY is used to intranasally inoculate mice IL-6, macrophage inflammatory protein (MIP)-2 and KC (the murine IL-8 homologue) are found in bronchiolar lavage fluid (BALF) and are responsible for the recruitment of polymorphonuclear leukocytes (PMNL) to the lungs (Rijneveld et al., 2002). PLY has been shown to upregulate transcription of a number of chemokines in an NF κ B, MAPK-dependent manner such as CCL2, CCL4, CCL5, CCL8, CXCL8 and CXCL10 (Bernatoniene et al., 2008; Dogan et al., 2011). Other *in vitro* models have also shown PLY-dependent production of TNF α and IL-1 α/β in a caspase-1, NLRP3-dependent manner (Houldsworth et al., 1994; Shoma et al., 2008). Pneumolysin has also been shown to enhance the production of IL-12, IL-23, IL-6, IL-1 α and IL-1 β , TNF α , IL-17A and IFN γ in response to various TLR ligands (McNeela et al., 2010). Production of nitric oxide in macrophages is induced by TNF- α , IL-1 β and LPS in synergy with IFN- γ , PLY has been shown to induce these cytokines and to induce nitric oxide in production in macrophages in an IFN- γ -dependent manner (Braun et al., 1999).

1.6.5 Interaction with the cell cytoskeleton, a mechanism for antigen uptake?

An interesting feature of PLY adjuvanticity is that antibody responses will not be generated towards the target antigen unless it is physically coupled to the toxin i.e. there is no by-stander effect. In the PATH project this was achieved genetically by creating fusion proteins of PLY/ Δ 6PLY and target antigens. The absence of a by-stander effect indicates that PLY mediates antigen uptake through direct contact with the cell, and that genetically coupled antigens are pulled into the cell, processed and presented along with PLY, whereas non-

coupled antigens are not taken up by the cell. The mechanism of PLY uptake/internalization is not well understood, it is unclear whether PLY is actively taken into the cell or whether the formation of pores allows PLY to pass through the membrane. However, increased endocytic activity and presence of cytoplasmic vacuoles had been observed in response to PLY treatment (Hirst et al., 2002). Additionally, there is strong evidence that PLY can interact directly with the cell cytoskeleton, further investigation of this interaction could lead to discovery of an uptake mechanism.

The changes in cell morphology have been attributed to PLY-induced changes to the actin cytoskeleton. At sublytic concentrations rearrangement of the actin cytoskeleton and microtubule stabilization (as indicated by increased acetylation and bundling) can be observed in astrocytes (Förtsch et al., 2011; Iliev et al., 2009). Although these effects were seen in the absence of observable pores, pore forming competency was required and non-lytic mutants did not induce these cytoskeletal changes. Cholesterol was also required for microtubule stabilization as these effects were abolished in cholesterol-depleted cells and when using cholesterol-treated PLY. This suggested that PLY must be bound to the cell surface in order to induce these effects. Recently, the mechanism of PLY-dependent cytoskeletal remodelling has been further elucidated, it has been shown that PLY has the ability to directly bind actin in vitro. Domains 123 and full length PLY bind strongly to actin, the non-lytic deletion mutant $\Delta 6$ PLY has comparatively reduced binding activity suggesting that the refolding and/or conformational changes that occur in D123 during pore formation are required for actin binding (Hupp et al., 2013).

1.6.6 The neutrophil response to pneumolysin

Rapid neutrophil infiltration occurs during bacterial pneumonia, this is both essential for protection and implicated in its pathogenesis (Craig et al., 2009). The chemotaxis and transendothelial migration of neutrophils during pneumococcal pneumonia is dependent on PLY (Moreland & Bailey, 2006) as are many of the subsequent inflammatory responses of recruited neutrophils. The

neutrophil response to PLY is well documented and various proinflammatory factors are induced or upregulated.

PLY induces activation of NF κ B and subsequent synthesis and release of IL-8 in a Ca²⁺-dependent manner (Cockeran et al., 2002; Fickl et al., 2005), thus creating a positive feedback loop for additional neutrophils recruitment. Neutrophils are exquisitely sensitive to PLY and calcium flux occurs even at apparently sublytic (≤ 100 ng/ml) concentrations of PLY, calcium flux does not occur in neutrophils treated with the non-lytic deletion mutant $\Delta 6$ PLY. The flux of Ca²⁺ is a prerequisite for most neutrophil responses to PLY which include production of the anti-microbial peptides prostaglandin E₂, Leukotriene B₄ and phospholipase A₂ (Cockeran et al., 2001). PLY also induces increased superoxide production and release of elastase in neutrophils activated with the chemotactic tripeptide FMLP (N-formyl-methionine-leucine-phenylalanine) (Cockeran et al., 2001). PLY is known to strongly induce production of neutrophil chemoattractants KC and IL-8, interestingly there is thought to be a positive feedback loop/crosstalk between Th17 cells and neutrophils, where each cell type is capable of recruitment and/or activation of the other (Pelletier et al., 2010). Given the cytokine profile induced by PLY, the essential role of Th17 cells in preventing pneumococcal colonization and the role of neutrophils in pneumococcal infection, it could be possible that PLY induces Th17 cellular immunity and the production of neutrophil chemoattractants such as KC in response to PLY deserves further investigation.

1.7 Aims of this study

Pneumolysin stimulates a vast range of responses from host cells, this is further complicated in that these responses are also influenced by the lytic action of PLY, sub-lytic or non-lytic doses provoke different responses. It would not have been possible to investigate all of the biological responses mentioned here and relate them to adjuvant activity in the time-frame allowed. Therefore, combinations of high-throughput and specific investigations were used to try and elucidate the role(s) of a few key features of pneumolysin's interactions with the host. Throughout this project comparisons were drawn between lytic, non-

lytic and truncated versions of PLY in an attempt to assign function to different regions of the toxin and to pore-forming capability.

The supposed interaction of PLY with TLR4 was a particular focus of this project; the aim was to confirm an interaction between PLY and TLR4 and to determine what effect (if any) this had on the cytokines/chemokines selected for analysis. The primary hypothesis of this project was that the increased potency of PLY based vaccines compared to $\Delta 6$ PLY based vaccines (in terms of antibody titres) was due to PLY-dependent IL-1 β production. It was hypothesised that PLY binding to TLR4 would result in upregulation of pro-IL-1 β and that subsequent activation of NLRP3 by pore formation would cleave pro-IL-1 β into its active form. This highly inflammatory cytokine could then result in increased magnitude of response compared to the non-lytic $\Delta 6$ PLY (which cannot form pores and therefore should not activate NLRP3).

As target antigens must be genetically coupled to PLY/ $\Delta 6$ PLY it was hypothesised that a specific uptake mechanism such as receptor mediated endocytosis was involved in vaccine uptake and processing and that this could be elucidated using a high-throughput pull-down method. Direct binding and internalization of PLY and its derivatives was assessed by fluorescence microscopy to try and assign binding and internalisation to a specific region (domains 1-3 or domain 4) of the toxin.

Initial studies into PLY-dependent gene expression were performed to give a comprehensive view of the immune mediators potentially upregulated by PLY (appendix 5). The potential role in adjuvant activity of differentially regulated genes was inferred and comparisons were drawn between PLY-dependent gene expression patterns and those of currently licensed adjuvants. Finally, an *in vivo* immunization model was used to translate the *in vitro* findings into a model for adjuvant activity of PLY.

2. Materials and Methods

2.1 Materials

2.1.1 Chemicals

Unless otherwise stated the chemicals used throughout this project were purchased from Sigma-Aldrich, Gillingham UK, Fisher Scientific, Loughborough UK or Melford, Suffolk UK.

2.1.2 Enzymes

All restriction enzymes and DNA polymerases used in this study were purchased from Promega, Southampton UK.

2.1.3 Protein purification supplies

Pre-packed HisTrap™ HP and HiTrap™ Canto™ Q affinity columns for the purification of His₆ tagged recombinant proteins by nickel-affinity chromatography (NAC) and anion-exchange chromatography (AEC), respectively, were purchased from GE Healthcare, Buckinghamshire UK. Pureproteome™ nickel magnetic beads for the separation of purified His₆ tagged recombinant proteins from their solvents were purchased from Millipore, Watford UK. Halo-link™ resin for the purification of Halo™ tagged recombinant proteins was purchased from Promega UK, Southampton UK.

2.1.4 Antibiotics

The antibiotics described in table 2-1 were used for the selection of positive clones following bacterial transformation as well as routinely to maintain plasmid presence in transformed strains. The antibiotics described in table 2-2 were used routinely to prevent microbial contamination of cultured mammalian cells as well as for plasmid maintenance in stable mammalian reporter cell lines.

Table 2-1 List of antibiotics, preparation guidelines and storage conditions.

Antibiotic	Stock Conc.	Working Conc.	Solvent	Storage
Ampicillin	100mg/ml	100µg/ml	dH ₂ O	-20 °C
Erythromycin	100mg/ml	1mg/ml	EtOH	-20 °C
Kanamycin	50mg/ml	50µg/ml	dH ₂ O	+4 °C to -20 °C

Table 2-2 List of antibiotics for tissue culture, preparation guidelines and storage conditions.

Antibiotic	Stock Conc.	Working Conc.	Solvent	Storage
Blastocidin	10mg/ml	10µg/ml	dH ₂ O	-20 °C
Geneticin/G418	500mg/ml	500µg/ml	dH ₂ O	-20 °C
Penicillin	5000U/ml	50U/ml	PBS	-20 °C
Puromycin	10mg/ml	5µg/ml	dH ₂ O	-20 °C
Streptomycin	5mg/ml	50µg/ml	PBS	-20 °C
Zeocin	100mg/ml	200µg/ml	dH ₂ O	-20 °C

2.2 Bacterial strains and vectors

2.2.1 Storage and growth conditions

E. coli strains were streaked onto Luria Bertani (LB) agar supplemented with the appropriate antibiotic to confirm purity before culturing O/N in LB broth at 37 °C with shaking at 220rpm. Frozen stocks of strains were prepared in 1ml aliquots of appropriate growth media supplemented with 15% vol/vol sterile glycerol and stored at -80 °C.

2.2.2 Bacterial strains

Table 2-3 summarizes the bacterial strains used in this project. *Escherichia coli* strains XL-1 blue and BL21 (DE3) were used for the propagation and storage of plasmid vectors and protein purification respectively.

Table 2-3 Bacterial strain information.

Species	Strain	Genotype	Description	Antibiotic Resistance
<i>E. coli</i>	XL-1 blue	<i>recA1 endA1 gyrA96 thi-1 hsdR17 supE44 relA1 lac [F2 proAB lacIqZ\otimesM15 Tn10 (Tetr)]</i>	Ideal host for long-term storage and propagation of plasmid vectors.	None
<i>E. coli</i>	BL21 (DE3)	<i>E. coli B F ompT hsdS_B(r_B⁻ m_B⁻) gal dcm λ(DE3)</i>	General protein expression host. Expression controlled by <i>lac</i> promoter.	None

2.2.3 Vectors

2.2.3.1 pET33b

pET33b is a commercially available plasmid vector (Novagen, UK) and was used for the expression and purification of recombinant His₆ tagged proteins. This vector contains His₆ sequences adjacent to the multiple cloning site allowing proteins to be tagged at either the N- or C-terminus. Pneumolysin is not amenable to fusion at the C-terminus and so all PLY-fusions were made at the N-terminus. Protein expression is under the control of an inducible T7*lac* RNA polymerase promoter, expression is induced by IPTG.

2.2.3.2 pFN18A HaloTag[®] Flexi[®] Vector

pFN18A is part of the Flexi[®] Vector range (Promega, UK). pFN18A encodes the HaloTag[®] such that it is appended to the N-terminus of the desired protein. The

HaloTag system allows multiple downstream applications such as protein purification, fluorescence microscopy and pull-downs to be performed after creating a single construct. The HaloTag itself is a 33kDa haloalkane dehalogenase derived from a prokaryotic hydrolase (Feature, 2006; Los et al., 2008). Promega have engineered a variety of haloalkane-based ligands that bind covalently to the HaloTag; for example a wide range of fluorochrome-tagged microscopy ligands exist and allow flexibility in protocols for cell localization and interaction studies. The cloning site of pFN18A is shown in figure 2-1. All Flexi[®] Vectors have a cloning site flanked by the rare restriction sites SgfI and PmeI, this allows easy interchange of a desired insert from one Flexi[®] Vector to another. A lethal Barnase gene within the cloning site and an ampicillin resistance selection marker allow positive selection of clones. This is designed as a shuttle vector and allows the expression of the desired protein in both *E. coli* and mammalian cells under the control of a T7 RNA polymerase promoter.

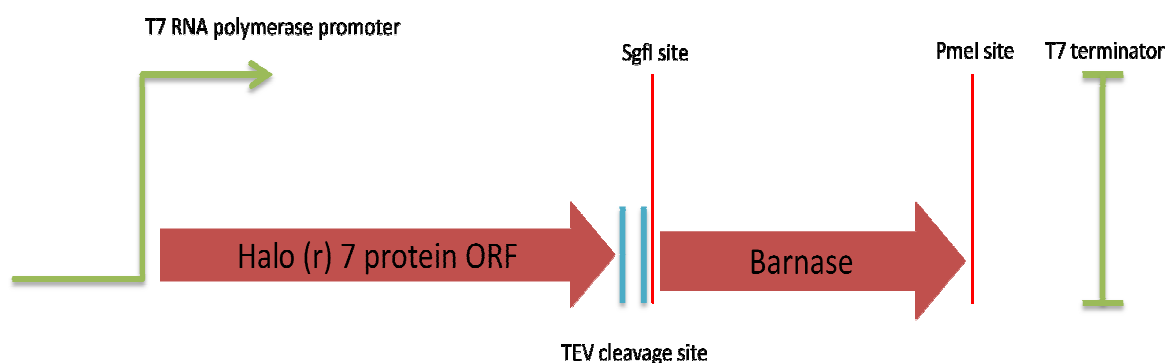


Figure 2-1 Diagram of pFN18A cloning site.

2.2.4 Electrocompetent cells

Electrocompetent cells were generated in-house for the *E. coli* strains XL-1 blue and BL21 as follows.

Under sterile conditions, 500ml of LB was inoculated with 5ml of an overnight culture. Cultures were incubated at 37°C, 200rpm until OD_{600nm} 0.6 was reached. Culture flasks were rapidly chilled on ice before centrifugation at 5000rpm for ten minutes at 4°C. The resulting pellet was washed four times in ice-cold sterile dH₂O by repeated resuspension and centrifugation. Finally, the

pellet was resuspended in 1-2ml of ice-cold sterile dH₂O containing 10% glycerol. The competent cells were aliquoted in 60µl volumes, snap frozen in liquid nitrogen and stored at -80° C until required.

2.3 Molecular cloning

2.3.1 Oligonucleotides

Oligonucleotide primers were purchased from either Sigma Aldrich (UK) or Eurofins MWG Operon (Germany). Oligonucleotides were supplied lyophilized and were reconstituted to 100µM stock concentration in molecular biology grade dH₂O. Oligonucleotides were stored at -20° C until required.

Table 2-4 Oligonucleotide primers.

Name	Description	Sequence
9Y	Forward sequence of pneumolysin in pET 33b(+) [i.e. start of Ply in pET]	CGG GAT CCG GCA AAT AAA GCA GTA AAT GAC TTT
9Z	Reverse sequence of pneumolysin in pET 33b(+) [i.e. end of Ply in pET]	GAC GGA GCT CGA CTA GTC ATT TTC TAC CTT ATC
20G	Amplification of GFP for cloning into pET 33b in frame with the ATG and HisTag. Contains Nhe 1 site and deletes ATG	GTC AGG CTA GCA TGA GTA AAG GAG AAG AAC
20H	Amplification of GFP for cloning into pET33b. Contains Bgl 11 site (compatible with Bam HI). Also in frame with HisTag (c-term) and stop	CCA CGC AGA TCT TTG TAT AGT TCA TCC
23B	Binds to bases 415-466 of Ply gene Introduces DA146R147 within Ply gene	GGT CAA TAA TGT CCC AAT GCA GTA TGA AAA AAT AAC GGC TC
23C	Reverse and compliment of LK6 (forward)	GAG CCG TTA TTT TTT CAT ACT GCA TTG GGA CAT TAT TGA CC

Table 2-4 continued		
48I	Amplification of PLY domains 1-3 for cloning into pET33b - ends at VTAYRN then adds a stop codon. SacI site	GACGGAGCTCGACTAGTTT CTGTAAGCTGTAAC
52Q	From: Suzuki et al. 2005. Discrimination of Streptococcus pneumoniae from Viridans Group Streptococci by Genomic Subtractive Hybridization. J. Clin. Microbiol. 43: 4528-4534.	ATTTCTGTAACAGCTACCAA CGA
52R	From: Suzuki et al. 2005. Discrimination of Streptococcus pneumoniae from Viridans Group Streptococci by Genomic Subtractive Hybridization. J. Clin. Microbiol. 43: 4528-4534.	GAATTCCTGTCTTTTCAA GTC
62P	Halo seq for	CCTGCCTAACTGCAAGGCTG
62Q	Halo seq rev	CAGCAGCCAACTCAGCTTCC
62R	Halo ply for	TAACGCGATCGCCATGGCAAAT AAAGCAGTAAATGAC
62S	Halo ply rev	TTCGTTTAAACCTAGTCATTTT CTACCTTATCC
62T	Halo d123 rev stop	ATTCGTTTAAACCTATCTGTAA GCTGTAACCTTA
62U	Halo D4 for	TAACGCGATCGCCTACAGAAAC GGAGATTTACTGCT
62V	Halo egfp for	GTCGCGATCGCCATGAGTAAAG GAGAAGAACTTTTC
62W	Halo egfp rev	GTTTAAACGACGGATCTTTGTA TAGTTCATCC

2.3.2 Polymerase chain reaction (PCR)

In this study PCR was used for the amplification or mutagenesis of target genes for molecular cloning as well as for screening subsequent bacterial colonies following transformation. The proof-reading enzyme *PfuUltra* II fusion high fidelity polymerase (Stratagene, Cheshire UK) was used to amplify targets for molecular cloning and to perform Site-directed Mutagenesis. Bacterial colony screening by PCR was performed using GoTaq DNA polymerase (Promega, Southampton UK). Reactions were performed according to the manufacturer's instructions; typical PCR conditions are detailed below.

2.3.2.1 Typical PCR conditions using GoTaq standard fidelity DNA polymerase

Table 2-5 GoTaq PCR mix
Reaction Component Volume Required

DNase/RNase free dH ₂ O	up to 50µl
5 x GoTaq green reaction buffer	10µl
dNTPs (10mM)	1µl
for primer (10µM)	1µl
rev primer (10µM)	1µl
DNA template	<0.5µg total/xµl
GoTaq DNA polymerase	0.5µl
Total reaction volume	50µl

Table 2-6 GoTaq PCR cycling conditions
Step Temperature Time No. of Cycles

Initial denaturation	95°C	2 minutes	1x
Melting	95°C	30 seconds	
Annealing	42-65°C	30 seconds	30x
Extension	72°C	1 minute/kb	
Final Extension	72°C	5 minutes	1x
Soak	4°C	Indefinite	1x

2.3.2.2 Typical PCR conditions using *PfuUltra II* fusion HS high fidelity DNA polymerase

Table 2-7 *PfuUltra II* PCR mix

Reaction Component	Volume Required
DNase/RNase free dH ₂ O	up to 50µl
5 x GoTaq green reaction buffer	10µl
dNTPs (10mM)	1µl
<i>for primer</i> (10µM)	1µl
<i>rev primer</i> (10µM)	1µl
DNA template	<0.5µg total/xµl
GoTaq DNA polymerase	0.5µl
Total reaction volume	50µl

Table 2-8 *PfuUltra II* PCR cycling conditions

Step	Temperature	Time	No. of Cycles
Initial denaturation	95°C	2 minutes	1x
Melting	95°C	30 seconds	30x
Annealing	42-65°C	30 seconds	
Extension	72°C	1 minute/kb	
Final Extension	72°C	5 minutes	1x
Soak	4°C	Indefinite	1x

2.3.3 Agarose gel electrophoresis

Agarose gel electrophoresis was used to visualise PCR products and separate products from restriction digests for further purification. Typically, 0.3µg of 1kbp+ DNA standard (Invitrogen, Paisley UK) and 10µl of PCR product or 50µl of a restriction digest reaction were run on a 0.8% w/v agarose gel in 1x Tris-Acetate-EDTA (TAE) buffer at 100 V for 20 minutes. The UVPro Gold gel-documentation system (UV Tech) was used to visualise and image gels.

2.3.4 Plasmid purification

The QIAspin miniprep kit (Qiagen) was used according to the manufacturer's instructions to purify plasmid DNA from O/N cultures of transformed bacteria.

2.3.5 Restriction digest

The conditions of restriction digests varied throughout this project and are described in more detail in section 2.4.

2.3.6 Gel extraction and PCR product purification

Following restriction digest the resulting DNA segments were separated by agarose gel electrophoresis and extracted from the gel using the Qiagen QIAquick gel extraction kit. PCR products to be used in downstream reactions were purified from their PCR mix using the SV Wizard PCR purification kit (Promega, UK). Where possible, gel extraction was avoided to reduce loss of digest products; digestion of pET33b constructs with *NheI* and *BglII* results in 6 undesirable base pairs, these can be separated from the desired product using a PCR clean-up protocol resulting in increased yield compared to gel extraction.

2.3.7 Ligation

T4 DNA ligase (Promega, UK) was used to ligate DNA fragments for ligation dependent cloning. The molecular ratio of vector to insert was 1:3 for cloning with "sticky ends" or 1:10 for blunt end cloning. Typically, 2µl of T4 DNA ligase and 2µl of 10X DNA ligase buffer were added to a reaction with a 20µl final volume. Reactions were incubated at room temperature for 4hrs before heat

inactivation at 65°C for 10min. 5µl of the ligation reaction was used for transformation into electrocompetent XL-1 blue *E. coli*.

2.3.8 Bacterial transformation

Electrocompetent *E. coli* were transformed with plasmid DNA using the Bio-rad gene pulser electroporation system. Briefly, 100µl of electrocompetent cells were allowed to thaw on ice, 5µl of salt-free plasmid DNA was added to the cells and incubated on ice for 20min. The mix was transferred to a pre-chilled 0.2cm gap electroporation cuvette and pulsed at 2.5kV. Following electroporation 200µl of SOC medium was quickly added to the cuvette and the mixture was transferred to a 1.5ml microcentrifuge tube. The transformed cells were incubated at 37°C at 220rpm for 1hr then plated onto selective LB. The plates were incubated overnight at 37°C.

2.4 Construction of plasmids

2.4.1 pET33bPLY: PLY derivatives and eGFP.

At the beginning of this work multiple PLY mutants had been constructed by previous researchers in the Mitchell group (see table 2-9). Figure 2-2 describes the regions of the toxin that are amplified for cloning and the region containing the delta 6 mutation. These mutants will allow the biological properties of PLY to be assigned to different regions of the toxin as well as differentiating between pore-dependent and independent interactions with the host. For the majority of PLY mutants fusion proteins also existed, where eGFP was fused to PLY and its derivatives; eGFP serves as both a model antigen and tool to examine PLY localisation and interactions with the host. In these studies PLY and PLY mutants were purified from existing constructs and several new constructs were created in the pET33b expression system, these are all listed in table 2-9.

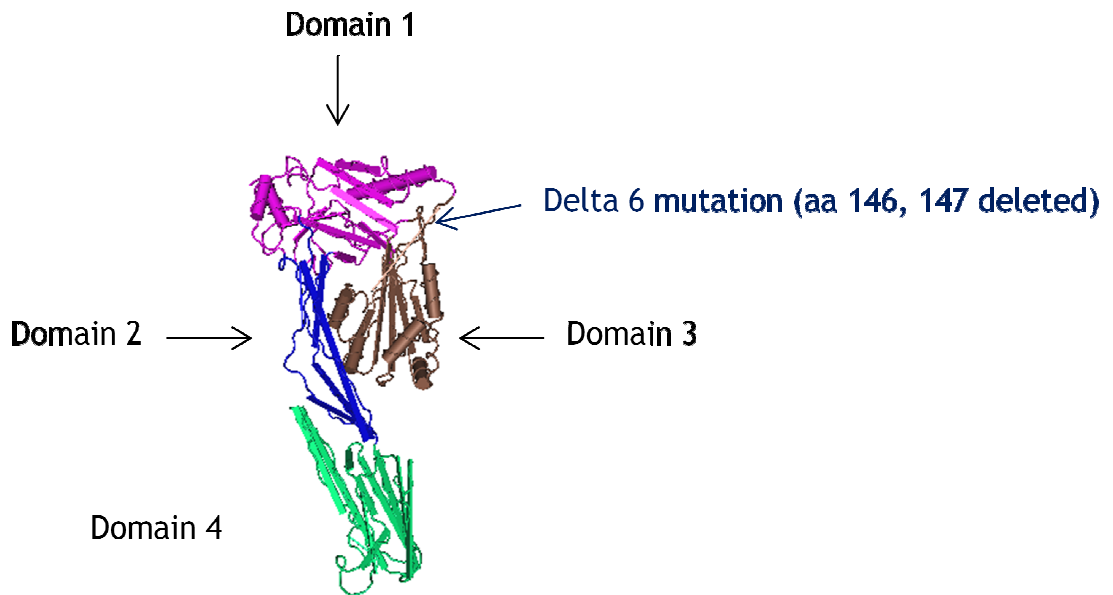


Figure 2-2 Mutation and truncation of pneumolysin.

As previously mentioned domain 1 (residues 6-21, 58-147, 198-243, 319-342), domain 2 (residues 22-57, 343-359) and domain 3 (residues 148-197, 244-318) are physically inseparable. The delta 6 mutation which renders PLY non-toxic is achieved by deleting residues 146 and 147 within domain 1 (directly before a stretch of domain 3). Domain 4 (residues 360-469) can be purified separately from the other domains.

Table 2-9 pET33b constructs available for use

Name of construct	Origin	Description
pET33b-PLY	Graeme Cowan	His ⁶ tagged full-length lytic PLY
pET33b- Δ 6PLY	Lea-Ann Kirkham	His ⁶ tagged full-length non-lytic PLY
pET33b-D123PLY	Graeme Cowan	His ⁶ tagged truncation mutant of domains 1, 2 and 3 of PLY
pET33b- Δ 6D123PLY*	Catherine Dalziel (Author)	His ⁶ tagged truncation mutant of domains 1, 2 and 3 of PLY with the Δ 6 mutation (aa146-147 removed)
pET33b-D4PLY	Graeme Cowan	His ⁶ tagged truncation mutant of domain 4 of PLY
pET33b-eGFPPLY	Graeme Cowan	Full-length lytic PLY tagged with both His ⁶ and eGFP
pET33b-eGFP Δ 6PLY	Jiang Tao Ma	Full-length non-lytic PLY tagged with both His ⁶ and eGFP
pET33b-eGFPD123PLY	Jiang Tao Ma	Truncation mutant of domains 1,2 and 3 of PLY tagged with both His ⁶ and eGFP
pET33b-eGFP Δ 6D123PLY*	Catherine Dalziel (Author)	Truncation mutant of domains 1,2 and 3 of PLY, with the Δ 6 mutation and tagged with both His ⁶ and eGFP
pET33b-eGFPD4PLY	Jiang Tao Ma	Truncation mutant of domain 4 PLY tagged with both His ⁶ and eGFP
pET33b-eGFP	Graeme Cowan	His ⁶ tagged enhanced Green Fluorescent Protein only

2.4.1.1 pET33b- Δ 6D123

The major difference in activity between PLY and Δ 6PLY is, of course, lack of cytolytic activity; however, it was not known whether the Δ 6 mutation had also introduced other deviations in function. To address this, a D123PLY mutant containing the Δ 6 mutation was constructed; this removed the confounding issue of pore formation from comparisons. A ligation-dependent cloning strategy was

used for the construction of pET33b- Δ 6D123. Primers 9Y and 48I were used to amplify domains 1-3 from pET33b Δ 6PLY adding *Bam*HI and *Sac*I sites, respectively (figure 2-3).

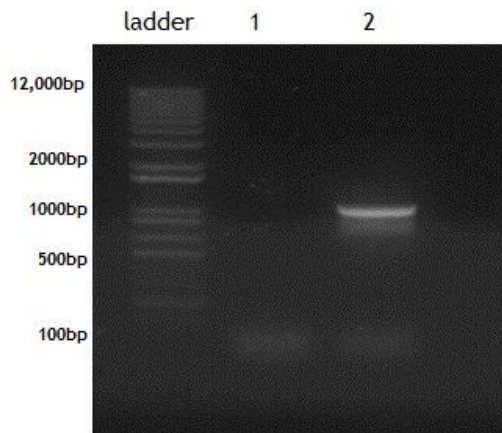


Figure 2-3 DNA insert Δ 6D123PLY.

Primers 48I and 9Y were used to amplify domains 1-3 from pET33b- Δ 6PLY creating a 1101bp PCR product (lane 2) for insertion into pET33b. Lane 1 shows the negative control. Following PCR amplification of the insert using GoTaq PCR mastermix (Promega), 10 μ l of the PCR and control were loaded into a 0.8% agarose gel and electrophoresed at 100 V for 20 minutes. PCR products were visualised using the UVPro Gold gel-documentation system (UV Tech).

The resulting PCR product and the vector pET33b were subjected to a 3 hour double digest at 37°C with *Sac*I and *Bam*HI. The digested products were cleaned and ligated using T4 DNA ligase at a molecular ratio of 3:1 (insert:vector) for 4 hours at room temperature. XL-1 blue electrocompetent *E. coli* were transformed with 3 μ l of the ligation reaction and plated onto LB agar plates containing 50 μ g/ml kanamycin. Positive colonies were screened by PCR for the presence of the insert using primers 9Y and 48I before storage as glycerol stocks (figure 2-4).

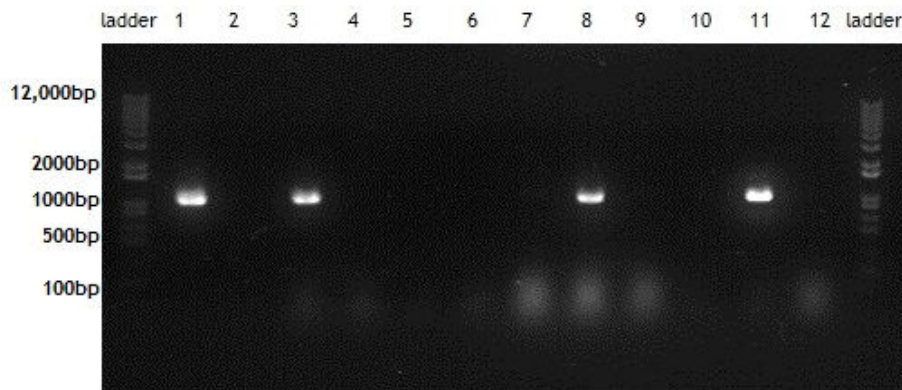


Figure 2-4 Colony screening PCR.

Following transformation of XL-1 blue *E. coli* with pET33b- Δ 6D123PLY any resulting colonies were screened for the presence of the insert using primers 48I and 9Y. Following PCR amplification of the insert using GoTaq PCR mastermix (Promega), 5 μ l of the PCR and control were loaded into a 0.8% agarose gel and electrophoresed at 100 V for 20 minutes. PCR products were visualised using the UVPro Gold gel-documentation system (UV Tech). Lanes 3, 8 and 11 are positive and give a band of 1101bp, identical to that of the positive control (lane 1, pET33b-D123PLY template).

The new plasmid sequence was verified by Sanger sequencing at the Source Biosciences facility in Nottingham. Following confirmation of sequence the new construct was then used to transform *E. coli* BL21 cells for protein expression and purification.

2.4.1.2 pET33b-eGFP Δ 6D123PLY

Site-directed mutagenesis was employed to create an eGFP-tagged version of Δ 6D123PLY in pET33b. The mutagenic primers 23B and 23C were used to create the Δ 6 deletion mutation in pET33bD123PLY. The SDM protocol was followed as detailed in section 2.3.2, following mutagenesis parental DNA template was removed by digestion with *DpnI* at 37°C for 1 hour. XL-1 blue electrocompetent *E. coli* were transformed with 3 μ l of the ligation reaction and plated onto LB agar plates containing 50 μ g/ml kanamycin. Positive colonies were screened by PCR for the presence of the insert using primers 9Y and 48I plus 20G and 20H before storage as glycerol stocks. The new plasmid sequence was verified by Sanger sequencing at the Source Biosciences facility in Nottingham. Following confirmation of sequence the new construct was then used to transform *E. coli* BL21 cells for protein expression and purification.

2.4.2 pFN18A: PLY derivatives and eGFP.

To construct HaloTagged versions of PLY, $\Delta 6$ PLY, D123PLY, $\Delta 6$ D123PLY, D4PLY and eGFP in the vector pFN18A the manufacturer's (Promega, UK) ligation-dependent cloning strategy was followed. The primers, templates and creators of the pFN18A constructs are detailed in table 2-2. Briefly, target genes were amplified using primers designed to append *SgfI* and *PmeI* sites to the target, both the PCR product and acceptor vector (pFN18A) were digested with *SgfI* and *PmeI* at 37°C for 30 minutes. The digest reactions were inactivated by incubation at 65°C for 10 minutes, the PCR product was cleaned but the vector digest was not. Digested insert and vector were ligated at a molecular ratio of 10:1 (insert: vector) using T4 DNA ligase at room temperature for 1 hour. XL-1 blue electrocompetent *E. coli* were transformed with 3 μ l of the ligation reaction and plated onto LB agar plates containing 100 μ g/ml ampicillin. Positive colonies were screened by PCR for the presence of the insert before storage as glycerol stocks. The new plasmid sequence was verified by Sanger sequencing at the Source Biosciences facility in Nottingham. Following confirmation of sequence the new construct was then used to transform *E. coli* BL21 cells for protein expression and purification.

Table 2-10 Table of primers and DNA templates used to clone PLY and its derivatives into pFN18A.

Construct Name	PCR Template	PCR Primers	Constructed By
pFN18A-PLY	pET33b-PLY	62R and 62S	Jiang Tao Ma
pFN18A-Δ6PLY	pET33b- Δ6PLY	62R and 62S	Catherine Dalziel (author)
pFN18A-D123	pET33b-D123	62R and 62T	Freiderike Vollmer/Catherine Dalziel (author)
pFN18A-Δ6D123	pET33b- Δ6D123	62R and 62T	Catherine Dalziel (author)
pFN18A-D4	pET33b-D4	62S and 62U	Freiderike Vollmer/Catherine Dalziel (author)
pFN18A-eGFP	pET33b-eGFP	62V and 62W	Catherine Dalziel (author)

2.5 Protein expression and purification

2.5.1 Protein expression in *E. coli* BL21 (DE3)

Proteins of interest were expressed in BL21 (DE3) *E. coli* cells transformed with the required plasmid (see tables 2-9 and 2-10). Typically, 4 x 1L flasks of LB broth containing 50μg/ml kanamycin were inoculated with 10ml of an O/N culture of transformed BL21 cells. The cultures were incubated at 37°C with shaking at 220rpm until an OD_{600nm} of 0.8-1 was reached. Protein expression was induced by the addition of Isopropyl-β-D-thio-galactopyranoside (IPTG) to a final concentration of 1mM. The cultures were grown for a further 6hr at 30°C with shaking before harvesting the cells by centrifugation at 5000rpm for 30min at 4°C. Cell pellets were stored at -20°C until required for protein purification.

2.5.2 Lysate preparation

Frozen culture pellets were resuspended in 10mls (per L of culture) of ice-cold PBS supplemented with 300 units of DNase I (Sigma-Aldrich, Gillingham UK) and 1 complete protease inhibitor tablet, EDTA-free (Roche, Welwyn UK). The bacterial cell suspension was passed through the One Shot Cell Disruptor (Constant Systems, Warwick UK) and the resultant lysates were centrifuged at 13000rpm for 30 mins to pellet cell debris. Lysates were sterilized by passing through a 0.22µm syringe filter (Sartorius, Hannover Germany) to remove any whole bacteria or remaining cell wall debris.

2.5.3 Purification of His-tagged Proteins

2.5.3.1 Nickel-affinity chromatography (NAC)

Using a peristaltic pump, a 5ml HisTrap™ HP affinity column was washed with sterile dH₂O then packed with 0.2M nickel sulphate solution. The column was washed again with PBS before loading with filtered lysate (section 2.5.2.1). A final wash with PBS removed unbound proteins from the column. The AKTA-PrimePlus system was used to remove His-tagged proteins from the column. Using a pre-programmed His-tag gradient elution programme, increasing concentrations of imidazole were used to compete with his-tagged proteins for binding space on the column. As the concentration of imidazole increases His-tagged proteins are removed from the column into collection tubes (fractions). The AKTA-PrimePlus analysis software uses UV spectrophotometry to indicate fractions that contain eluted protein; these fractions were electrophoresed on an SDS-PAGE gel, stained with coomassie and destained. Figure 2-5 shows an example of NAC purification of Δ6D123PLY. The fractions that contained the most protein with the fewest contaminating bands on the gel were then selected for dialysis at 4°C O/N in anion-exchange chromatography (AEC) start buffer.

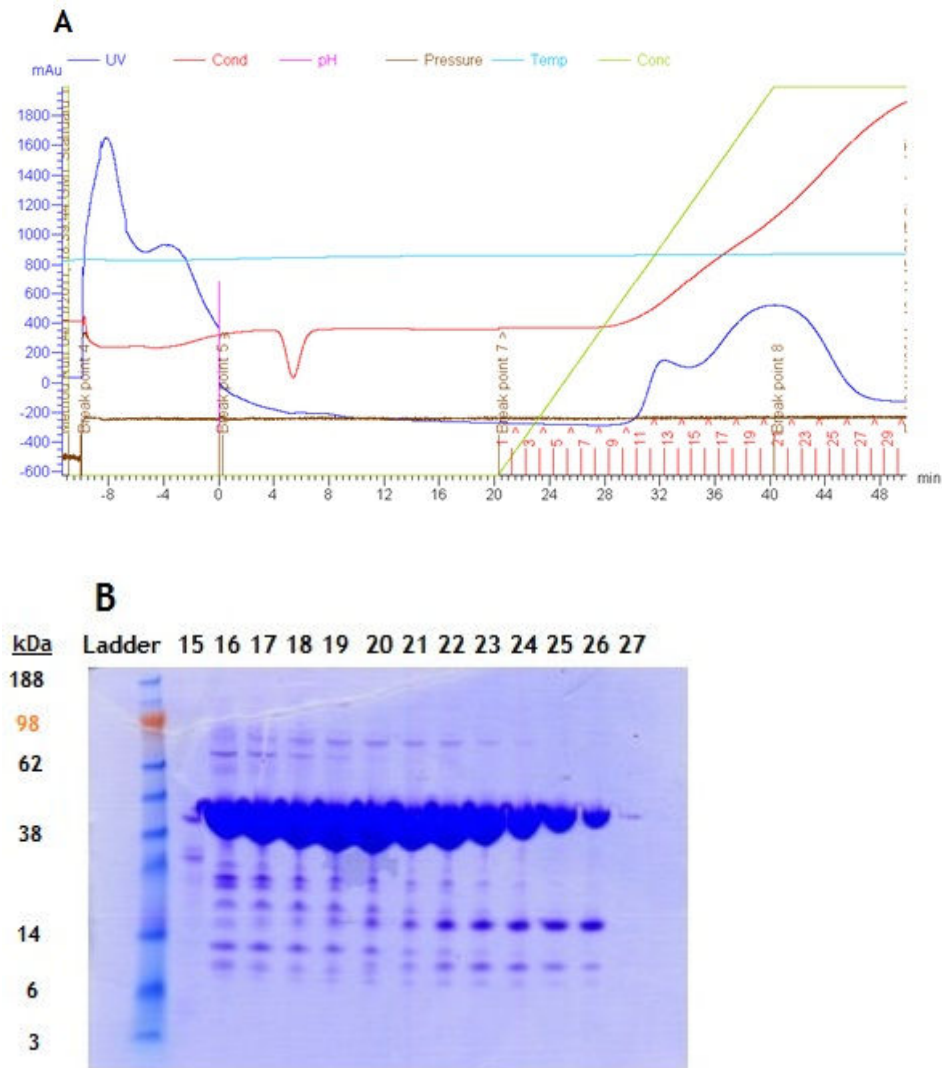


Figure 2-5 Example purification of $\Delta 6D123PLY$ by NAC.

The Akta PrimePlus UV absorption trace (A) indicated that $\Delta 6D123PLY$ was eluted from the HisTrap column into fractions 16-26. The peaks shown in fraction 11-14 routinely appear and are always identified as contaminants. To check for the presence of $\Delta 6D123PLY$, fractions 15-27 were analysed by SDS-PAGE (B). Fraction samples were diluted 1:5 in sample buffer and 10 μ l of each was loaded into a 10%SDS-PAGE gel, the fraction proteins were separated by electrophoresis at 180 V for 40 minutes and the gel was stained with coomassie blue.

2.5.3.2 Anion-exchange chromatography (AEC)

Following nickel-affinity chromatography proteins were further purified by anion-exchange chromatography. A peristaltic pump was used to load proteins purified by NAC onto a 1ml HiTrap™ Capto™ Q affinity column, to ensure the entire sample had been passed through the column a final wash with 15mls of AEC start buffer was performed. The Akta-PrimePlus system was utilised again, this time using the pre-programmed anion exchange Capto Q gradient. As with

NAC, fractions containing eluted protein were analysed by SDS-PAGE (figure 2-6(B)). The purest fractions were pooled and dialysed twice in a 50-fold volume of sterile PBS at 4 °C for 24hrs.

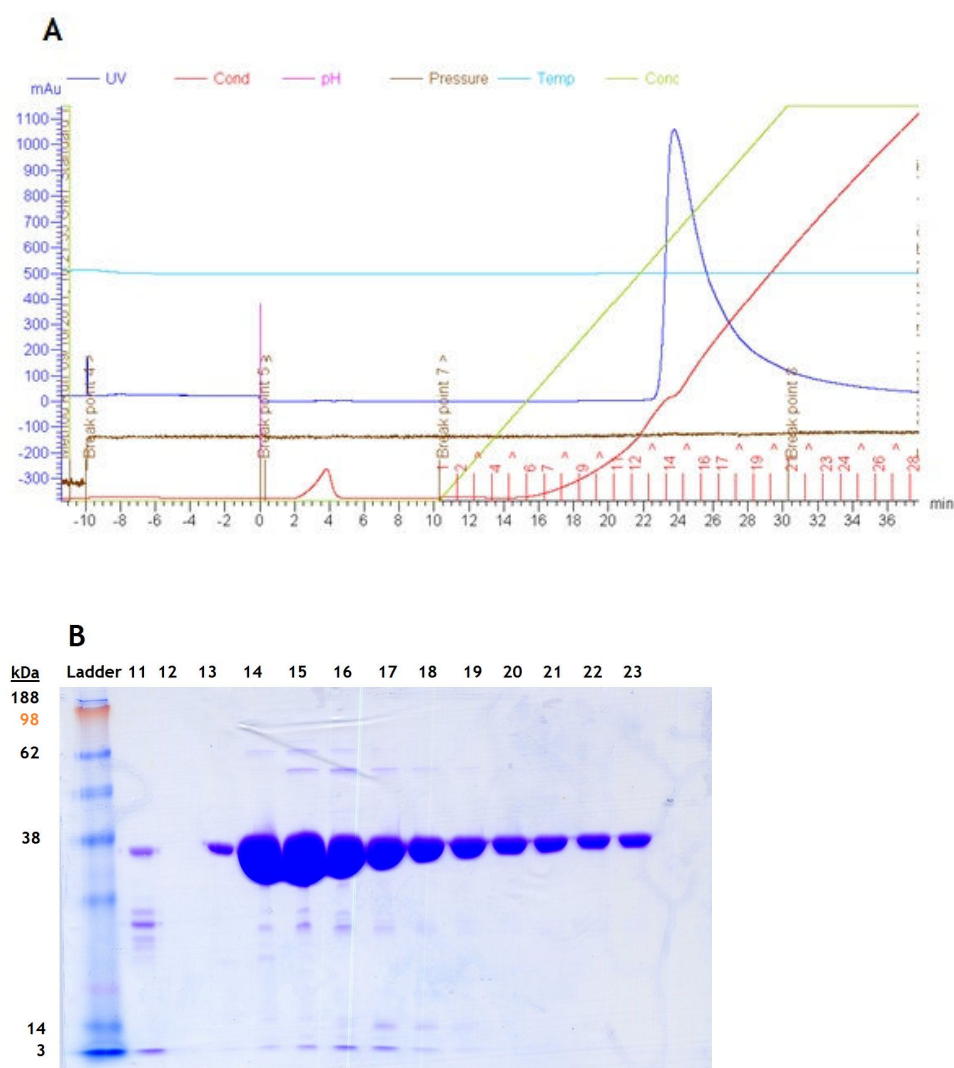


Figure 2-6 Example purification of $\Delta 6D123PLY$ by AEC.

The Akta Primeplus UV absorption trace (A) indicated that $\Delta 6D123PLY$ was eluted from the HiTrap Capiro column into fractions 13-23. Fractions 11-23 were analysed for the presence of $\Delta 6D123PLY$ by SDS-PAGE (B). Fraction samples were diluted 1:5 in sample buffer and 10 μ l of each was loaded into a 10%SDS-PAGE gel, the fraction proteins were separated by electrophoresis at 180 V for 40 minutes and the gel was stained with coomassie blue.

Following dialysis purified proteins were concentrated using Amicon ultra centrifugal filters (Millipore, Watford UK) with an appropriate molecular weight cut-off. Purified proteins were aliquoted and stored at -20 °C for further analysis.

2.5.4 Purification/Isolation of HaloTagged Proteins

Although the HaloTag can also be used for protein purification the covalent binding of the HaloTag to Halo-link resin requires cleavage of the desired protein from the tag using TEV protease. If desired, the proteins could be purified by size-exclusion chromatography but for the purposes of this study whole bacterial cell lysates were deemed suitable. Lysates were obtained from BL21 cells expressing HaloTagged proteins as described in sections 2.5.1 and 2.5.2.

2.6 Analysis of Isolated proteins

2.6.1 SDS-PAGE and western blotting

SDS-PAGE and western blotting were used to check for the presence and purity of recombinant proteins, figure 2-7 shows an example analysis of $\Delta 6D123PLY$. SDS-PAGE gels were either purchased as pre-cast 4-12% gels (Invitrogen, Paisley UK) or cast using the Bio-Rad mini protean system with a 10% resolving gel and a 4% stacking gel (appendix).

Samples were diluted in 5 X SDS-PAGE sample buffer (see appendix) and denatured at 70°C for 20min. 10 μ l of sample and 5 μ l Seeblue® Plus 2 pre-stained molecular weight marker were loaded onto the gel. The gel was electrophoresed at 180v for 40min then stained with coomassie R250 stain, destain was applied several times to remove excess stain followed by several washes of dH₂O to obtain a clear background. Alternatively, silver staining was performed using the SilverQuest™ kit (Invitrogen). Silver staining can detect as little as 0.3ng of protein and was used to detect proteins of low abundance.

Western blotting was performed using SDS-PAGE gels prepared as above, instead of performing a coomassie stain the proteins were transferred onto a Hybond-C nitrocellulose membrane (Amersham biosciences, Buckinghamshire UK) using an Xcell™ blot module (Invitrogen, UK) at 30v for 1hr. The membranes were blocked at 4°C in 3% skimmed milk overnight. After blocking, the membranes were washed x 4 in 0.05% PBS-Tween™ and incubated with the primary antibody for 3hrs at 37°C with shaking. The membranes were washed again and

incubated with the secondary antibody for 1hr at 37°C with shaking. After a final wash step the membranes were developed by enhanced chemiluminescence (ECL) (Millipore, UK) following the manufacturer's instructions. Alternatively, membranes were developed using 4-chloronaphthol developer (see appendix).

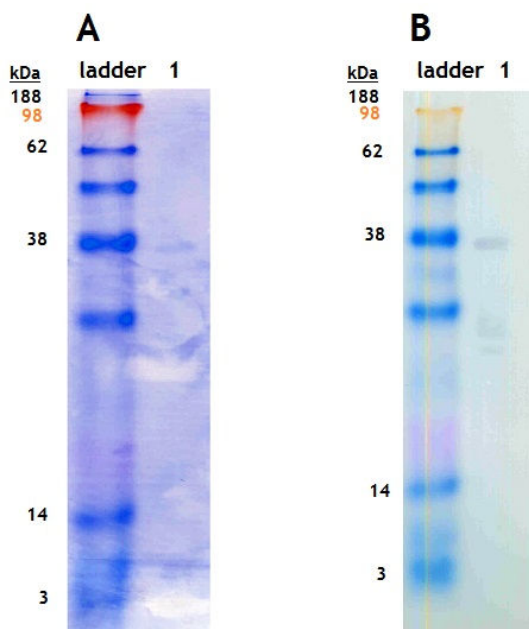


Figure 2-7 Analysis of purified protein by SDS-PAGE and western blotting.

SDS-PAGE of purified $\Delta 6D123PLY$ (A) and corresponding western blot using rabbit anti-PLY developed using 4-chloronaphthol (B). Purified $\Delta 6D123PLY$ was diluted to 1mg/ml and mixed 1:5 with SDS-PAGE loading buffer. 5 μ l of Seeblue Plus 2 molecular weight marker and 10 μ l of the protein were loaded into the wells of a 10% SDS-PAGE gel and electrophoresed at 180 V for 40 minutes. The proteins were transferred onto nitrocellulose membrane and detected by western blotting using rabbit anti-PLY (1:1000) and donkey anti-rabbit-HRP (1:2000). The blot was developed using 4-chloro 1-naphthol.

2.6.2 Haemolytic assay

The haemolytic activity of PLY and its derivatives was measured by haemolytic assay. Briefly, 50 μ l of PBS was added to each required well of a round-bottomed 96-well plate, purified PLY of a known concentration was diluted 1/1000 and 50 μ l of this was added to the plate in duplicate, serial dilutions of PLY were performed along both rows. This step was repeated with test samples of either purified protein (diluted 1/1000) or bacterial lysates (1/5 dilution). 50 μ l of 10mM DTT was added to each well before incubating the plate at 37°C for 15-30min. 1ml of sheep blood was washed by centrifugation at 13000rpm for 1min, the supernatant was removed and replaced with PBS and the process repeated

until the supernatant was clear. The blood was then used to prepare a 2% erythrocyte solution; 50µl of this solution was added to each well. The plate was incubated at 37°C for a further 30min. After incubation 50µl PBS was added to each well and the plate as centrifuged at 1000rpm for 1min. 100µl of supernatant was transferred from each well to a flat-bottomed 96-well plate and the absorbance at 540nm was measured. Figure 2-8 shows an example haemolytic assay using purified PLY.

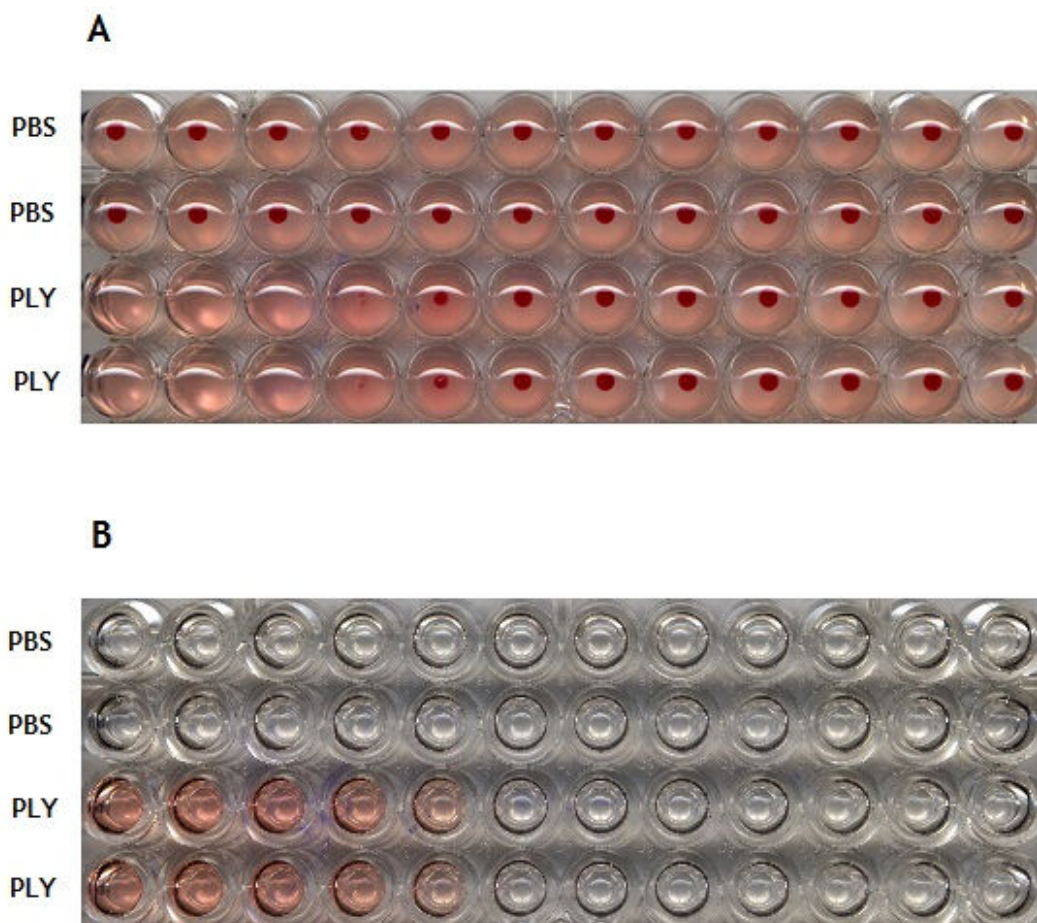


Figure 2-8 Example haemolytic assay.

Sheep erythrocytes were treated with either PBS or serial dilutions of PLY (1µg/ml starting conc.) in duplicate for 30 mins. 50µl of purified PLY (1µg/ml) and 50µl of PBS was added in duplicate to the first wells of a 96-well plate and serially diluted (1:2) horizontally across the plate. Following incubation with a 2% sheep RBC solution for 30 minutes the plate was centrifuged at 1000rpm for 1 min, intact erythrocytes were visible as pellets (A). Released haemoglobin from lysed erythrocytes was analysed by measuring the absorbance at 540nm of cell supernatants using a Fluostar Optima plate reader (B).

The absorbance data from haemolytic assays were used to calculate % lysis for each test using the calculation:

$$\text{Percentage lysis} = ((X-Y)/(Z-Y))*100$$

Where X = the A540 for the sample, Y = the background A540 and Z = the A540 from a positive control sample (i.e. 100 lysis).

By plotting % lysis values against log toxin concentration the specific activity in HU/pmol of a sample can be calculated.

2.6.3 Determination of protein concentration

2.6.3.1 Lysates

Total protein concentration of lysates was measured by Bradford assay. Briefly, protein standards were prepared by diluting a 2µg/ml solution of bovine serum albumin (BSA) in PBS as described in table 2-11.

Table 2-11 Preparation of Protein standards for Bradford Assay

Final BSA Concentration (µg/ml)	Volume of BSA (2µg/ml) required (µl)	Volume of PBS required (µl)
1500	75	25
1000	50	50
750	33	67
500	25	75
250	12.5	87.5
125	6.25	93.75
62.5	3.12	96.83
0	0	100

10µl of both standards and test solutions were added in duplicate to a flat-bottomed 96-well plate, 200µl of Bradford reagent (Sigma) was added to each well and incubated for 5-60 minutes. The A570 of each well was determined using the BMG fluostar Optima. The protein concentration of samples was determined by extrapolating A570 values against the BSA standard curve.

2.6.3.2 HaloTagged Proteins

To assess the concentration of HaloTagged proteins in lysates a TEV cleavage was performed. Briefly, 200µl of lysate was mixed with 100µl of HaloLink resin and incubated at room temperature with rotation for 2 hours. The resin was washed and treated with 100µl of Turbo TEV protease (Geneway, USA) overnight at 4°C. The concentration of cleaved proteins was then measured using the NanoDrop ND-1000 (Fisher scientific, Loughborough UK) as detailed in section 2.6.3.3, the calculated protein concentrations for HaloTagged proteins can be found in the appendix.

2.6.3.3 Purified proteins

Protein concentration was determined by UV spectrophotometry using a NanoDrop ND-1000 (Fisher scientific, Loughborough UK) at absorbance 280nm (A280). At A280 the amino acid residues tyrosine and tryptophan contribute significantly to absorption; it is necessary to account for this to obtain an accurate protein concentration. Beer's law states that the concentration of a protein is equal to its absorbance at 280nm divided by its molecular extinction coefficient. The molecular extinction coefficient is the molecular weight of a protein divided by its molar extinction coefficient. These calculations were used to determine accurate protein concentration following purification.

2.6.4 Separation of His-tagged protein from solvent using nickel magnetic beads

In this study vehicle controls for purified protein were generated by removal of the His₆-tagged proteins from solution using PureProteome nickel magnetic beads. The protein free solvents were then used in equal volumes to purified

protein solutions when analysing cellular responses to the toxins. This allowed confidence that the observed results were due to the purified protein in question and not contaminants such as LPS. The PureProteome nickel magnetic beads were used according to the manufacturer's instructions; approximately 200µl of nickel bead solution was used for every 100µg of protein removed.

2.6.5 Determination of LPS concentration in purified protein preparations

The Charles River Endosafe® portable testing system was used to accurately measure the LPS concentration in purified proteins.

2.7 Tissue culture techniques

2.7.1 Generation and analysis of bone marrow derived macrophages (BMDM)

2.7.1.1 Preparation of L929 conditioned culture medium

The cell line L929 secretes monocyte colony stimulating factor (MCSF) into culture supernatant. This supernatant can be harvested and used for the differentiation of primary macrophages. L929 were cultured in complete RPMI + pen/strep and maintained at 50-90% confluency for 10 days. Once established culture supernatant was harvested during routine subculturing and sterilized by filtration through a 2µm syringe filter. Sterile L929 conditioned medium was stored at -20°C until required.

2.7.1.2 Isolation and differentiation of BMDM

To generate primary BMDM female mice were euthanized under CO₂ by exsanguination and cervical dislocation. The femurs and tibiae were dissected out and the joints removed. Under sterile conditions, using a 10ml syringe and 25G needle complete RPMI 1640 was flushed through the bones to expel the bone marrow. The resulting suspension was then repeatedly drawn up and

expelled through the needle and syringe to create a single cell suspension. The bone marrow was pelleted by centrifugation at 2000rpm for 2min; the pellet was resuspended in 1ml of ACK lysis buffer (LONZA) and allowed to stand for 1min to lyse RBCs. The suspension volume was made up to 10ml with complete RPMI and centrifuged at 2000rpm for 2min to wash off the lysis buffer. After a final resuspension in complete RPMI the cells were counted using a haemocytometer and the cell concentration was adjusted to 3×10^6 /ml. BMDM were cultured by adding 2ml of cell suspension + 4ml of L929 conditioned medium + 14ml of complete RPMI to a 75cm² vented TC flask and incubating at 37°C, 5% CO₂. After 3 days in culture the cells were fed by the addition of another 14mls of complete RPMI + 4ml of L929 conditioned medium. On day 6 the cells were harvested manually by scraping after incubation for 5min in ice-cold PBS.

2.7.1.3 Analysis of BMDM culture phenotype by flow cytometry

Bone marrow derived macrophages were cultured from 6-week-old female MF1 mice; on day 6 of BMDM culture 1×10^6 cells were harvested. Half of the harvested cells were stained with Fluorescein Isothiocyanate (FITC) anti-mouse F4/80 -Pan macrophage marker (eBioscience), half were left as an unstained control population and both samples were run on the FACscalibur flow cytometer following appropriate user instructions (figure 2-9).

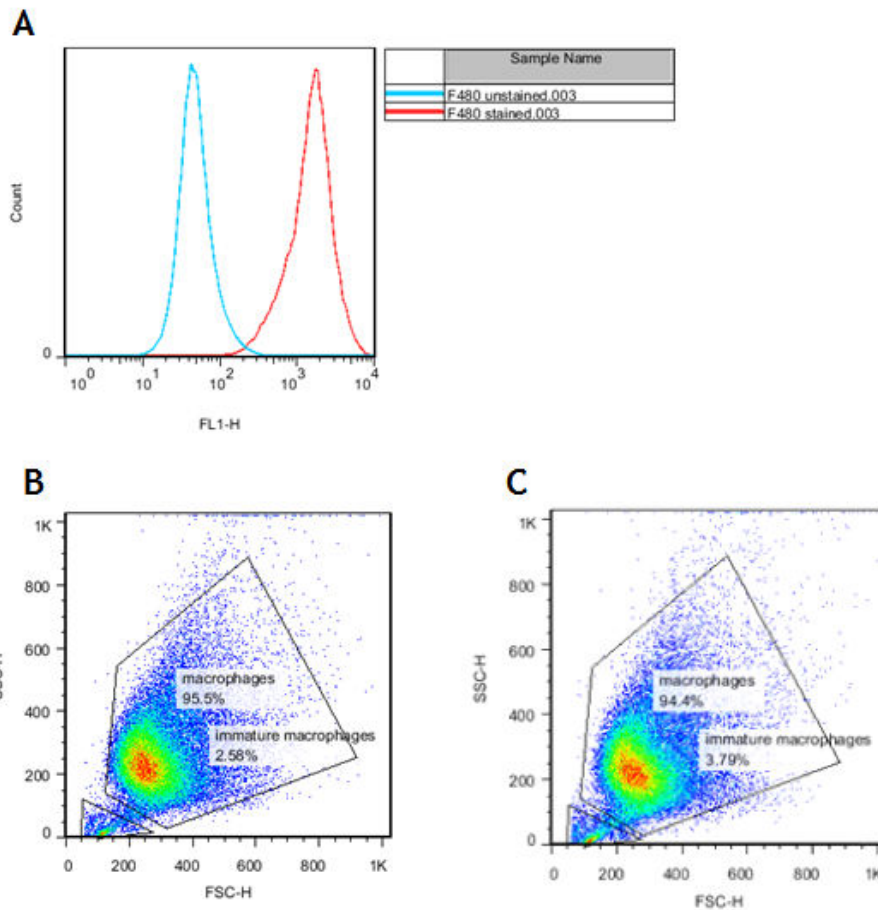


Figure 2-9 Analysis of BMDM culture phenotype by flow cytometry.

On day 6 of culture BMDM were harvested, 1×10^6 cells were stained with anti-mouse F4/80 (FITC) and 1×10^6 cells were left unstained. Samples were analyzed for fluorescence intensity (A). The size and granularity of the stained sample was analyzed and groups were created for mature and immature macrophages, indicating percentage of the total sample (B). The percentage of cells that were positive for F4/80 was analyzed and grouped according to size and granularity (C).

2.7.2 Cell line information and culture requirements

Table 2-12 Description of Cell line Origins, Characteristics and Growth Requirements

HEK293- NF κ B/TLR4/MD2	Human	Complete DMEM/G418 + blasticidin + puromycin
HEK293- NF κ B/TLR5	Human	Complete DMEM/G418 + blasticidin

The HEK293 reporter cell lines (Imgenex) are stably transformed with full length human TLR/co-receptors and an SEAP reporter gene under the control of an NF κ B response element. Following exposure to appropriate TLR ligands these cells express SEAP which can be detected with the use of quanti-blue media (Invivogen). SEAP expression increases linearly with increasing ligand dose. These cell lines have epithelial-like morphology and are adherent.

L929	Murine	Complete RPMI/none
------	--------	--------------------

The L929 cell line was isolated from induced sarcomas in a male C3H mouse. It is used routinely for cytotoxicity testing; its culture supernatant also provides a source of MCSF for the differentiation of primary macrophages from mouse bone marrow. This cell line has fibroblastic morphology and is adherent.

RAW264.7	Murine	Complete RPMI/none
----------	--------	--------------------

RAW 264.7 is a monocyte/macrophage cell line isolated from an Abelson leukaemia virus-induced tumour in a BALB/c mouse. This cell line is useful for studying some aspects of host response and as a transfection host. This cell line has fibroblastic morphology and is adherent.

THP1-blue TM - CD14	Human	Complete RPMI/ blasticidin + zeocin
--------------------------------	-------	-------------------------------------

The THP1 cell line is derived from an acute monocytic leukaemia found in the peripheral blood of a 1year old male. These cells can be differentiated to a macrophage-like phenotype by the addition of phorbol 12-myristate 13-acetate (PMA) to culture media. THP1-blueTM-CD14 cells are reporters expressing full-length human TLR1-10 as well as CD14, a co-receptor for some TLRs. Interaction between TLRs and their cognate ligand results in the expression of SEAP under the control of a promoter induced by NF κ B and AP-1. SEAP expression increases linearly with increasing ligand dose. This cell line has lymphoblast-like morphology and grows in suspension.

2.7.3 Resuscitation of frozen cell lines

Cell lines were resuscitated from liquid nitrogen by quick thawing in a 37°C water bath followed by suspension in 9ml of appropriate culture medium. The cell suspension was pelleted by centrifugation at 2000rpm for 2min followed by resuspension in 5mls of appropriate culture medium before removal to a 25cm² vented tissue culture flask. Cells were cultured until 90% confluent at 37°C, 5%

CO₂ and then sub-cultured into 75cm² vented tissue culture flasks to be bulked up for use.

2.7.4 Routine sub-culturing techniques

Adherent cell lines were harvested for sub-culture when between 80-90% confluent. All adherent cell lines were harvested by trypsinization with the exception of the RAW 264.7 cell line which is harvested manually using a cell scraper. Cells were treated with 2 or 4ml of trypsin-EDTA (Sigma Aldrich, UK) for 25cm² or 75cm² culture sizes, respectively. Following addition of trypsin-EDTA cells were incubated at 37°C for no more than 5min until all cells had dissociated from the flask surface. Active trypsin was inhibited by a 5x dilution in appropriate culture media and removed by centrifugation of the cell suspension at 2000rpm for 2min. Non-adherent cells were harvested simply by centrifugation at 2000rpm for 2min. Harvested cells were counted using a haemocytometer and sub-cultured at the appropriate density for the particular cell line used.

2.7.5 Storage of cell line aliquots in liquid nitrogen

Additional aliquots of cell lines were prepared from 80-90% confluent T75cm² cultures. Cells were harvested as detailed in section 2.7.3 and cell pellets were resuspended in 5ml of appropriate freeze media (either FBS + 10% DMSO or complete media + 10% DMSO as dictated by the cell line supplier). 5 x 1ml aliquots of the resuspended cells were prepared and stored at -80°C for 24hr before removal to liquid nitrogen.

2.8 Microscopy

2.8.1 Analysis of PLY interactions with RAW 264.7 macrophages

2.8.1.1 Staining with CellMask deep red plasma membrane stain and Halo TMR-direct ligand

1 x 10⁶ RAW 264.7 cells were seeded on cover slips in 6 well plates and allowed to adhere overnight at 37°C, 5% CO₂. Non-adherent cells were removed by

gently washing twice with warm complete media. 1ml of 2.5µg/ml CellMask Deep Red Plasma membrane stain (Invitrogen, Paisley UK) was added to each cover slip and incubated for 5 mins at 37°C. Cover slips were then washed three times with warm complete media to remove the stain. HaloTag® fusion lysates were added to the cells (100µl lysate in 900µl warm complete media) and incubated for 30mins at 37°C. After incubation the cells were washed gently three times with warm sterile PBS and fixed by incubation for 10 mins at room temperature with 1 ml of warm 4% paraformaldehyde/0.2M sucrose/1xPBS (pH 7.5). Following fixation the HaloTag® TMRDirect Ligand (Promega, Southampton UK) was added to the cells to label fusion proteins; a 1:200 dilution of the ligand was prepared in warm media to create a 5X stock solution, 100µl of stock was then added to 400µl of warm PBS and cells were incubated for a further 2hrs at 37°C. After the final incubation cells were washed three times with PBS and mounted onto microscope slides using Dako fluorescence mounting media (Dako).

Images were captured using a Zeiss M1 Axioskop microscope at 100x magnification with filter set TRITC and lasers 555ex/580em and Alexa647. Images were taken as z - stacks 0.25µm apart to allow 3D visualization of cells following analysis using the Volocity software package (PerkinElmer, UK).

2.8.1.2 Staining with rhodamine phalloidin and eGFP tagged PLY variants

RAW 264.7 macrophages were cultured and prepared for staining as detailed in section 2.8.1.1. 1ml of a 1µg/ml solution of eGFP- tagged WT-, Δ6-, D123- and D4-PLY and an eGFP only control were added to the cover slips and incubated at 37°C for 30mins. The cover slips were washed and fixed as detailed above. Cells were permeabilized by adding 1ml of 0.1% triton x-100 and incubating at - 20°C for 3mins. Cells were washed twice with PBS and stained by adding 5µl of methanolic rhodamine phalloidin (Invitrogen) stock to 200µl of PBS and incubating at room temperature for 20mins. The cells were washed and mounted as described in section 2.8.1.1 and imaged using eGFP and RFP filter sets.

2.8.2 Image analysis

Following image acquisition images were analysed using the Volocity image analysis software package (PerkinElmer, UK). The captured Z- stacks were

compiled to produce 3D images and colocalization of stained cell features was analysed using the software's colocalization tools and Pearson's correlation coefficient (PCC).

2.9 *In Vitro* analysis of recombinant PLY and its derivatives

2.9.1 *Analysis of PLY cytotoxicity*

2.9.1.1 Lactate Dehydrogenase Release

Lactate dehydrogenase is a stable cytosolic enzyme that is released upon cell lysis. The CytoTox 96® Non-Radioactive Cytotoxicity Assay (Promega) is a colourimetric assay that allows % lysis in treated cells to be calculated by measuring LDH presence in cell culture supernatants. This assay was performed according to the manufacturer's instructions.

2.9.1.2 Analysis of Apoptosis

The ApoTox-Glo™ Triplex assay (Promega) is capable of measuring viability, cytotoxicity and apoptosis simultaneously in treated cells. Cells were treated with PLY and its derivatives by serially double diluting the proteins from an initial concentration of 175nM in duplicate. The cells were incubated at 37 °C for 6 hours before performing the assay according to the manufacturer's instructions.

2.9.2 *Treatment of mammalian cells with PLY and its derivatives*

Cellular responses to purified PLY and its derivatives were analysed by a variety of techniques. In all cases PLY derivatives such as truncation mutants were added at equimolar concentrations e.g 1µg of PLY in 1ml is equivalent to a 17.56nM solution therefore all PLY derivatives were used at the same molarity to account for differences in molecular weight. To maintain consistency between assays the number of PLY monomers per cell was kept constant, for example, if 1×10^5 macrophages were treated with 200µl of PLY at a concentration of 17.5nM this would give approximately 2.3×10^7 PLY monomers per cell. This allowed the

use of optimum cell number and culture volume without compromising treatment dose.

Note - where whole mouse serum was added to *in vitro* assays the total assay volume was kept constant as detailed above. Serum (prepared as detailed in section 2.10.3) was added to each well to a concentration of 10%, i.e. 20µl of serum per well.

2.9.3 Analysis of cytokine expression

Culture supernatants from PLY treated cells were tested for the presence of IL-1 beta, IL-6 and KC using R and D systems ELISA Duosets. The manufacturer's instructions were followed with the exception of volumes used; half-volumes of samples, antibodies and developing reagents were used, this did not affect assay sensitivity.

2.9.4 Analysis of gene expression by RT² qPCR

2.9.4.1 Isolation of RNA from PLY treated mammalian cells

2x10⁶ Bone marrow derived macrophages were treated with 100ng/ml of LPS, 100ng/ml (or equimolar equivalent) of PLY or its derivatives or left untreated and incubated for 6hrs at 37°C at 5% CO₂. RNA was immediately harvested using the GeneJet RNA isolation kit (Fermentas). RNA samples were aliquoted and stored at -80°C for future analysis.

2.9.4.2 Analysis of RNA quality and concentration

The concentration of RNA in samples was determined using the Qubit™ fluorimeter (Invitrogen), according to the manufacturer's instructions.

RNA quality was then determined using the Agilent Nano-, or Pico-chip depending on the concentration of RNA available. The quality of RNA is given as the RNA integrity number (RIN). RINs are given on a scale of 1-10, only samples with a RIN of 8 or above are taken for further analysis.

2.9.4.3 cDNA synthesis

The RT² first strand cDNA synthesis kit (Qiagen) was used to synthesize cDNA from RNA samples; the manufacturer's instructions were followed. Typically, 1µg of starting RNA was used. The amount of starting RNA was kept constant where samples were to be directly compared.

2.9.4.4 Real-Time PCR using RT² qPCR primer assays or RT² qPCR profiler assays and RT² SYBR green mastermixes

RT² qPCR profiler assays were used to analyse the expression of genes associated with the murine antibacterial response (cat. PAMM-148) and inflammatory cytokine and chemokine response (cat. PAMM-112) following PLY treatment of BMDM. A selection of genes was chosen to validate these assays by individual PCR using the RT² qPCR primer assays. In both cases the manufacturer's instructions for use were followed, including cycling conditions for a Chromo4, DNA engine opticon cycler.

2.9.5 QUANTI-Blue™ assay for detection of SEAP secreted by reporter cell lines

The QUANTI-Blue™ (Invivogen) assay is an enzymatic colourimetric assay that is used to detect alkaline phosphatase in biological samples. In this case the assay was used to detect secreted embryonic alkaline phosphatase (SEAP) in reporter cell culture supernatants. The assay media was prepared and used according to the manufacturer's instructions. In addition a standard curve of SEAP was created using cell-based alkaline phosphatase standard (Cayman Chemical), an eight point standard was created by performing double dilutions from a top concentration of 50mU/ml to 0mU/ml. 50µl of standard or sample was added to 150µl of QUANTI-Blue™ media in a flat-bottomed 96-well plate, the plate was incubated at 37°C for 24hrs. The OD 625-655nm of samples, standards and controls were measured using the BMG Fluostar Optima.

2.9.6 Analysis of protein-protein interaction by pull-down using HaloTagged proteins

The HaloTag® Mammalian Pull-down system (Promega, G6500) was used according to a modified version of the manufacturer's instructions. 50µl samples were taken at every step of the protocol for analysis by SDS-PAGE and western blotting to ensure stringency of the protocol. Briefly, 400µl of HaloTag® fusion lysate was diluted in 800µl of 1 x TBS and added to 200µl of prepared Halo-link resin; binding reactions were incubated at room temperature for 1hr on a tube rotator. Unbound proteins were removed by washing x 5 with 1x TBS + 0.05% IGEPAL (Sigma-Aldrich, CA-630). Mammalian cell lysate was prepared for each reaction from 1 x 10⁶ RAW 264.7 cells by resuspending pelleted cells with 300µl of mammalian lysis buffer and 30µl protease inhibitor (kit components). The mammalian cell lysate + 700µl of 1 x TBS was added to the Halo-link resin and incubated at 37°C for 1hr with shaking. The resin preparation was washed x5 with 1 x TBS + 0.05% IGEPAL. Bound proteins were eluted by incubation at room temperature for 30min with 100µl of SDS-elution buffer (kit component). Finally, to confirm the presence of fusion proteins the resin preparation was treated with 100µl of Turbo TEV protease (Genaway, USA) overnight at 4°C. Cleaved proteins were harvested by centrifugation of the resin at 2000 RPM for 2 minutes before removal of the supernatant. Fraction samples were initially analysed by SDS-PAGE, western blot and silver staining (Invitrogen, LC6070) to ensure absence of proteins in the wash fractions and absence of PLY in the elution fractions. Samples were then run on a large SDS-PAGE gel (Hoefer, USA) and stained with coomassie blue. Bands of interest were excised and stored at -20°C until ready for analysis by mass spectrometry.

Mass Spectrometry

Proteins within the excised bands were identified by tandem mass spectrometry (MS/MS) at the Burchmore lab mass spectrometry facility at the University of Glasgow. Results were provided as analysed Mascot files.

2.9.7 Analysis of Actin Binding by ELISA

2.9.7.1 Preparation of actin solution

This assay was replicated from Hupp et al, 2013. Briefly, non-muscle actin (Cytoskeleton Inc.) was reconstituted in dH₂O to a conc. of 0.4mg/ml and incubated on ice for 60 minutes. The resulting monomeric actin solution was diluted 1:10 in actin polymerization buffer (APB, appendix) and incubated at room temperature for 1 hour. The solution was centrifuged for 1 hour at 100,000g at room temperature for 1 hour to pellet polymerized actin. 25.2µl of the resulting supernatant was diluted in 4974.8µl of PBS + 0.1% BSA.

2.9.7.2 Actin binding ELISA

A 96-well high binding ELISA plate (Costar) were coated in duplicate with 350, 175 and 87.5nM of PLY, Δ6PLY, D123PLY, D4PLY or 1µg/ml BSA as a negative control and incubated overnight at 4°. The plates were washed x5 with PBS/Tween and blotted before addition of 50µl of actin solution. After a two hour incubation at room temperature the plate was washed x5 and 50µl of anti-actin antibody (Cytoskeleton, Inc.) (diluted 1:1000) was added to each well, the plate was incubated for a further 1 hour at room temperature. The plate was washed x5 and 50µl of anti-rabbit HRP (1:1000) was added to the plate. After 30 minutes at room temperature 50µl of streptavidin (1:200) was added. The plate was incubated for 20 minutes, washed x5 and developed using 50µl of Fast OPD (Sigma), development was stopped after 5 min by addition of 50µl 3M HCL. The OD at 485-10nm was read using the BMG labtech Fluostar Optima.

2.10 *In Vivo* analysis of recombinant PLY and its derivatives

All *in vivo* experiments were carried out in accordance with the UK animals (scientific procedures) act 1986. Mice had access to food and water *ad libitum* and were kept at a constant room temperature of 20-22°C with a 12 hour light/dark cycle. All animal procedures were performed under the project

license of Professor Tim Mitchell and received ethical approval from the Ethical Review Board at the University of Glasgow. Unless otherwise stated all animal handling, sample processing and analysis was performed by the author, Catherine Dalziel.

2.10.1 Intranasal vaccination

To study murine mucosal and systemic immune responses to pneumolysin fusion vaccines, animals were vaccinated intranasally according to the schedule detailed in table 2-13. Briefly, mice were lightly anaesthetized using 3.5% isofluorane/1.5% O₂ (1.5L per minute) (Astra-Zeneca, Macclesfield UK) and 20µl of prepared pneumolysin fusion vaccine was instilled into the nares by gentle pipetting. The doses used were 0.2µg of lytic fusions or 2µg of non-lytic fusions in a total volume of 20µl PBS, 10µl was added to each nostril. Following vaccination the animals were monitored until they had recovered from the effects of anaesthesia. As indicated in table 2-13 animals were vaccinated 3 times over a 42 day schedule with a 14 day period between each vaccination, blood samples were taken from the lateral tail vein before each dose of vaccine. On day 42 animals were humanely sacrificed and terminal samples were taken by cardiac puncture (blood) and nasopharyngeal wash.

Table 2-13 Immunization schedule.

Day	Procedure
0	Take 20µl sample of venous blood from lateral tail vein (PB). Intranasally immunize with 20µl of test vaccine.
14	Take 20µl sample of venous blood from lateral tail vein (B1). Intranasally immunize with 20µl of test vaccine.
28	Take 20µl sample of venous blood from lateral tail vein (B2). Intranasally immunize with 20µl of test vaccine.
42	Humanely sacrifice animal by exsanguination under terminal anaesthetic (B3), perform nasal wash.

Table 2-14 Table of transgenic animals and their genetic backgrounds

Transgenic animal	Genetic background
C3-/-	C57BL/6
NLRP3-/-	BALB/c
TLR4-/-	BALB/c
IL-17-/-	C57BL/6

2.10.2 Analysis of Antibody Response in Immunized Mice

2.10.2.1 Analysis of immunoglobulin G presence in serum

Sera obtained following intranasal vaccination were tested for the presence of IgG by ELISA. 96-well EIA plates (Corning) were coated with 50µl of capture antigen at a concentration of 1µg/ml (except those in the second column which are negative control wells) and incubated O/N at 4°C. The plates were washed X3 with PBST (PBS + 0.05% tween-20) and blotted dry. Free binding sites were blocked by adding 150µl of 1% BSA in PBS and incubating for 1hr at 37°C. The wash step was repeated. The plates were prepared for sample addition by adding 98µl of PBS to each well across the top row and 80µl to every other well. 2µl of positive control sera was added to the first two wells and 2µl of test sera was added in duplicate to the rest of the top row. The samples and control were diluted 1 in 5 by transferring 20µl from the top row to the second row and mixing well, this was repeated until all rows had been diluted. The plate was incubated for 2hr at 37°C. The wash step was repeated. The detection antibody, anti-mouse gamma (γ chain) biotin conjugate (Sigma) was diluted 1 in 1000 and 50µl of this solution was added to each well of the plate. The plate was incubated for 1hr at 37°C. The wash step was repeated. Streptavidin HRP conjugate (Sigma) was also diluted 1 in 1000 and 50µl was added to every well of the plate and incubated for 30min at 37°C. A final wash step was performed. The plates were developed using 50µl of Fast OPD (Sigma) and development

stopped after 5 min by addition of 50µl 3M HCL. The OD was read using the BMG labtech Fluostar Optima.

2.10.2.2 Analysis of IgA presence in nasal washes

Nasal washes were collected from immunized mice at the end of the immunization schedule (Day 42). The presence of IgA in nasal washes was measured by ELISA as detailed in section 2.10.2.1 with the following exceptions; nasal wash samples were added neat to the top well of the ELISA plate before serial dilution, the detection antibody used is anti-mouse IgA alpha-chain specific (Sigma) at a 1:500 dilution and the plates are incubated for 1 hour with streptavidin HRP solution rather than 30 minutes.

2.10.2.3 Determining IgG clonotype generated in response to PLY-fusion vaccines

Following confirmation of an IgG antibody response in immunized mice the Southern Biotech Antibody Clonotyping ELISA kit was used to determine the clonotype(s) of the response i.e (IgG1, 2a, 2b or 3). The manufacturer's protocol was altered slightly to give optimized performance with available reagents and samples. Briefly, 96-well EIA plates (Corning) were coated with 50µl of capture antigen at a concentration of 1µg/ml and incubated O/N at 4°C. The plates were washed X3 with PBST (PBS + 0.05% tween-20) and blotted dry. Free binding sites were blocked by adding 200µl of 1% BSA in PBS and incubating for 2 hours at room temperature. The wash step was repeated. The plates were prepared for sample addition by adding 98µl of PBS to wells A2-12 and 80µl to every other well, except A1 to which 100µl of diluent was added. 2µl of test sera was added to every well in the top row. The samples were diluted 1 in 5 by transferring 20µl from the top row to the second row and mixing well, this was repeated down the plate until discarding 20µl from row H. The plate was incubated for 2hr at room temperature. The wash step was repeated. The Southern Biotech kit provides HRP conjugated antibodies directed against the following antibody isotypes/subclasses - Ig, IgG1, IgG2a, IgG2b, IgG3 and IgA, these antibodies were diluted 1:500 and added to the plate as shown in table 2-15.

Table 2-15 Subclasses ELISA Secondary Antibody Layout.

	1	2	3	4	5	6	7	8	9	10	11	12
A	alg	alg	algG1	algG1	algG2a	algG2a	algG2b	algG2b	algG3	algG3	algA	algA
B	alg	alg	algG1	algG1	algG2a	algG2a	algG2b	algG2b	algG3	algG3	algA	algA
C	alg	alg	algG1	algG1	algG2a	algG2a	algG2b	algG2b	algG3	algG3	algA	algA
D	alg	alg	algG1	algG1	algG2a	algG2a	algG2b	algG2b	algG3	algG3	algA	algA
E	alg	alg	algG1	algG1	algG2a	algG2a	algG2b	algG2b	algG3	algG3	algA	algA
F	alg	alg	algG1	algG1	algG2a	algG2a	algG2b	algG2b	algG3	algG3	algA	algA
G	alg	alg	algG1	algG1	algG2a	algG2a	algG2b	algG2b	algG3	algG3	algA	algA
H	alg	alg	algG1	algG1	algG2a	algG2a	algG2b	algG2b	algG3	algG3	algA	algA

The plates were incubated at room temperature for 1 hour, the wash step was repeated and 50µl of extravidin HRP (1:2000) was added to each well. The plates were incubated at room temperature before performing a final wash step. The plates were developed using 50µl of Fast OPD (Sigma) and development stopped after 5 min by addition of 50µl 3M HCL. The OD at 485-10nm was read using the BMG labtech Fluostar Optima.

2.10.3 Preparation of whole mouse serum and preservation of complement activity.

Briefly, mice were anaesthetized using 3.5% isoflurane/1.5% O₂ (1.5L per minute), while under anaesthesia the animals were humanely culled by performing a terminal bleed via cardiac puncture, followed by cervical dislocation. Harvested blood was immediately transferred to a pre-chilled 15ml Falcon tube and allowed to clot on ice for 1 hour. Serum was separated from clotted blood by centrifugation at 15,000rpm for 20 minutes at 4°C and immediately aliquoted and stored at -80°C. It is essential that harvested serum

is thawed on ice, kept chilled and handled carefully until point of use; allowing the serum to reach room temperature or rough handling risks activating the alternative pathway of complement activation and depleting/exhausting complement components in the sample.

2.11 Statistical analysis

All statistical analysis was performed using GraphPad® instat (GraphPad® software, San Diego, California, USA). ELISA, LDH and Quanti-blue assay results were analysed by one-way analysis of variance (one-way ANOVA) followed by a Bonferroni's post-test. The only exception to this was analysis of antibodies present in the sera of immunised mice (chapters 5), this was analysed by unpaired t test. Probability (p) values of <0.05 were considered statistically significant. Statistically significant differences in this work are indicated by * ($p<0.05$), ** ($p<0.01$), *** ($p<0.001$).

3. Functional Analysis of Recombinant Pneumolysin and its Derivatives

This chapter describes preliminary studies into the biological functions of PLY potentially responsible for its adjuvant activity.

As previously discussed, there is evidence in the literature that PLY can directly bind TLR4. However, there is not a consensus in the field and it is often suggested that biological responses attributed to PLY are in fact due to contaminating LPS. This work sought to further elucidate the relationship between PLY and TLR4, with particular reference to cytokine induction via this pathway.

Throughout this project it was essential to appropriately control for potential contaminating TLR ligands; a novel process for creating vehicle controls was devised and used to test for contaminating TLR ligands that could generate false positive results. Additionally, the quality and cytolytic activity for all PLY variants was analyzed and *in vitro* treatment models were devised and optimized.

The nomenclature of proteins used in this project has been refined for ease of understanding and to conserve space, the key in table 3-1 defines all abbreviations used in this project.

Table 3-1 Abbreviations and Definitions of PLY variants used in this Project

Abbreviation	Description
PLY	Full-length lytic pneumolysin
Δ6	deletion of the amino acids alanine and arginine at positions 146-147, removes lytic activity in full-length PLY
D123	A truncation mutant consisting of domains 1,2 and 3 of PLY (aa 1-359)
D4	A truncation mutant consisting of domain 4 of PLY (aa 360-471)
e-	Indicates the protein has been N-terminally tagged with eGFP
h-	Indicates the protein has been N-terminally tagged with the Halo-Tag.
No precursor	Where there is no precursor a protein should be assumed to be N-terminally His-tagged for purification purposes only.

3.1 Analysis of Cytolytic Activity in Purified Recombinant PLY and its Derivates

To determine the optimum conditions for analyzing immunological properties of PLY *in vitro*, the cytolytic activity of PLY and its derivatives was determined in multiple cell types.

3.1.1 Haemolytic Activity

The haemolytic activity of all proteins used in this project was determined prior to use. The haemolytic activity of PLY and its derivatives is measured in haemolytic units per picomole (HU/pmol) of toxin; one haemolytic unit is defined as the concentration of toxin required to lyse 50% of a 2% erythrocyte solution.

Analysis of haemolytic activity showed that all PLY truncation mutants and those containing the delta 6 mutation did not have lytic activity, all other full length versions of PLY including retained lytic activity (figure 3-1).

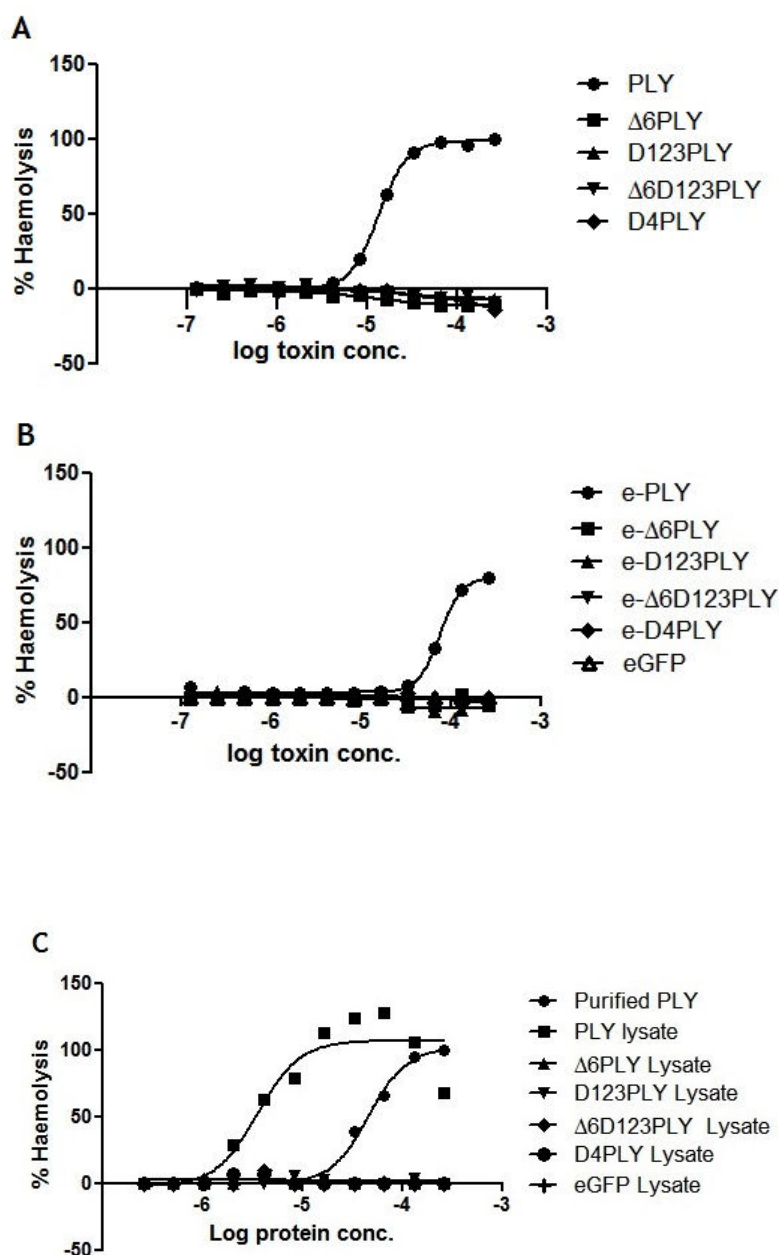


Figure 3-1 Analysis of haemolytic activity of PLY variants.

Haemolytic assays were performed to calculate the specific activity of His-tagged PLY variants (A), eGFP-tagged PLY variants (B) and Halo-tagged PLY variants (C). 50 μ l of purified PLY or derivatives (17.5nM) and 50 μ l of lysates (diluted 1:5) was added in duplicate to the first wells of a 96-well plate and serially diluted (1:2) horizontally across the plate. Following incubation with a 2% sheep RBC solution released haemoglobin was measured at 540nm using a Fluostar Optima plate reader. O.D. measurements were used to create dose response curves in Graphpad Prism indicating % haemolysis and subsequently to calculate specific activity (HU/pmol). Data points are mean % haemolysis and represent technical duplicates.

The log dose response curves shown in figure 3-1 were used to calculate specific activity for each lytic version of PLY; these values are given per picomole in table 3-2.

Table 3-2 Calculated Haemolytic Activity of Lytic PLY Variants

Protein	HU/pmol
PLY	41.27
e-PLY	10.40
h-PLY	49.87

3.1.2 Cytotoxic Activity/Lysis

Analysis of the haemolytic activity of PLY and its derivatives showed that only full-length wild-type PLY was capable of causing erythrocyte lysis. This is also true in nucleated cells, none of the truncation or $\Delta 6$ mutants caused lysis of bone marrow derived macrophages (BMDM), L929 fibroblasts or RAW264.7 macrophages as determined by LDH release (data not shown except where figure 3-3 shows $\Delta 6$ PLY treated BMDM). The purpose of the lactate dehydrogenase assay (LDH) was two-fold, firstly LDH release was used as an indicator of pore formation (it should be noted that apoptotic cells do not release LDH and so this is a measure of necrosis and/or pore formation rather than total cell death). Secondly, as IL-1 β initially exists in a precursor form (Pro-IL-1 β) which is also detected by ELISA, the % pore formation was used to adjust IL-1 β measured by ELISA to account for pro-IL-1 β that may have ‘leaked’ into the supernatant as a result of pore formation.

It has been shown previously that human monocytic and epithelial cell lines have different sensitivities to PLY (Hirst et al., 2002); analysis of LDH release by L929, RAW264.7 and BMDM concurs with these findings (figures 3-2 and 3-3). Both the L929 and RAW264.7 cell line were equally resistant to lysis at treatment durations of 1 and 3 hours, even at high doses of 175nM PLY both cell lines showed less than 20% lysis. After 6 hours of treatment with PLY there is a marked difference in survival between the cell lines. Analysis of dose response curves revealed that 50% lysis was achieved in PLY treated L929 at 100nM, in comparison only 25nM PLY was required to lyse 50% of RAW264.7 cells.

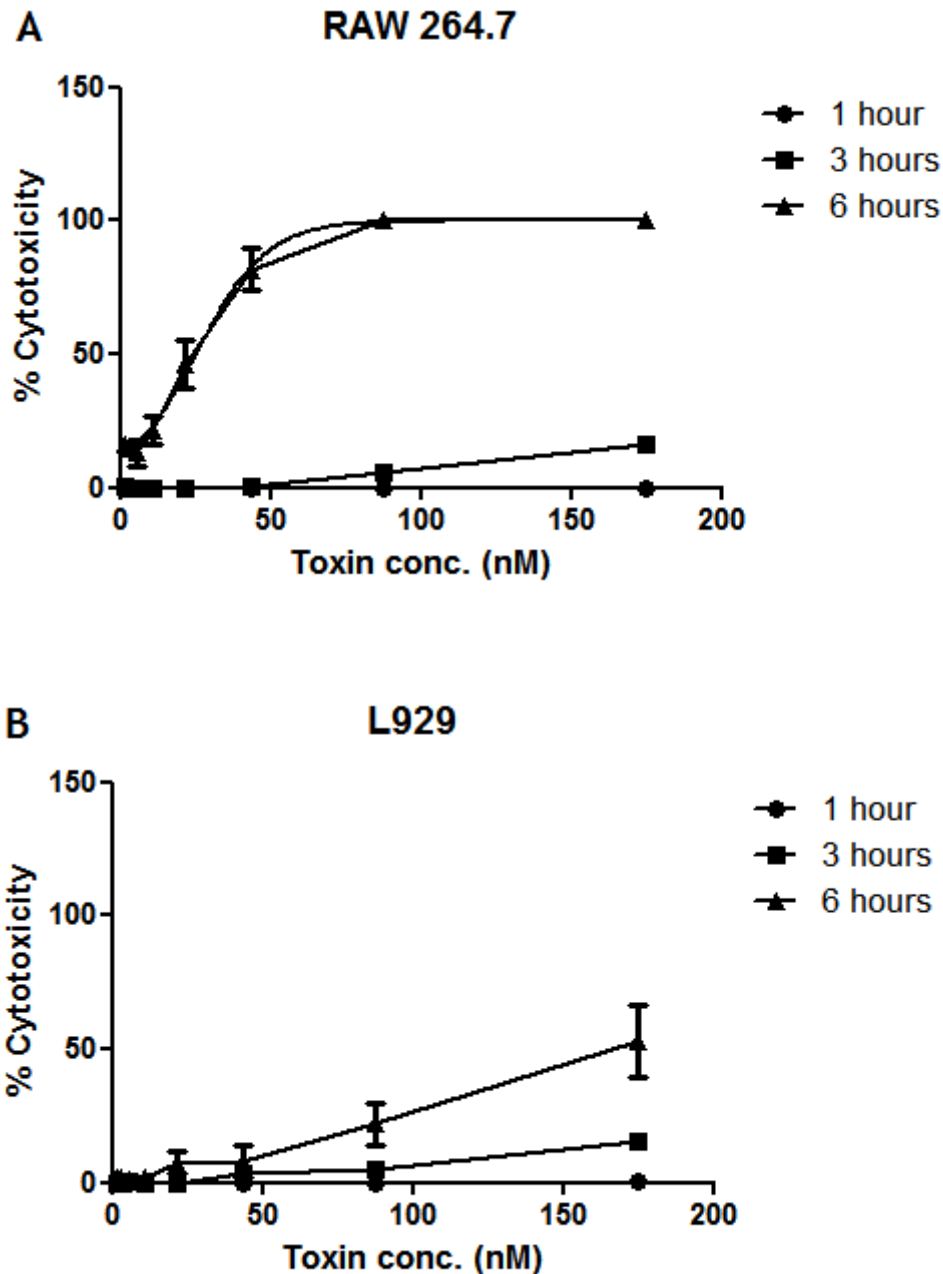


Figure 3-2 Analysis of cytolytic activity of PLY against L929 and RAW264.7 macrophages.

L929 and RAW 264.7 cell lines were seeded at 1×10^5 cell/well in $100 \mu\text{l}$ complete RPMI in a 96-well plate. In a separate 96-well plate PLY was serially diluted (1:2) across the plate in triplicate from a starting conc. of 350 nM . $100 \mu\text{l}$ of PLY dilutions were transferred to the plate containing L929 and RAW 264.7, this resulted in a top PLY conc. of 175 nM . The cells were incubated at 37°C for 1, 3 and 6 hours. Supernatants were collected and analysed for LDH release using the Cytotox®96 Non-radioactive Cytotoxicity Assay (Promega). LDH release from both cell lines was used to create dose-response curves in Graphpad Prism and subsequently to calculate percentage lysis. These experiments were performed once, data are mean % lysis from three technical replicates.

Bone marrow derived macrophages were used in *in vitro* models of PLY treatment to investigate cytokine/chemokine and gene expression. To optimize the treatment conditions the degree of cytotoxicity caused in PLY treated BMDM was measured by LDH release at PLY conc. of 175, 17.5 and 1.75nM and incubation periods of 3, 6, 12 and 24 hours (figure 3-3). The percentage of lysed cells in PLY treated BMDM is significantly increased compared to untreated or LPS treated BMDM. The cytotoxic activity of PLY was dose-dependent; PLY conc. of 175, 17.5 and 1.75nM caused ~50, 30 and 10% lysis, respectively. The percentage lysis does not significantly increase after 3 hours of treatment. In addition BMDM were more resistant to lysis than either L929 or RAW264.7, 175nM of PLY was required to achieve 50% lysis.

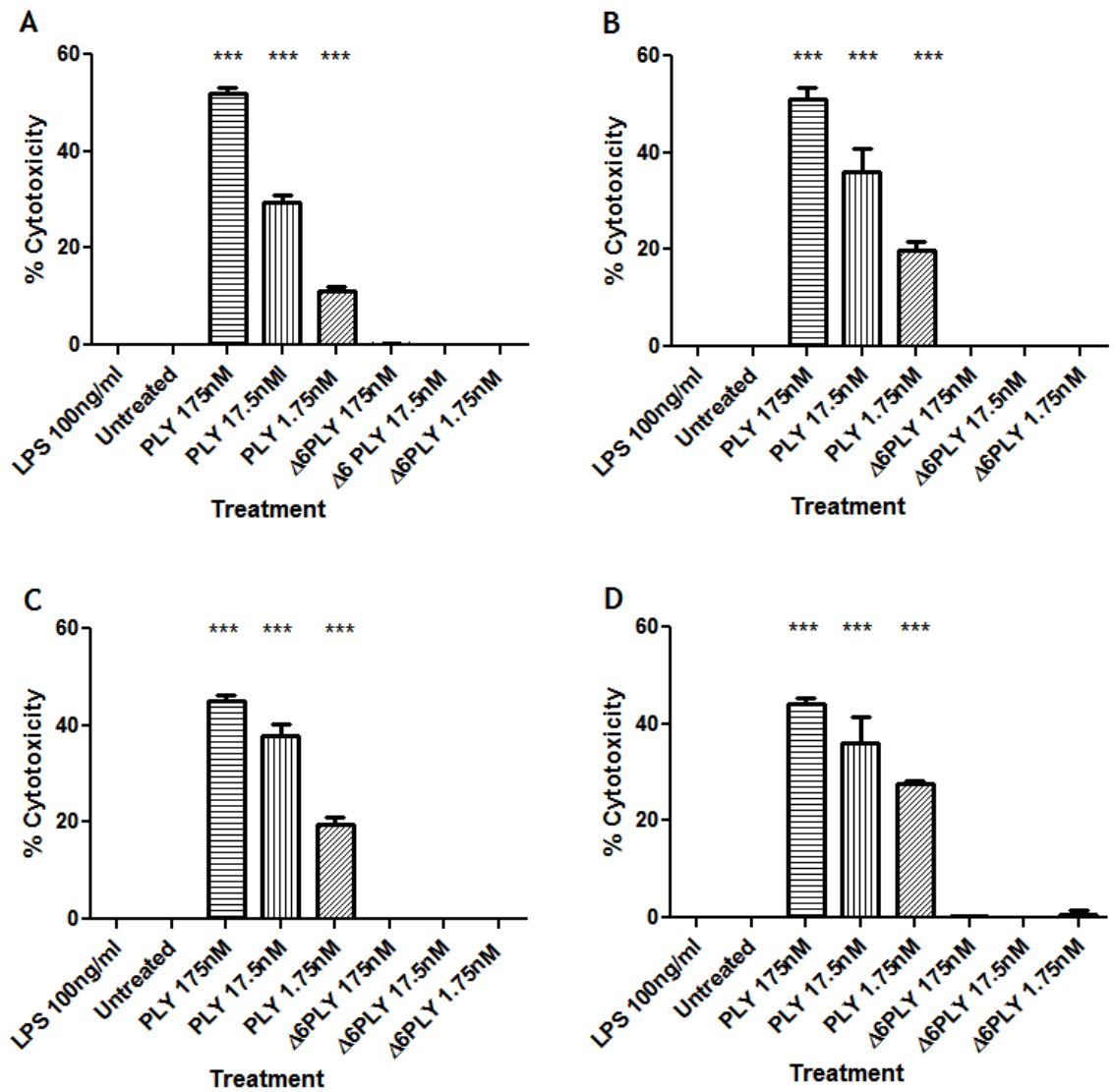


Figure 3-3 LDH release in PLY treated bone marrow derived macrophages at 3(A), 6(B), 12(C) and 24(D) hours.

BMDM were seeded at 1×10^5 cell/well in a 96-well plate and treated with PLY at concentrations of 175, 17.5 and 1.75nM for 3, 6, 12 and 24 hours in a total well volume of 200 μ l. Supernatants were collected and analysed for LDH release using the Cytotox®96 Non-radioactive Cytotoxicity Assay (Promega). LDH release from cells was used to calculate percentage lysis. Statistical significance was tested by one-way ANOVA comparing all columns to the control column (untreated), *($p < 0.05$), **($p < 0.01$), ***($p < 0.001$). Two experiments were performed with three technical replicates per condition, data are mean+SEM.

PLY has previously been shown to induce apoptosis in dendritic cells and cochlear hair cells (Beurg et al., 2005; Littmann et al., 2009). Figure 3-4 confirms an apoptotic response to PLY in BMDM and also demonstrates that this is dependent on lysis as $\Delta 6$ PLY, D123PLY and D4PLY did not induce apoptosis.

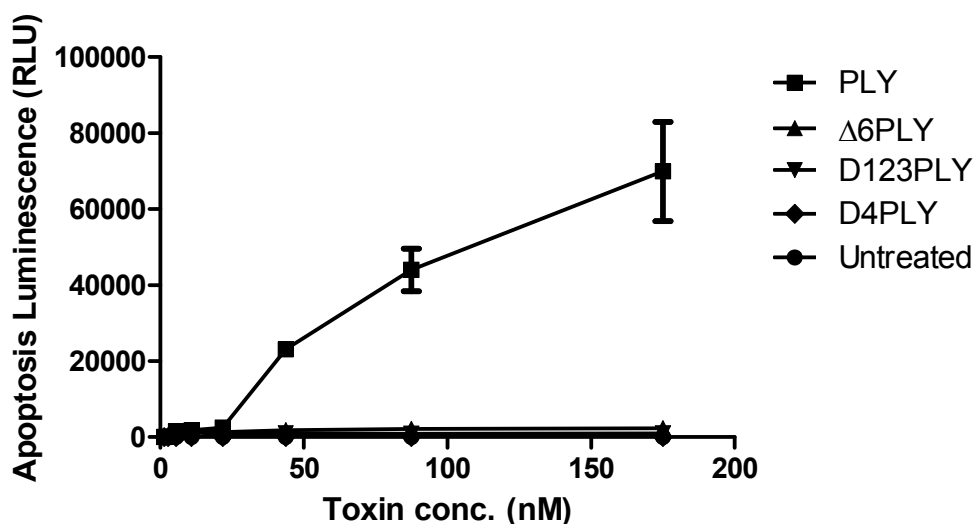


Figure 3-4 Apoptosis in BMDM treated with PLY, Δ6PLY, D123PLY, D4PLY.

BMDM were seeded at 1×10^5 (100 μ l total volume) in a 96-well plate and incubated for 6 hours at 37°C with 100 μ l of either PLY, Δ6PLY, D123PLY or D4PLY at a final conc. ranging from 175 nM to 1.36 nM (serial double dilutions), an untreated control was included. The Promega Apotoglo assay was used to measure caspase3/7 by luminescence as per the manufacturer's instructions. Data shown are mean+SEM from three technical replicates, this experiment was performed once.

3.2 Analysis of LPS Content and Preparation of Vehicle Controls

As the recombinant proteins for this study were expressed and purified from *E. coli* it was necessary to ensure that contamination with endogenous proteins etc. was negligible. One particular concern when purifying proteins from *E. coli* is the presence of contaminating LPS, anion-exchange chromatography is able to separate LPS from the desired protein, however, LPS is extremely difficult to remove entirely and so must be quantified to ensure levels are acceptably low. To ensure that trace contaminants were not responsible for any observed biological activity in these studies vehicle controls were prepared using Ni-magnetic beads to remove the toxin. The Ni-magnetic beads were used to remove His-tagged proteins from solution, leaving behind any contaminants. The remaining solutions were used as vehicle controls to demonstrate that the responses seen to PLY and its derivatives were due to the specific proteins and not contaminants.

3.2.1 LPS testing

As this study centred around the immune response to PLY, with a particular focus on TLR4, it was vital that responses observed were due to PLY and not LPS. The minimum threshold dose of LPS required to elicit an inflammatory response in macrophages is 1ng/ml (Pestka & Zhou, 2006; Zhang & Morrison, 1993). Table 3-3 gives the LPS concentration of a range of proteins purified by the same methods as those used in this project. Given that in this study the maximum treatment dose of PLY *in vitro* is 175nM and that 1ng of LPS is equivalent to 10EU, the purified proteins are below the defined LPS concentration cut-off (table 3-3).

Table 3-3 LPS Concentration in Purified Recombinant PLY and its Derivatives.

Protein	LPS (EU/ μ g of protein)
PLY	0.10
Δ 6PLY	0.073
D123PLY	0.047
D4PLY	0.068
e-PLY	0.37
e- Δ 6PLY	0.98
e-D123PLY	0.37
e-D4PLY	0.067

3.2.2 Preparation of vehicle controls

Vehicle controls were prepared from His-tagged PLY and its derivatives using PureProteome nickel-magnetic beads. The beads were washed with PBS to remove the storage buffer and resuspended in the undiluted protein preparations. Following an incubation period the nickel-bead bound proteins were removed from the suspension using a magnetic rack; the resulting solutions were used as vehicle controls. Finally, proteins were eluted from the beads

using the recommended elution buffer as additional controls. It was not possible to elute either D123PLY or D4PLY from the beads (table 3-4); however, it was possible to achieve total protein removal in all vehicle controls (figure 3-5 shows complete removal of PLY and $\Delta 6$ PLY from vehicle controls). Equal volumes (200 μ l) of protein solution and elution buffer were used and so the reduced protein concentration in elution controls is not a consequence of dilution.

Table 3-4 Protein Concentration of Controls Created using Ni-magnetic Beads

Protein	Starting Conc.	Vehicle Conc.	Elution Conc.
PLY	1.065mg/ml	0mg/ml	0.253mg/ml
$\Delta 6$ PLY	0.786mg/ml	0mg/ml	0.053mg/ml
D123PLY	1.900mg/ml	0mg/ml	0
$\Delta 6$ D123PLY	1.200mg/ml	0mg/ml	0
D4PLY	0.530mg/ml	0mg/ml	0

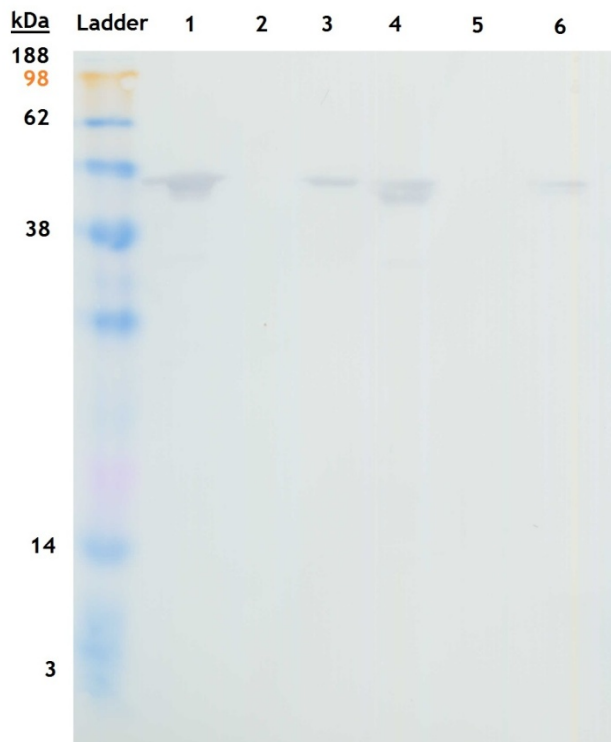


Figure 3-5 Analysis of vehicle controls and eluted proteins following Ni-magnetic bead treatment of PLY and Δ 6PLY.

Purified and eluted proteins were diluted to 1mg/ml (vehicle controls were undiluted) and mixed 1:4 with SDS-PAGE loading buffer. 5 μ l of Seeblue Plus 2 molecular weight marker and 10 μ l of the proteins were loaded into the wells of a 10% SDS-PAGE gel and electrophoresed at 180 V for 40 minutes. The proteins were transferred onto nitrocellulose membrane and detected by western blotting using rabbit anti-PLY (1:1000) and donkey anti-rabbit-HRP (1:2000). The blot was developed using 4-chloro 1-naphthol. Lane 1 =purified PLY, 2= PLY vehicle, 3= eluted PLY, 4=purified Δ 6PLY, 5= Δ 6PLY vehicle, 6= eluted Δ 6PLY.

The haemolytic activity in PLY, PLY vehicle control and PLY eluted control from nickel-magnetic beads was assessed by haemolytic assay (figures 3-6 and 3-7). Haemolytic activity was absent in the vehicle control as expected, however, haemolytic activity was also absent in the eluted PLY control. There is no obvious explanation for the absence of haemolytic activity following nickel-magnetic bead treatment; this is further explored in the discussion section of this chapter.

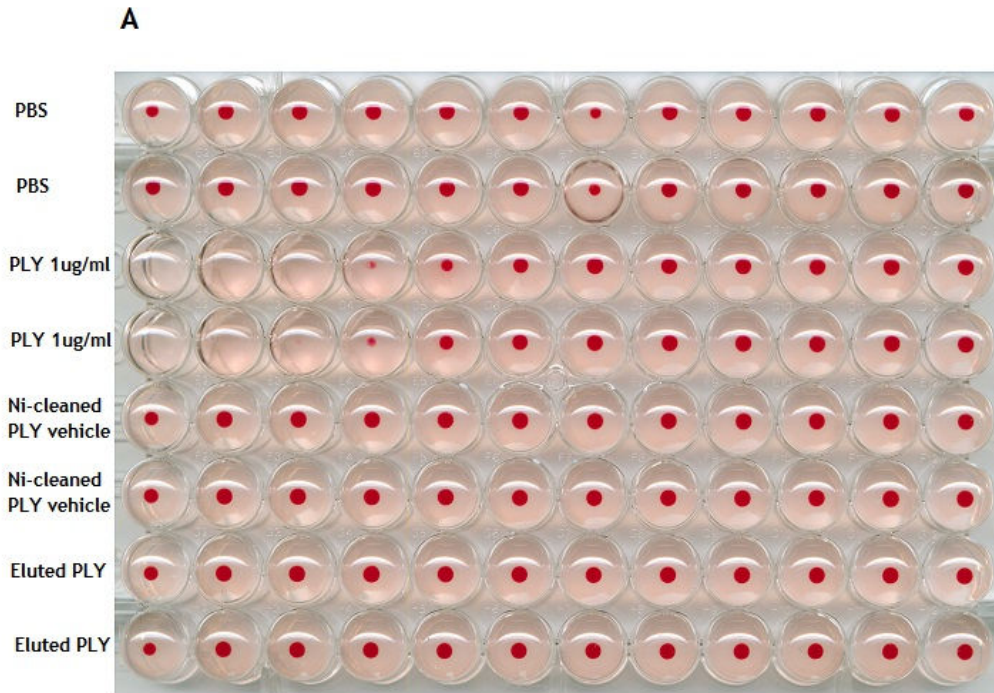


Figure 3-6 Haemolytic assay of purified PLY, Ni-cleaned PLY vehicle and eluted PLY.

Purified PLY was serially diluted from a starting conc. of 1 μ g/ml whereas PLY vehicle and eluted PLY were added neat. Intact erythrocytes were pelleted (A) by centrifugation and supernatants (B) were collected and analysed for the presence of haemoglobin by measuring absorbance at 540nm.

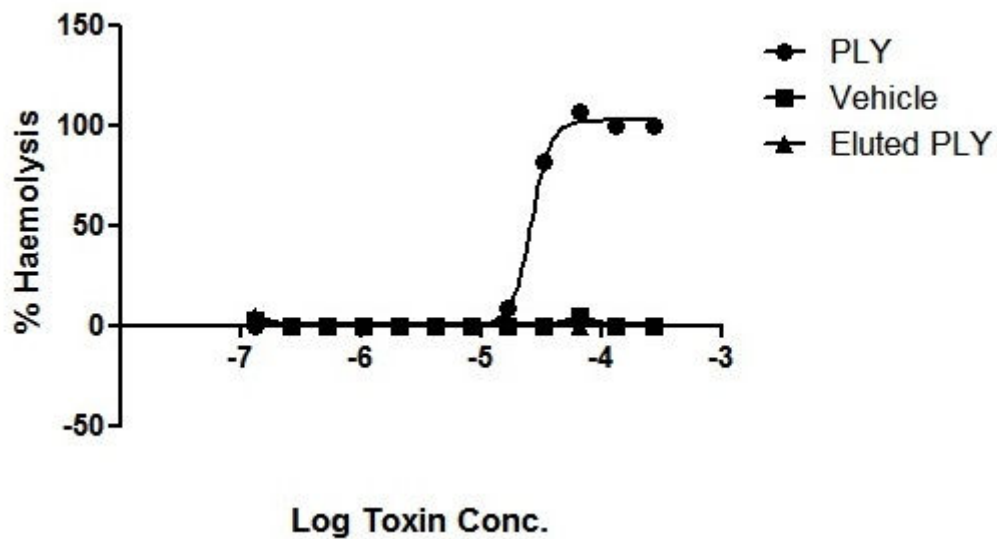


Figure 3-7 Analysis of haemolytic activity of PLY, PLY vehicle and eluted PLY following Ni-magnetic bead treatment.

50 μ l of purified PLY (17.5nM) and 50 μ l of vehicle and eluted PLY controls (prepared with equal volumes as PLY control) were added in duplicate to the first wells of a 96-well plate and serially diluted (1:2) horizontally across the plate. Following incubation with a 2% sheep RBC solution released haemoglobin was measured at 540nm using a Fluostar Optima plate reader. OD measurements were used to create dose response curves in Graphpad Prism and calculate % haemolysis. Data points are mean % haemolysis from two technical replicates per dilution, this experiment was performed once.

Figure 3-8 shows the final SDS-PAGE analysis of PLY, Δ 6PLY, D123PLY, Δ 6D123PLY, D4PLY and their respective vehicle controls. All the proteins and vehicle controls are free from contaminating proteins.

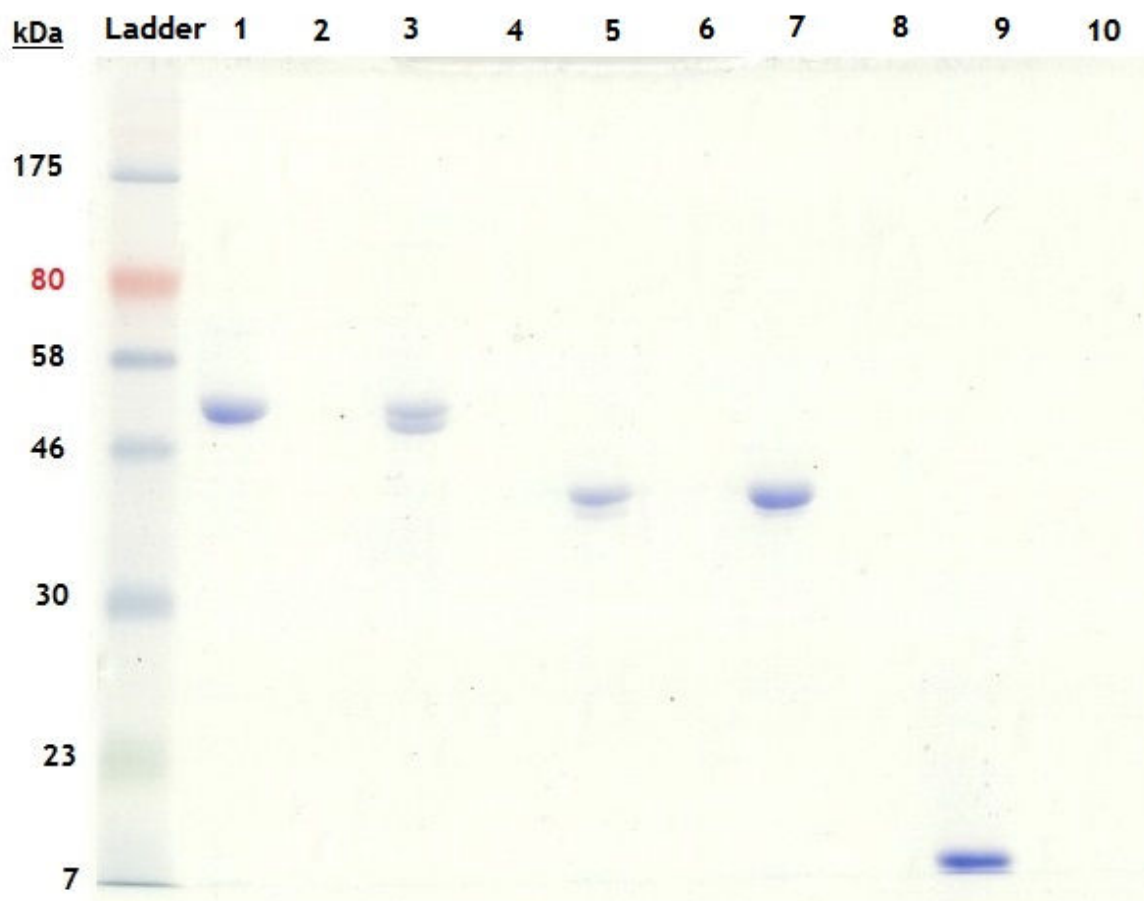


Figure 3-8 SDS-PAGE analysis of purified PLY derivatives.

Purified proteins were diluted to 1mg/ml (vehicle controls were undiluted) and mixed 1:4 with SDS-PAGE loading buffer. 5 μ l of Seeblue Plus 2 molecular weight marker and 10 μ l of the proteins were loaded into the wells of a 10% SDS-PAGE gel and electrophoresed at 180 V for 40 minutes. The gel was subsequently stained using coomassie blue stain. PLY (1), Δ 6PLY (3), D123PLY (5), Δ 6D123PLY (7), D4PLY (9) and their respective vehicle control (2,4,6,8 and 10).

3.3 Is PLY a TLR4 ligand?

The THP-1 blue CD14 cell line (table 2-12) is a reporter cell line stably transformed with a plasmid expressing secreted embryonic alkaline phosphatase (SEAP) in a dose-dependent manner upon ligation of TLR. Human TLR1-10 are expressed by this cell line, upon ligation the transcription factors Nf κ B and AP-1 induce expression of SEAP. A colourimetric assay, QUANTI-Blue™, is used to detect SEAP in cell culture supernatants.

To determine if there were any TLR ligands in the purified proteins THP-1 blue CD14 cells were treated for 24 hours with either purified proteins, their vehicle controls or (where possible) eluted proteins. Protein solutions were prepared

for a final concentration of 175, 17.5 or 1.75nM and vehicle controls solutions were prepared using the same volumes as their respective protein at 175nM. After 24 hours the culture supernatants were collected and analysed for SEAP presence using the QUANTI-blue™ assay (figure 3-9).

The THP-1 blue CD14 cells did not report any TLR activity in the vehicle controls. Interestingly, the cells did respond in a dose-dependent manner to all PLY variants. The production of SEAP was restored in response to vehicle controls when eluted PLY and $\Delta 6$ PLY was added back into the solution. No SEAP is produced in response to 175nM PLY (A), this is likely because of early cell death. As seen in figures 3-6 and 3-7 the elution process abrogated lytic activity in PLY, this results in significant SEAP production in response to eluted PLY at 175nM demonstrating that TLR activation is not dependent on lytic activity. This is mirrored in figure 3-9 (B), non-lytic $\Delta 6$ PLY treatment results in significant SEAP production at all three doses. However, the production of SEAP in response to $\Delta 6$ PLY at doses of 17.5 and 1.75nM was lower than that induced by PLY at the same concentrations; it was for this reason that the $\Delta 6$ D123PLY truncation mutant was created to test the effects of the delta 6 deletion without the confounding factor of pore formation. Both D123PLY and D4PLY induced SEAP production in the THP-1 blue CD14 cell line indicating TLR ligand sites in both domains.

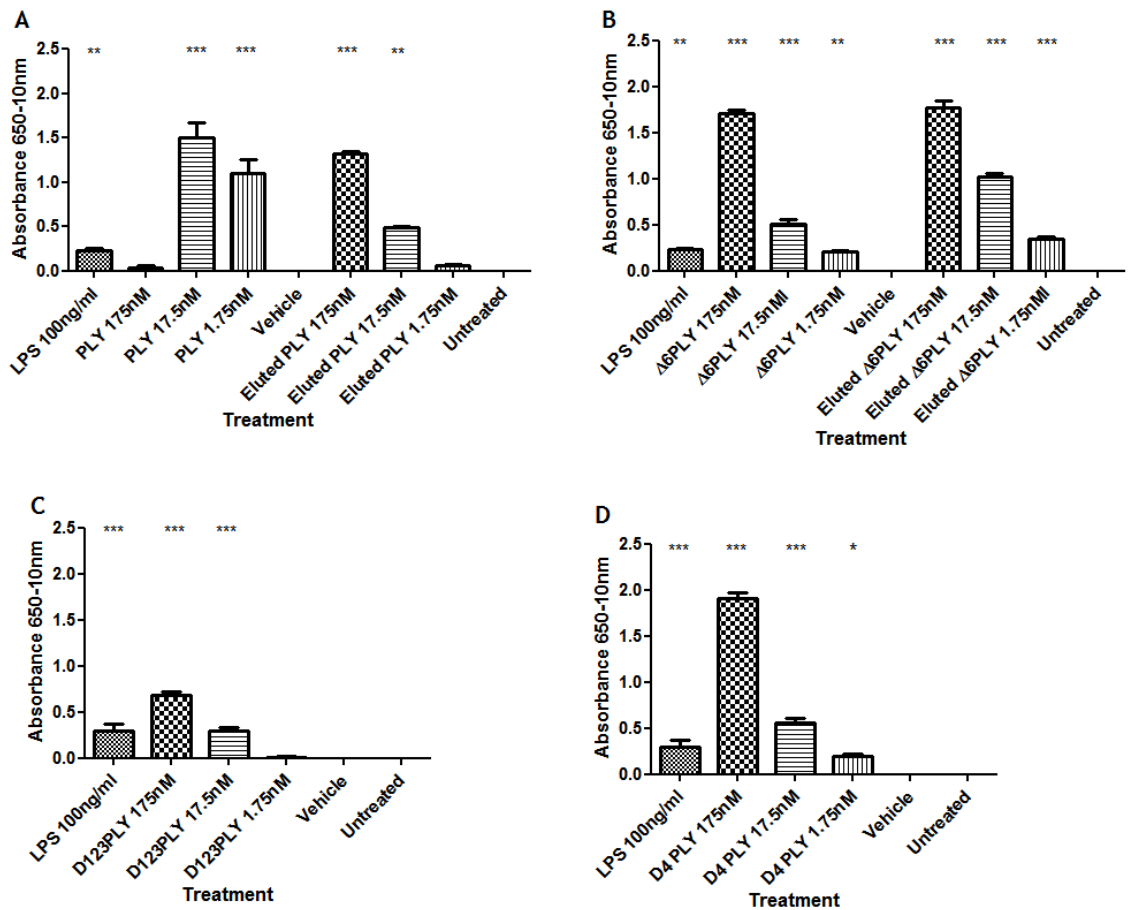


Figure 3-9 SEAP production in THP1-blue CD14 reporter cells following treatment with PLY variants.

Cells were treated with (A) - PLY, (B) - Δ6PLY, (C) – D123PLY and (D) – D4PLY, their respective vehicle controls and where possible eluted proteins. THP1-blue CD14 cells were seeded at 1×10^5 cells/well and treated with PLY variants at 175, 17.5 and 1.75nM in a total well volume of 200μl. Vehicle controls were prepared identically to PLY variants. Following a 24 hour incubation at 37°C supernatants were harvested from treated cells and tested for the presence of SEAP using QUANTI- Blue medium. Statistical significance was tested by one-way ANOVA comparing all columns to the control column (untreated), *(p<0.05), ** (p<0.01), *** (p<0.001). The experiments were performed twice with three technical replicates per condition, data are mean+SEM.

The results using THP-1 blue CD14 cells gave strong indications that PLY could be a TLR4 ligand, to test this further HEK293/TLR4/MD2/SEAP and HEK293/TLR5/SEAP reporter cell lines were tested with full length and truncation versions of PLY. The HEK293 cell lines (table 2-12) are reporters that function similarly to THP-1 blue CD14 cells. The only TLR endogenously expressed by HEK293 cells is TLR5, therefore, it is possible to isolate interactions between individual TLR and PLY using the HEK293/TLR5/SEAP reporter as a control. The HEK293/TLR5/SEAP cell line produced SEAP in response to flagellin but not to LPS or any of the PLY variants (figure 3-10). The HEK293/TLR4/MD2/SEAP cell line responded to both LPS and flagellin (due to

the presence of endogenous TLR5). Figure 3-11 shows that the HEK293/TLR4/MD2/SEAP cell line reported TLR4 ligation in response to $\Delta 6$ PLY, D123 and $\Delta 6$ D123 but not PLY or D4PLY. There was no significant difference in SEAP production between D123 and $\Delta 6$ D123.

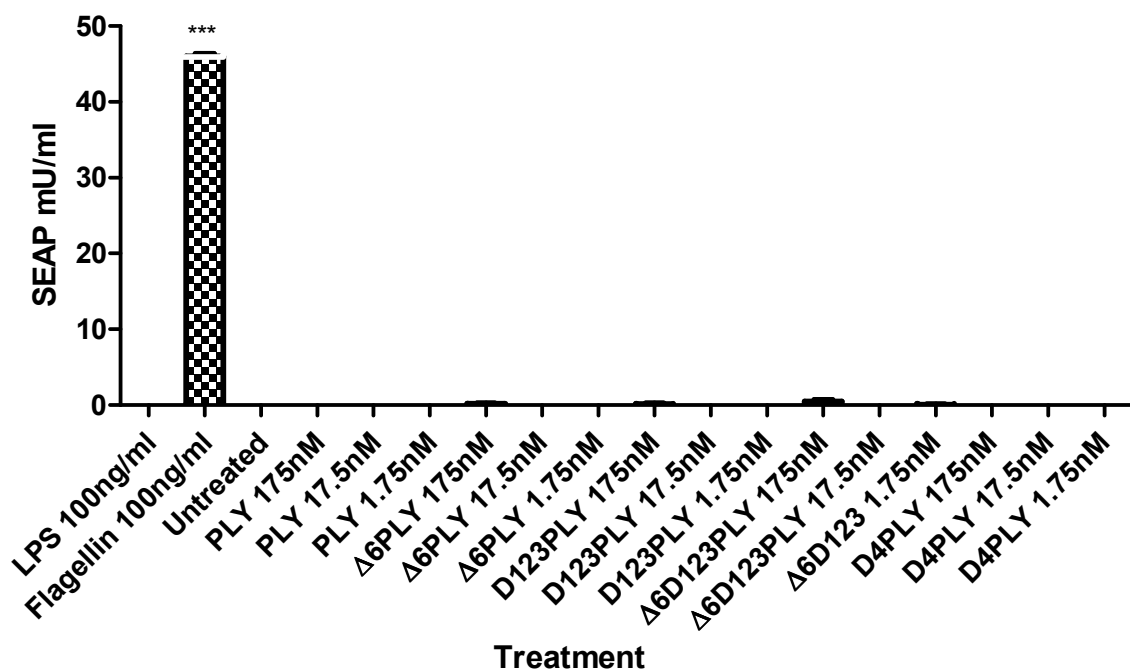


Figure 3-10 SEAP production in HEK293/SEAP/TLR5 reporter cells following treatment with PLY variants.

HEK293/SEAP/TLR5 cells were seeded at 1×10^4 and treated with PLY, $\Delta 6$ PLY, D123PLY, $\Delta 6$ D123PLY or D4PLY at 175, 17.5 or 1.75nM in a total assay volume of 200 μ l for 24 hours at 37°C. Supernatants were harvested from treated cells and the presence of SEAP was tested using QUANTI- Blue medium. A standard curve of purified SEAP was used to quantify the concentration of SEAP in supernatants. Statistical significance was tested by one-way ANOVA comparing all columns to the control column (untreated), *($p < 0.05$), **($p < 0.01$), ***($p < 0.001$). This experiment was performed once with three technical replicates per condition, data are mean+SEM.

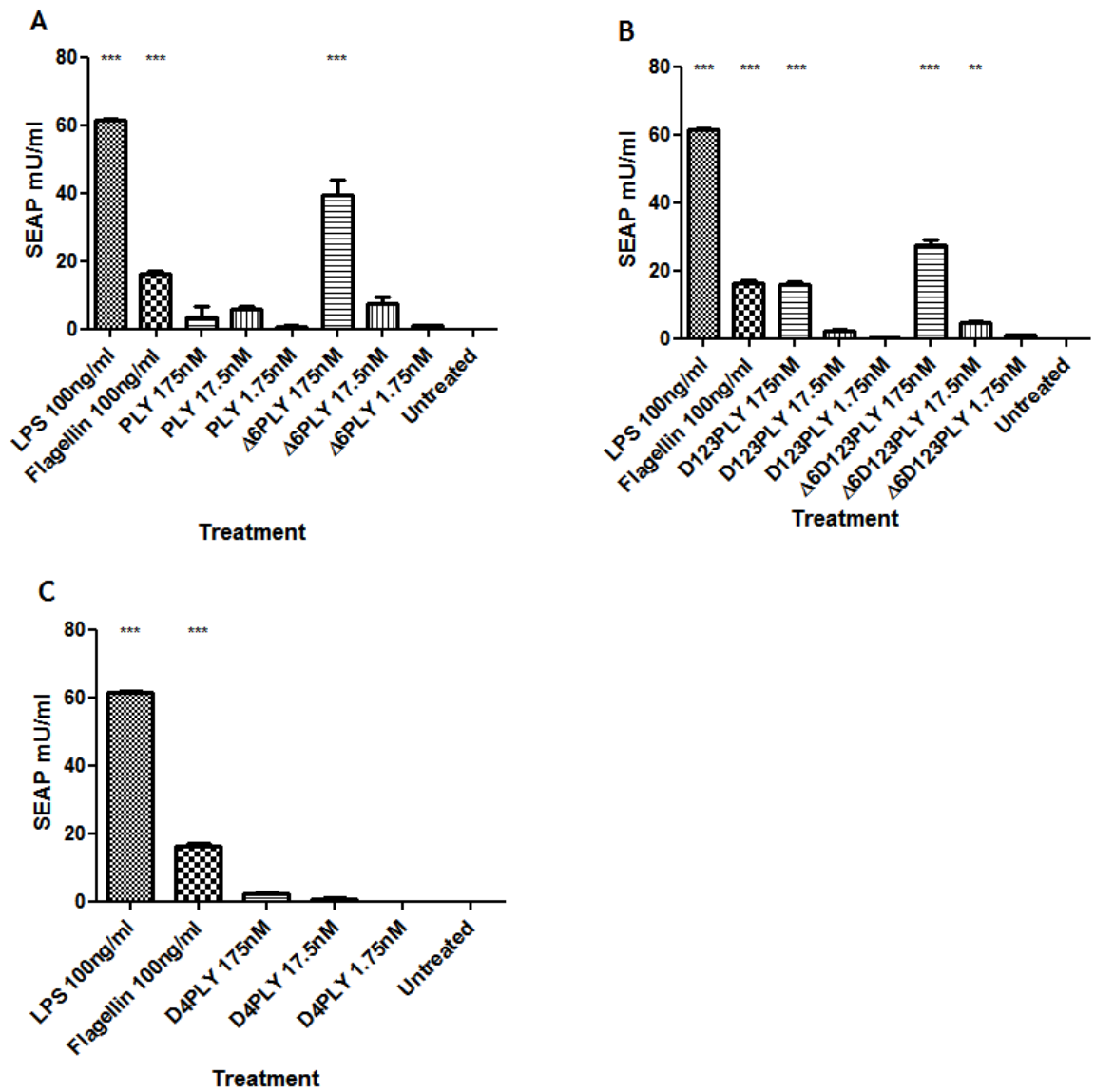


Figure 3-11 SEAP production in HEK293/SEAP/TLR4/MD2 reporter cells following treatment with PLY variants.

HEK293/SEAP/TLR4/MD2 cells were seeded at 1×10^4 cells/well and treated with either (A) – PLY or $\Delta 6$ PLY, (B) – D123PLY or $\Delta 6$ D123PLY or (C) – D4PLY. Cells treated with PLY variants at 175, 17.5 or 1.75nM in a total well volume of 200 μ l for 24 hours at 37°C. Supernatants were harvested from treated cells and the presence of SEAP was tested using QUANTI- Blue medium. A standard curve of purified SEAP was used to quantify the concentration of SEAP in supernatants. Statistical significance was tested by one-way ANOVA comparing all columns to the control column (untreated), *($p < 0.05$), **($p < 0.01$), ***($p < 0.001$). This experiment was performed once with three technical replicates per condition, data are mean+SEM.

These findings concur with those in the literature that show PLY to be capable of binding TLR4, in addition this study identified that domains 1-3 contain the TLR4 binding site. Interestingly, D4PLY showed TLR activity in the THP-1 CD14 blue screen but further analysis has shown that this did not belong to TLR4. This would suggest that D4 also contains an as yet unidentified TLR binding site.

3.4 Cytokine expression in PLY treated BMDM

The cytokine and chemokine profile induced in the initial response to an adjuvant instructs the phenotype of the final immune response (cell type, antibody isotype and clonotype etc.). Initial investigations into the cytokine profile induced by PLY were focussed on IL-6, KC and IL-1 β . PLY has previously been shown to induce IL-6 *in vitro* (Malley et al., 2003; Rijneveld et al., 2002) is induced during pneumococcal infection (Antunes et al., 2002) and has a protective role in pneumococcal disease (van der Poll et al., 1997), little or no IL-6 was found in the BMDM treatment model. In a pilot study of PLY-induced gene expression in the BMDM model, IL-6 was found to be upregulated (appendix). It is possible that the production of IL-6 is a late response and additional time points should be added to the *in vitro* assay as IL-6 was found in BALF of mice following instillation of PLY into the lungs (Kirkham, 2006).

3.4.1 The IL-1 β hypothesis

Interleukin-1 beta is a pleiotropic inflammatory cytokine and its production is tightly controlled, this process can be simplified into two stages caused by pathogen associated molecular patterns (PAMP). The first stage is transcription of pro-IL-1 β mediated by TLR ligation, the second is assembly of the inflammasome which culminates in the catalytic cleavage of Pro-IL-1 β into its active form. Pro-IL-1 β must be catalytically cleaved by caspase-1, which itself exists in precursor form (Pro-caspase-1). Pro-caspase-1 is cleaved into its active form by the inflammasome, a multi-protein platform. The Nod-like receptors NLRC4, NLRP1 and NLRP3 are involved in the assembly of inflammasomes (Franchi et al., 2009), the NLRP3 inflammasome (described in section 1.6.1) is known to be activated by PLY via pore formation.

It was hypothesized that as PLY is a putative TLR4 ligand and induces NLRP3 activation via pore formation that IL-1 β would be expressed and secreted in BMDM in response to PLY treatment. As IL-1 β is a highly inflammatory cytokine it was thought that this could explain the difference in the magnitude of antibody titres seen in response to e-PLY and e- Δ 6PLY immunization (figure 3-12).

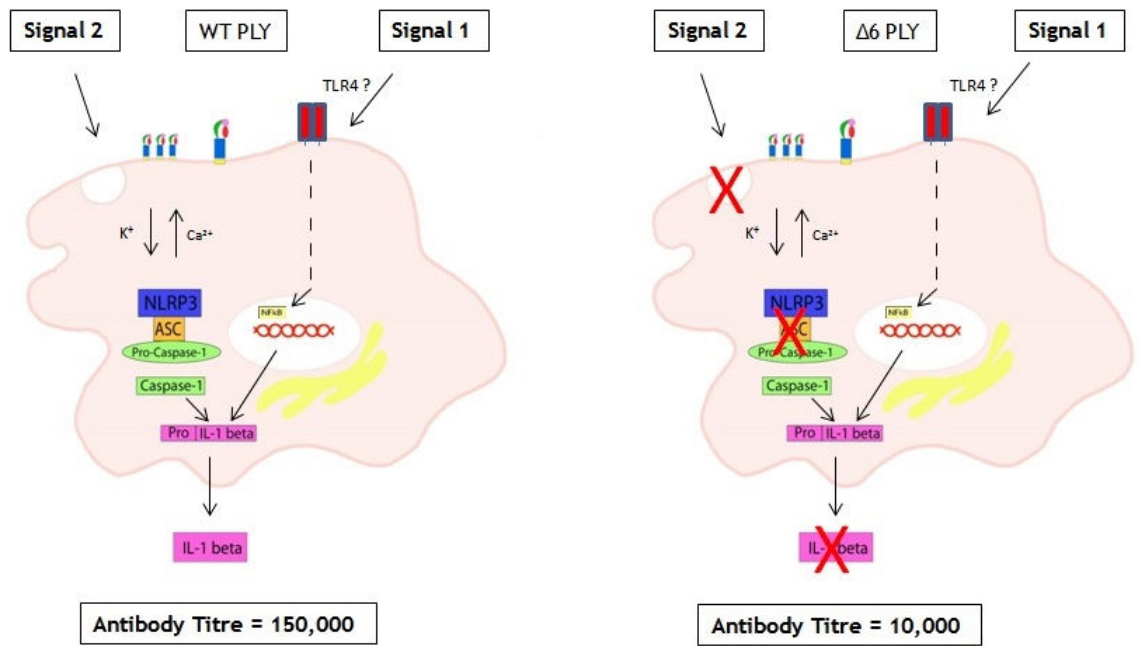


Figure 3-12 The IL-1 β hypothesis.

As shown in figure 3-13 PLY treated BMDM do not produce IL-1 β in response to treatment with either PLY or $\Delta 6$ PLY alone. However, IL-1 β is produced in a dose-dependent manner in response to PLY where a 2 hour pre-treatment with 100ng/ml LPS has been given.

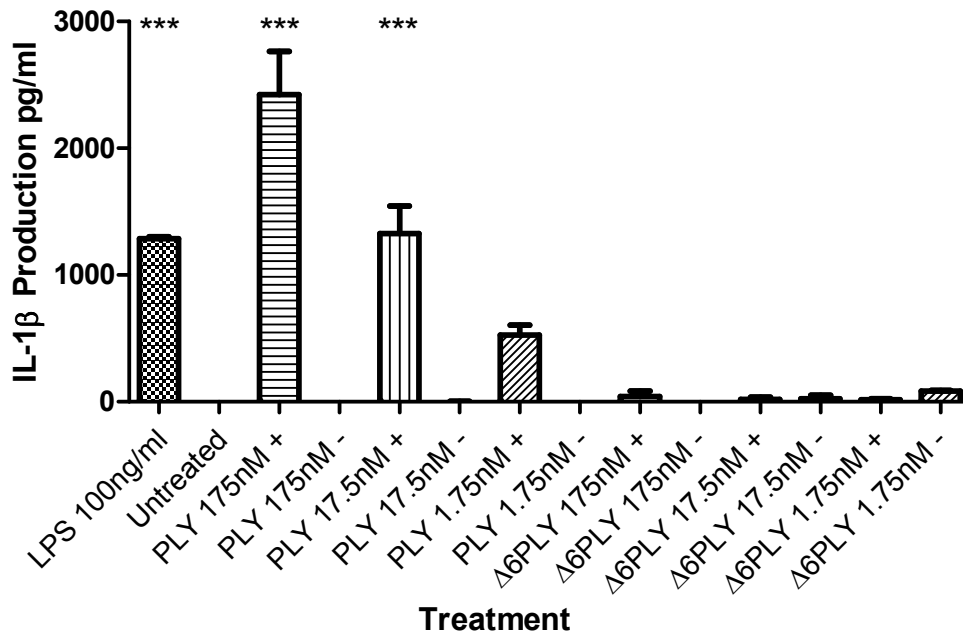


Figure 3-13 IL-1 β production in BMDM treated with PLY or Δ 6PLY.

BMDM were seeded at 1×10^5 /well in a 96-well plate. A 2 hour pre-treatment with 100ng/ml LPS was given to half of the seeded cells (200 μ l total well volume). After two hours all cell supernatants were removed and replaced with either 100ng/ml LPS, medium, PLY or Δ 6PLY at 175, 17.5 or 1.75nM (200 μ l total well volume) and incubated for 6 hours at 37°C. The cell supernatants were harvested and IL-1 β was measured by ELISA. Statistical significance was tested by one-way ANOVA comparing all columns to the control column (untreated), *($p < 0.05$), **($p < 0.01$), ***($p < 0.001$). This experiment was performed three times with three technical replicates per condition, data are mean+SEM.

This study has shown that in the BMDM model of PLY treatment IL-1 β is not produced in response to PLY alone, this is unexpected as results from this chapter clearly show that PLY is capable of TLR-binding and PLY is known to activate the NLRP3 inflammasome (McNeela et al., 2010). Therefore the hypothesis of IL-1 β production initially proposed is not true (at least in this cell type) as shown in figure 3-14.

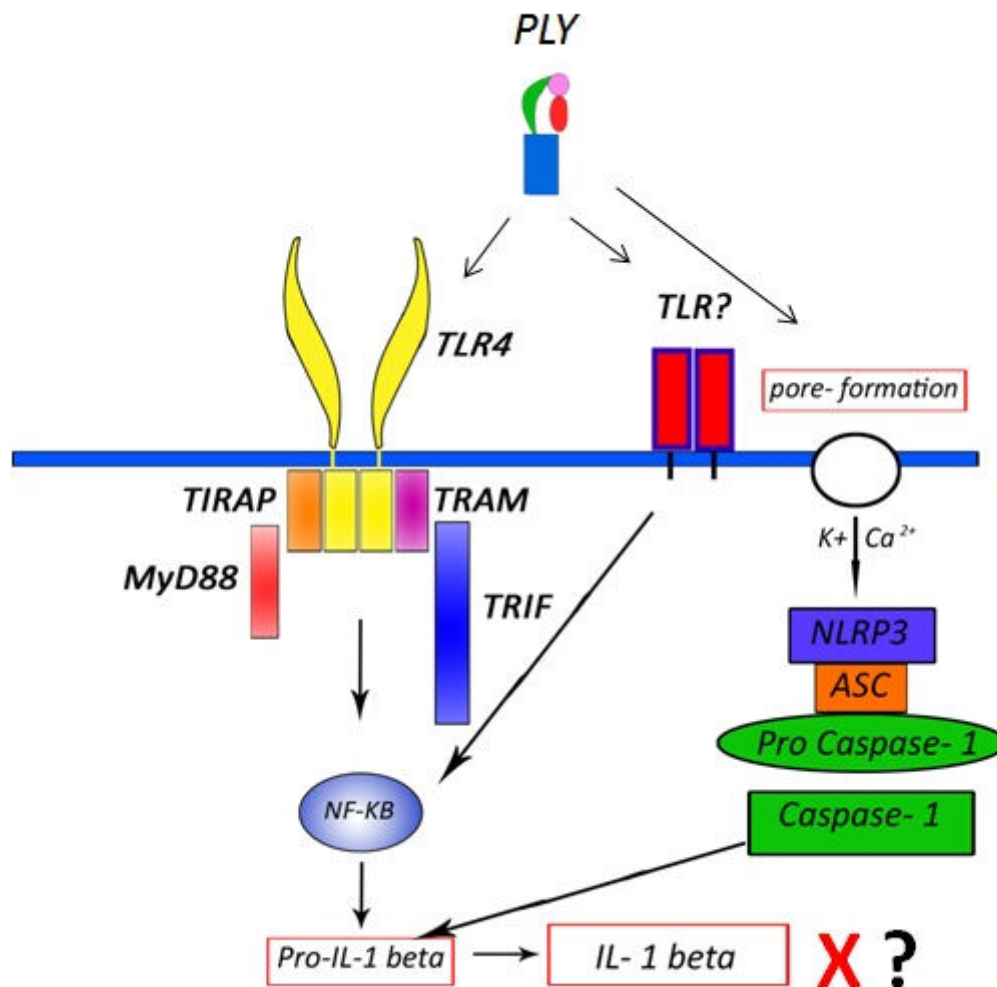


Figure 3-14 Putative model of PLY-dependent IL-1 beta production, version 1.

This model of IL-1 β production, where PLY induces Pro-IL-1 β via TLR stimulation and mediates its cleavage into active IL-1 β through activation of the NLRP3 inflammasome by pore formation does not result in IL-1 β production in BMDM.

3.4.2 KC expression in response to PLY and the role of TLR4

KC is the murine homologue of IL-8 (CXCL-1). This chemokine is highly chemotactic for neutrophils and is rapidly upregulated by tissue resident macrophages in response to ligation of TLR2, 3 and 4 (Filippo et al., 2013a). BMDM produced significant concentrations of KC in response to PLY, Δ 6PLY and D123 but not D4PLY (figure 3-15(A)). In a model using BMDM generated from TLR4^{-/-} mice KC was produced in response to full length PLY variants only and the KC previously seen in response to D123 was lost (figure 3-15(B)).

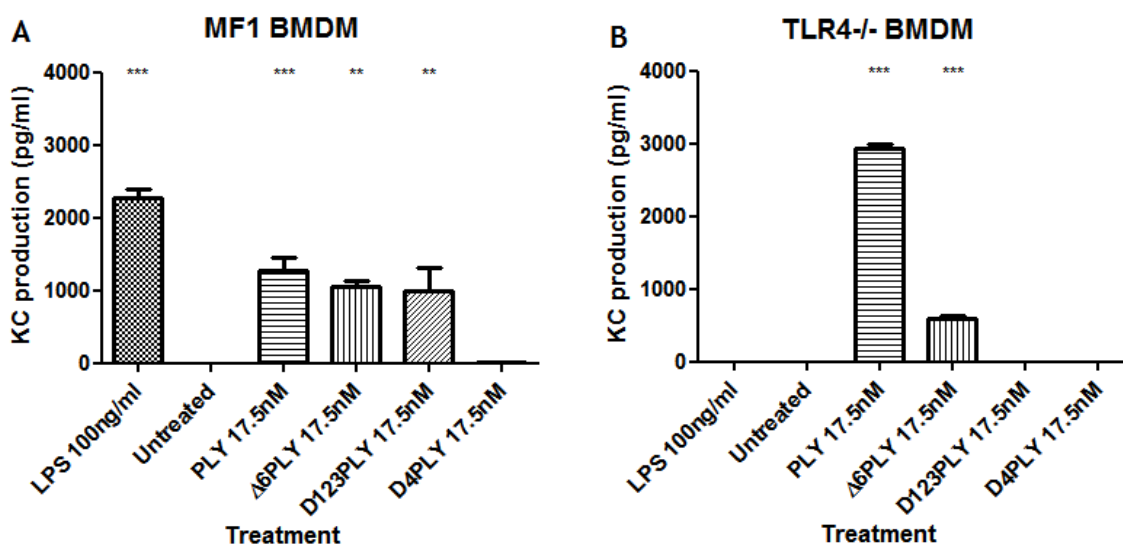


Figure 3-15 KC production in (A – MF1) or (B – TLR4^{-/-}) BMDM treated with either PLY, Δ6PLY, D123PLY or D4PLY.

BMDM were seeded at 1×10^5 cells/well and treated with either 100ng/ml LPS, culture medium (untreated control) or PLY variants at 17.5nM (200μl total well volume) for 6 hours at 37°C. The cell supernatants were harvested and KC was measured by ELISA (R AND D SYSTEMS). Statistical significance was tested by one-way ANOVA comparing all columns to the control column (untreated), *($p < 0.05$), **($p < 0.01$), ***($p < 0.001$). This experiment was performed twice with three technical replicates per condition, data are mean+SEM.

3.5 Discussion

All PLY variants were tested for haemolytic activity and behaved as expected, only Δ6 deletion and truncation mutants lacked lytic activity (figure 3-1). There is variability in the HU/pmol between lytic versions of PLY, particularly where PLY has been N-terminally tagged with eGFP. This is possibly due to variability in the quality of protein preparations; PLY is known have reduced haemolytic activity following long-term storage, particularly if stored above -80°C or if subjected to freeze-thaw. If the reduction in haemolytic activity is due to N-terminal fusion it may give insight into the process of pore formation; there is still some debate as to whether pore formation begins with assembly of the pre-pore on the cell surface before insertion into the membrane, or, if PLY monomers assemble into a pore after insertion of individual monomers. The fact that haemolytic activity is retained demonstrates that PLY is amenable to N-terminal tagging and that structural integrity of the protein is unaffected, this is important as it suggests that other functions of the toxin are unlikely to be affected by fusion to potential vaccine antigens. It is possible that fusion

proteins physically inhibit formation of a complete pore in some instances by interrupting oligomerization or preventing the domain rotation necessary for membrane insertion; this could be visualized by electron microscopy. If the tag is indeed interrupting oligomerization it is likely to have a greater effect once PLY is membrane bound (as the monomer would be less mobile) suggesting that the pre-pore assembles on the cell surface. A study of pore-formation by cryo-electron microscopy has visualised the conformational change required for pore-formation occurring after oligomerization (Tilley et al., 2005) and the evidence put forward in this chapter would concur with that model.

Analysis of pore formation by LDH release revealed that there were dramatic differences in PLY sensitivity in different cell types. In figure 3-2, both L929 and RAW 264.7 cells showed less than 20% lysis following 1 and 3 hours incubation with PLY at 175nM, however by 6 hours there was a marked difference in lysis at the highest PLY concentration (50 and 100%, respectively). In contrast, following 3 hours incubation with 175nM PLY BMDM showed ~50% lysis and this did not increase significantly with time (figure 3-3). This would suggest that BMDM are initially more susceptible to PLY-mediated pore formation compared to L929 and RAW 264.7 cells but have greater resistance to pore formation/membrane disruption over time. A study by Hirst et al. examining the differences in PLY sensitivity between epithelial and monocytic cells suggested that differences in both membrane cholesterol levels and dynamics of the plasma membrane could explain the variation in sensitivity, for example, certain cell types have been shown to shed toxin-bound membrane and even repair damaged areas of membrane by excising pores via endocytosis (Cassidy & O’Riordan, 2013). It could also be possible that differences in the differentiation state of these cells results in variations in sensitivity, THP-1 cells are monocytic, RAW264.7 are in fact an immature macrophage or monocyte/macrophage phenotype whereas BMDM are fully differentiated, mature (but not activated) macrophages and may be more capable of membrane repair by endocytosis. A study of sensitivity to SLO in monocyte/macrophage cell lines demonstrated that cells with a more mature phenotype were more resistant to SLO-mediated lysis (Tanigawa et al., 1996). Furthermore, in a study of cell susceptibility to streptolysin-O (SLO) mediated lysis it was found that inhibition of cholesterol synthesis had a protective effect. It may be of interest

to investigate the variation in membrane cholesterol between the cell types studied as well as the possibility of PLY-induced changes in cholesterol synthesis.

Compared to nucleated cells RBC are far more sensitive to PLY-mediated lysis; although the assays are not directly comparable (due to variations in cell number, assay volume, duration and output) by extrapolating the number of PLY monomers/cell at the point at which 50% lysis occurs the equivalent number at the same cell concentration as the LDH assays can be calculated as 5.4nM. This level of lysis is reached after a treatment time of 30 minutes, far earlier than any of the nucleated cells tested which at 30 minutes showed no observable lysis. An approximate ranked order of PLY sensitivity for all cells types studied is shown in table 3-5. Following analysis of PLY-dependent lysis in L929, RAW264.7 and BMDM PLY conc. of 175, 17.5 and 1.75nM were chosen for future treatment models to ensure a wide range of lytic activity.

Table 3-5 Ranked Order of Cell Sensitivity to PLY-mediated Lysis.

* LDH release was not investigated for THP-1 or HEK 293 reporters, however, based on observations of reduced SEAP at 175nM PLY at 6 hours they are judged to be at least as sensitive to PLY mediated lysis as the RAW264.7 cells.

Name	Cell Type	PLY conc. at which 50% lysis Occurs (nM)/time
RBC	Erythrocyte	5.4nM/30 mins
HEK293	Unknown/ epithelial-like	*
THP-1	Monocyte	*
RAW 264.7	Monocyte/immature macrophage	25nM/6 hours
L929	Fibroblast	100nM/6 hours
BMDM	Macrophage	175nM/6 hours

The use of Ni-magnetic beads has proven to be an effective method for creating vehicle controls and is able to remove all toxin/toxoid from solution (table 3-4, figure 3-5). However, this method would not be a suitable alternative for protein purification as elution of bound protein from the beads was not possible

for truncation mutants and resulted in total loss of cytolytic activity in PLY (figures 3-6 and 3-7). It appears that PLY has been in some way denatured or damaged in the binding or elution process. It may be possible to optimize the elution buffer to improve removal from the beads; the elution buffer is a simple solution of 50mM sodium phosphate, 300mM sodium chloride and 300mM imidazole (pH8) and does not differ substantially from the elution buffer used in NAC (appendix). Increasing the concentration of imidazole could cause elution of the truncations; however, it seems unlikely that modifying the elution buffer would allow retention of lytic activity in PLY. It will be of interest to investigate the loss of lytic activity during Ni-magnetic bead treatment as this could lead to a method for chemical detoxification of PLY.

Although purified proteins were shown to have acceptably low levels of LPS, the absence of response in reporter cells treated with vehicle controls has increased confidence that the presence of even low levels of LPS can be ruled out as a cause of TLR4 activation in PLY treated cells (figures 3-9, 3-10 and 3-11).

New evidence has been found to support the claim that PLY is a TLR4 ligand and additionally suggests that there could potentially be more than one TLR site within PLY. The TLR4 binding site was found to reside in domains 1-3 of PLY and was not affected by the $\Delta 6$ mutation (figure 3-11). As discussed above, the THP-1 blue CD14 cell line is particularly susceptible to PLY at the highest conc. (175nM) and this resulted in absent or weak SEAP responses at this dose, the same was true of the HEK293 cell line. Interestingly, when PLY eluted from Ni-magnetic beads lacking lytic activity was used to treat the cell line a higher SEAP response than that of $\Delta 6$ PLY was observed; this suggested that the delta 6 mutation did in some way interfere with TLR ligation. However, when this was investigated using the $\Delta 6$ D123PLY truncation mutant no difference could be found, this may suggest that the delta 6 mutation has an effect on the full-length protein but not on domains 1-3 in isolation. Previously, it has been shown that the apoptotic response to PLY is mediated by TLR4 (Srivastava et al., 2005), the data presented in this chapter would suggest that the apoptotic mechanism is also dependent on pore formation, as the presence of a TLR4 site in domains 1-3 did not induce apoptosis where cells were treated with the truncation mutant D123PLY (figure 3-4).

Interestingly, THP-1 blue CD14 cells indicated a TLR site within domain 4 of PLY, however, this should be confirmed with the use of HEK293/SEAP reporter cell lines to clearly demonstrate if an additional TLR is inducing the response seen in THP-1 blue CD14 cells. This is particularly important as both reporter cell lines produce SEAP in an NF κ B-dependent manner; although the HEK293/TLR5 reporter could be interpreted as showing that the SEAP response is not a result of non-specific PLY-mediated NF κ B activation, a HEK293/NF κ B/SEAP control cell line should be used as a definitive control. Domain 4 of PLY is essential for pore formation (Baba et al., 2001) and contains the undecapeptide common to the cholesterol-dependent cytolysin family (Jacobs et al., 1999). The identification of a TLR-binding site within domain 4 could help to identify further functions of domain 4 in the immunological response to PLY.

The role of TLR4 in cytokine production has been investigated and has given insights into the immunogenic properties of the different domains of PLY. Analysis of KC production in PLY treated BMDM has shown that D4PLY alone is not capable of stimulating KC production but that D123PLY alone is (figure 3-15). Both PLY and Δ 6PLY induced KC in a TLR4-independent manner, however, the production of KC in response to D123PLY alone was TLR4-dependent. As the production of KC in macrophages is mediated by stimulation of TLR2, 3 and 4 (Filippo et al., 2013) this provides further evidence that PLY may contain Toll-like receptor binding sites other than TLR4. This could also suggest that there is either an additive effect where both domains are required or that in creating the truncation mutants an immunogenic region of the protein has been disrupted or removed.

Initial studies into the production of IL-1 β have shown that PLY alone is not capable of inducing IL-1 β production. This concurs with other studies of PLY-treated BMDM where an additional TLR ligand was required to induce release of IL-1 β into the cell supernatants (Malley et al., 2003). This does not rule out the hypothesis that IL-1 β is involved in the adjuvant activity of PLY and this hypothesis is further investigated in chapter 5. BMDM were chosen for this *in vitro* model as IL-1 β production is regulated by a two signal process (detailed in chapter one). Unlike BMDM, human blood monocytes are capable of producing mature IL-1 β following treatment with TLR2 and TLR4 ligands, this is due to a

combination of constitutive caspase-1 activation and upregulation of ATP in response to TLR ligation (Netea et al., 2009). Cell types such as THP-1 and RAW264.7 are monocytic and therefore do not have the same requirements for IL-1 β production as mature macrophages, this may explain why IL-1 β has been seen in response to other PLY treatment models.

To conclude, this chapter has shown that the proteins used throughout this project are of high purity and has increased confidence that the immunological responses observed are due to PLY or its variants and not contaminants such as LPS. An essential role for domains 1-3 in the production of KC has been identified and this has been shown to be at least partially TLR4-dependent. Finally, analysis of TLR activation by PLY and its derivatives has identified TLR binding sites within PLY, a TLR4 site within domains 1-3 and potentially an additional TLR binding site within domain 4 of PLY. This could prove to be an essential feature of the adjuvant activity of PLY.

4. Investigating Direct Interactions between PLY and Mammalian Cell Receptors and Cytoskeleton

PLY is known to interact with cholesterol (Tveten, 2005b) and is thought to interact with TLR4 (Malley et al., 2003); we sought to discover other potential interactions with host cell molecules that may contribute to adjuvanticity through both fluorescence microscopy and pull-down experiments.

The multifunctional HaloTag® technology (Promega) was utilized in this study as the HaloTag® can interact with multiple synthetic ligands to allow microscopy, protein purification and pull-down studies to be performed after creating a single construct. We analysed cell localization and protein: protein interactions by fluorescence microscopy and mass spectrometry. Interactions between full-length PLY, $\Delta 6$ PLY and the functional domains D123PLY and D4PLY with the mouse macrophage cell line RAW 264.7 were analyzed.

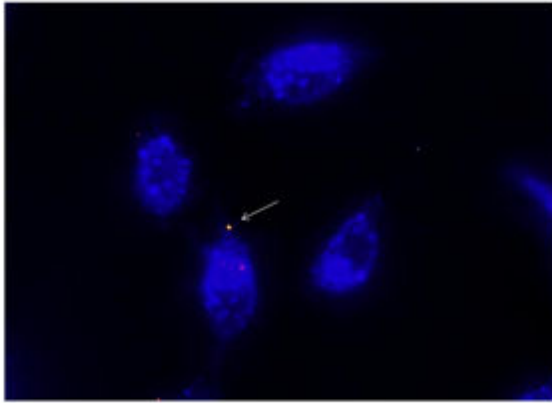
4.1 Analysis of Binding of PLY and its Derivatives to Mammalian Cells by Confocal Fluorescence Microscopy

In this study, the binding patterns of PLY variants were analyzed as well as the gross morphological changes induced in PLY treated cells. It was shown that all HaloTag-PLY variants were able to bind directly to the cell surface and that this was not dependent on the HaloTag itself. It was also shown that each PLY variant had a unique pattern of distribution across the cell surface.

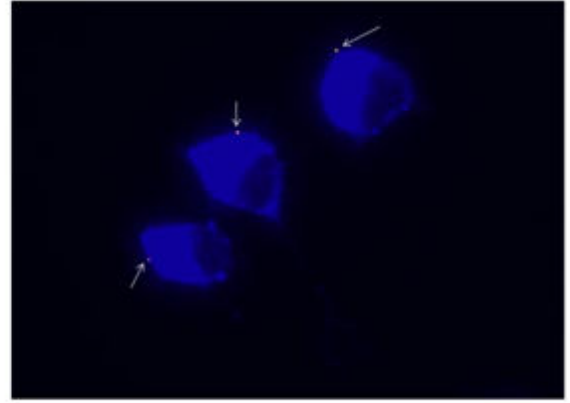
Initially, the rapidity of PLY binding to the RAW 264.7 cell lines was analysed to gauge the most appropriate time point for image capture. Although the RAW 264.7 cell line was particularly susceptible to lysis by PLY at later time points (3-6hrs) (figure 3-2) it was resistant to lysis up to 1 hour after toxin addition at 17.5nM. Too high a concentration of toxin could disrupt the cell membranes to the extent that visualisation by microscopy is impossible. A toxin concentration of 17.5nM typically gave the greatest biological response (e.g. SEAP production), therefore, this concentration struck a balance between cellular responses and cytotoxicity. Incubation times of 30 seconds, 2, 5, 10 and 30 minutes were

selected for analysis. In figure 4-1 h-PLY can be seen to bind RAW 264.7 cells rapidly, within thirty seconds a single focus of h-PLY binding can be observed, the image at 2 minutes shows a similar level of binding however by 5 minutes there are multiple h-PLY foci on the cells. The observable binding of h-PLY increases over time and by 30 mins there is considerable binding of h-PLY to the cells. Figure 4-1 also shows the changes in cell morphology that develop over time and with increased PLY-binding; after 30 seconds exposure to the toxin RAW 264.7 cells have a healthy morphology, although signs of increased filopodia can be observed, this is even more noticeable after 2 minutes and the cells now appear “stressed”. The cells have become distinctly rounded after 5 minutes exposure and this increases up to 30 minutes where the cells appear obviously rounded and have no visible projections such as filopodia, this may be a sign of imminent detachment. For future binding analysis a concentration of 17.5nM and 30 minutes incubation was used for all PLY variants.

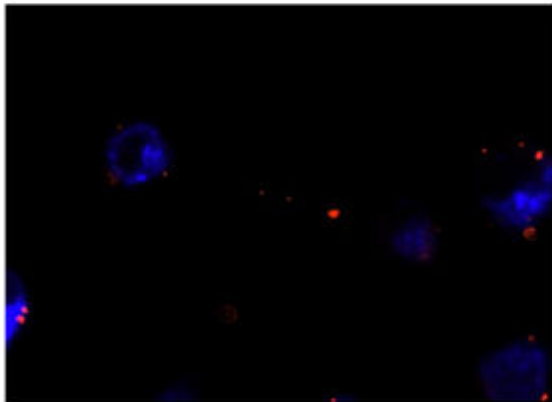
30 seconds



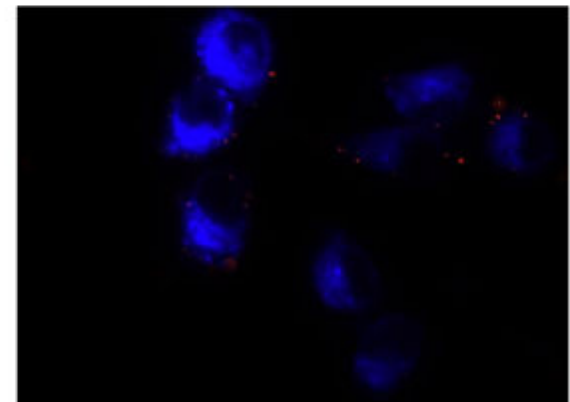
2 minutes



5 minutes



10 minutes



10 minutes

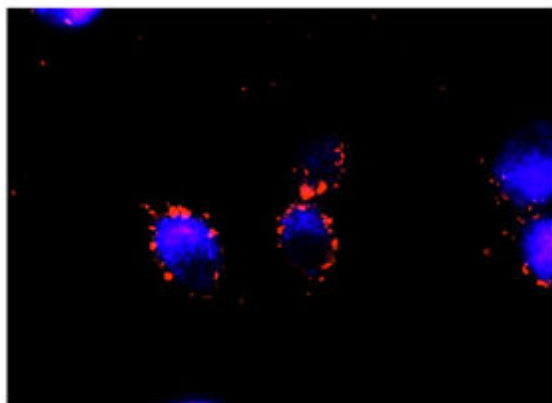


Figure 4-1 Analysis of h-PLY binding to RAW264.7 cells at different incubation times.

RAW 264.7 cells were seeded at 1×10^6 /well in a 6-well flat bottomed plate containing cover slips and allowed to adhere O/N. The cells were treated with approximately $1 \mu\text{g/ml}$ h-PLY (1ml total well volume) from lysates and incubated with the toxin for 30 seconds, 2, 5, 10 or 30 minutes before washing with warm PBS and staining with Deep-red plasma membrane stain (Alexa 647) and Halo-TMR direct ligand (RFP). The cells were fixed in 4% paraformaldehyde before a final rinse in PBS. The cover slips were removed and mounted onto microscope slides using Dako Fluorescent Mounting Media, images were captured using the Zeiss-axio imager at 100X magnification. This experiment was performed once, multiple images were taken at each time point and the above were selected as representative images. The arrows in images taken at 30 seconds and 2 minutes highlight areas of h-PLY binding that are less obvious than those in subsequent images.

4.1.1 Analysis of PLY binding using HaloTag technology

Figure 4-2 shows that the distribution of PLY across the cells is punctate and there does not seem to be a particular focal binding site. Instead PLY is evenly distributed across the image, membrane shedding can be observed and deep-red plasma membrane staining shows that membrane integrity has been disrupted. Compared to cells treated with the control h-eGFP which have a bipolar or tripolar morphology, around 50% of the h-PLY treated cells have become rounded indicating that the cells are in the process of detaching.

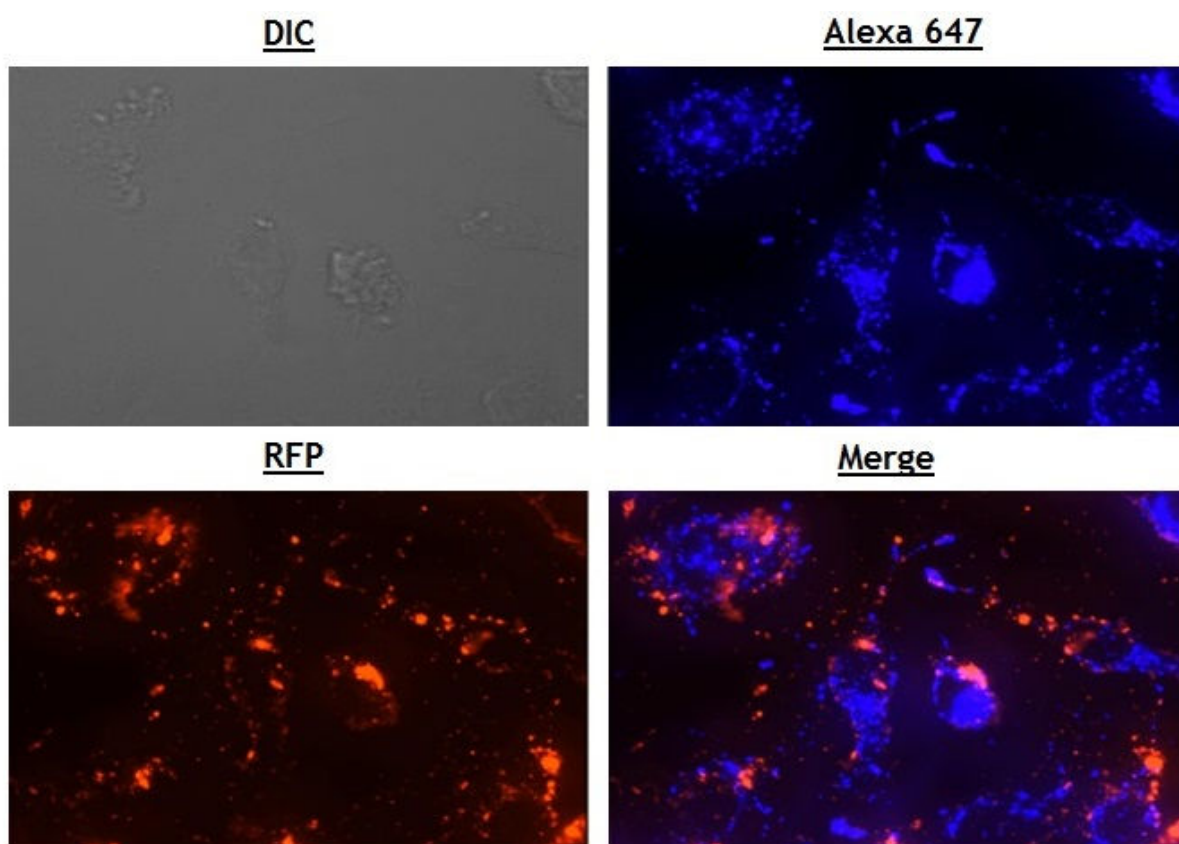


Figure 4-2 2D merged image of h-PLY treated RAW 264.7 cells stained with CellMask Deep-red plasma membrane stain and HaloTag TMR-direct ligand.

RAW 264.7 cells were seeded at 1×10^6 /well in a 6-well plate containing cover slips and allowed to adhere O/N at 37°C. The cells were treated with h-PLY lysate diluted in culture medium to a final conc. of 17.5nM (1ml total well volume). The cells were incubated for 30 minutes before staining with CellMask Deep Red plasma membrane stain and HaloTag TMR-direct ligand according to the protocol in section 2.8.1.1. The cells were fixed in 4% paraformaldehyde before a final rinse in PBS. The cover slips were removed and mounted onto microscope slides using Dako Fluorescent Mounting Media, images were captured using the Zeiss-axio imager at 100X magnification. Images of the cells were captured using DIC (differential interference contrast) and using RFP and Alexa-647 channels to create a merged image. This experiment was performed twice, multiple images were taken of each slide and the above was selected as a representative image.

3D image analysis (figure 4-3) shows PLY distributed both around the edges of the cells and visible within the cell; it is unclear if PLY has entered the cell passively (either through pores formed by cytolysis or lack of membrane integrity) or has been actively taken into the cell by endocytosis.

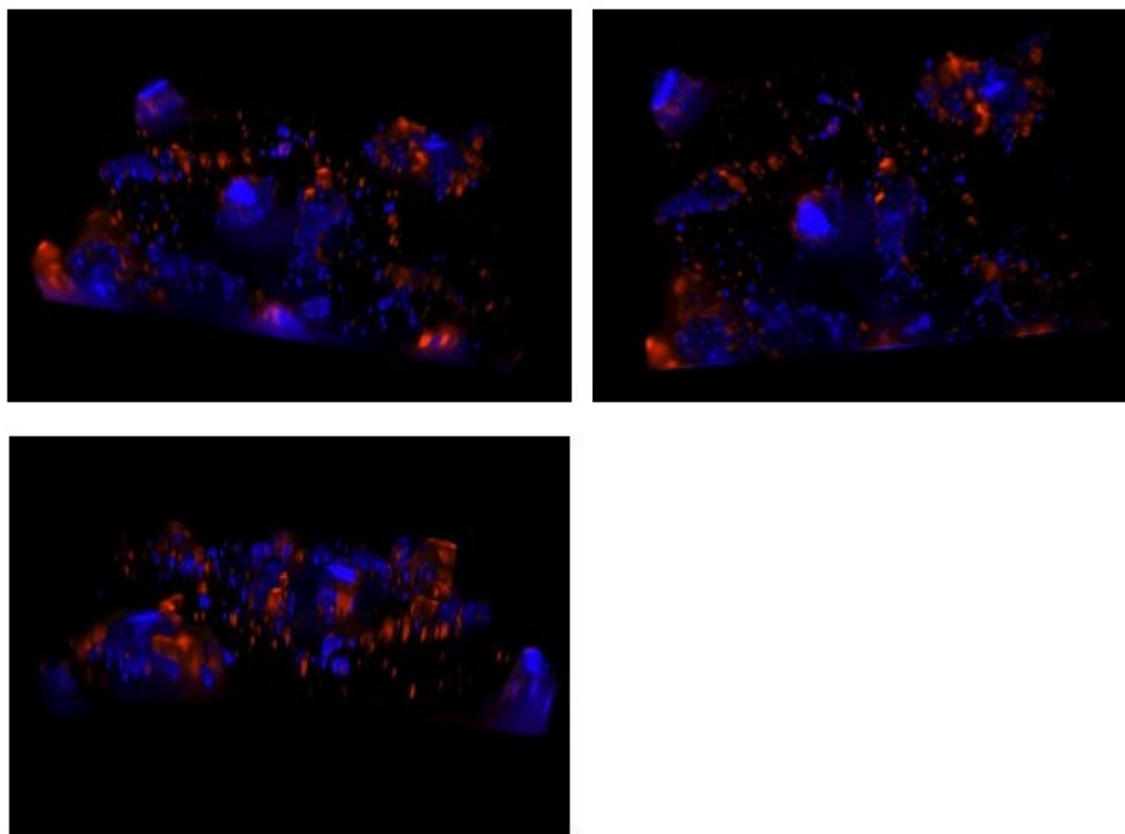


Figure 4-3 3D image of h-PLY treated RAW 264.7 cells stained with Deep-red plasma membrane stain and Halo TMR-direct ligand.

The z-stacks of image 4-2 were combined using Volocity® software to create a 3D image of h-PLY binding to the RAW 264.7 cell lines. The software was also used to create a movie of this image by compiling snapshots taken from different angles, this movie can be viewed in the compact disk accompanying this thesis.

4.1.2 Analysis of $\Delta 6$ PLY binding using HaloTag technology

While h-PLY clearly damaged the cell membranes of treated cells, h- $\Delta 6$ PLY treated cells maintained cell membrane integrity (figure 4-4). The punctate distribution pattern seen with h-PLY is also seen with h- $\Delta 6$ PLY. In addition, the binding particles appear to be larger.

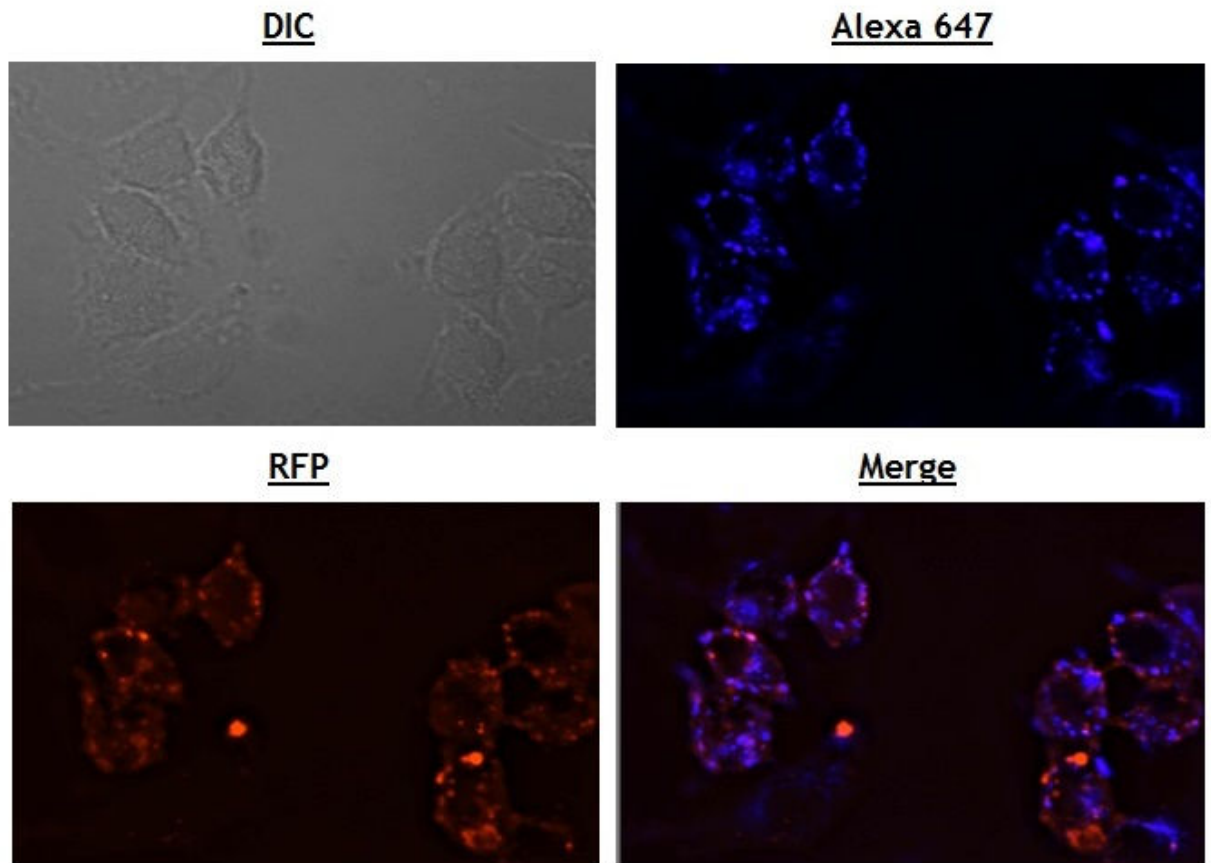


Figure 4-4 2D merged image of h- Δ 6PLY treated RAW 264.7 cells stained with CellMask Deep Red plasma membrane stain and HaloTag TMR-direct ligand.

RAW 264.7 cells were seeded at 1×10^6 /well in a 6-well plate containing cover slips and allowed to adhere O/N at 37°C. The cells were treated with h- Δ 6PLY lysate diluted in culture medium to a final conc. of 17.5nM (1ml total well volume). The cells were incubated for 30 minutes before staining with CellMask Deep Red plasma membrane stain and HaloTag TMR-direct ligand according to the protocol in section 2.8.1.1. The cells were fixed in 4% paraformaldehyde before a final rinse in PBS. The cover slips were removed and mounted onto microscope slides using Dako Fluorescent Mounting Media, images were captured using the Zeiss-axio imager at 100X magnification. Images of the cells were captured using DIC (differential interference contrast) and using RFP and Alexa-647 channels to create a merged image. This experiment was performed twice, multiple images were taken of each slide and the above was selected as a representative image.

It is clearer from the 3D analysis of h- Δ 6PLY treated cells in figure 4-5 that the protein has been internalized; as membrane integrity remains intact this is most likely due to an active process such as endocytosis. The CD accompanying this thesis contains a movie of figure 4-5 where internalized h- Δ 6PLY can be observed more clearly. It would be possible to test this using inhibitors of endocytosis, for example by treating the cells with cytochalasin D it would be possible to distinguish actin-dependent endocytosis from, for instance, endocytosis via clathrin-coated pits (Lamaze, 1997).

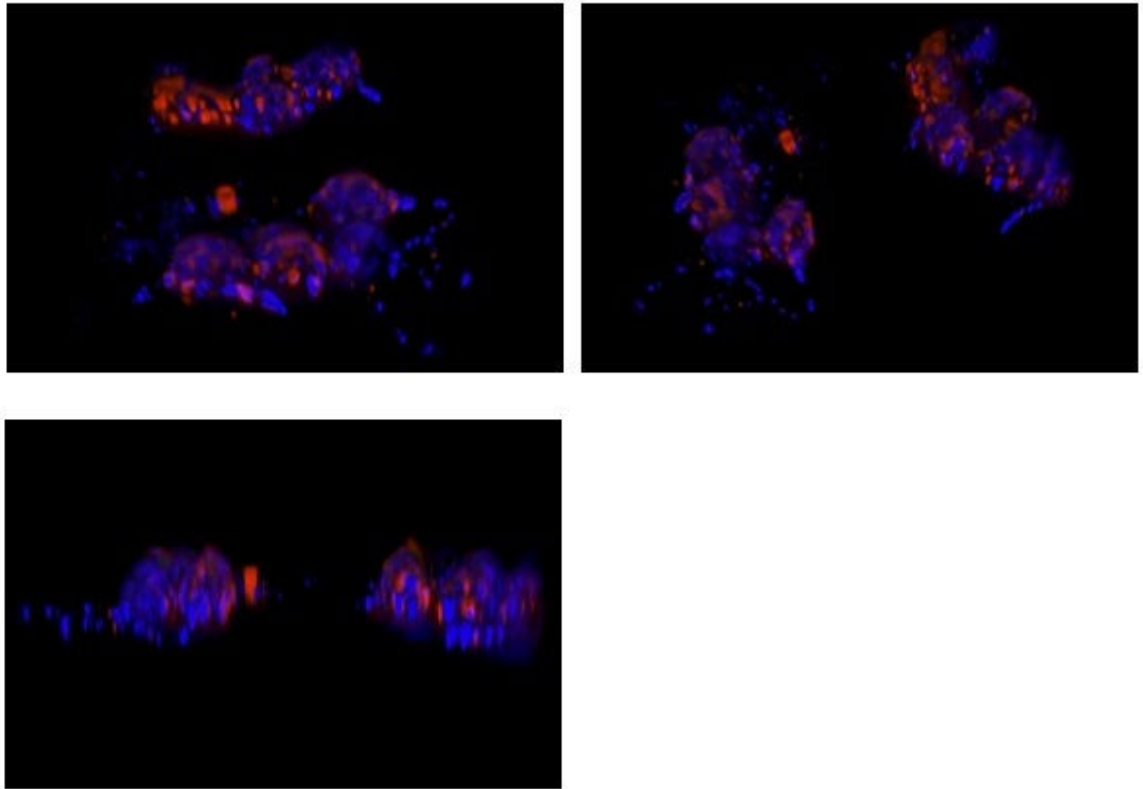


Figure 4-5 3D image of h- Δ 6PLY treated RAW 264.7 cells stained with Deep-red plasma membrane stain and Halo TMR-direct ligand.

The z-stacks of image 4-4 were combined using Velocity® software to create a 3D image of h- Δ 6PLY binding to the RAW 264.7 cell lines. The software was also used to create a movie of this image by compiling snapshots taken from different angles; this movie can be viewed in the compact disk accompanying this thesis.

4.1.3 Analysis of D123PLY binding using HaloTag technology

Previously, PLY binding to the cell surface has been attributed almost exclusively to domain 4, h-D123PLY was not expected to bind to the cell surface at all; however, h-D123PLY can be seen to form large aggregates on the cell surface in figure 4-6. The distribution is not punctate or distributed as in h-PLY and h- Δ 6PLY treated cells but instead appears as large single foci.

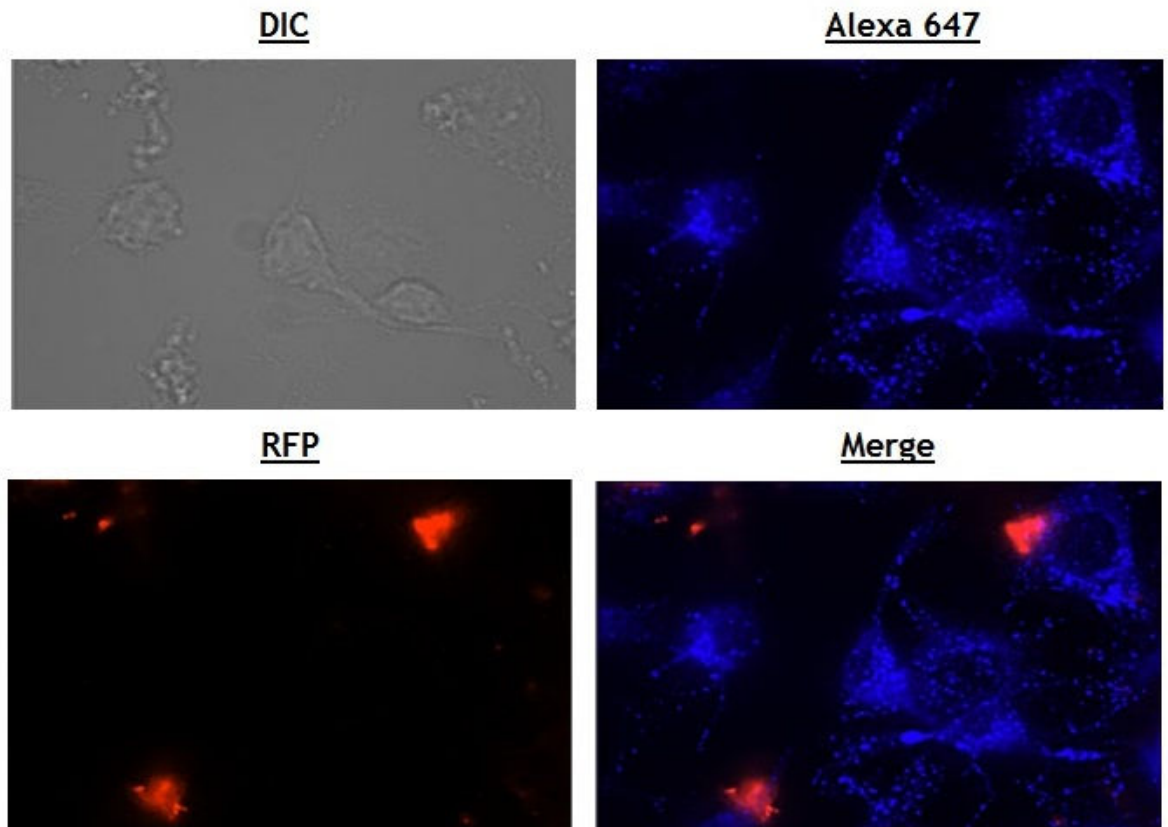


Figure 4-6 2D merged image of h-D123PLY treated RAW 264.7 cells stained with CellMask Deep Red plasma membrane stain and HaloTag TMR-direct ligand.

RAW 264.7 cells were seeded at 1×10^6 /well in a 6-well plate containing cover slips and allowed to adhere O/N at 37°C. The cells were treated with h-D123PLY lysate diluted in culture medium to a final conc. of 17.5nM (1ml total well volume). The cells were incubated for 30 minutes before staining with CellMask Deep Red plasma membrane stain and HaloTag TMR-direct ligand according to the protocol in section 2.8.1.1. The cells were fixed in 4% paraformaldehyde before a final rinse in PBS. The cover slips were removed and mounted onto microscope slides using Dako Fluorescent Mounting Media, images were captured using the Zeiss-axio imager at 100X magnification. Images of the cells were captured using DIC (differential interference contrast) and using RFP and Alexa-647 channels to create a merged image. This experiment was performed twice, multiple images were taken of each slide and the above was selected as a representative image. Further analysis of individual z-stacks for this image has shown that it is not an extended image of the entire cell and is in fact a cross-sectional image, this is likely due to user error when determining the depth settings for image capture.

At first glance the image analysis of h-D123PLY binding does not appear to show internalization of PLY, however, looking at the image from both above and below it is clear that h-D123PLY appears on both sides of the image (figure 4-7). Further analysis of the z-stacks used to compile this 3D image shows that the defined height of the cell (set by the user within the image capture software - top and bottom of the cell) before capturing the z-stacks was too narrow and has in fact captured a cross-section of the cells. It is unclear if this cross-section

captures an internal image. The unusual binding pattern of h-D123PLY is further assessed in section 4.3.4.

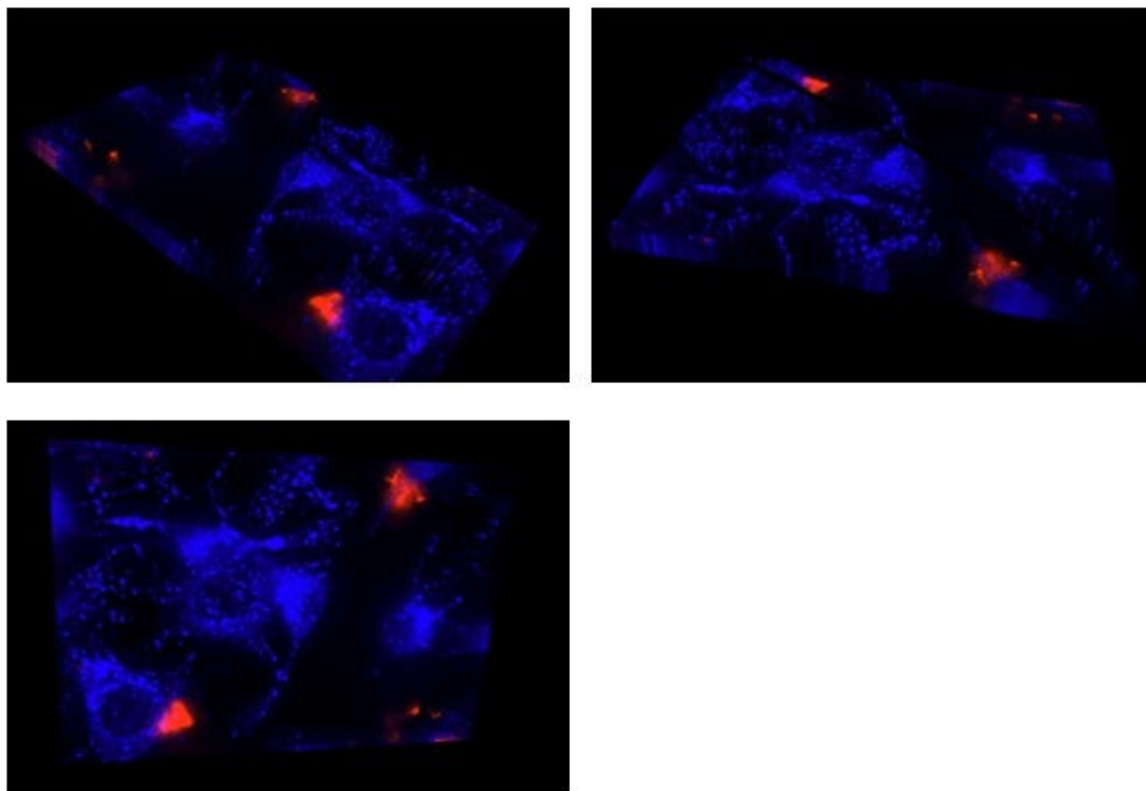


Figure 4-7 3D image of h-D123PLY treated RAW 264.7 cells stained with Deep-red plasma membrane stain and Halo TMR-direct ligand.

The z-stacks of image 4-6 were combined using Volocity® software to create a 3D image of h-D123PLY binding to the RAW 264.7 cell lines. The software was also used to create a movie of this image by compiling snapshots taken from different angles; this movie can be viewed in the compact disk accompanying this thesis.

4.1.4 Analysis of D4PLY binding using HaloTag technology

In figure 4-8 h-D4PLY can be seen to bind around the edges of cells as well as extending along the adherens junctions. h-D4PLY can also be seen binding to the edges of two daughter cells in the process of dividing in this image. Unlike h-D123PLY, h-D4PLY has a punctate binding pattern, much like that of h-PLY and h- Δ 6PLY. However, h-D4PLY does not have the even cellular distribution of h-PLY and h- Δ 6PLY; it may be that domain 4 of PLY binds to a specific molecule that is present in high concentrations at these cellular locations, for instance cytoskeletal proteins.

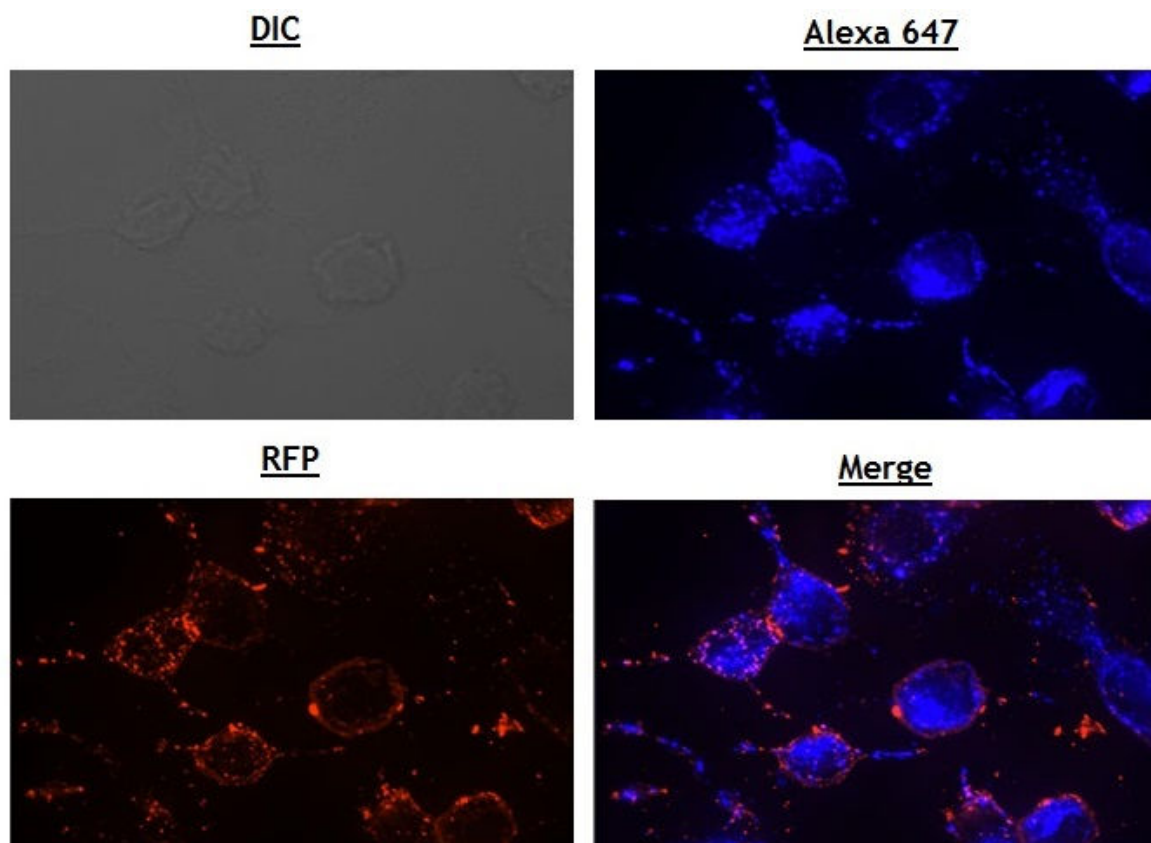


Figure 4-8 2D merged image of h-D4PLY treated RAW 264.7 cells stained with CellMask Deep Red plasma membrane stain and HaloTag TMR-direct ligand.

RAW 264.7 cells were seeded at 1×10^6 /well in a 6-well plate containing cover slips and allowed to adhere O/N at 37°C. The cells were treated with h-D4PLY lysate diluted in culture medium to a final conc. of 17.5nM (1ml total well volume). The cells were incubated for 30 minutes before staining with CellMask Deep Red plasma membrane stain and HaloTag TMR-direct ligand according to the protocol in section 2.8.1.1. The cells were fixed in 4% paraformaldehyde before a final rinse in PBS. The cover slips were removed and mounted onto microscope slides using Dako Fluorescent Mounting Media, images were captured using the Zeiss-axio imager at 100X magnification. Images of the cells were captured using DIC (differential interference contrast) and using RFP and Alexa-647 channels to create a merged image. This experiment was performed twice, multiple images were taken of each slide and the above was selected as a representative image.

As shown in figure 4-9 3D image analysis of h-D4PLY binding does not show internalization of the protein. The binding of h-D4PLY around the edges of the cells is more clearly visible in these images. It would be of interest to extend the time-course of h-D4PLY treatment; at 30 minutes there is no evidence of internalization, this could indicate that uptake of PLY is mediated by a different region of the toxin.

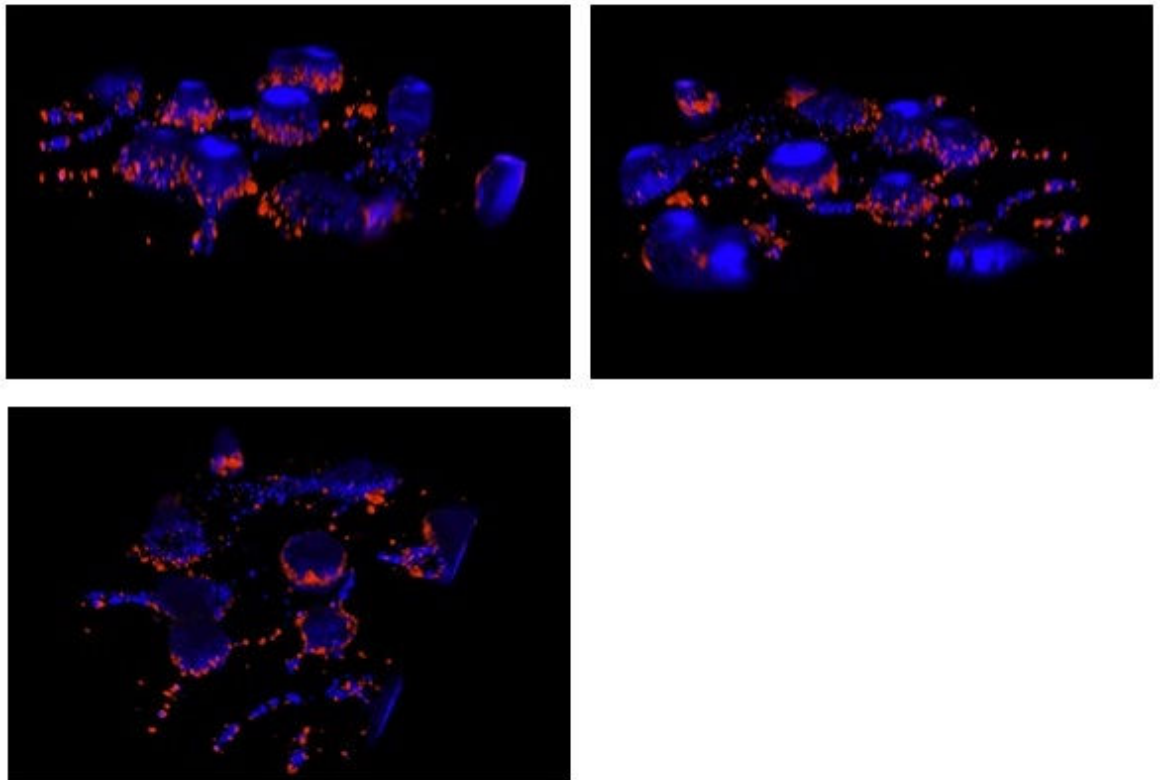


Figure 4-9 3D image of h-D4PLY treated RAW 264.7 cells stained with Deep-red plasma membrane stain and Halo TMR-direct ligand.

The z-stacks of image 4-8 were combined using Volocity® software to create a 3D image of h-D4PLY binding to the RAW 264.7 cell lines. The software was also used to create a movie of this image by compiling snapshots taken from different angles; this movie can be viewed in the compact disk accompanying this thesis.

4.1.5 Analysis of eGFP (control) binding using HaloTag technology

To control for any endogenous binding properties of the HaloTag, a HaloTagged version of eGFP was constructed. No bound protein is observed under these conditions demonstrating that the binding of previously shown PLY derivatives was not mediated by the HaloTag (figure 4-10).

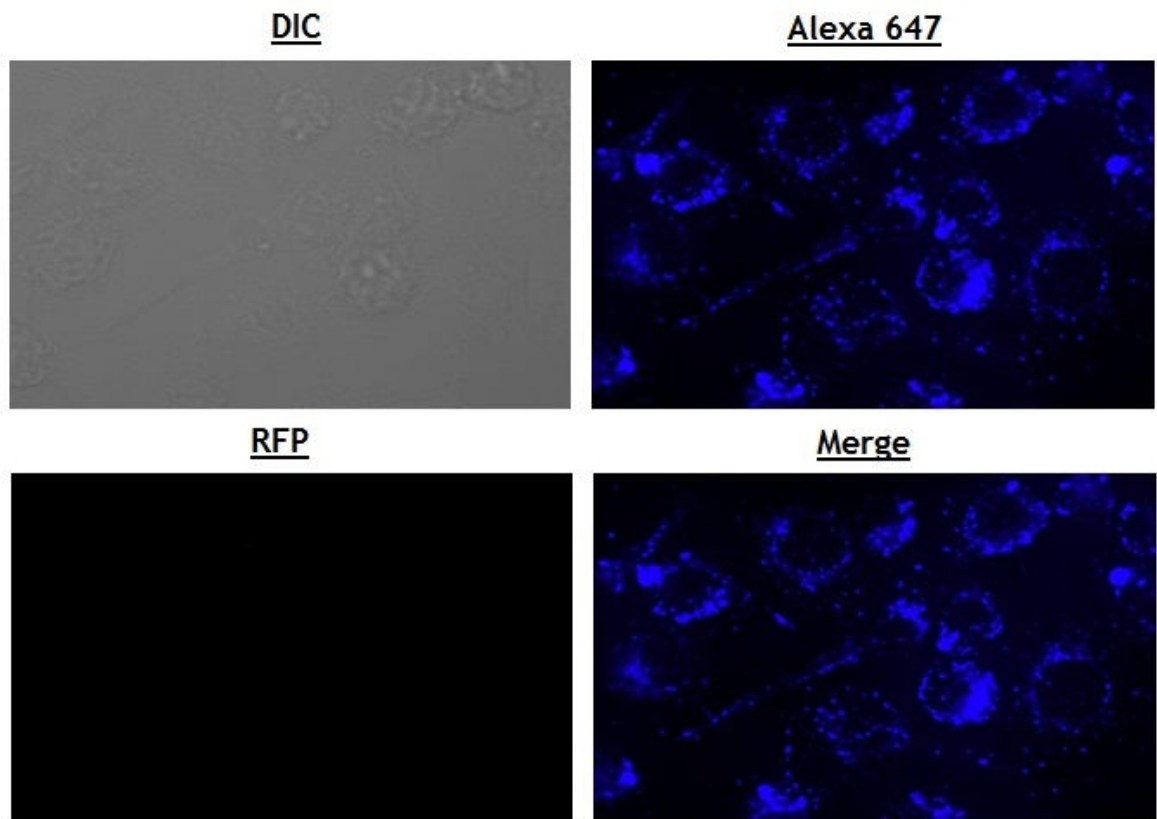


Figure 4-10 2D merged image of h-eGFP treated RAW 264.7 cells stained with CellMask Deep Red plasma membrane stain and HaloTag TMR-direct ligand.

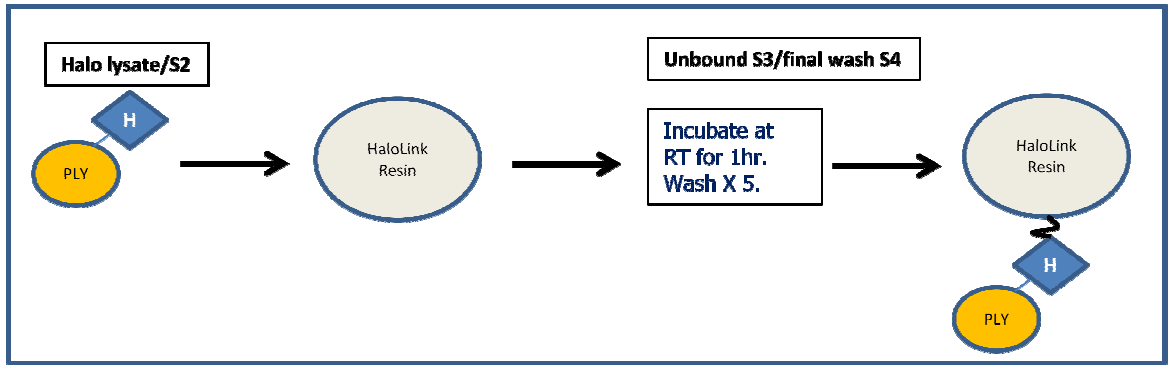
RAW 264.7 cells were seeded at 1×10^6 /well in a 6-well plate and allowed to adhere O/N at 37°C . The cells were treated with h-eGFP lysate diluted in culture medium to a final conc. of 17.5nM . The cells were incubated for 30 minutes before staining with CellMask Deep Red plasma membrane stain and HaloTag TMR-direct ligand according to the protocol in section 2.8.1.1. The cells were fixed in 4% paraformaldehyde before a final rinse in PBS. The cover slips were removed and mounted onto microscope slides using Dako Fluorescent Mounting Media, images were captured using the Zeiss-axio imager at 100X magnification. Images of the cells were captured using DIC (differential interference contrast) and using RFP and Alexa-647 channels to create a merged image. This experiment was performed once, multiple images were taken from the slide and the above was selected as a representative image.

This investigation of PLY and its derivatives binding to host cells has revealed that the individually purified domains exhibit strikingly different binding patterns and suggests specific binding interaction with molecules on the host cell surface. The following section describes a high-throughput method used to discern what these molecules may be.

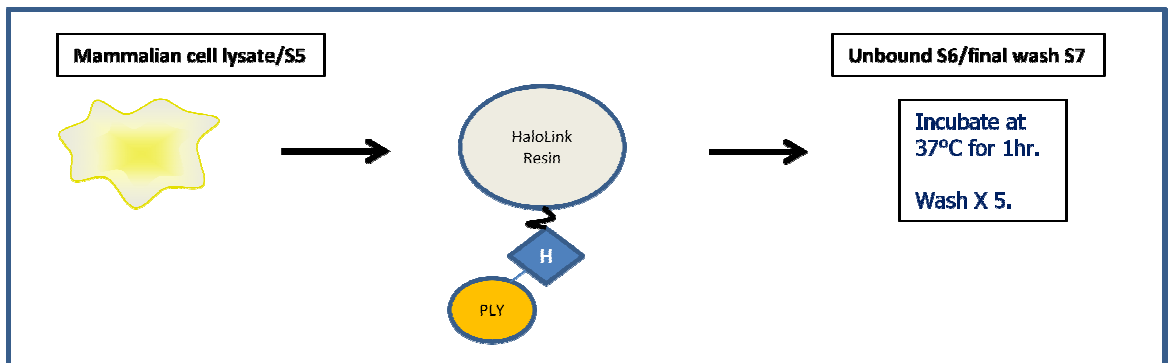
4.2 Investigating PLY-Host Interactions by Protein Pull-down

To investigate potential binding partners for PLY a modified version (Figure 4-11) of the Promega mammalian pull-down system protocol was devised. The pull-down method was used as a screening approach both to identify novel interactions between PLY and the host and also to confirm those already presented in the literature e.g. TLR4. It was of particular interest to assign interaction to different regions of the toxin, therefore, following the pull-down and sample separation by SDS-PAGE, only samples from h-D123PLY and h-D4PLY were sent for identification by mass spectrometry.

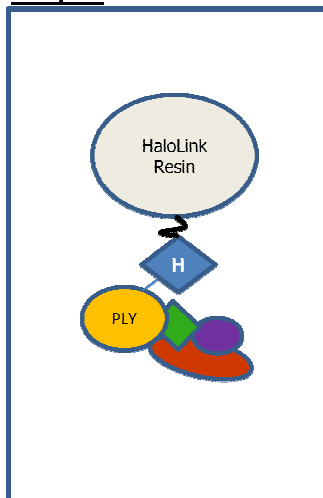
Stage 1 – coupling of Halo-lysate to Halo-link resin and removal of unbound proteins



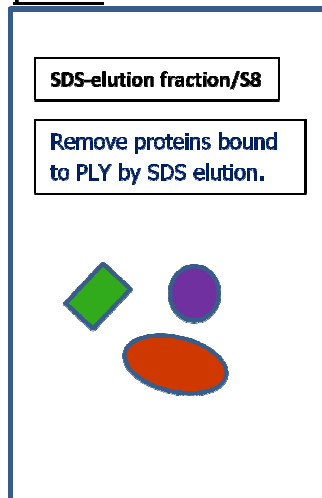
Stage 2 - addition of mammalian cell lysate to Halo complex and removal of unbound proteins



Stage 3 - Final pull-down complex



Stage 4 - Elution of bound proteins



Stage 5 – cleavage of protein from Halo-tag

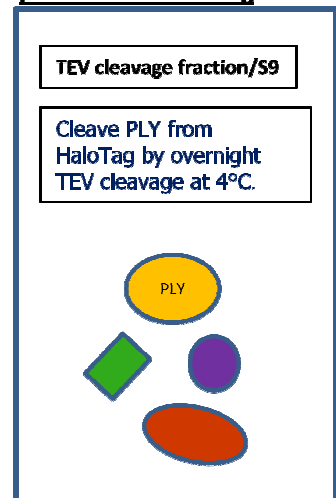


Figure 4-11 Schematic of a modified Halo-tag pull-down protocol. The full pull-down protocol is detailed in section 2.9.6.

4.2.1 Analysis of Pull-down efficiency by western blot and SDS-PAGE

At each stage of the pull-down samples were taken for analysis of protein content. Table 4-1 indicates the samples analyzed and whether HaloTagged proteins or their purified His-tagged controls are expected to be present. Silver staining was employed initially as its higher sensitivity range compared to coomassie staining would allow sensitive detection of contaminating carry-over following wash steps, additionally, it was possible that PLY or its derivatives could interact with less abundant mammalian proteins and silver staining would give a greater chance of their detection.

Table 4-1 Fractions Analyzed Following Protein Pull-down Protocol

Sample name	Description	PLY variant expected to be detected by western blot
(S1) - Positive control (purified protein)	Relevant His-tagged protein at 1µg/ml.	Yes
(S2)H-protein lysate	Undiluted lysate containing HaloTagged protein.	Yes
(S3) Unbound 1	Supernatant removed after incubating halo lysate with Halo-link resin.	Either acceptable, excess protein may carry over into this fraction.
(S4) Wash fraction 5	Resin is washed 5 times with PBS, final wash is sampled.	No
(S5) Mammalian cell lysate	Obtained from RAW 264.7 cells treated with lysis buffer.	No
(S6) Unbound 2	Supernatant removed after incubating mammalian cell lysate with Halo-link resin.	No
(S7) Wash fraction 10	Resin is washed a further 5 times with PBS, final wash is sampled.	No
(S8) SDS-elution fraction	Bound proteins are eluted with SDS-elution buffer.	Yes
(S9) TEV cleavage fraction	Proteins are cleaved from the HaloTag with TEV protease.	Yes

A distinct band of between 55-65 kDa can be seen in the wash fractions of most of the silver stained gels (figures 4-12 to 4-13). This is most likely human keratin as it is a commonly observed contaminant in silver stained SDS-PAGE gels (Xu et al., 2011). HaloTagged PLY and its derivatives are detectable in all of the lysates. The wash fraction 5 samples were free from contaminating HaloTagged protein carry over with the exception of the h-D4PLY pull down. In figure 4-13 (D) h-D4PLY carry over can be seen until lane 6 (Unbound 2) this is likely an artefact caused by the intense signal in lanes 1 and 2, in any case, no h-D4PLY is detected in lane 7 (wash fraction 10) and so any proteins pulled down in the SDS-elution fraction will have bound to h-D4PLY bound to resin and not in solution. $\Delta 6$ PLY was not detectable in the TEV cleavage fraction (figure 4-12 (D)). In figure 4-13 (C) and (D) several bands are observed in the SDS-elution and TEV cleavage fractions, this is potentially because h-D123PLY and h-D4PLY have complexed with other proteins however, it is more likely that h-D123PLY has degraded during the TEV cleavage process. It also seems likely that the Halo-tag has been cleaved from the protein (in the absence of TEV protease) as in lanes 2 and 3 bands of the correct size for non-tagged D123PLY and D4PLY (41 and 13 kDa respectively) are present.

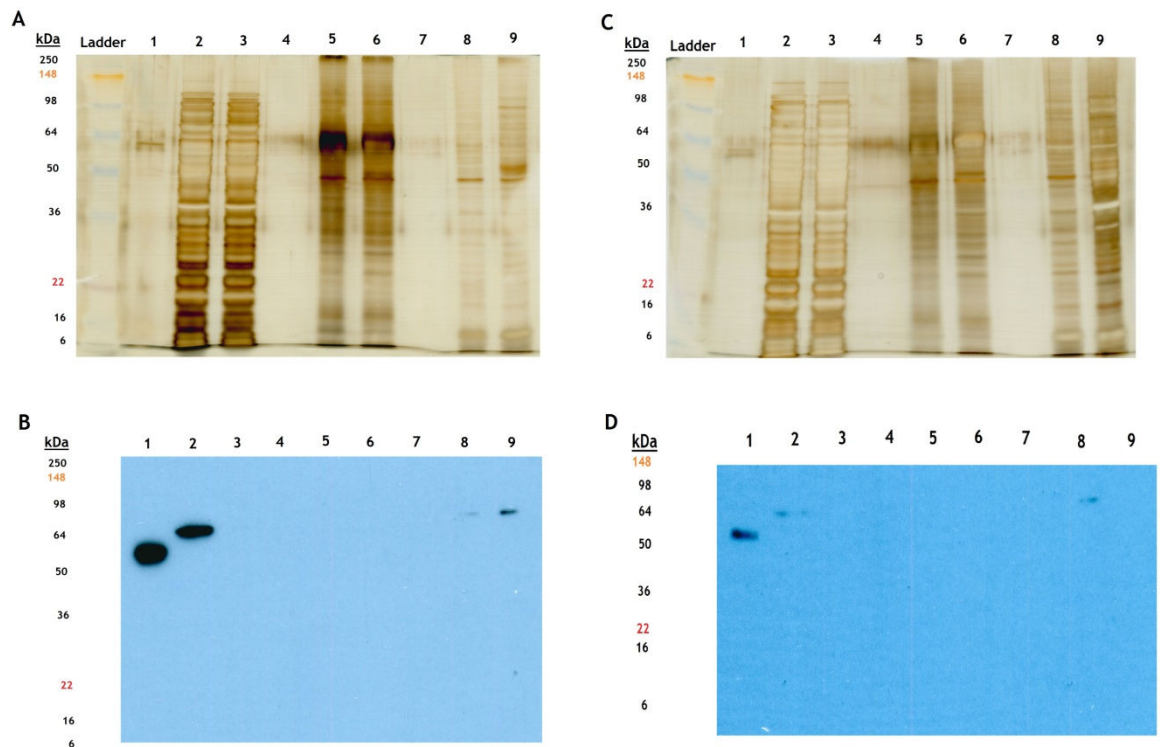


Figure 4-12 Analysis of pull-down efficiency by silver staining and western blot.

h-PLY pull-down silver staining (A) and western blot (B), h- Δ 6PLY pull-down silver staining (C) and western blot (D). Lane 1 = purified His-tagged protein, 2 = Halo lysate, 3 = unbound fraction 1, 4 = wash fraction 1, 5 = mammalian cell lysate, 6 = unbound fraction 2, 7 = wash fraction 2, 8 = SDS elution fraction, 9 = TEV cleavage fraction. Purified PLY/ Δ 6PLY was diluted to 1mg/ml, pull-down samples were undiluted and mixed 1:4 with SDS-PAGE loading buffer. 5 μ l of Seebule Plus 2 molecular weight marker and 10 μ l of the proteins or pull-down samples were loaded into the wells of a 10% SDS-PAGE gel and electrophoresed at 180 V for 40 minutes. The presence or absence of PLY and Δ 6PLY or mammalian proteins was determined by silver staining (SilverQuest, Invitrogen) and western blot using rabbit anti-PLY antibodies. The proteins in unstained gels were transferred onto nitrocellulose membrane and detected by western blotting using rabbit anti-PLY (1:1000) and donkey anti-rabbit-HRP (1:40,000) using enhanced chemiluminescence (ECL) (Millipore).

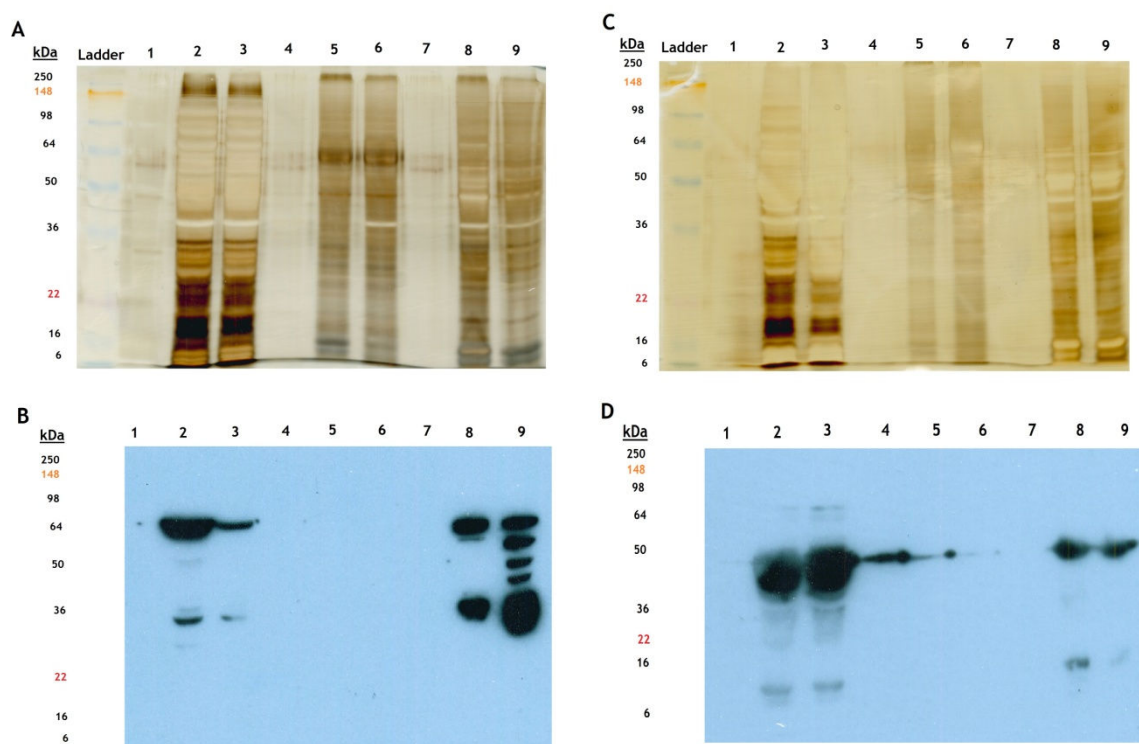


Figure 4-13 Analysis of pull-down efficiency by silver staining and western blot.

h-D123PLY pull-down silver staining (A), and western blot (B), h-D4PLY pull-down silver staining (C) and western blot (D). Lane1 = purified His-tagged protein, 2 = Halo lysate, 3 = unbound fraction 1, 4 = wash fraction 5, 5 = mammalian cell lysate, 6 = unbound fraction 2, 7 = wash fraction 10, 8 = SDS elution fraction, 9 = TEV cleavage fraction. Purified D123PLY/D4PLY was diluted to 1mg/ml, pull-down samples were undiluted and mixed 1:4 with SDS-PAGE loading buffer. 5 μ l of Seebule Plus 2 molecular weight marker and 10 μ l of the proteins or pull-down samples were loaded into the wells of a 10% SDS-PAGE gel and electrophoresed at 180 V for 40 minutes. The presence or absence of D123PLY and D4PLY or mammalian proteins was determined by silver staining (SilverQuest, Invitrogen) and western blot using rabbit anti-PLY antibodies. The proteins in unstained gels were transferred onto nitrocellulose membrane and detected by western blotting using rabbit anti-PLY (1:1000) and donkey anti-rabbit-HRP (1:40,000) using enhanced chemiluminescence (ECL) (Millipore).

4.2.2 Separation and extraction of Pull-down proteins by SDS-PAGE

This initial analysis of the pull-down fractions indicated that it had been successful and that eluted proteins should be sent for identification by mass spectrometry, however, the eluted proteins were not sufficiently separated making it impossible to excise individual protein bands. Additionally, the sensitivity of silver staining means that bands of insufficient concentration for mass spectrometry could be excised. For these reasons the elution and TEV

cleavage fractions were separated on larger gels cast and electrophoresed using the Hoeffer 2600 system. The gels were stained with coomassie blue rather than silver stained to ensure proteins were of a high enough concentration to be identified by mass spectrometry.

As shown in Figures 4-14 and 4-15 seventy-two potential binding partners across the four pull-downs were identified. It was decided that only bands from h-D123PLY and h-D4PLY pull-downs would be sent for analysis by mass spectrometry so that any proteins identified could be assigned to different domains of the toxin. Although the final wash fractions were clean and did not identify any carry-over of unbound proteins we decided to only send those bands that were present in both the elution and TEV cleavage fractions. The reasoning for this was that those bands were most likely to have a strong interaction with PLY and therefore not be entirely dissociated by SDS-elution.

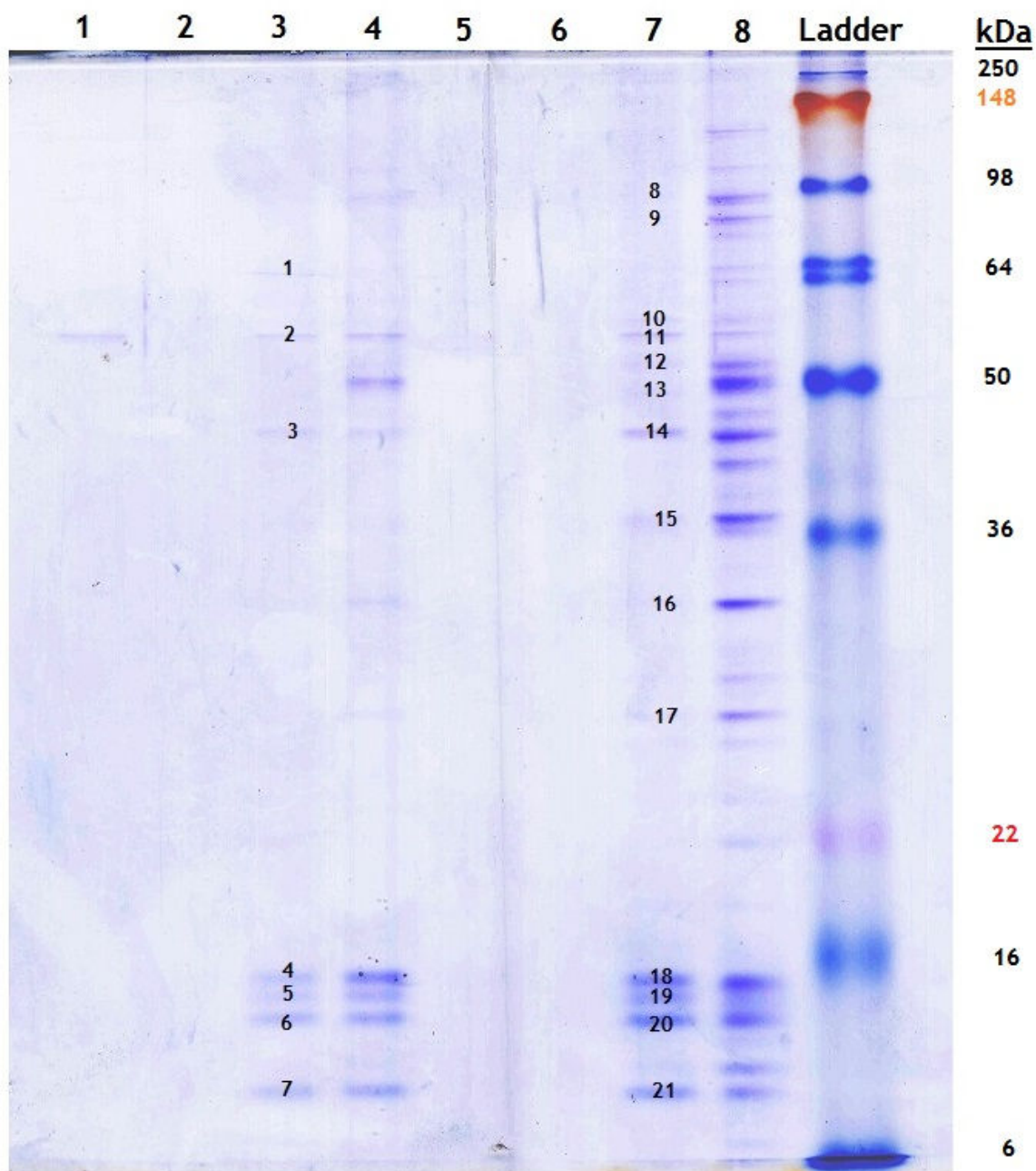


Figure 4-14 Separation and excision of proteins from h-PLY and h-Δ6PLY pull-down.

The Hoefer SE600 system was used to separate proteins isolated from the pull-down protocol. Lane 1 = purified PLY, 2 = final wash fraction (h-PLY), 3 = SDS-elution fraction (h-PLY), 4 = TEV cleavage fraction (h-PLY), 5 = purified Δ6PLY, 6 = final wash fraction (h-Δ6PLY), 7 = SDS-elution fraction (h-Δ6PLY), 8 = TEV cleavage fraction (h-Δ6PLY). Purified PLY/Δ6PLY was diluted to 1mg/ml, pull-down samples were undiluted and mixed 1:4 with SDS-PAGE loading buffer. 20μl of Seeblue Plus 2 molecular weight marker and 50μl of the proteins or pull-down samples were loaded into the wells of a large 10% SDS-PAGE gel and electrophoresed at 50V for 2 hours followed by 3 hours at 250V. The gel was stained in coomassie blue stain for 1 hour and destained O/N followed by several washes in dH₂O. As protein bands were identified they were numbered, excised and stored at -80°C for future analysis by mass spectrometry.

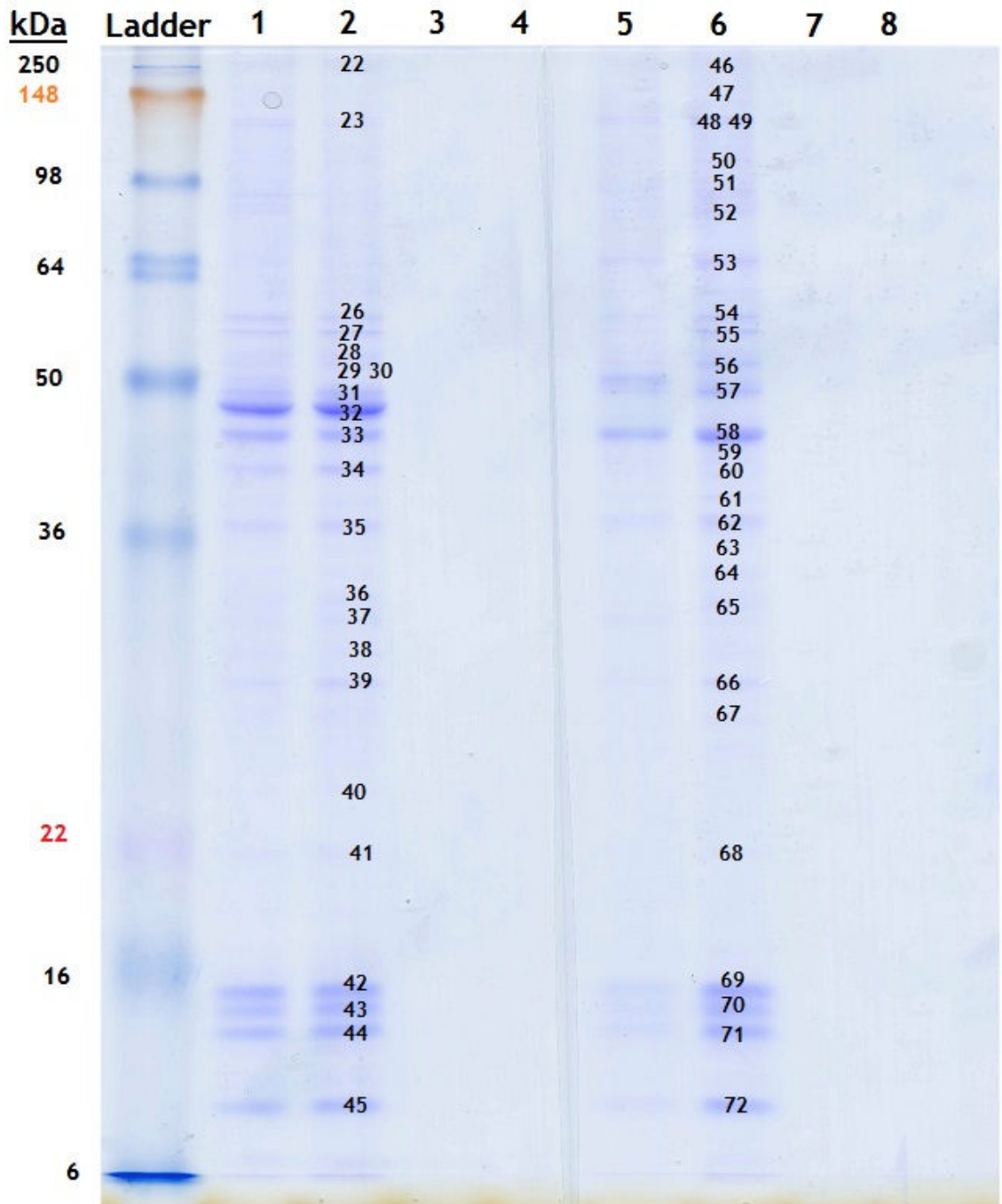


Figure 4-15 Separation and excision of proteins from h-D123PLY and h-D4PLY pull-down.

The Hoefer SE600 system was used to separate proteins isolated during the pull-down protocol. Lane 1 = TEV cleavage fraction (h-D4PLY), 2 = SDS-elution fraction (h-D4PLY), 3 = final wash fraction (h-D4PLY), 4 = purified D4PLY, 5 = TEV cleavage fraction (h-D123PLY), 6 = SDS-elution fraction (h-D123PLY), 7 = final wash fraction (h-D123PLY), 8 = purified D123PLY. Purified D123PLY/D4PLY was diluted to 1mg/ml, pull-down samples were undiluted and mixed 4:1 with SDS-PAGE loading buffer. 20 μ l of Seeblue Plus 2 molecular weight marker and 50 μ l of the proteins or pull-down samples were loaded into the wells of a large 10% SDS-PAGE gel and electrophoresed at 50V for 2 hours followed by 3 hours at 250V. The gel was stained in coomassie blue stain for 1 hour and destained O/N followed by several washes in dH₂O. As protein bands were identified they were numbered, excised and stored at -80°C for future analysis by mass spectrometry. As protein bands were identified they were numbered, excised and stored for analysis by mass spectrometry.

4.2.3 Mass Spectrometry results

Of the bands sent for identification by mass spectrometry six returned positive hits for *M. musculus* (mouse) proteins; one protein was identified as *Bos taurus* (bull), however there is 100% sequence homology between *Bos taurus* and *Mus musculus* tubulin β -5 chain (appendix) and so this was taken as a positive hit. The identified proteins and their functions are detailed in table 4-2, probability scores over 42 indicate confirmed identity or extensive homology ($p < 0.05$).

Table 4-2 Proteins identified by MS/MS mass spectrometry.

Band No.	Protein Identity and Species	Probability Score	Description
26	pyruvate kinase (<i>Mus musculus</i>)	305	Pyruvate kinase is a transferase with key role in glycolysis. Typically located in the cytosol. Has been linked with caspase-dependent cell death.
27	vimentin (<i>Mus musculus</i>)	305	Vimentin is a cytoskeletal protein involved in supporting cell organelles; it has direct attachments to the nucleus, ER and mitochondria (Katsumoto, 1990).
28	tubulin β -5 chain (<i>Bos taurus</i>)	178	A subunit of microtubules; cytoskeletal structures that provide structural support and act as platforms for intracellular transport (Hammond et al., 2008).
29	ATP synthase subunit β (<i>Mus musculus</i>)	306	Mitochondrial membrane ATP synthase (F_1F_0 ATP synthase or Complex V) produces ATP from ADP in the presence of a proton gradient across the membrane which is generated by electron transport complexes of the respiratory chain (Jonckheere et al., 2011).
30	ATP synthase subunit β (<i>E. coli</i>)	404	
31	transcription termination factor rho (<i>E. coli</i>)	434	

Table 4-2 continued			
32	Trypsin	108	Protease added by MS facility.
33	elongation factor (<i>E. coli</i>)	451	
34	outer membrane protein F (<i>E. coli</i>)	349	
35	60s acidic ribosomal protein PO (<i>Mus musculus</i>)	143	Located in the cytoplasm this ribosomal protein forms pentamers with P1 and P2 dimers.
51	heat shock protein 1 (<i>Mus musculus</i>)	392	Hsp90AB1, also known as Hsp84, is a chaperon and belongs to the HSP90 class of heat shock proteins in mammals. It plays a role in response to temperature elevation and cytotoxic stresses and is expressed constitutively in the cytosol (Fukuyama et al., 2008).
52	Leucine rich PPR containing protein (<i>Mus musculus</i>)	103	LLPPRC is thought to have a role in many cellular processes (such as trafficking) through regulation of the cytoskeleton (Fukuda et al., 2004).

Bands 26, 27 and 52 were of particular interest, they corresponded to vimentin, tubulin β -5 chain and leucine rich PPR containing protein, respectively. As these proteins were all associated with the cell cytoskeleton/cellular trafficking they could potentially be involved in the antigen uptake mechanism of PLY-based vaccines. Additionally, there is already evidence in the literature that PLY associates with the actin cytoskeleton (Hupp et al., 2013; Iliev et al., 2009), therefore the interaction(s) between PLY and the actin cytoskeleton in macrophages was further investigated.

4.3 Interactions between PLY and the Actin Cytoskeleton

The initial microscopy results using HaloTag-PLY variants and the results of mass spectrometry indicated direct interactions between PLY and the cell cytoskeleton. To further investigate this theory phalloidin staining was used to visualize the actin cytoskeleton of RAW 264.7 macrophages stimulated with eGFP-PLY variants. The binding patterns observed were consistent with those seen with HaloTag-PLY variants. In addition there were obvious conformational changes to the actin cytoskeleton in PLY treated cells.

4.3.1 Visualising interactions between eGFP and the actin cytoskeleton using purified eGFP

In figure 4-16 the actin of eGFP treated control cells is visible as podosomes (actin dense foci that may facilitate adherence, usually visible as ring like structures at the substrate binding edges of cells (Linder et al., 2000)) around the edges of the macrophages and along adherens junctions but is also visible throughout the cytoplasm.

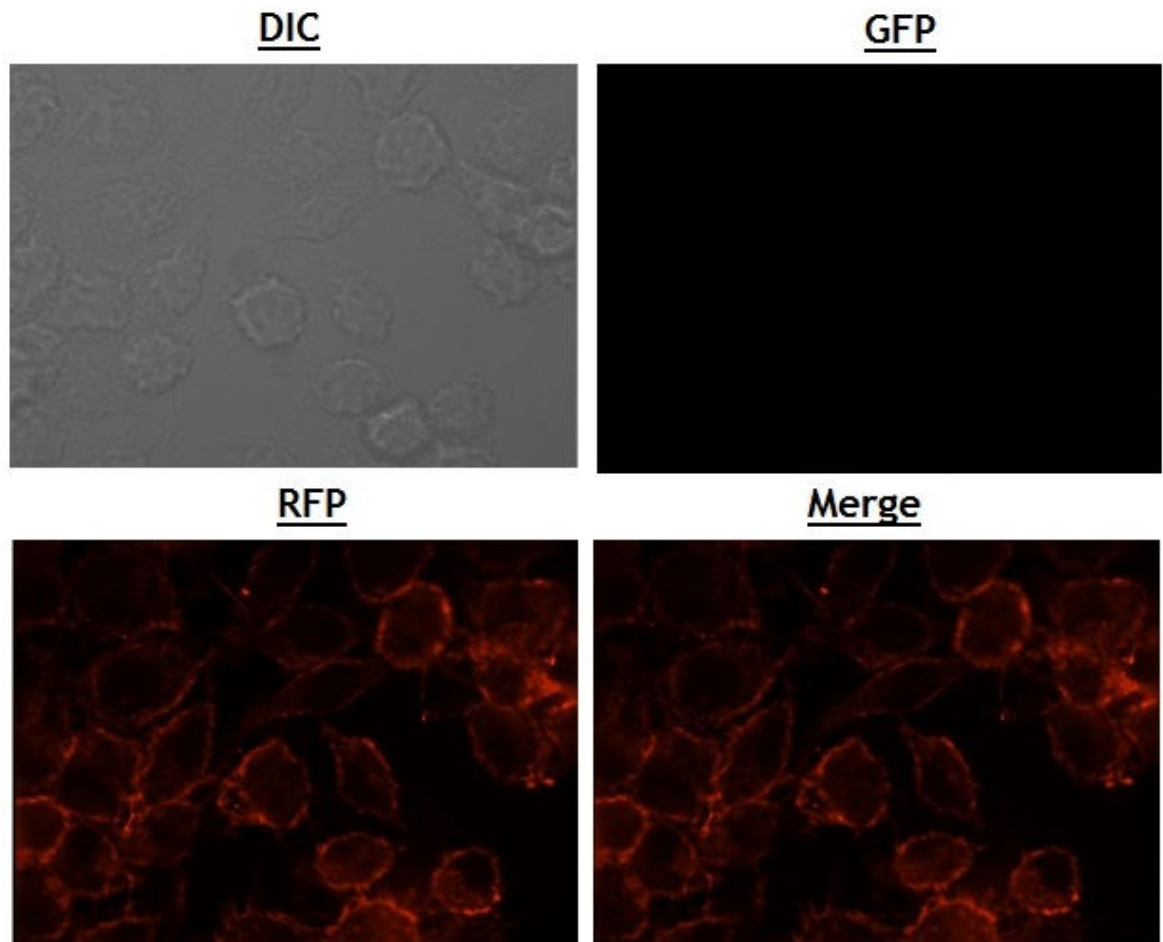


Figure 4-16 2D merged image of eGFP treated RAW 264.7 cells stained with rhodamine phalloidin.

RAW 264.7 cells were seeded at 1×10^6 /well in a 6-well plate containing cover slips and allowed to adhere O/N at 37°C. The cells were treated with 1ml 17.5nM eGFP for 30 minutes; the cells were washed and stained with rhodamine phalloidin according to the protocol in section 2.8.1.2. The cells were fixed in 4% paraformaldehyde before a final rinse in PBS. The cover slips were removed and mounted onto microscope slides using Dako Fluorescent Mounting Media, images were captured using the Zeiss-axio imager at 100X magnification. Images of the cells were captured using DIC (differential interference contrast) and using RFP and GFP channels to create a merged image. This experiment was performed twice, multiple images were taken of each slide and the above was selected as a representative image.

4.3.2 Visualising interactions between PLY and the actin cytoskeleton using eGFP-tagged PLY

The binding pattern and morphological changes seen in response to h-PLY are replicated in e-PLY treated cells (figure 4-17). In e-PLY treated cells there appears to be widespread actin destabilization and podosome degradation, the actin cytoskeleton seems granular in appearance. In the merged image there does seem to be colocalization of e-PLY and actin (seen as a yellow spots).

3D analysis of the same image (figure 4-18) shows that the actin cytoskeleton is condensed and flattened, e-PLY can be observed both centrally within the cells and peripherally, binding to the edges and adherens junctions of cells.

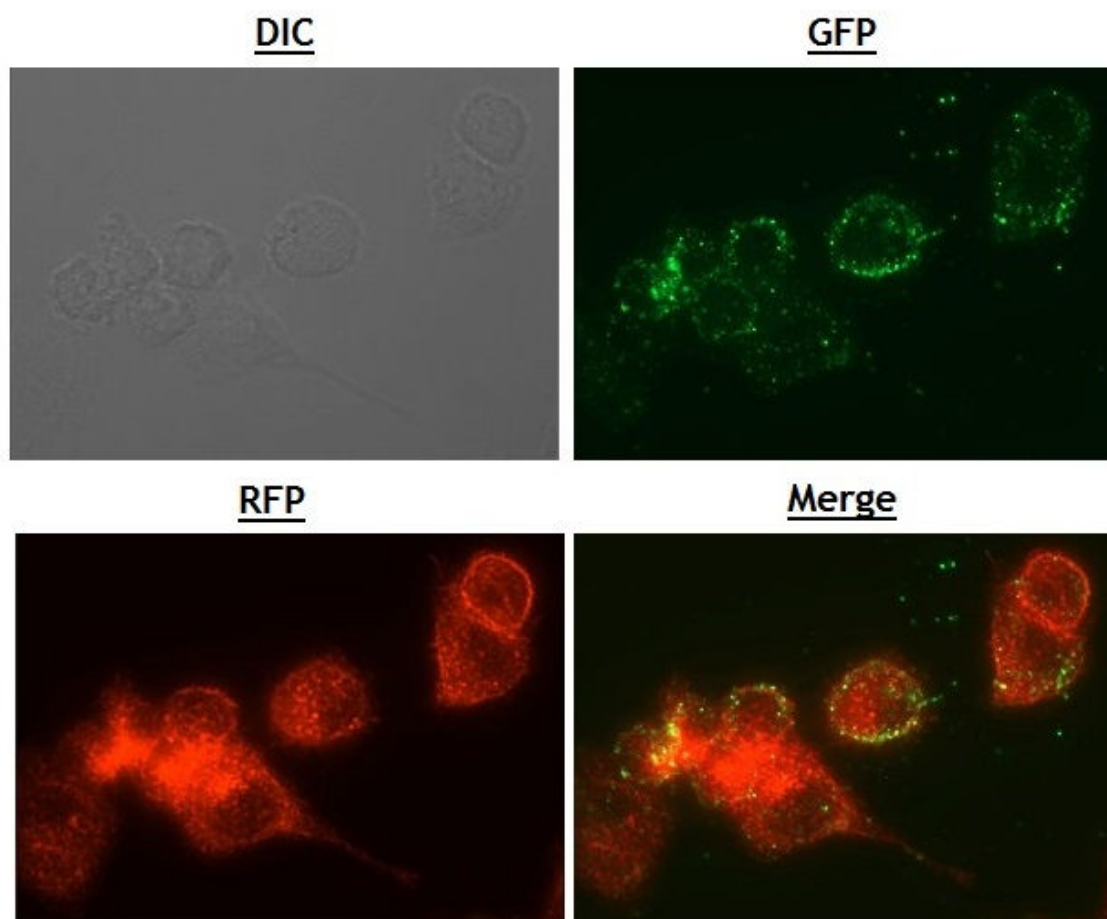


Figure 4-17 2D merged image of e-PLY treated RAW 264.7 cells stained with rhodamine phalloidin.

RAW 264.7 cells were seeded at 1×10^6 /well in a 6-well plate containing cover slips and allowed to adhere O/N at 37°C. The cells were treated with 1ml 17.5nM e-PLY for 30 minutes; the cells were washed and stained with rhodamine phalloidin according to the protocol in section 2.8.1.2. The cells were fixed in 4% paraformaldehyde before a final rinse in PBS. The cover slips were removed and mounted onto microscope slides using Dako Fluorescent Mounting Media, images were captured using the Zeiss-axio imager at 100X magnification. Images of the cells were captured using DIC (differential interference contrast) and using RFP and GFP channels to create a merged image. This experiment was performed twice, multiple images were taken of each slide and the above was selected as a representative image.

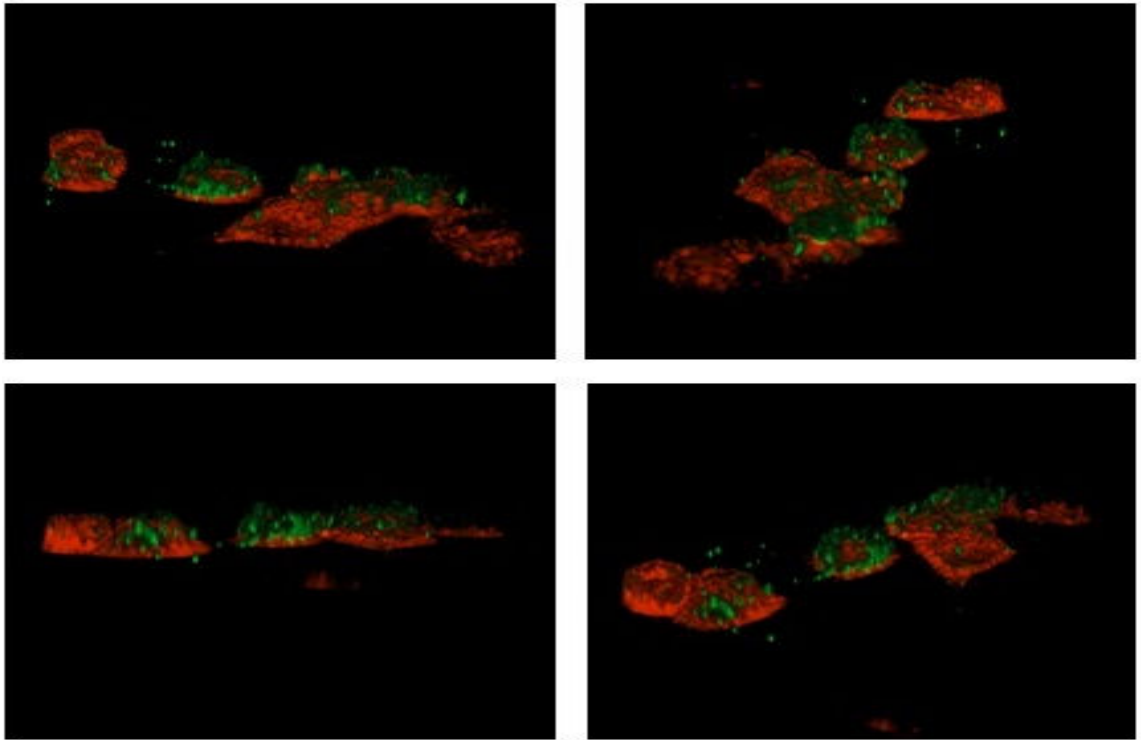


Figure 4-18 3D image of e-PLY treated RAW 264.7 cells stained with rhodamine phalloidin.

The z-stacks of image 4-17 were combined using Volocity® software to create a 3D image of e-PLY binding to the RAW 264.7 cell lines. The software was also used to create a movie of this image by compiling snapshots taken from different angles; this movie can be viewed in the compact disk accompanying this thesis.

4.3.3 Visualising interactions between $\Delta 6$ PLY and the actin cytoskeleton using eGFP-tagged $\Delta 6$ PLY

The actin destabilization and podosome degradation seen in e-PLY treated cells is also observed in e- $\Delta 6$ PLY treated cells though to a lesser degree, perhaps to due greater membrane integrity (figure 4-19).

The 3D image analysis in figure 4-20 shows that in contrast to e-PLY treated cells, the actin cytoskeleton of e- $\Delta 6$ PLY treated cells is not flattened and appears less condensed.

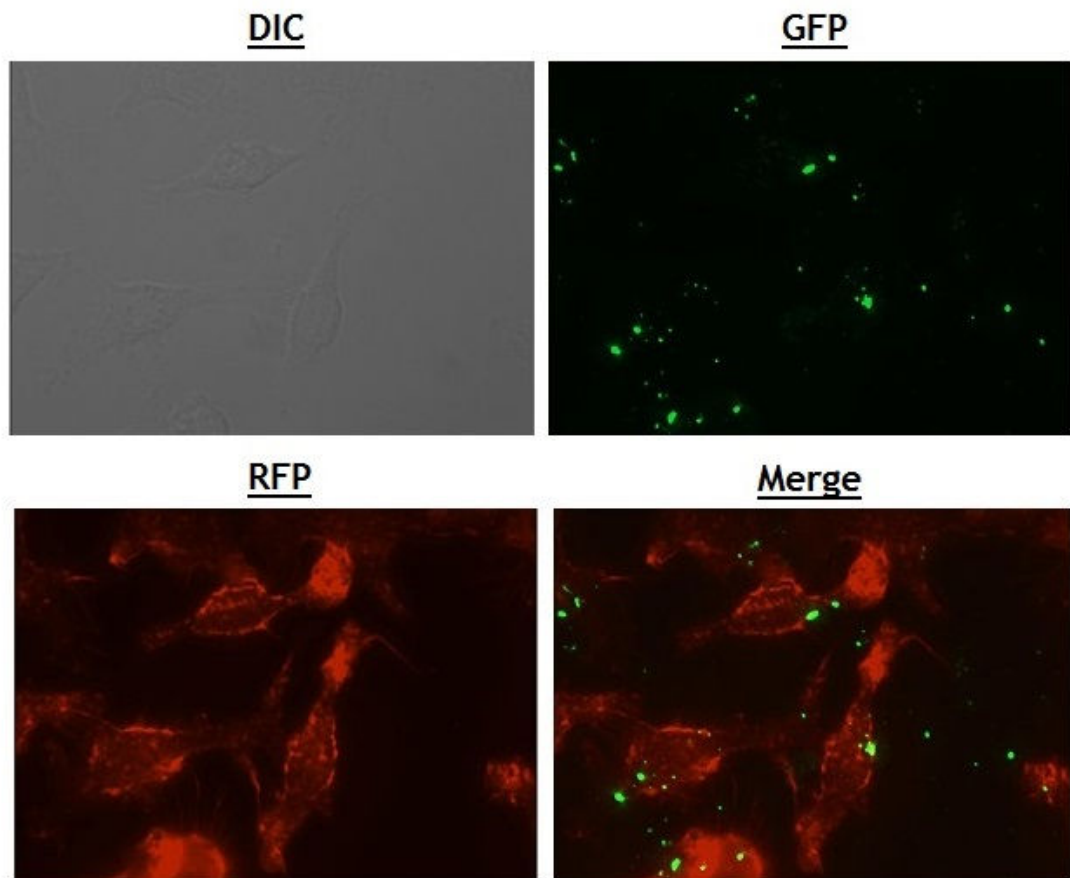


Figure 4-19 2D merged image of e- Δ 6PLY treated RAW 264.7 cells stained with rhodamine phalloidin.

RAW 264.7 cells were seeded at 1×10^6 /well in a 6-well plate containing cover slips and allowed to adhere O/N at 37°C . The cells were treated with 1ml 17.5nM e- Δ 6PLY for 30 minutes; the cells were washed and stained with rhodamine phalloidin according to the protocol in section 2.1.1.2. The cells were fixed in 4% paraformaldehyde before a final rinse in PBS. The cover slips were removed and mounted onto microscope slides using Dako Fluorescent Mounting Media, images were captured using the Zeiss-axio imager at 100X magnification. Images of the cells were captured using DIC (differential interference contrast) and using RFP and GFP channels to create a merged image. This experiment was performed twice, multiple images were taken of each slide and the above was selected as a representative image.

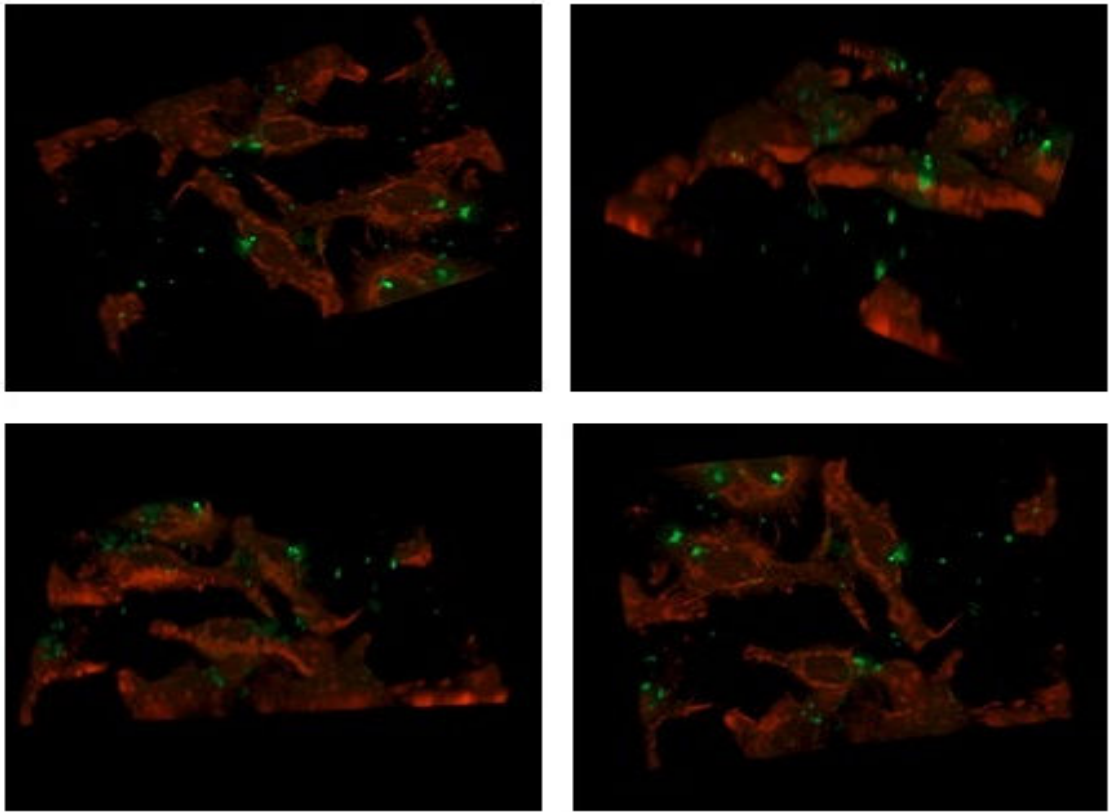


Figure 4-20 3D image of e- Δ 6PLY treated RAW 264.7 cells stained with rhodamine phalloidin.

The z-stacks of image 4-19 were combined using Volocity® software to create a 3D image of e- Δ 6PLY binding to the RAW 264.7 cell lines. The software was also used to create a movie of this image by compiling snapshots taken from different angles; this movie can be viewed in the compact disk accompanying this thesis.

4.3.4 Visualising interactions between D123PLY and the actin cytoskeleton using eGFP-tagged D123PLY

In figure 4-21 RAW 264.7 cells treated with e-D123PLY have a rounded appearance and increased number of filopodial projections. The podosomes of treated cells appear intact; and there does not seem to be a reduction in cytoplasmic actin compared to control cells.

The binding pattern of h-D123PLY is replicated in figure 4-22 using e-D123PLY, in this 3D image analysis the binding pattern is striking and in some cases the entire surface of the cell is coated in protein. This image would indicate that the 3D composite in figure 4-6 was too narrow and is in fact a slice from the inside of the cell potentially suggesting internalization of D123PLY.

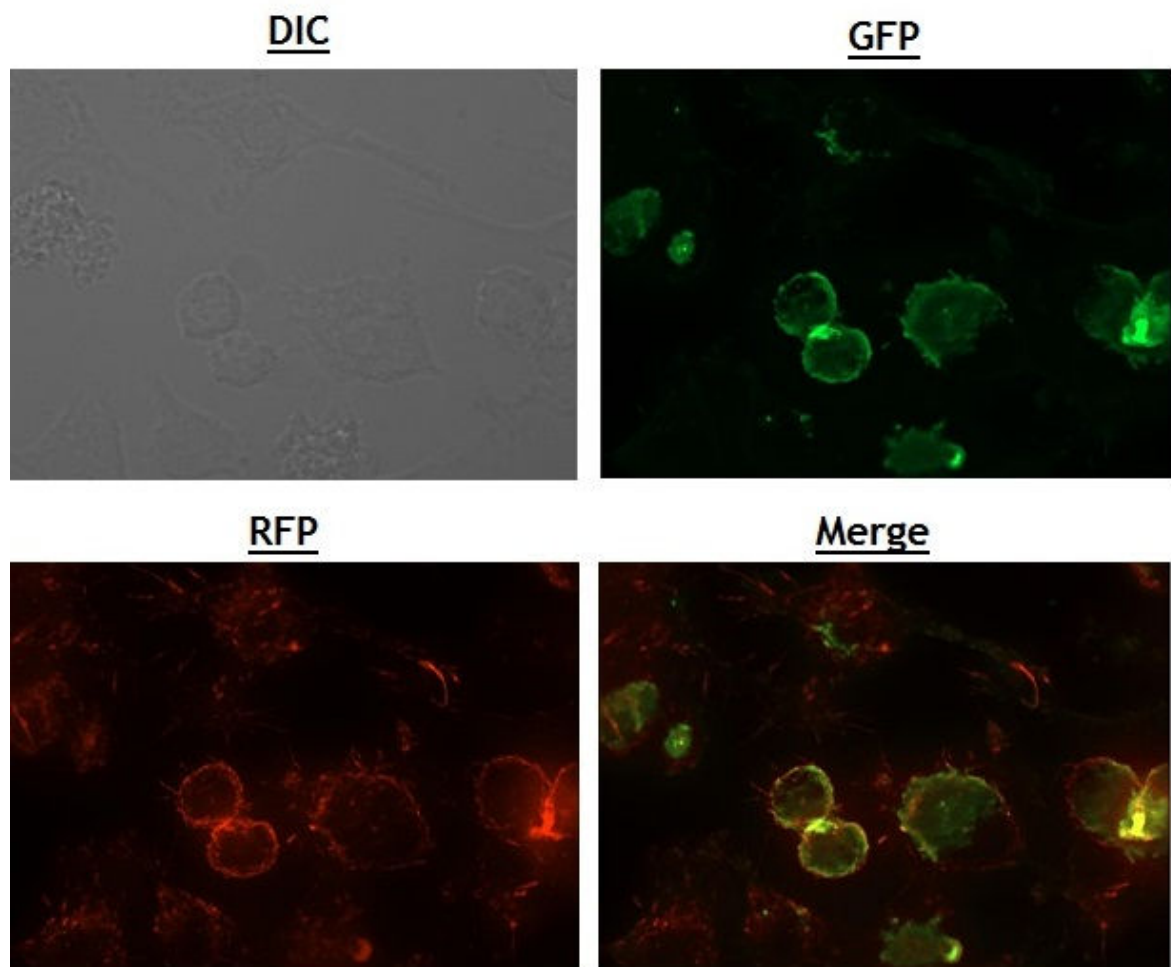


Figure 4-21 2D merged image of e-D123PLY treated RAW 264.7 cells stained with rhodamine phalloidin.

RAW 264.7 cells were seeded at 1×10^6 /well in a 6-well plate containing cover slips and allowed to adhere O/N at 37°C. The cells were treated with 1ml 17.5nM e-D123PLY for 30 minutes; the cells were washed and stained with rhodamine phalloidin according to the protocol in section 2.8.1.2. The cells were fixed in 4% paraformaldehyde before a final rinse in PBS. The cover slips were removed and mounted onto microscope slides using Dako Fluorescent Mounting Media, images were captured using the Zeiss-axio imager at 100X magnification. Images of the cells were captured using DIC (differential interference contrast) and using RFP and GFP channels to create a merged image. This experiment was performed twice, multiple images were taken of each slide and the above was selected as a representative image.

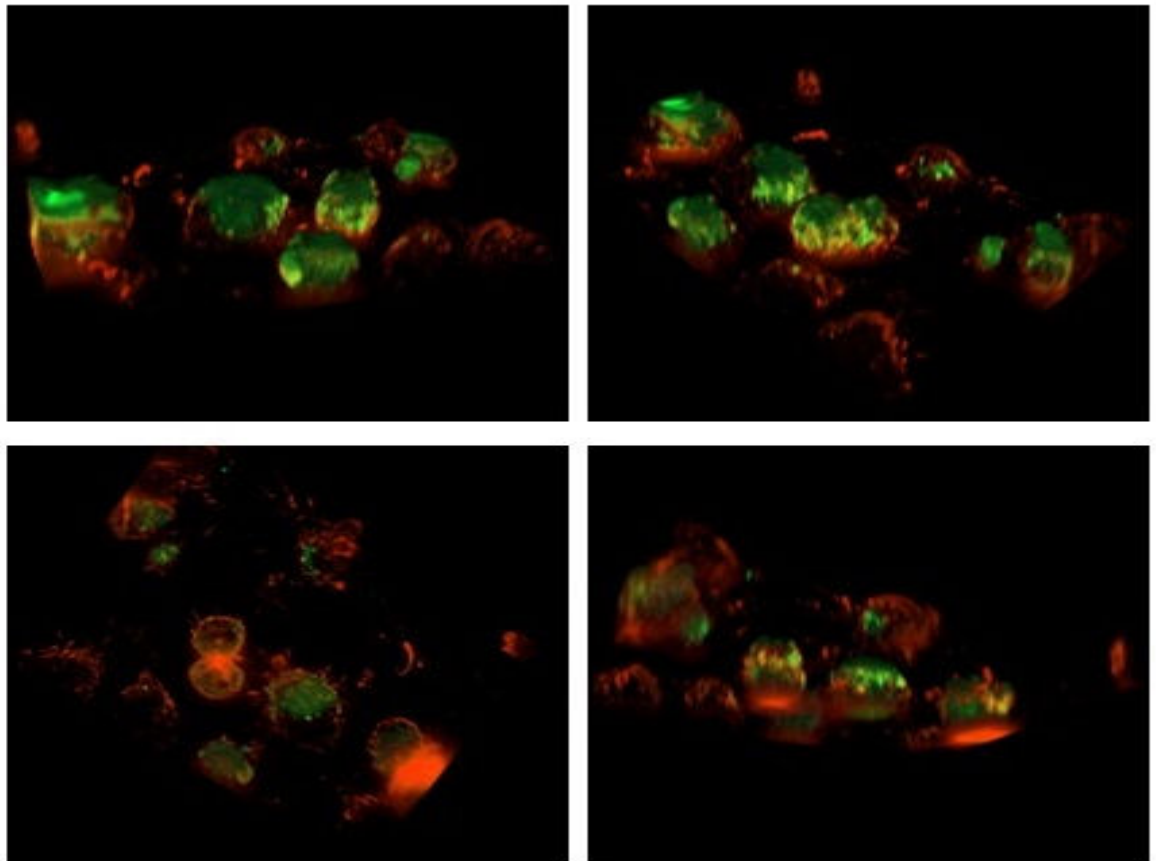


Figure 4-22 3D image of e-D123PLY treated RAW 264.7 cells stained with rhodamine phalloidin.

The z-stacks of image 4-21 were combined using Volocity® software to create a 3D image of e-D123PLY binding to the RAW 264.7 cell lines. The software was also used to create a movie of this image by compiling snapshots taken from different angles; this movie can be viewed in the compact disk accompanying this thesis.

4.3.5 Visualising interactions between D4PLY and the actin cytoskeleton using eGFP-tagged D4PLY

In contrast to e-D123PLY treated cells, in figure 4-23 e-D4PLY treated cells the ‘rings’ of actin around the edges of the cells are less visible and are condensed in a punctate formation. Additionally, there is no actin visibly associated with e-D4PLY, which could suggest that D4PLY disrupts the actin cytoskeleton upon binding, this could potentially indicate podosome degradation and may be associated with the cell rounding and detachment observed in PLY-mediated cell death.

In figure 4-24 the 3D image analysis shows that in common with e-D123PLY treated cells there is an absence of cytoplasmic actin in e-D4PLY treated cells.

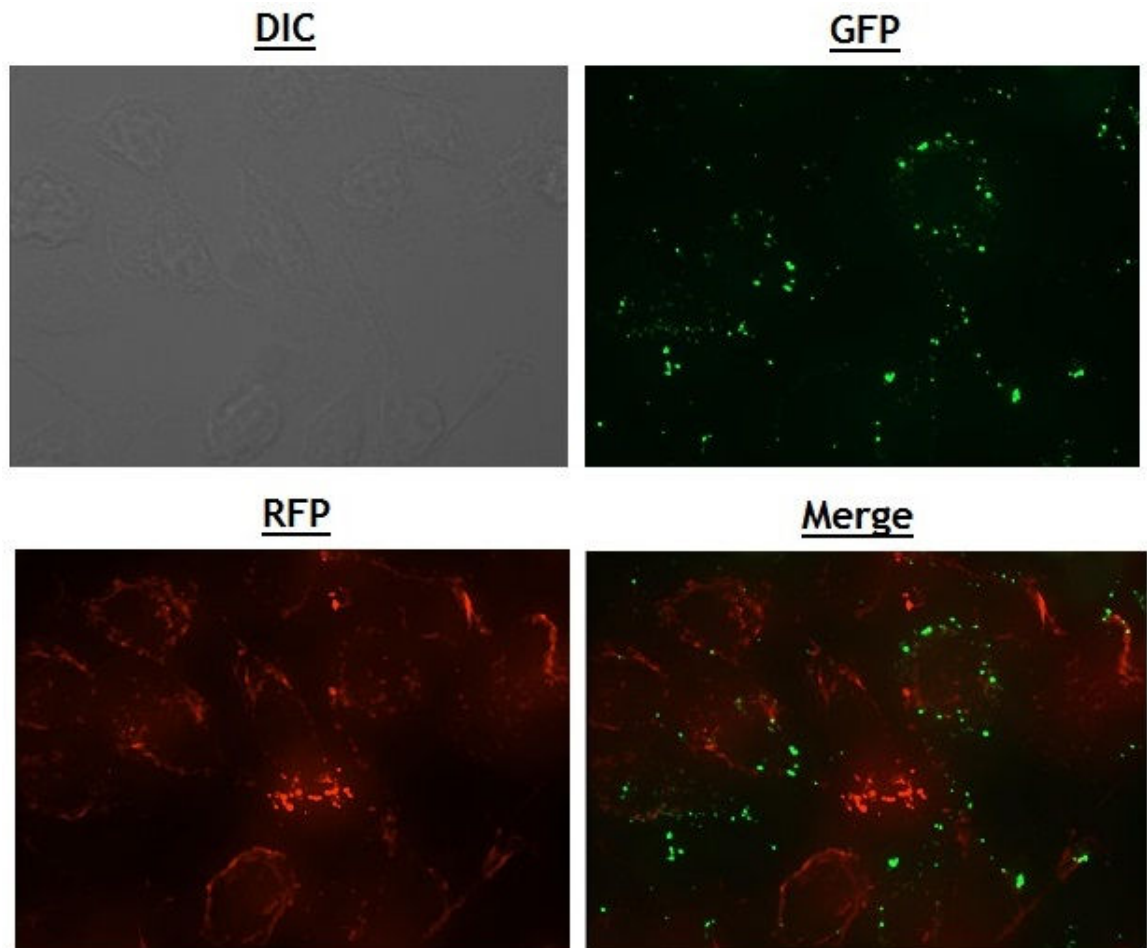


Figure 4-23 2D merged image of e-D4PLY treated RAW 264.7 cells stained with rhodamine phalloidin.

RAW 264.7 cells were seeded at 1×10^6 /well in a 6-well plate containing cover slips and allowed to adhere O/N at 37°C . The cells were treated with 1ml 17.5nM e-D4PLY for 30 minutes; the cells were washed and stained with rhodamine phalloidin according to the protocol in section 2.8.1.2. The cells were fixed in 4% paraformaldehyde before a final rinse in PBS. The cover slips were removed and mounted onto microscope slides using Dako Fluorescent Mounting Media, images were captured using the Zeiss-axio imager at 100X magnification. Images of the cells were captured using DIC (differential interference contrast) and using RFP and GFP channels to create a merged image. This experiment was performed twice, multiple images were taken of each slide and the above was selected as a representative image.

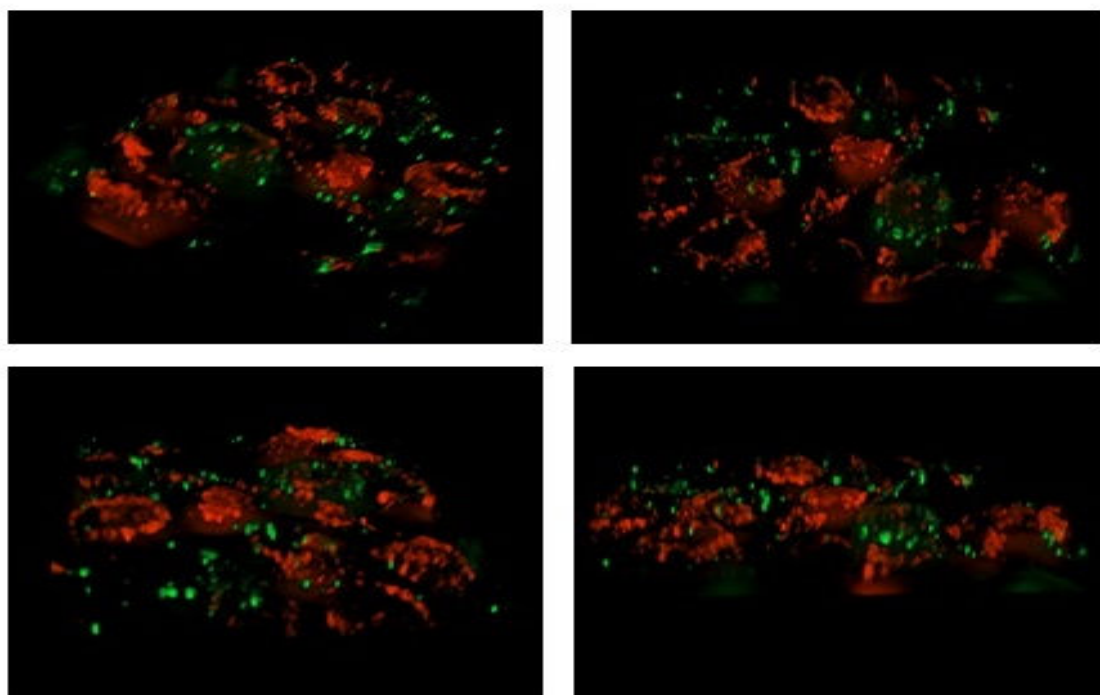


Figure 4-24 3D image of e-D4PLY treated RAW 264.7 cells stained with rhodamine phalloidin.

The z-stacks of image 4-23 were combined using Volocity® software to create a 3D image of e-D4PLY binding to the RAW 264.7 cell lines. The software was also used to create a movie of this image by compiling snapshots taken from different angles; this movie can be viewed in the compact disk accompanying this thesis.

4.3.6 Analysis of colocalization by thresholded Pearson's correlation coefficient (PCC)

The thresholded Pearson's correlation coefficient (PCC) is a statistical tool for demonstrating the strength of a relationship between two variables. PCC analysis cannot be used as confirmation of a direct interaction, however, it can be used to demonstrate colocalization and to indicate interactions for further analysis. Rather than relying on visible overlap from different channels (e.g red and green equals yellow/orange) PCC defines values (thresholds) within each channel, this removes objectivity when assessing colocalization. Briefly, the pixels within a pair of fluorescent images are mapped, the mean pixel intensity for the each image is subtracted from the intensity of each pixel. The individual pixel values from each image are multiplied to give the product of the difference of the mean. The products of the difference of the mean are summed for the entire image and divided by the maximum possible sum for the difference of the mean for the entire image. PCC analysis generates values

between 1 and -1, where 1 = a perfect correlation, 0 = no correlation and -1 = a perfect but inverse correlation. Table 4-3 shows the PCC values for the relationships between PLY variants and actin, the strongest correlation is between e-D123PLY (0.75) and actin followed by e-PLY and actin (0.45), both e- Δ 6PLY and e-D4PLY have weak, positive relationships with actin.

Table 4-3 PCC values for PLY variants and actin

Protein	PCC	Strength and direction of correlation
e-PLY	0.45	Moderate, positive.
e- Δ 6PLY	0.32	Weak, positive.
e-D123PLY	0.75	Strong, positive.
e-D4PLY	0.24	Weak, positive.

4.3.7 Quantifying binding affinity between PLY and actin by ELISA

The ability of PLY and its derivatives to directly bind actin was recently described (Hupp et al., 2013), following microscopic analysis of interactions with the actin cytoskeleton, an ELISA based binding assay described in this paper was replicated to see if similar results were obtained. It was seen that all PLY variants tested were capable of directly binding actin in a dose-dependent manner; D4PLY had both the strongest and weakest binding affinity at the highest and lowest concentrations, respectively. At 175nM and 17.5nM Δ 6PLY has the weakest binding affinity compared to other PLY variants, this replicates what was observed in the Hupp et al., 2013 study. This also fits with the changes in cytoskeleton structure observed microscopically, where e- Δ 6PLY caused the least disruption to the actin cytoskeleton.

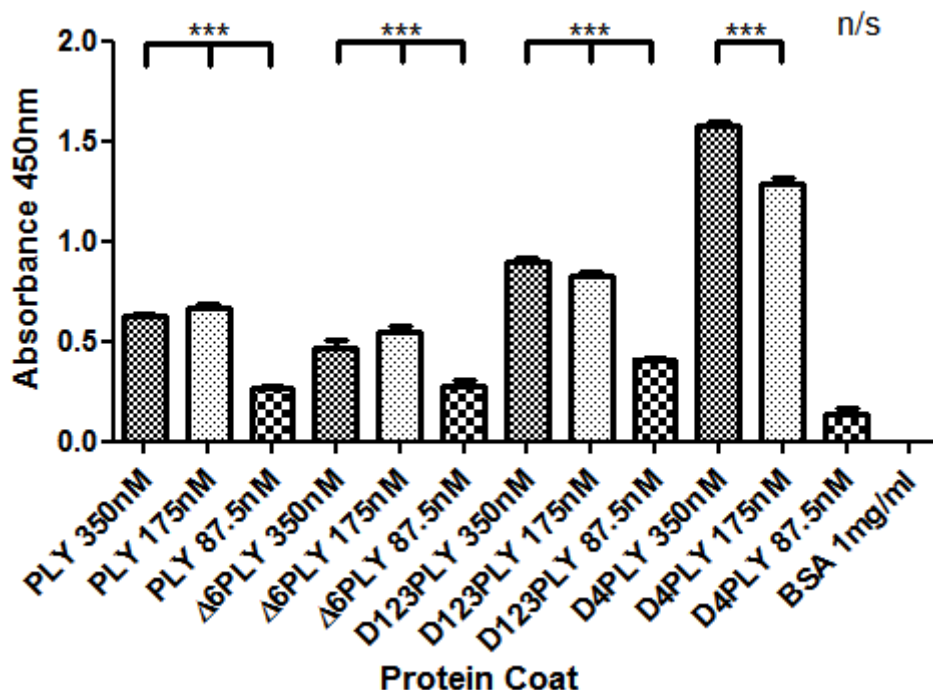


Figure 4-25 Actin Binding ELISA.

ELISA plates were coated with 50 μ l purified PLY and its derivatives (plus BSA control 1mg/ml) O/N at 4°C. The plates were washed x5 with PBS/Tween before incubating with 50 μ l non-muscle actin (Cytoskeleton, Inc.) Bound actin was detected using monoclonal anti-actin antibody (1:1000, Cytoskeleton, Inc.) followed by anti-rabbit-HRP (1:1000, Promega) and developing with OPD, absorbance at 405nm was measured using a BMG fluostar Optima. Statistical significance was assessed by one-way ANOVA with a Bonferroni post-test (comparing all pairs of columns). To conserve space, as all but one condition (D4PLY 87.5nM) was significantly (***) higher than the control (BSA 1mg/ml), the different protein conc. were grouped together, *(p<0.05), **(p<0.01), ***(p<0.001). This experiment was performed once with three technical replicates per condition, data are mean+SEM.

4.4 Discussion

The HaloTag® system was an ideal platform for these studies which have given key insights into interactions with host cells that may contribute to adjuvanticity. We have found that all PLY variants studied were capable of binding to the cell surface of RAW 264.7 macrophages and that this was not due to the HaloTag (as h-eGFP did not bind to cells). The morphology of RAW 264.7 cells was most changed in response to h-PLY, unsurprising as this was the only cytolytic protein tested. The h-PLY treated cell were visibly rounded and membrane shedding could be observed (figure 4-2), this a documented cellular reaction to pore-forming toxins (Walev et al., 1994) and may be linked to cellular recovery, however, as seen in chapter 3, RAW 264.7 cells are not

particularly resistant to PLY-mediated lysis and so this could be a sign of necrosis (Hirst et al., 2004; Zysk et al., 2001).

This study has highlighted the ability of domains 1-3 to directly bind host cells, a function not previously recognized in pneumolysin. This has however been noted previously in domain 1-3 of listeriolysin (LLO) and could be a common attribute of CDCs, it was also found that separately purified domains 1-3 and domain 4 of LLO could recombine on the cell surface and cause lysis of RBCs (Dubail et al., 2001); this experiment was replicated using D123PLY and D4PLY but lysis of RBC did not occur, this could however be due to the His⁶ tag. The unusual binding pattern of D123PLY could indicate aggregation of a specific receptor. In the previous chapter a TLR4 binding site was identified in domains 1-3, D123PLY was also shown to induce KC production. Combined, these findings identify domains 1-3 as a region of interest for future studies into host cell binding and interactions that are conducive to adjuvanticity. In the case of D4PLY it is already known that binding to membrane cholesterol is an essential process in adherence to the cell membrane, the distinct binding pattern may simply be a reflection of cholesterol localization within this cell type. As the binding patterns differed so obviously between the truncation mutants and full-length PLY variants it may be assumed that the individual binding properties of the different domains combine to create that of the full-length proteins. The punctate distribution pattern seen in both PLY and $\Delta 6$ PLY suggests that the delta 6 mutation does not interrupt oligomerization, but instead somehow prevents insertion or coherent formation of the pre-pore. This has previously been demonstrated in electron microscopy, where $\Delta 6$ PLY was seen to form structures like pores on the cell surface as well as dysfunctional structures such as arcs (figure 4-26) (Kirkham, 2006; Nöllmann et al., 2004).

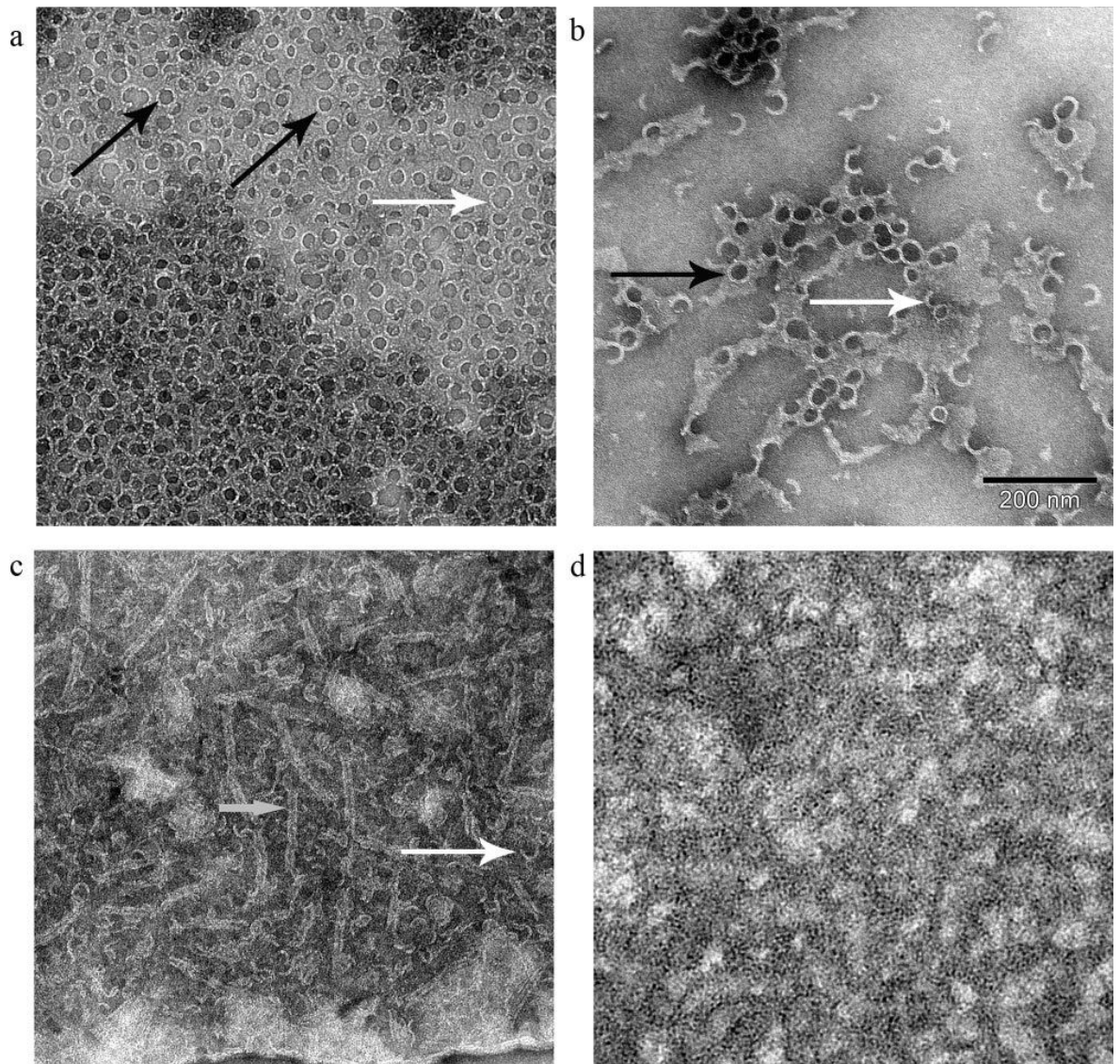


Figure 4-26 Electron microscopy image of pore formation.

This image was taken from (Kirkham et al., 2006) and shows a) 0.2mg/ml PLY, b) 0.2mg/ml PdB, c) 0.2mg/ml Δ 6PLY and d) PBS bound to horse erythrocytes.

Current knowledge of the adjuvant activity of Δ 6PLY suggests that internalization of the protein does occur and is necessary to generate adaptive immune responses to target antigens. In a study of adjuvanticity antibody responses to the model antigen eGFP were only observed when eGFP was genetically fused to PLY/ Δ 6PLY, no response was generated to eGFP admixed with the protein (Douce et al., 2010). Internalization of either truncation domain was not clearly observable, however, h- Δ 6PLY had clearly been taken into the cell, this cannot be due to passive passage through pores therefore we can hypothesize a specific uptake mechanism such as receptor mediated endocytosis is involved. This could be further investigated using a model of antigen presentation; an antigen presentation assay was devised using PLY variants genetically fused to OVA₃₂₃₋₃₃₉ and a T-cell hybridoma reporter cell line

specific to this peptide, however, at the time of writing this thesis the preliminary results were inconclusive.

Using HaloTag technology to perform protein pull-down has identified seven potential binding partners for PLY; of particular interest are the cytoskeletal components vimentin and tubulin β -5 chain as other studies have also shown interactions between PLY and the cytoskeleton (Iliev et al., 2007). One aim of this study was to verify the interaction between D123PLY and TLR4, bands of the expected size (90kDa) were analyzed by mass spectrometry however TLR4 was not identified. It is possible that the interaction between PLY and TLR4 is weak or transient; therefore its identification by pull-down would be difficult, if this experiment were repeated it would be useful to test for the presence of TLR4 in the mammalian cell lysate by western blot. No immune receptors were identified following the pull-down; however, not all of the excised bands were analyzed so it is possible that these may be identified in the remaining bands. It is important to understand that the pull-down results may not necessarily indicate direct interactions with PLY or its variants. Following a direct interaction with PLY any other molecules complexed with the target protein could also be pulled out, this may explain some of the less expected hits from mass spectrometry. For example, PLY has been shown to directly interact with the actin cytoskeleton, therefore it is feasible that other proteins associated with cellular structure and transport such as vimentin and LLPPRC would be associated with actin and could be pulled out simultaneously. These proteins in turn could be associated with other proteins, for example, vimentin provides support to organelles such as the nucleus, endoplasmic reticulum and mitochondria, this could explain the presence of the proteins pyruvate kinase and 60s acidic ribosomal protein P0. Although the h-eGFP microscopy experiments showed no binding of h-eGFP to RAW264.7 cells a further pull-down using a HaloTag only control would be appropriate to conclusively demonstrate that proteins identified are binding only to PLY variants and not the HaloTag. To further confirm protein-protein interactions between PLY and mammalian cells it may be essential to perform direct binding assays such as that performed using actin (figure 4-25). In particular, it may be of interest to confirm a direct interaction between PLY and tubulin β -5 chain, this protein is a subunit of microtubules and binding to this protein could be essential for the ability of PLY

to inhibit ciliary beat, an important factor in pneumococcal colonization and spread of infection (Beurg et al., 2005; Rubins et al., 1992).

The pull-down showed a clear relationship between PLY and the cytoskeleton, this has previously been described in the literature. Studies by the Iliev group have recently shown that PLY directly interacts with cytoskeletal actin (Hupp et al., 2013). These findings were replicated in this work, PCC analysis of colocalization (table 4-3) produced the same pattern as that of binding affinity, where PLY and D123PLY have the highest affinity followed by $\Delta 6$ PLY and finally D4PLY. The analysis of direct binding by ELISA (figure 4-25) did not replicate these results exactly and assigned the highest binding affinity to D4PLY; however, these results are from a single assay and should be repeated to provide statistical validity. Previously, it has also been shown by the same group that the changes in cell morphology observed in PLY treated cells are dependent on cholesterol-binding and pore formation (Förtsch et al., 2011; Iliev et al., 2009), these studies did not include truncation mutants and could explain why the most dramatic changes in the actin cytoskeleton were observed in cells treated with e-PLY and e-D4PLY. In contrast to eGFP treated cells the actin cytoskeleton in cells treated with PLY and its derivatives is clearly altered, actin destabilisation and podosome degradation can be observed in response to both e-PLY and e- $\Delta 6$ PLY (figures 4-17 and 4-19, respectively), in contrast the actin cytoskeleton in e-D123PLY (figure 4-21) treated cells does not differ significantly from control cells. The proposed model for interaction between D123PLY and the actin cytoskeleton only allows for contact between the two proteins following insertion of full-length PLY into the cell membrane, a portion of domains 1-3 could then feasibly interact with the cytoskeleton. The evidence presented in this chapter indicates that D123PLY is capable of interacting with cellular actin in a solid phase binding assay. The strong correlation seen by PCC analysis may simply be a reflection of the ubiquitous presence of both proteins and the proximity of membrane bound D123PLY to intracellular actin rather than a direct interaction. It is unlikely that domains 1-3 of PLY are capable of interacting with the actin cytoskeleton unless present in the context of lytic PLY. In e-D4PLY treated cells the actin cytoskeleton is visibly condensed and disrupted (figure 4-23). In addition e-D4PLY does not appear to be associated with actin (which correlates with PCC analysis) suggesting that some aspects of PLY-dependent changes in the actin cytoskeleton do not require direct binding and

could be a consequence of/induced by distal interactions with the cell such as cholesterol binding.

The work presented in this chapter has given insight into interactions with the cells that could be further investigated as mechanisms of adjuvant activity; for example, the role of the different domains in internalization and antigen presentation. Given that the binding patterns of the separated domains are markedly different, it will be of interest to discover whether they are trafficked or processed by different mechanisms and how this relates to the same processes in the full-length protein(s). As mentioned earlier, as an adjuvant PLY does not create a bystander effect i.e. antibody responses are not mounted against antigens unless they are genetically coupled to the toxin; this suggests that both PLY and the fusion antigen are pulled into the cell by a specific uptake mechanism. It will be of interest to further study localization of PLY and its derivatives (particularly after longer incubation periods) and to isolate the mechanism of antigen uptake through the use of specific endocytosis inhibitors such as cytochalasin D. These studies have also revealed new properties of D123PLY and increased the recognition of its potential role(s) in adjuvanticity. The use of truncation mutants in this study has unveiled properties of the domains in isolation, it remains to be seen if this gives insight into how the toxin works as a complete protein or confuses the study by unmasking properties not belonging to the whole molecule.

5. The Role of TLR4, Complement and IL-1 β in the Adjuvant Activity of Pneumolysin

As described in chapter three TLR ligation is the first step (signal one) in IL-1 β production, and given the increasing evidence that PLY is a TLR4 ligand and can activate the NLRP3 inflammasome through pore formation (signal two) (McNeela et al., 2010; Witzernath et al., 2011) it was expected that IL-1 β would be produced in PLY treated BMDM. However, as shown in figure 3-13 PLY alone cannot stimulate IL-1 β production in BMDM and an exogenous TLR ligand such as LPS is required. Initial studies into PLY-dependent gene expression (appendix 5, table 1) showed that IL-1 β was upregulated at the mRNA level in a single sample of PLY treated BMDM. It therefore seemed possible that PLY was providing TLR4 ligation and IL-1 β was upregulated in response (signal one). However, at this time it was unclear why IL-1 β was not then found in the supernatants of PLY treated cells.

In recent years the role of complement in both innate and adaptive immunity has been expanded, of particular relevance are several studies demonstrating a synergistic relationship between complement activation and TLR ligation (Fang et al., 2009; Zhang et al., 2007). In particular, complement activation has been shown to increase the production of pro-inflammatory cytokines such as IL-1 β . Analysis of gene expression in response to PLY treatment showed an upregulation of complement C3 in response to PLY treatment in BMDM (appendix 5, table 5). PLY is known to activate the classical complement pathway (Paton & Ferrante, 1984; Yuste et al., 2005) and therefore a new hypothesis was generated, where the activation of complement and TLR ligation by PLY would synergize to alter the cytokine expression profiles of PLY treated BMDM. The *in vitro* BMDM PLY treatment model used in this thesis was altered to include a complement source (whole serum) and the presence of complement in conjunction with PLY treatment was found to induce secretion of IL-1 β into cell supernatants.

The first hypothesis, detailed in chapter 3, figure 3-12, which proposed a model of adjuvanticity where IL-1 β production in response to PLY led to increased antibody magnitude compared to $\Delta 6$ PLY immunization was now further investigated. Using a previously published (Douce et al., 2010) *in vivo* model of

immunization the role(s) of both complement and IL-1 β in the adjuvant activity of e-PLY and e- Δ 6PLY were investigated. These studies provide a new model of PLY adjuvanticity where complement and NLRP3 activation and subsequent IL-1 β production are beneficial but not essential for the adjuvant activity of PLY.

5.1 The production of IL-1 β in PLY Treated BMDM is Dependent on Pore Formation and NLRP3 Activation

Evidence in the literature has shown that PLY is able to activate the NLRP3 inflammasome through pore formation (Chu et al., 2009; McNeela et al., 2010). Using BMDM generated from NLRP3 $^{-/-}$ transgenic mice it is shown that PLY-dependent IL-1 β production is entirely dependent on the NLRP3 inflammasome (figure 5-1).

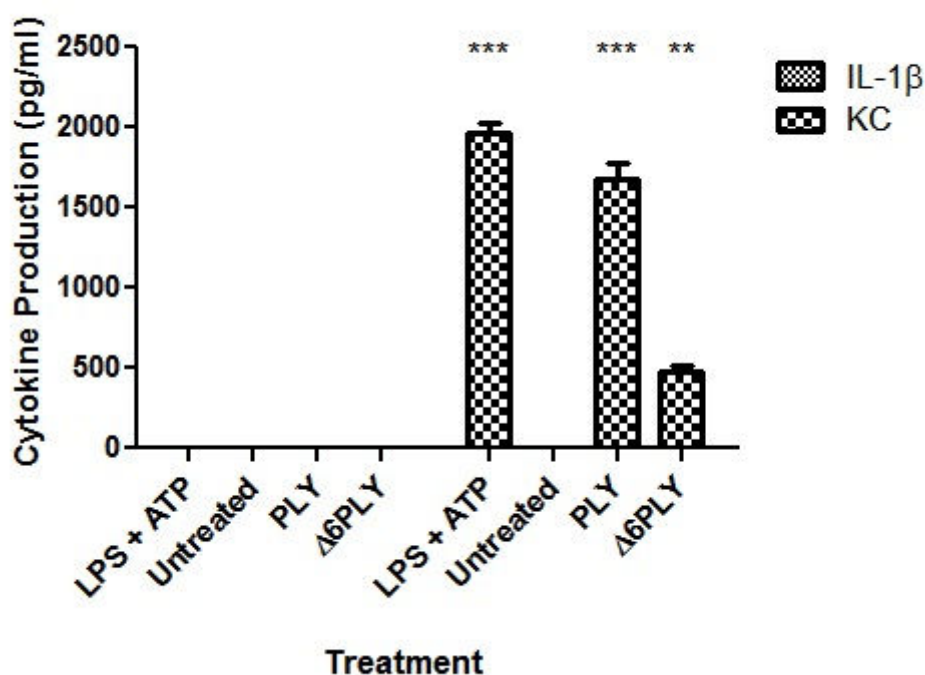


Figure 5-1 IL-1 beta and KC production in NLRP3 $^{-/-}$ BMDM treated with PLY and Δ 6PLY.

Transgenic BMDM were seeded at 1×10^5 cells/well in a 96-well plate and allowed to adhere. The cells were treated with either PLY or Δ 6PLY (17.5nM final conc.) alone or in the presence of 10% C3 $^{-/-}$ sera or complement sufficient sera (total well volume 200 μ l) and incubated for 6 hours at 37 $^{\circ}$ C. A positive control of 100ng/ml LPS + 5mM ATP was performed. The cell supernatants were harvested and IL-1 β and KC were measured by ELISA (R and D systems). Statistical significance was tested by one-way ANOVA comparing all columns to the control column (untreated), *($p < 0.05$), **($p < 0.01$), ***($p < 0.001$). This experiment was performed three times with three technical replicates per condition, data are mean+SEM.

Although NLRP3^{-/-} BMDM are incapable of producing IL-1 β in response to the standard positive control (LPS+ ATP), KC production in response to LPS is unaffected. Similarly, the KC response to PLY treatment is unchanged; however, the KC response to Δ 6PLY is reduced compared to BMDM from MF1 mice.

5.2 The Role of Complement in IL-1 β Production in PLY Treated BMDM

The *in vitro* PLY treatment assay previously used was altered by the addition of 10% whole, fresh mouse serum as a complement source. This assay was used to investigate the effect on cytokine production of simultaneous complement activation during BMDM treatment with PLY variants.

Figure 5-2 shows that the addition of complement sufficient serum significantly increased IL-1 β in PLY treated cells. IL-1 β production was dependent on lytic activity of PLY (most likely through activation of the NLRP3 inflammasome), however, there is a balance between lytic activity and IL-1 β production as treatment with 175nM PLY results in less IL-1 β than treatment with 17.5nM, and this is likely due to cell death. Where complement sufficient serum was replaced with serum from mice lacking the C3 component of the complement cascade IL-1 β production was reduced but still present. IL-1 β production in BMDM treated with 17.5nM PLY in the presence of C3^{-/-} sera was significantly lower than those treated with 17.5nM PLY in the presence of complement sufficient (MF1) sera ($p = <0.05$).

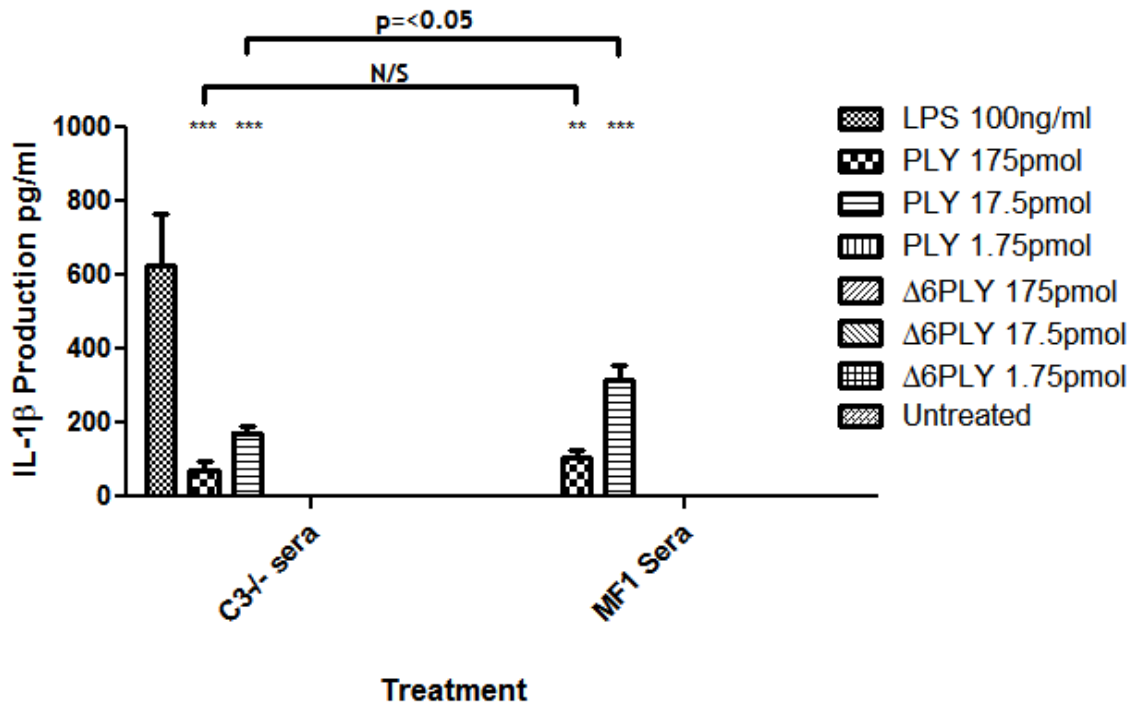


Figure 5-2 IL-1 β production in BMDM treated with PLY plus sera.

BMDM were seeded at 1×10^5 cells/well in a 96-well plate and allowed to adhere. The cells were treated with PLY or $\Delta 6$ PLY at 175, 17.5 or 1.75nM (final conc.). Before addition of the proteins 20 μ l of the cell supernatant was replaced with whole, fresh serum obtained from complement sufficient (MF1) or C3-/- mice (final well volume 200 μ l). The cells were treated with the proteins or LPS positive control for 6 hours at 37°C. Assay supernatants were harvested and tested for the presence of IL-1 β by ELISA (R and D systems). Statistical significance was tested by one-way ANOVA with a Bonferroni's post test (comparing all pairs of columns), shown above each column is significance compared to the control (untreated), comparisons between other columns are indicated by solid black lines, *($p < 0.05$), **($p < 0.01$), ***($p < 0.001$). This experiment was performed three times with three technical replicates per condition, data are mean+SEM.

To further investigate the role of complement in IL-1 β production *in vitro* increasing ratios of complement sufficient serum of either heat treated complement sufficient sera or C3-/- sera were added to PLY treated cells. The production of IL-1 β increased proportionally in response to the increasing presence of complement components (figure 5-3), demonstrating a dose-response curve.

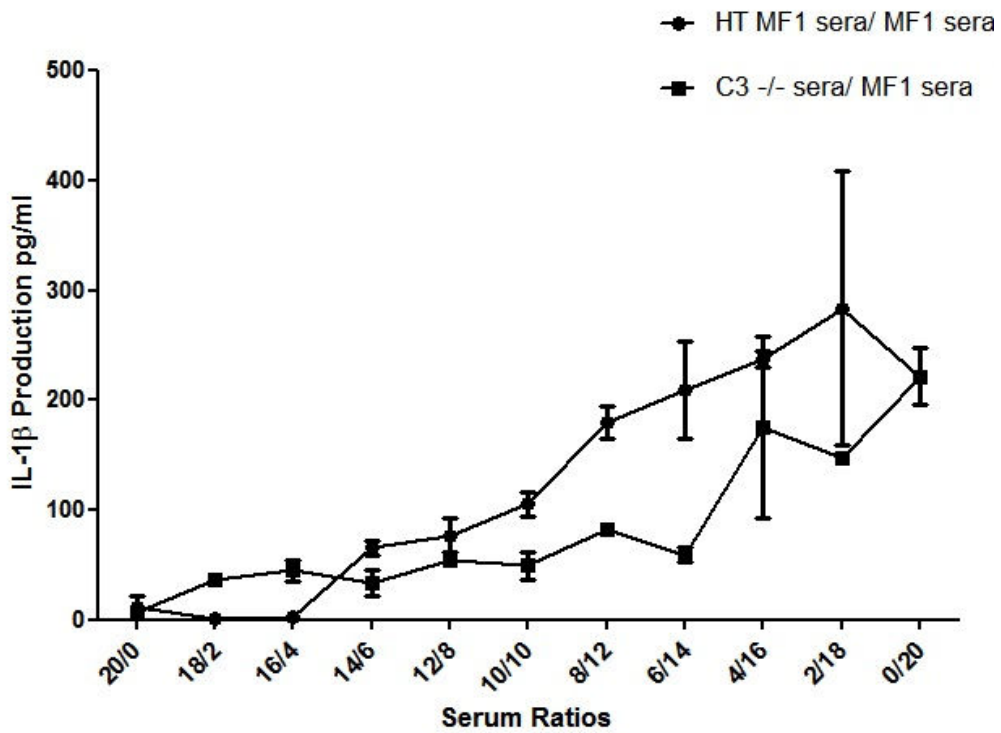


Figure 5-3 IL-1 β production in BMDM treated with PLY in the presence or absence of complement.

BMDM were seeded at 1×10^5 cells/well and allowed to adhere. The cells were treated with PLY or $\Delta 6$ PLY at 17.5nM (final conc.) for 6 hours. Before addition of the proteins 10% of the cell supernatant was replaced with sera. Heat treated (HT) or C3-/- sera were mixed with increasing ratios of complement sufficient sera (MF1). Assay supernatants were harvested and tested for the presence of IL-1 β by ELISA (R and D systems). This experiment was performed once with two technical replicates per condition, data are mean+SEM.

These initial experiments demonstrated that simultaneous complement activation plays a role in the immune response to PLY, specifically IL-1 β production. Figure 5-4 shows an updated model of PLY-dependent IL-1 β production. Now that it had been demonstrated that PLY treated BMDM were capable of producing IL-1 β under certain conditions, the IL-1 β hypothesis (figure 3-12) was further investigated.

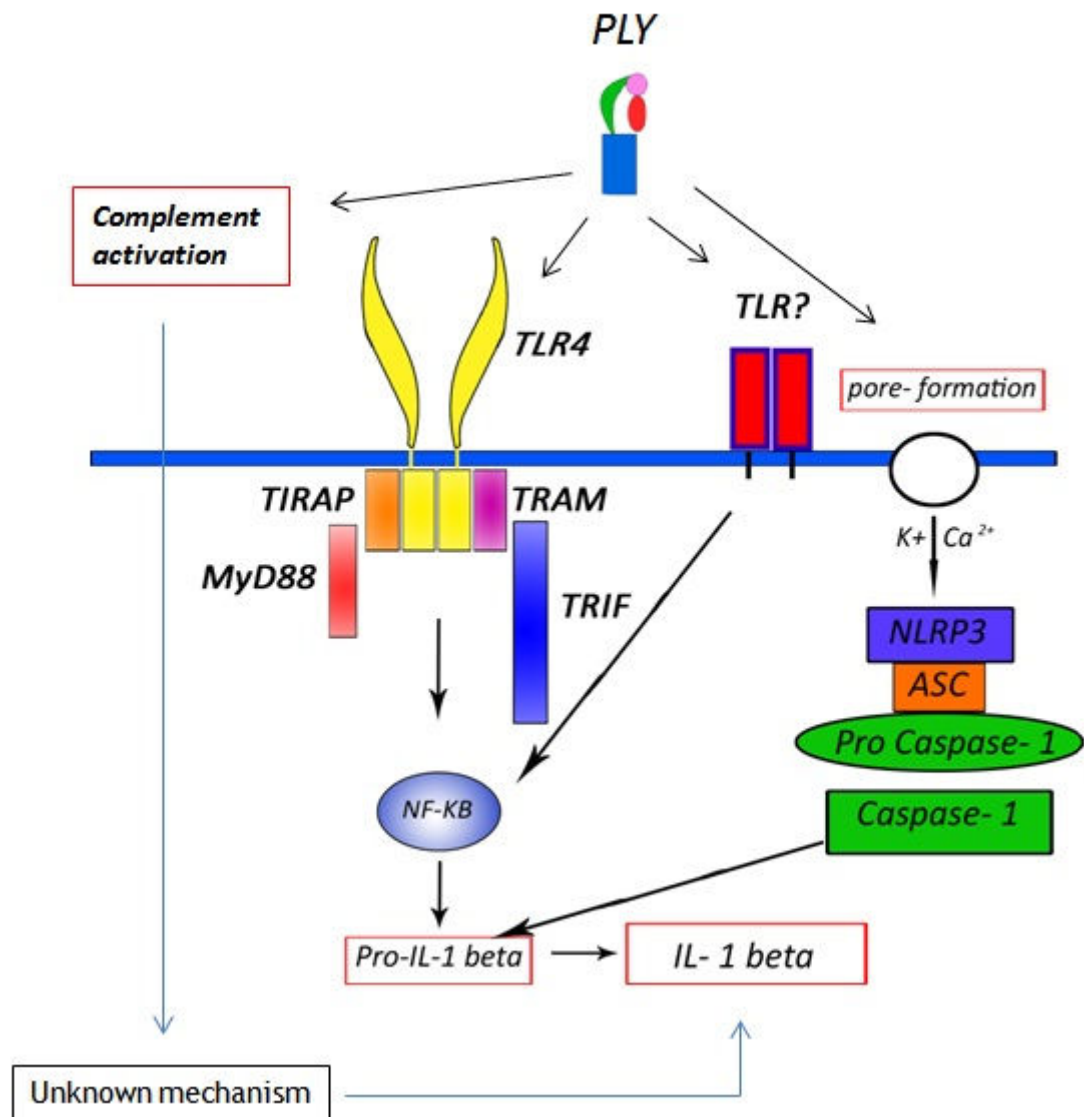


Figure 5-4 Putative model of PLY-dependent IL-1 beta production, version 2.

In this model the production of IL-1 β occurs in response to PLY treatment and simultaneous complement activation, the mechanism remains undefined but is possibly due to synergy between complement components and TLR stimulation.

5.3 Cytokine Production in PLY Treated Transgenic BMDM

Given the evidence in the literature for synergy between TLR ligation and complement activation (Fang et al., 2009; Zhang et al., 2007) and the increasing evidence of PLY as a TLR4 ligand (chapter 3), the contributions of these immune components in the cytokine responses of BMDM to PLY treatment were further investigated.

5.3.1 C3^{-/-} BMDM

Macrophages are a known source of peripheral complement C3 production (Strunk et al., 1983) and as C3 was upregulated in response to PLY treatment (table 5-5) it was possible that *in situ* C3 production could be responsible for the residual IL-1 β production in BMDM treated with PLY and C3^{-/-} serum. To investigate this hypothesis BMDM were generated from C3^{-/-} transgenic mice and used in the treatment assay (figure 5-5). It was found that the complete absence of complement component C3 (from either exogenous or endogenous sources) resulted in no significant change in IL-1 β production compared to control cells or C3^{-/-} cell treated with complement sufficient serum. However, all other complement components are assumed to be present at normal concentrations, the potential involvement of other complement components is considered in the discussion section of this chapter.

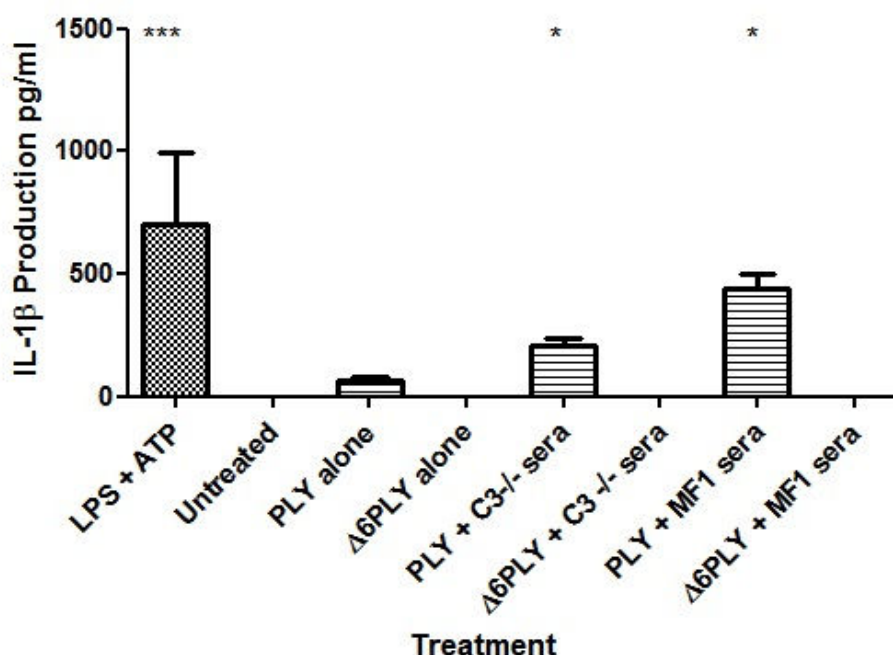


Figure 5-5 IL-1 β production in C3^{-/-} BMDM.

Transgenic macrophages were seeded at 1×10^5 cells/well and allowed to adhere. The cells were treated with PLY or Δ 6PLY at 17.5nM (final conc.) either alone or in the presence of 10% C3^{-/-} sera or complement sufficient sera for 6 hours at 37°C. A positive control of 100ng/ml LPS + 5mM ATP was performed. Assay supernatants were tested for the presence of IL-1 β by ELISA (R AND D SYSTEMS). Statistical significance was tested by one-way ANOVA comparing all columns to the control column (untreated), *(p<0.05), **(p<0.01), ***(p<0.001). This experiment was performed twice with three technical replicates per condition, data are mean+SEM.

A lack of complement C3 had no effect on the production of KC in response to PLY treatment. KC was used a control for response to PLY, neither a lack of complement C3 (figure 5-6(A)) nor addition of complement sufficient serum (figure 5-6(B)) significantly altered the production of KC in response to PLY.

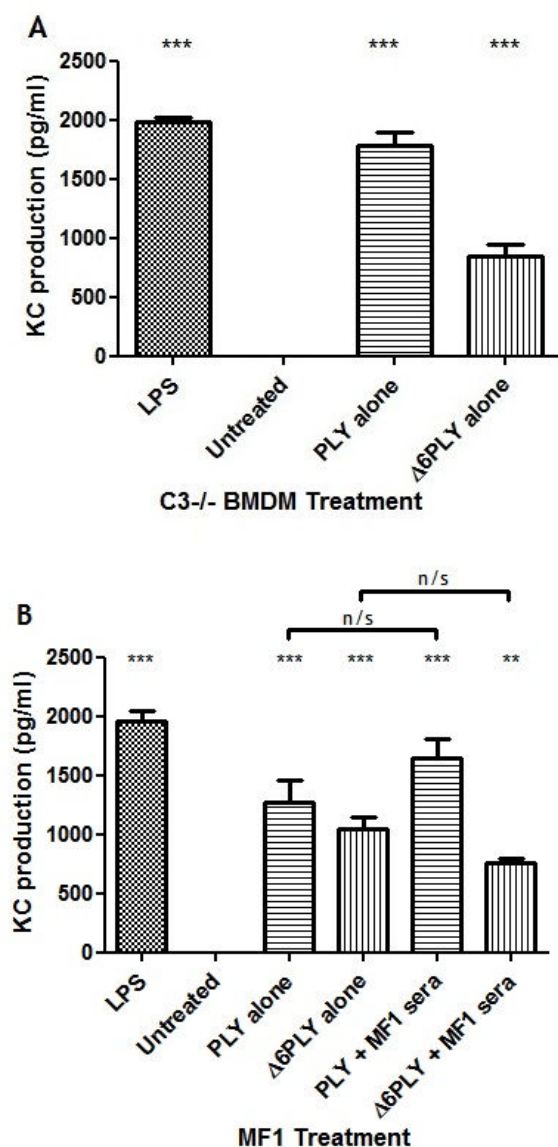


Figure 5-6 KC production in (A) C3^{-/-} and (B) MF1 BMDM.

BMDM generated from (A) C3^{-/-} and (B) MF1 mice were seeded at 1×10^5 cells/well and allowed to adhere. The cells were treated with PLY or Δ6PLY at 17.5nM (final conc.) and LPS (100ng/ml) for 6 hours at 37°C. PLY/Δ6PLY treated MF1 BMDM were additionally treated with 10% complement sufficient sera (200μl total well volume). Assay supernatants were tested for the presence of KC by ELISA (R and D systems). Statistical significance was tested by one-way ANOVA with a Bonferroni's post test (comparing all pairs of columns), shown above each column is significance compared to the control (untreated), comparisons between other columns are indicated by solid black lines, *(p<0.05), **(p<0.01), ***(p<0.001). This experiment was performed three times with three technical replicates per condition, data are mean+SEM.

5.3.2 TLR4^{-/-} BMDM and VIPER treated BMDM

It has been demonstrated that PLY is a TLR4 ligand; therefore it was thought this would provide 'signal 1' (figure 3-12) and induce transcription of pro-IL-1 β for subsequent cleavage by the NLRP3 inflammasome 'signal 2'. To further investigate this BMDM generated from TLR4^{-/-} transgenic mice were used in the PLY treatment assay (figure 5-7). Interestingly, it was found that IL-1 β was produced in response to PLY alone as well as in the presence of complement sufficient sera; the concentration of IL-1 β in cell supernatants was approximately six-fold less than that produced by BMDM generated from MF1 mice when comparing PLY treated cells in the presence of complement sufficient sera. The production of IL-1 β in response to the standard positive control (LPS+ATP) was completely lost.

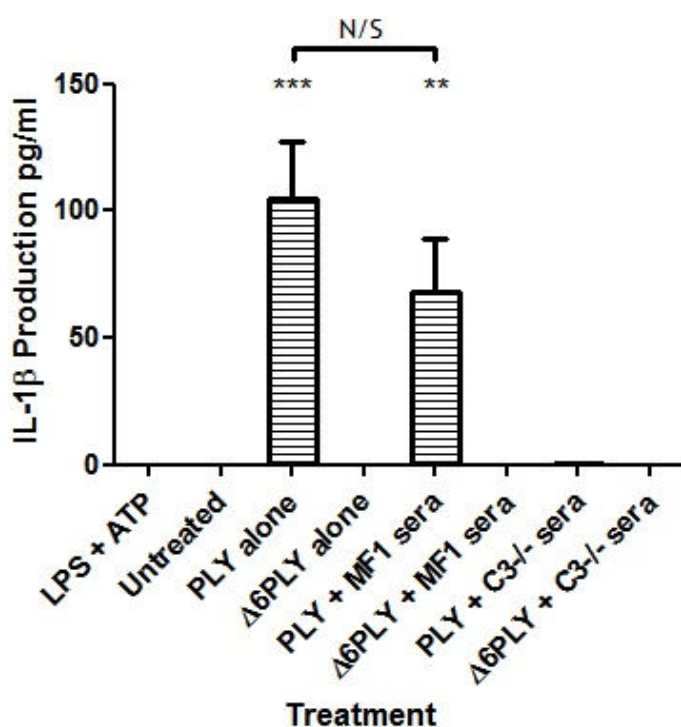


Figure 5-7 IL-1 β production in TLR4^{-/-} BMDM.

BMDM generated from TLR4^{-/-} mice were seeded at 1×10^5 cells/well and allowed to adhere. The cells were treated with PLY or Δ 6PLY at 17.5nM (final conc.) either alone or in the presence of 10% C3^{-/-}sera or complement sufficient sera (200 μ l total well volume) for 6 hours at 37 $^{\circ}$ C. A positive control of 100ng/ml LPS + 5mM ATP was performed. Assay supernatants were tested for the presence of IL-1 β by ELISA (R and D systems). Statistical significance was tested by one-way ANOVA with a Bonferroni's post test (comparing all pairs of columns), shown above each column is significance compared to the control (untreated), comparisons between other columns are indicated by solid black lines, *($p < 0.05$), **($p < 0.01$), ***($p < 0.001$). This experiment was performed twice with three technical replicates per condition, data are mean+SEM.

As an additional method for determining the role of TLR4 in IL-1 β production, BMDM were treated with a TLR4 inhibitor (VIPER) before PLY treatment (figure 5-8). The pattern of IL-1 β production in this variation of the treatment assay was virtually identical to that observed in a TLR4 $^{-/-}$ model. Again, the LPS+ATP positive control did not induce IL-1 β but IL-1 β production was seen in response to PLY alone as well as PLY + complement sufficient serum.

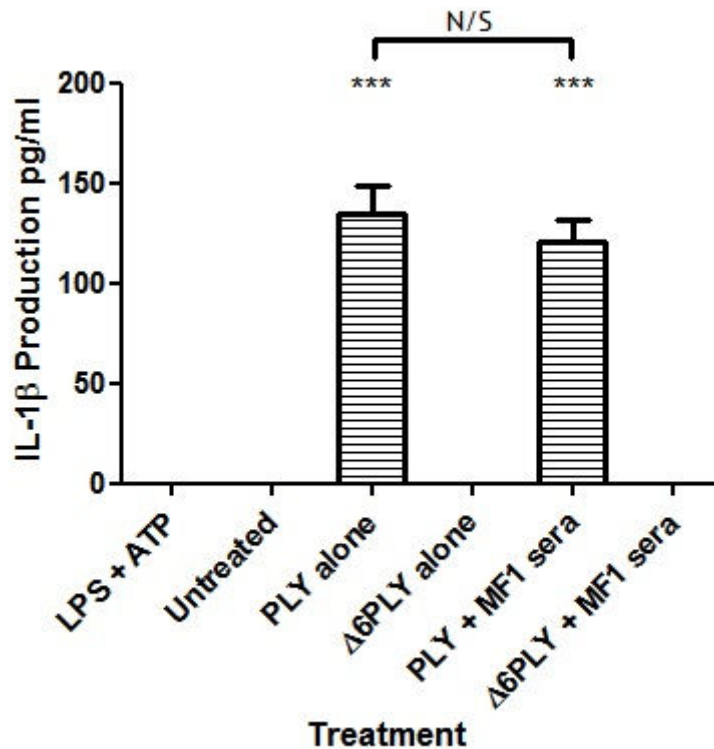


Figure 5-8 IL-1 β production in VIPER treated BMDM.

BMDM were seeded at 1×10^5 cells/well and allowed to adhere. The BMDM were pre-treated for 2 hours with VIPER (TLR4 inhibitor) at a final conc. of $30 \mu\text{M}$. The supernatant was removed and replaced with fresh medium. Macrophages were then treated with PLY or Δ 6PLY at 17.5 nM (final conc.) either alone or in the presence of 10% complement sufficient sera for 6 hours at 37°C . A positive control of 100 ng/ml LPS + 5 mM ATP was performed. Assay supernatants were tested for the presence of IL-1 β by ELISA (R and D systems). Statistical significance was tested by one-way ANOVA with a Bonferroni's post test (comparing all pairs of columns), shown above each column is significance compared to the control (untreated), comparisons between other columns are indicated by solid black lines, *($p < 0.05$), **($p < 0.01$), ***($p < 0.001$). This experiment was performed once with three technical replicates per condition, data are mean+SEM.

In contrast to the model in chapter 1 (figure 3-14), PLY alone was capable of inducing IL-1 β production, but only in the absence or inhibition of TLR4

signalling. The putative model of PLY-dependent IL-1 β production was updated to show this (figure 5-9).

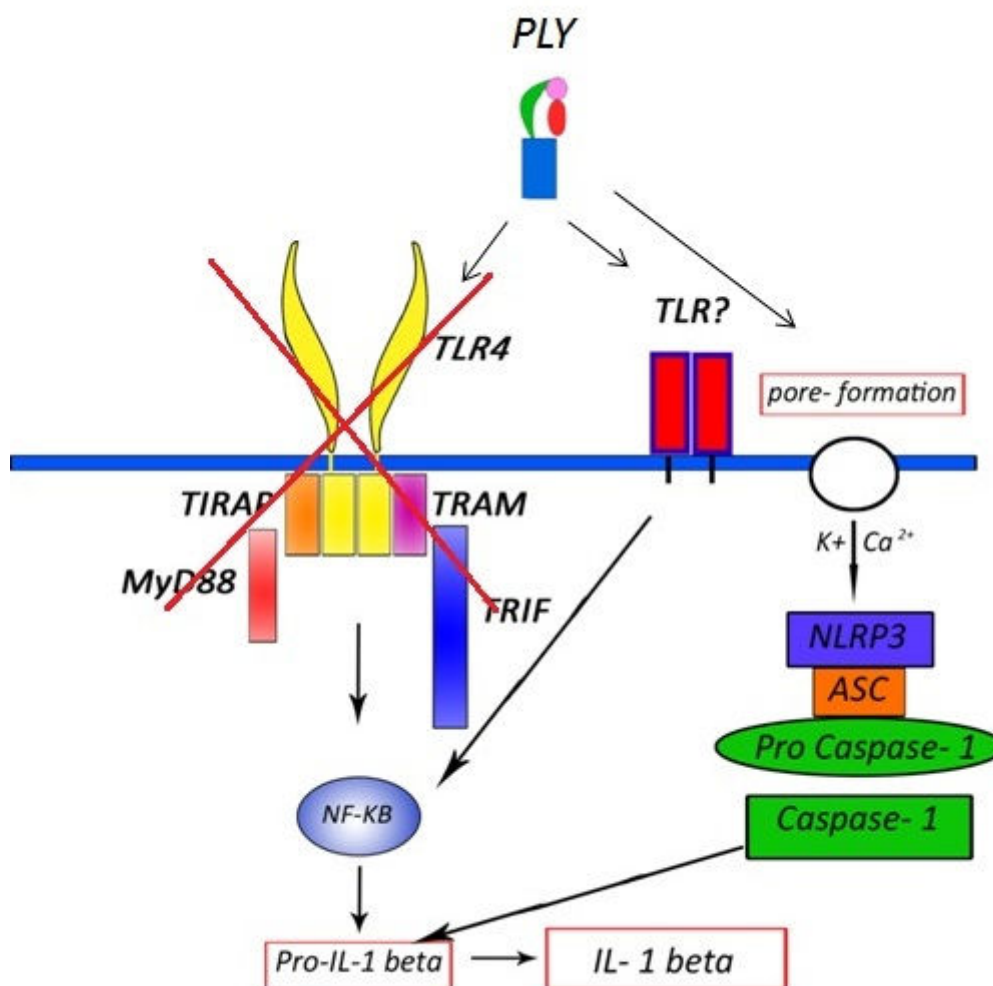


Figure 5-9 Putative model of PLY-dependent IL-1 beta production, version 3.

In contrast to IL-1 β models 1 and 2, PLY alone was capable of inducing IL-1 β production when TLR4 was genetically absent or its signalling was inhibited with VIPER peptide.

Before the PLY treatment model was performed in the absence of TLR4 signalling it was thought that perhaps the proposed interaction between PLY and TLR4 was too weak or transient to induce IL-1 β secretion unless an additional proinflammatory factor such as LPS or complement activation occurred simultaneously. The response now seen to PLY alone (figures 5-7 and 5-8) challenges the model of IL-1 β production proposed until now; it would seem that the presence of TLR4 and subsequent ligation is actively inhibiting the secretion of mature IL-1 β (figure 5-10).

In chapter 3 (section 3.3), evidence was presented that the TLR4 binding site of PLY is within domains 1-3 of the protein, in addition TLR activating ability was

found in D4PLY that could not be attributed to TLR4. In the new model proposed above IL-1 β is produced even in the absence of TLR4, this could be due to an additional TLR binding site (potentially within domain 4) causing transcription of pro-IL-1 β .

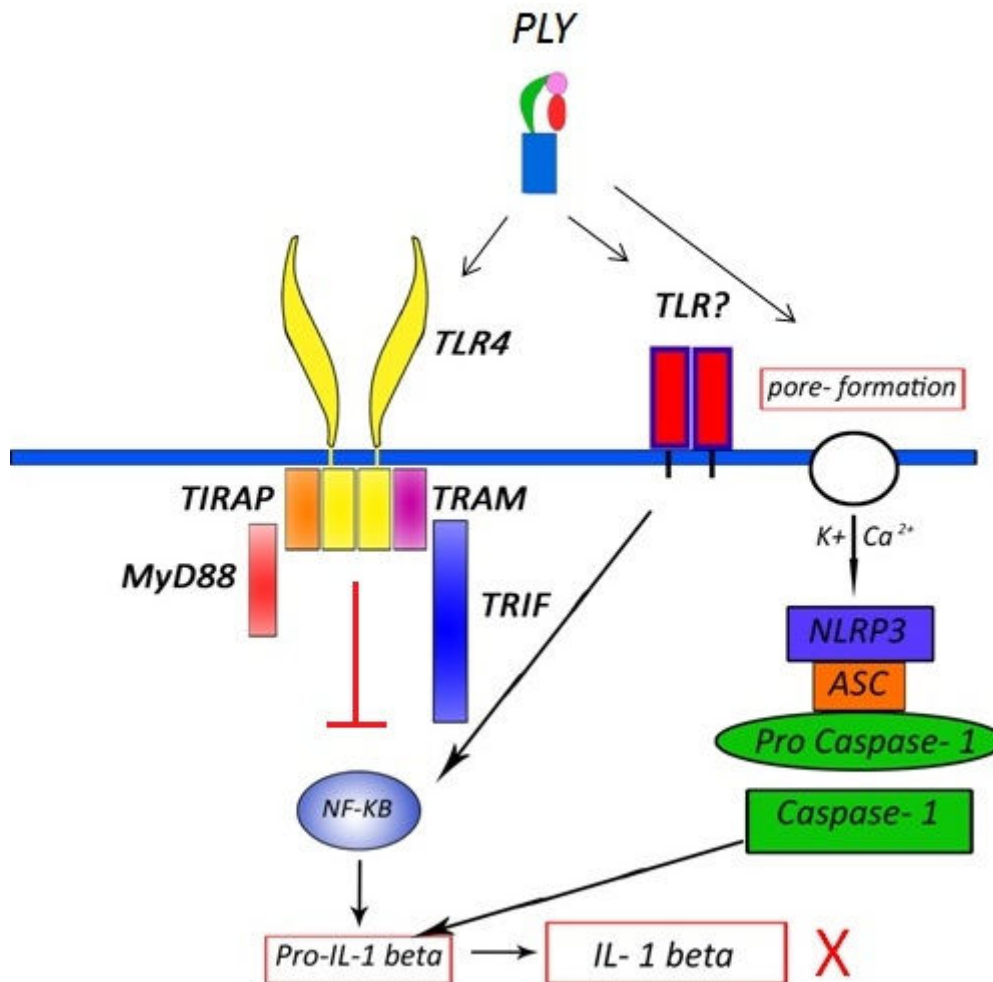


Figure 5-10 Putative model of PLY-dependent IL-1 beta production, version 4.

As stated in model 3, the absence of TLR4 results in IL-1 β production to PLY alone. This could suggest that TLR4 specifically inhibits IL-1 β production and/or processing.

In appendix 5 table 5-1 upregulation of IL-1 receptor type II (IL1RII) was found in response to D123PLY and D4PLY (no significant difference in expression in response to PLY or Δ 6PLY), this receptor is capable of binding both pro-IL-1 β (preventing processing) and mature IL-1 β (preventing binding to the type I IL-1 receptor) (Symons et al., 1995). This could indicate a possible mechanism for

TLR4-mediated suppression of IL-1 β and it would be of interest to assess PLY-mediated upregulation of IL1RII in TLR4-/- BMDM.

In conclusion, the *in vitro* data from this chapter supports a model where PLY can induce IL-1 β production (without the need for exogenous TLR ligands, this is more biologically plausible), although this model is more complex than initially thought.

5.4 The Role of Complement and IL-1 β in PLY Adjuvant Activity

Using a previously published mouse model of immunization the role(s) of both IL-1 β and complement in PLY adjuvant activity were investigated (Douce et al., 2010).

5.4.1 The Role of Complement in Adjuvant Activity

As the complement system was shown to have a synergistic role in cytokine production in response to PLY it was hypothesized that it could potentially have a role in adjuvant activity. Due to the number of available transgenic animals only immunization with e- Δ 6PLY was possible, there was no statistically significant difference in anti-eGFP IgG produced in C3-/- mice compared to their genetic background controls (C57BL/6). This is discussed further in the discussion section of this chapter.

5.4.2 The Role of IL-1 β in Adjuvant Activity

It was hypothesized that IL-1 β may play a role in the magnitude of the antibody response seen in mice immunized with PLY or its derivatives. This would explain the difference in antibody titres between mice immunized with Δ 6PLY fusions compared to PLY fusions. Figure 5-11 expands the IL-1 β hypothesis put forward in figure 3-12 to include the possibility of a third signal (complement activation) in the PLY-induced production of IL-1 β .

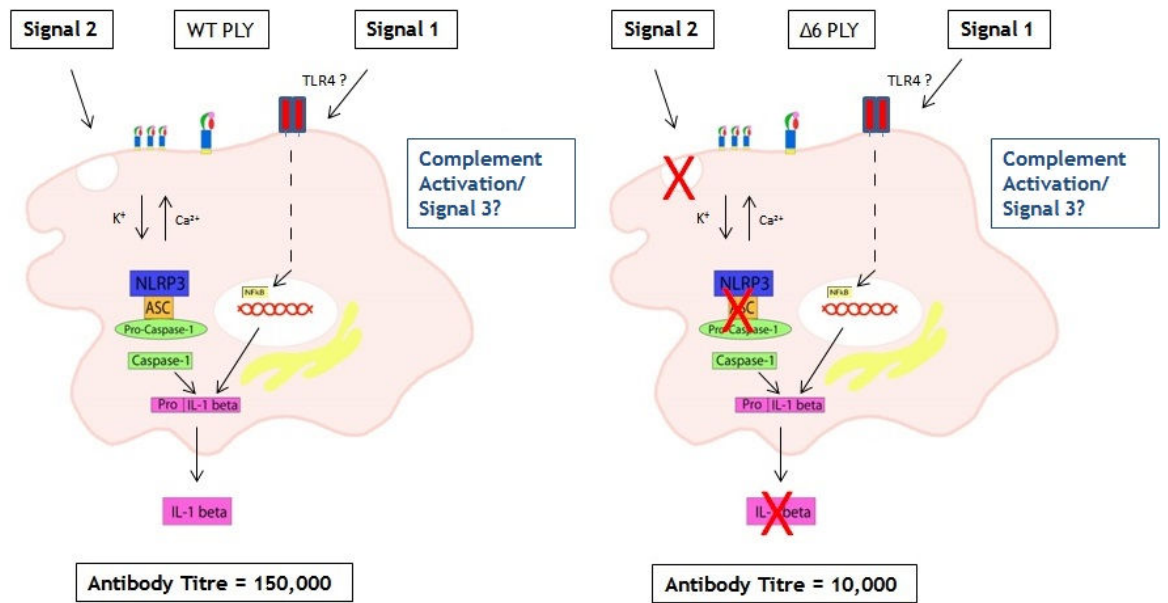


Figure 5-11 IL-1 beta Hypothesis - expanded.

Figures 5-12 and 5-13 show antibody responses in NLRP3^{-/-} mice (that are incapable of producing IL-1 β) and their genetic background controls (BALB/c) following immunisation with either e- $\Delta 6$ PLY or e-PLY. In the absence of NLRP3 there is no significant difference in anti-eGFP titres between mice immunized with e- $\Delta 6$ PLY or e-PLY. In comparison, in the genetic background control mice the response to e-PLY is significantly higher than the response to e- $\Delta 6$ PLY.

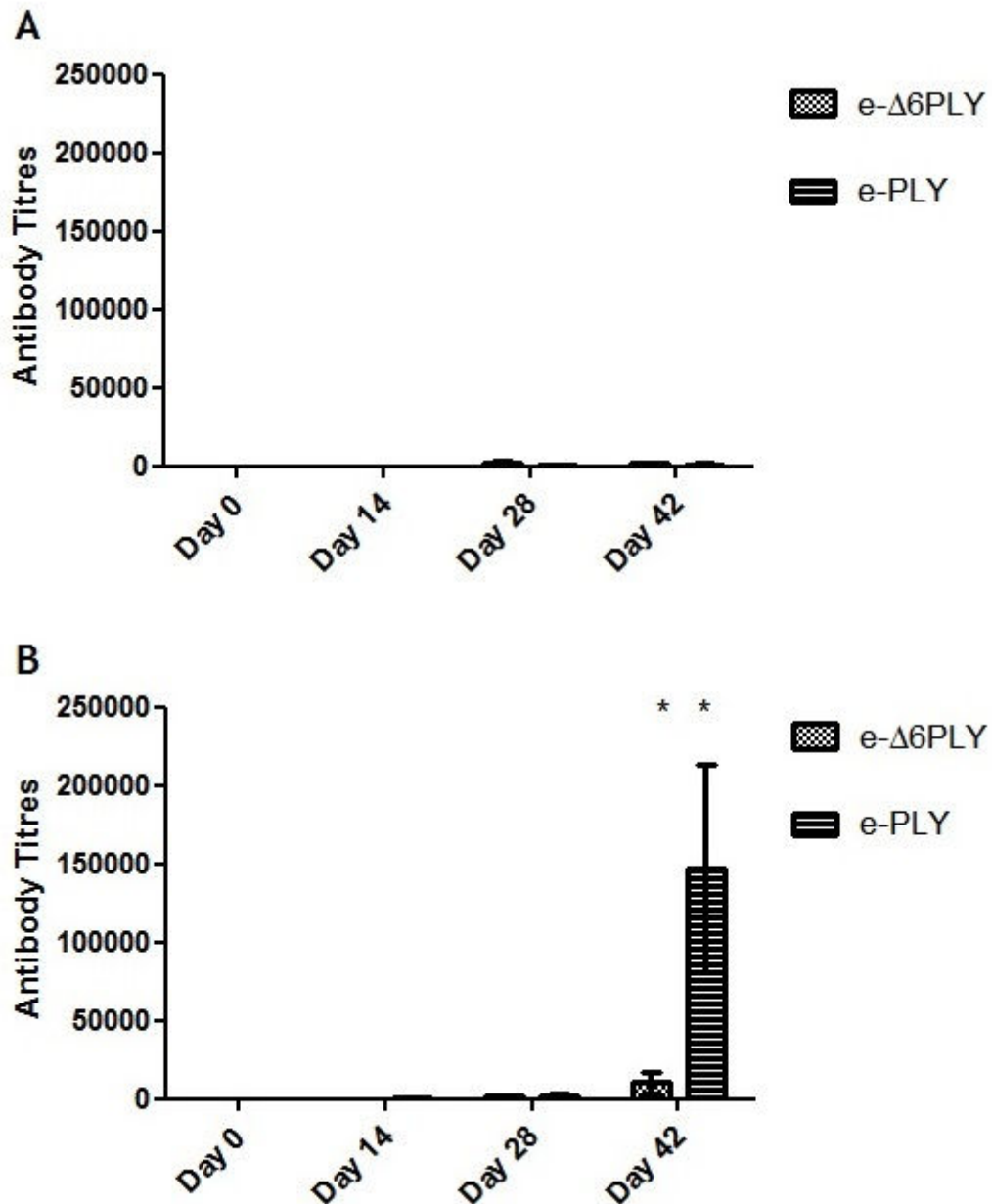


Figure 5-12 Anti-eGFP IgG titres in NLRP3^{-/-} (A) and BALB/c (B) mice immunized with e-Δ6PLY or e-PLY.

NLRP3^{-/-} (A) and BALB/c (B) mice were intranasally immunized with 20ng e-Δ6PLY or 2ng PLY prepared in PBS to a volume of 20μl. Immunizations were performed under light anaesthesia (3.5% isoflurane/1.5% O₂, 1.5L per minute) by instilling the prepared vaccines into the nares by gentle pipetting. Immunizations were performed and blood samples were taken by tail bleed on days 0, 14 and 28. On day 42 terminal blood samples were taken by cardiac puncture under anaesthesia. Anti-eGFP titres were analysed by ELISA. Statistical significance was measured by unpaired t test, comparing test serum samples to unimmunized control serum, *(p>0.05), ** (p>0.01), *** (p>0.001). This experiment was performed once using 5 mice per condition, serum samples were tested in duplicate, data are mean+SEM.

The difference in anti-eGFP antibody titres between mice immunized with either e-Δ6PLY or e-PLY in the presence or absence of NLRP3 (and therefore IL-1β) is

best demonstrated in figure 5-13 where it can be clearly observed that removing NLRP3 from the *in vivo* system reduces the adjuvanticity of PLY to that of $\Delta 6$ PLY.

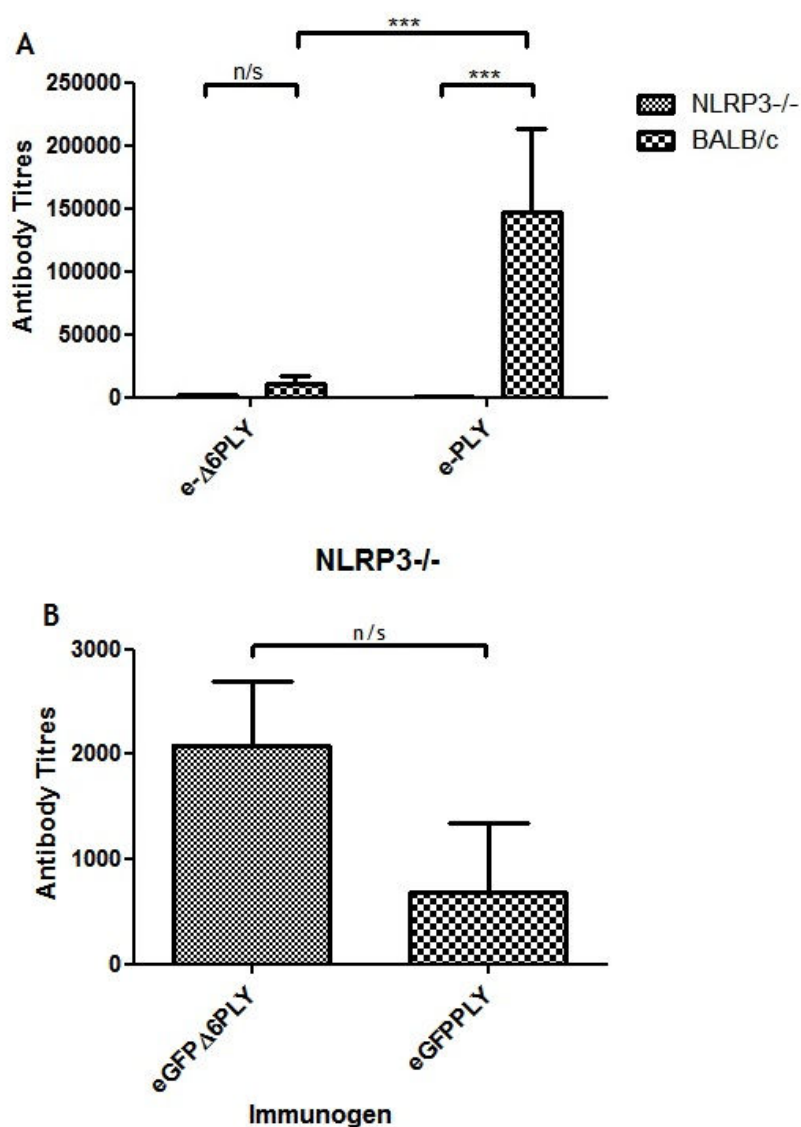


Figure 5-13 Anti-eGFP IgG titres in NLRP3^{-/-} (A) and BALB/c (B) mice immunized with e- $\Delta 6$ PLY or e-PLY.

Results shown are the same as in figure 5-12 but with a reduced scale. (A) Direct comparison of anti-eGFP IgG present in NLRP3^{-/-} and BALB/c mice immunized with e- $\Delta 6$ PLY or e-PLY on day 42. (B) Anti-eGFP antibody titres on day 42 in NLRP3^{-/-} mice immunized either e-PLY or e- $\Delta 6$ PLY. Shown above each column is significance compared to the control (untreated), comparisons between other columns are indicated by solid black lines, *($p < 0.05$), **($p < 0.01$), ***($p < 0.001$). This experiment was performed once using 5 mice per condition, serum samples were tested in duplicate, data are mean+SEM.

Anti-PLY antibodies were not found in blood or nasal washes under any of the immunization conditions (data not shown). This is consistent with previous immunization experiments performed within the Mitchell group (Douce et al., 2010)(unpublished data).

In figure 5-14 anti-eGFP titres in the four groups were also assessed, however, although there is a trend towards greater anti-eGFP IgA titres in BALB/c mice immunized with e-PLY there are no significant differences between the four groups, this is potentially due to the relatively low antibody titres and variation within groups.

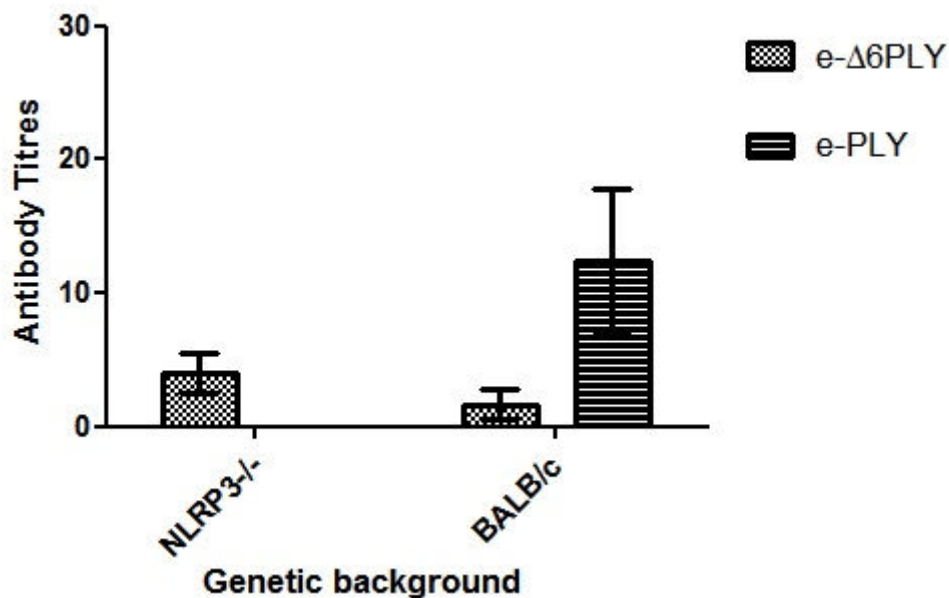


Figure 5-14 Anti-eGFP IgA titres in NLRP3^{-/-} and BALB/c mice immunized with e-Δ6PLY.

Mice were intranasally immunized with 20ng e-Δ6PLY on days 0, 14 and 28. On day 42 animals were humanely sacrificed by terminal bleed under anaesthesia and nasal washes were collected for analysis of specific IgA by ELISA. Statistical significance was measured by unpaired T-test, comparing test nasal wash samples to nasal washes from unimmunized mice, *(p>0.05), ** (p>0.01), *** (p>0.001). This experiment was performed once using 5 mice per condition, nasal wash samples were tested in duplicate. Data are mean+SEM.

Based on these experiments the increased magnitude of antibodies seen in fusion vaccines where lytic PLY is the adjuvant can be attributed to the following immunological events/premises -

- 1) - PLY ligates Toll-like receptors (TLR4, plus other TLR?) on host cells and induces transcription of Pro-IL-1 β . 'Signal 1'.
- 2) - PLY inhibits IL-1 β processing or release, (mediated by TLR4?).
- 3) - PLY forms pores on the cell surface and activates the NLRP3 inflammasome. 'Signal 2'.
- 4) - PLY-induced IL-1 β production *in vitro* was enhanced or dependent on simultaneous complement activation. 'Signal 3'?
- 5) - Increased antibody magnitude was NLRP3-dependent *in vivo*.
- 6) - IL-1 β production was NLRP3-dependent *in vitro*.

These data suggest that the IL-1 β hypothesis is correct and that the reduced antibody titres seen in mice immunized with $\Delta 6$ PLY-based vaccines compared to PLY-based vaccines is due to a lack of IL-1 β production.

5.5 Analysis of IgG Subclasses Produced in Response to e-PLY and e- $\Delta 6$ PLY Immunization in NLRP3-/- and BALB/c Mice

In addition to measuring titres of the antibody isotypes IgA and IgG, the specific subsets of IgG present in immune sera were analyzed. There are four subclasses of IgG; this gives a greater breadth and specificity of IgG function (described in table 5-2) (Clark, 1997) and is thought to be based on differential affinities for Fc receptors (Nimmerjahn & Ravetch, 2005). During isotype switching helper T cells (Th) secrete cytokines that inform B cells which antibody isotype to produce (IgA, IgE etc.), in addition, where IgG is induced these cytokines also determine which IgG subclass will be produced (table 5-1). By analyzing the IgG subsets present in immune sera from mice immunized with PLY fusions, conclusions can be drawn about the type of T helper response generated in response to immunization. Pinpointing the elements of fusion vaccines responsible for different adaptive immune phenotypes could allow manipulation of future fusion vaccines for increased efficacy.

Table 5-1 Role of Cytokines in Regulating Ig Isotype Expression (recreated from Immunobiology, 6th edition, Janeway et al.)

Cytokines	IgM	IgG3	IgG1	IgG2b	IgG2a	IgE	IgA
IL-4	inhibits	inhibits	induces		inhibits	induces	
IL-5							augments
IFN γ	inhibits	induces	inhibits		induces	inhibits	
TGF β	inhibits	inhibits		induces			induces

Table 5-2 Description of IgG Subsets and their Functions

IgG Subclass	Function
IgG1	Recognition of carbohydrate epitopes.
IgG2a	Complement fixation and binding of protein antigens.
IgG2b	Complement fixation and binding of protein antigens.
IgG3	Mast cell binding.

The role of IL-1 β in influencing IgG subsets was determined by measuring anti-eGFP IgG subsets in the final bleeds of NLRP3^{-/-} and BALB/c mice immunized with e- Δ 6PLY or e-PLY (figure 5-15). As shown in figures 5-12 and 5-13 the IgG response to eGFP is reduced in mice immunized with e- Δ 6PLY and in NLRP3^{-/-} mice immunized with either of the vaccines. This is reflected in the IgG subsets, cumulatively the IgG response in BALB/c mice immunized with e- Δ 6PLY is lower than that of BALB/c mice immunized with e-PLY, the pattern of IgG subsets between the two groups is however the same, IgG1 is the dominant subset, followed by IgG2a and IgG2b. Although IgG3 is present in BALB/c mice immunized with e- Δ 6PLY it is only present at very low concentrations (titre is 15.3).

NLRP3^{-/-} mice immunized with either e-Δ6PLY or e-PLY do not produce the IgG2b subset, additionally, e-PLY immunization did not induce production of IgG2a in this model. There is no difference in IgG1 production between the two groups (A and B).

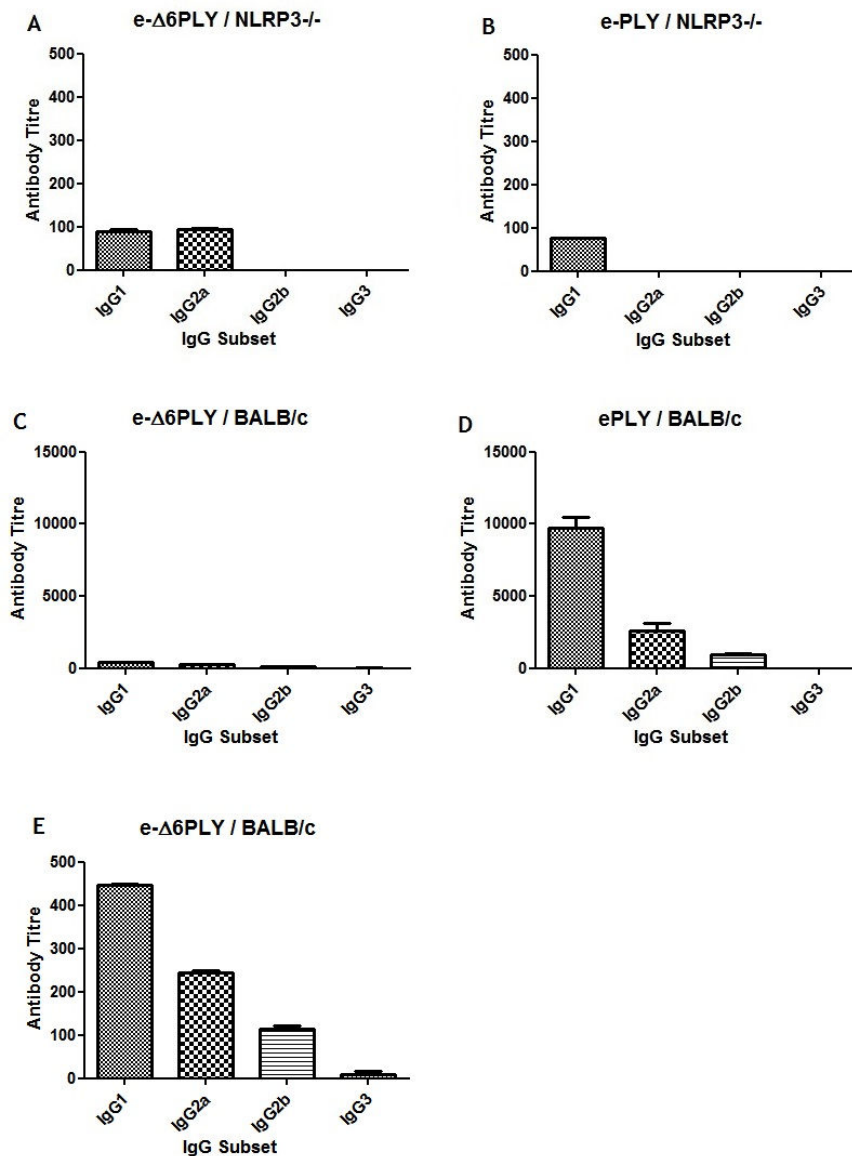


Figure 5-15 Analysis of anti-eGFP IgG subsets.

Terminal serum samples from NLRP3^{-/-} mice immunized with e-Δ6PLY (A) or e-PLY (B) and from BALB/c mice immunized with either e-Δ6PLY (C) or e-PLY (D) were analysed for the presence of IgG subsets using the Southern Biotech ELISA based clonotyping system. The IgG subsets from BALB/c mice immunized with e-Δ6PLY (C) have also been included on a smaller scale (E) so that the ratios of IgG subsets can be better observed. This experiment was performed once using 5 mice per group, serum samples were pulled and tested in duplicate, data are mean+SEM.

Inbred mouse strains with the *Igh1-b* allele such as C57BL/6 mice do not produce the IgG2a antibody subclass, in its place they produce a unique subclass, IgG2c (Morgado et al., 1989). There is no cross-reactivity between IgG2a and IgG2c (Martin & Brady, 1998), and no alternative detection antibody was available, therefore, considering immunization with e- Δ 6PLY did not result in different antibody titres between C3 sufficient and deficient mice the influence of complement on IgG subclass was not investigated.

5.6 Discussion

This work has revealed a synergistic relationship between the complement system and PLY. Establishing this mechanism of IL-1 β production then allowed further investigation of the role(s) of TLR4 and the NLRP3 inflammasome in the immune response to PLY, it was shown that the IL-1 β response in PLY treated BMDM is entirely dependent on activation of the NLRP3 inflammasome (figure 5-1). However, IL-1 β production is not entirely dependent on TLR4 ligation and may even be suppressed in a TLR4-dependent manner (figure 5-7 and 5-8). Using two TLR4 exclusion models it was found that IL-1 β was produced in response to both PLY alone and PLY plus complement sufficient serum, albeit the concentration of IL-1 β was less than that found in TLR4 sufficient models in the presence of PLY plus complement sufficient sera; this suggests two possible modes of PLY-mediated IL-1 β production.

1 - PLY binds TLR and up-regulates Pro-IL-1 β transcription. Simultaneously, IL-1 β production is controlled in a TLR4-dependent manner. PLY activates the classical complement pathway, this proinflammatory signal overrules the regulation of IL-1 β and allows its processing and export to culture supernatants.

2 - In the absence of TLR4 signalling PLY binds to an as yet unidentified TLR (possibly through a binding site located in domain 4) and pro-IL-1 β is upregulated. In the absence of TLR4 pro-IL-1 β is processed and exported to the cytoplasm normally and without the need for additional pro-inflammatory signals such as complement activation.

Figure 5-16 incorporates these two modes of action into a final putative model of PLY-dependent IL-1 β production.

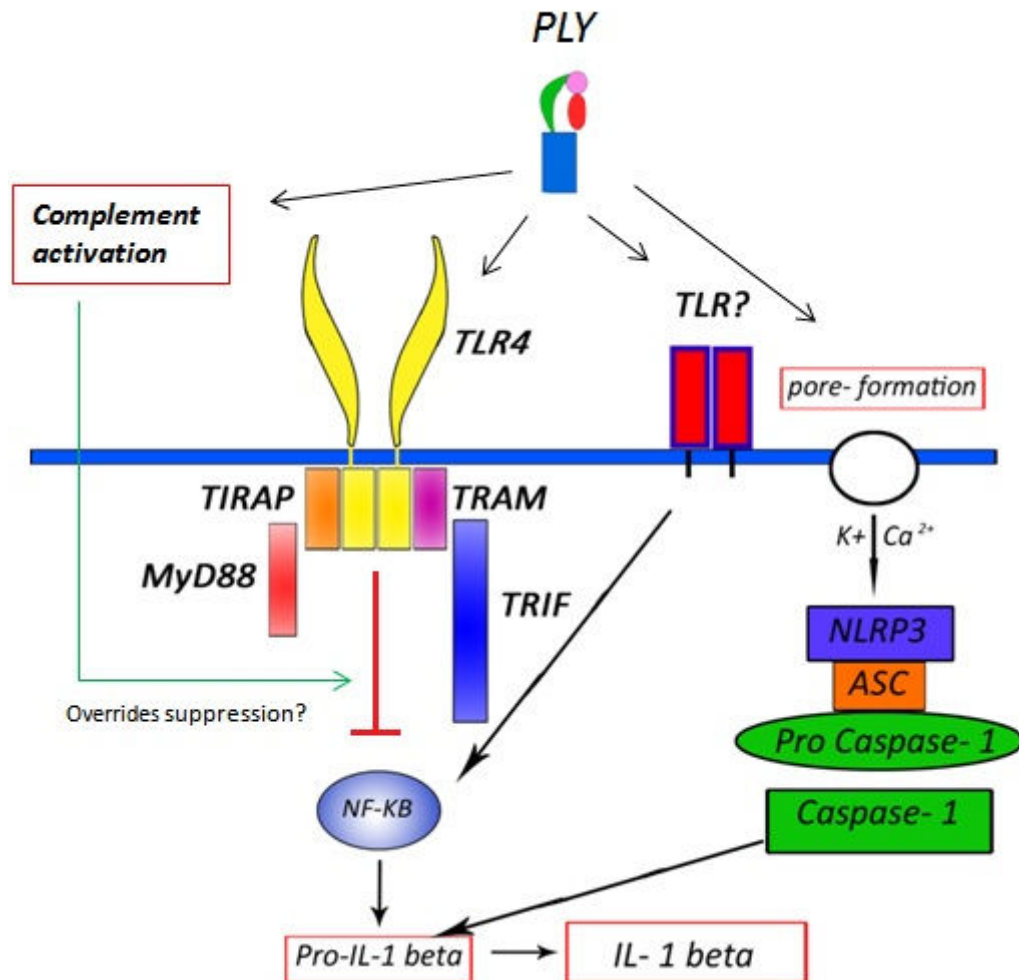


Figure 5-5-16 Final putative model of PLY-dependent IL-1 β production.

The results presented in this chapter have revealed a complex mechanism for the PLY-dependent production of IL-1 β . In the above diagram these results have been compiled to create a putative model of PLY-dependent IL-1 β production. In this model PLY stimulates TLRs resulting in the transcription of pro-IL-1 β , it also activates the NLRP3 inflammasome by pore formation. However, the stimulation of TLR4 inhibits either transcription or processing of pro-IL-1 β into its active form, complement activation by PLY is then required to override this inhibition.

The use of transgenic C3^{-/-} mice for both sera and BMDM has suggested that C3 presence increases the magnitude of IL-1 β production but is not essential suggesting that complement components from higher in the classical activation pathway are involved. In figure 5-7 the difference in IL-1 β production between BMDM treated with complement sufficient or C3^{-/-} sera is striking compared to other experiments. Although VIPER was used in this experiment it seems

unlikely that this difference is due to TLR4 inhibition; as detailed in section 2.10.3 the preparation of complement sufficient sera is a delicate process as mishandling of the sera can activate the alternative complement pathway and deplete complement components in the sample, in addition there will be inherent variability in the concentration and ratios of complement components in serum samples. This could also explain the low IL-1 β response to C3-/- sera in figure 5-2. It is likely that more experimental replicates would reduce this variation. As figure 5-17 shows there are several complement components that precede C3 in the classical complement cascade, while C3a and C5a (anaphylotoxins) are known pro-inflammatory mediators, C4a and C2a are increasingly being recognized as important mediators of inflammatory immune responses as well as essential components of the classical complement cascade (Mattsson et al., 2011). It would be of interest to further investigate the role(s) of individual components of the complement cascade using Quidel's depleted sera (where individual complement components have been removed), the use of commercially prepared sera could also reduce inter-experiment variation. Additionally, in an initial investigation into PLY dependent gene expression (appendix 5) complement C3 was shown to be upregulated in BMDM treated with both Δ 6PLY and PLY, the production of C3 *in situ* could help to create an 'inflammatory focus' at the site of fusion vaccine administration and is potentially an important factor in adjuvant activity. Complement activation would clearly not be the only factor in adjuvant activity as demonstrated by the unchanged KC response to PLY and Δ 6PLY in the presence or absence of exogenous (sera) or endogenous (C3 upregulation) complement. However, it will be important to investigate the effect complement activation has on the production of other cytokines.

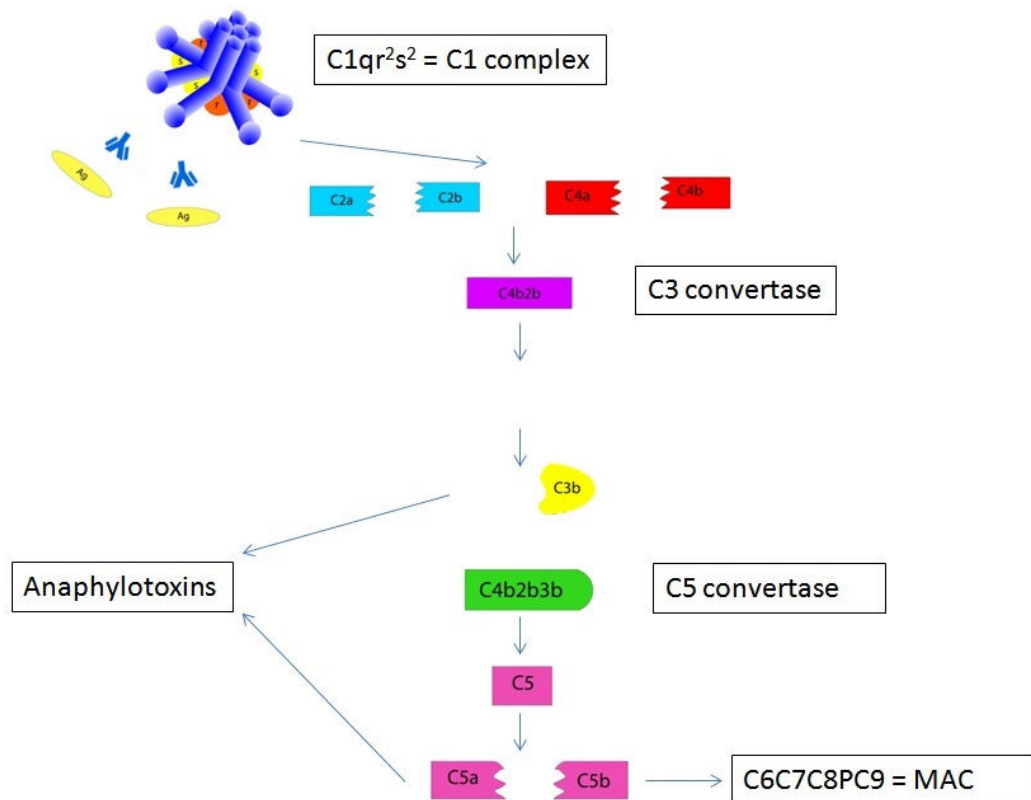


Figure 5-17 Diagram of the classical complement cascade.

All complement activation pathways converge on the C3 convertase, the classical pathway is typically initiated by the cross-linking of surface bound antibody with the C1 complex. In the case of PLY-dependent activation a structural homology with antibody Fc within D4 of PLY may be recognized by the C1 complex.

It was thought that complement activation could play a direct role in the adjuvant activity of PLY, however, C3^{-/-} mice responded equally to their genetic background controls (C57BL/6) (data not shown). This could however, be a reflection of the capabilities of this mouse strain rather than the role of complement in PLY adjuvant activity. C57BL/6 mice have an unusual antibody phenotype in that the IgG subset IgG2a is not produced and instead a subclass named IgG2c is produced (Mestas & Hughes, 2012). This is also an important consideration for *In vitro* experiments, while control conditions such as LPS + ATP suggest that BMDM generated from different backgrounds respond similarly in these experiments (e.g. figures 5-2 and 5-5) it would be more appropriate to use BMDM generated from mice of the same genetic background for control experiments where transgenic BMDM are used. If a transgenic complement deficient strain could be found on an alternative background it would be of interest to see if this alters the IgG subclass profile compared to complement

sufficient mice. Additionally, as $\Delta 6$ PLY induces a lower magnitude of antibody response compared to PLY, immunization of C3^{-/-} mice with e-PLY could potentially highlight differences in antibody magnitude compared to complement sufficient strains. This would also add strength to IL-1 β hypothesis laid out in this thesis, where complement provides ‘signal 3’ in PLY-induced IL-1 β production, thereby increasing the magnitude of an antibody response.

It has been shown that complement activation can synergize with TLRs and IL-6 to promote Th17 biased adaptive immune responses (Fang et al., 2009). While in this study antibody levels were assessed no T-cell outputs were measured. As described in chapter 1, cell-based immunity (particularly Th17) is an essential component in protective immune responses against *Streptococcus pneumoniae*, and so in future experiments the impact of complement in promoting T-cell phenotypes in response to PLY-based vaccines should be assessed.

Immunization of NLRP3^{-/-} mice demonstrated that a lack of NLRP3 (and therefore IL-1 β) reduces antibody titres in response to e-PLY to the same level as those raised against e- $\Delta 6$ PLY (figure 5-13). This suggests that the IL-1 β hypothesis first described in chapter three is correct and a lack of IL-1 β in response to non-lytic PLY variants is responsible for the reduction in antibody magnitude. It could also be said that complement activation has an indirect role in adjuvant activity as its activation enhances IL-1 β production *in vitro* and therefore could be involved in IL-1 β production *in vivo* increasing antibody magnitude. It cannot be determined from these experiments whether pre-formed IL-1 β stores (such as those found in PBMC, particularly monocytes) are involved in the immune response to PLY vaccines, although it is likely that they do. As TLR4 alone is not responsible for the upregulation of IL-1 β this would not be a suitable model for investigation, however, if an additional TLR site is found within PLY a double knock-out mouse model could be devised. Previously, TLR4^{-/-} mice have been used in the Mitchell group immunization model to investigate the role of TLR4 in adjuvanticity, however, a mixed response arose with no difference in mean antibody titres between TLR4^{-/-} mice and their genetic background controls (BALB/c) (Ma, 2012). It is possible that as with complement and IL-1 β , TLR4 plays a non-essential role in the adjuvant activity of PLY but aids in the magnitude of response. Combined these data suggest that

the adjuvant activity of PLY is pleiotropic and that the immune system is able to compensate for missing elements such as TLR4 making it difficult to identify a single essential component responsible for adjuvant activity.

Analysis of IgG subsets in e- Δ 6PLY and e-PLY immunized NLRP3^{-/-} and BALB/c mice has suggested that NLRP3 may play a role in the induction of an IgG2b response (figure 5-15); in the absence of NLRP3 the IgG2b subset is not induced in response to either vaccines and the IgG2a response is lost in response to e-PLY. However, it is unlikely that this is due to IL-1 β as aside from the magnitude of response there is little difference in IgG subsets raised against either vaccine (with the exception of small quantities of IgG3 raised against e- Δ 6PLY). This analysis suggests that the fundamental composition/phenotype of the immune response raised by PLY/ Δ 6PLY vaccines is the same regardless of lytic activity.

6. Effect of Fusion Antigens on Immunization Outcome

As discussed in detail in the introduction (section 1.3.5) the Mitchell group have studied the efficacy of PLY based vaccines extensively in the form of pneumococcal protein fusion vaccines. Briefly, the project was funded by the Programme for Appropriate Technology in Healthcare (PATH), PLY and delta6PLY were used as fusion partners for four chosen antigens based on evidence of some protective immunity induced by the proteins. The four fusion antigens chosen were PsaA, PspA, PspC and PhtD, PATH nomenclature is detailed in table 6-1.

The PATH vaccines were administered either intranasally or subcutaneously following the immunization schedule detailed in the materials and methods section 2.10. After completion, sera from the PATH project were available as research materials; the IgG subsets within these sera were measured to give insight into the influence of both administration route and fusion antigen(s) on immune outcome following immunization with PLY based vaccines. This study also gave further insight into the cytokine milieu generated by PLY that would influence the phenotype of the adaptive immune response to PLY immunization.

Table 6-1 PATH Grant Experimental Nomenclature

Experiment Name	Fusion Antigen	Immunization Route
PATH 1	PsaA-PLY/ Δ 6PLY	Intranasal
PATH 2	PsaA-PLY/ Δ 6PLY	Subcutaneous
PATH 3	PspA-PLY/ Δ 6PLY	Intranasal
PATH 4	PspA-PLY/ Δ 6PLY	Subcutaneous
PATH 5	PspC-PLY/ Δ 6PLY	Intranasal
PATH 6	PspC-PLY/ Δ 6PLY	Subcutaneous
PATH 7	PhtD-PLY/ Δ 6PLY	Intranasal
PATH 8	PhtD-PLY/ Δ 6PLY	Subcutaneous
PATH 9	PsaA/PspA/PspC/PhtD- Δ 6PLY	Intranasal
PATH 10	PsaA/PspA/PspC/PhtD- Δ 6PLY	Subcutaneous

Anti-PLY responses were not generated against PsaA or PspA fusion vaccines and so have not been included in those figures. Antibody titres in all experiments were determined by calculating the reciprocal titre of the last well in which signal could be detected above background ($OD_{485-10nm} 0.3$), it is for this reason that some readings are identical. Due to the small sample volumes available sera were pooled within groups and tested in duplicate.

6.1 IgG subclasses induced by Immunization with PsaA fusion vaccines

Antibodies generated against PsaA in the PATH 1 experiment (figure 6-1) were predominantly of the IgG1 subtype, IgG2b was generated in response to PsaA-PLY but not PsaA- $\Delta 6$ PLY.

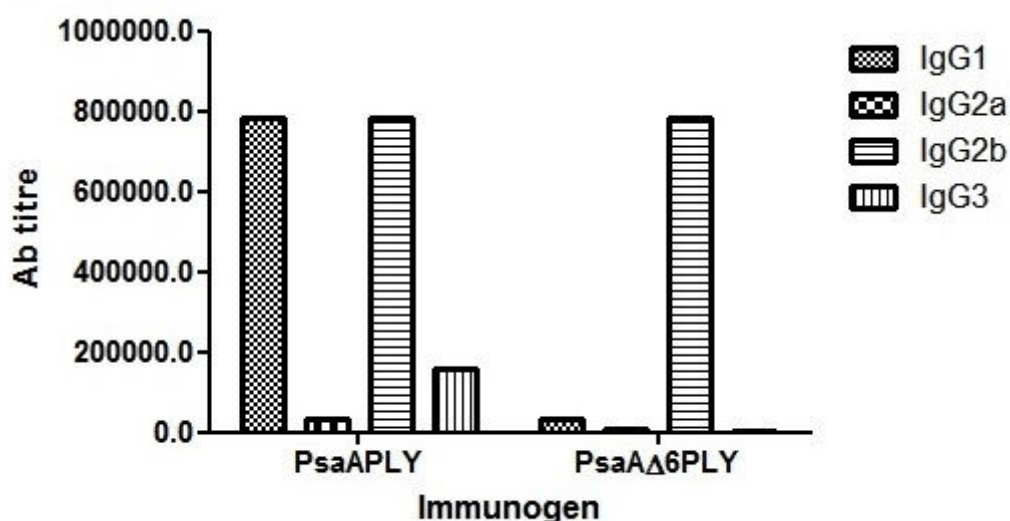


Figure 6-1 PATH 1.

IgG subsets were determined in terminal serum samples from MF1 mice immunized intranasally with either PsaA-PLY or PsaA- $\Delta 6$ PLY (following schedule detailed in table 2-13). Anti-PsaA antibodies were assessed by ELISA (Southern Biotech antibody clonotyping kit). Serum samples were pooled from 5 immunized mice, samples were added to the first well at 1:50 dilution and serially diluted 1:5 vertically down the plate. Antibody (Ab) titres were determined by calculating the reciprocal titre of the last well in which signal could be detected above background ($OD_{485-10nm} 0.3$).

Subcutaneous immunization with PsaA-PLY or PsaA- Δ 6PLY (figure 6-2) resulted in an altered IgG subset pattern compared to intranasal immunization. Similarly to intranasal immunization, IgG2a did not feature as a dominant IgG subset in the PATH 2 group, IgG2b was also unaffected by immunization route. There is an interesting trend reversal in IgG1 production; given intranasally PsaA- Δ 6PLY does not induce substantial titres of IgG1 whereas PsaA-PLY does, the opposite is true when the fusion vaccines are given subcutaneously. In addition subcutaneous immunization results in IgG3 production in response to PsaA- Δ 6PLY where intranasal immunization does not, and IgG3 production in response to PsaA-PLY is approximately 4 times higher via this route compared to intranasal immunization.

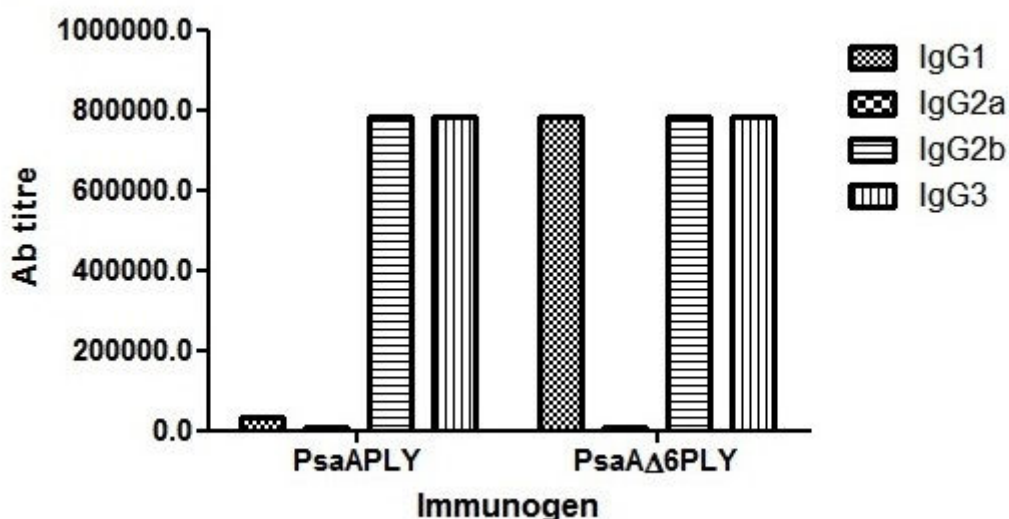


Figure 6-2 PATH 2.

IgG subsets were determined in terminal serum samples from MF1 mice immunized subcutaneously with either PsaA-PLY or PsaA- Δ 6PLY (following schedule detailed in table 2-13). Anti-PsaA antibodies were assessed by ELISA (Southern Biotech antibody clonotyping kit). Serum samples were pooled from 5 immunized mice, samples were added to the first well at 1:50 dilution and serially diluted 1:5 vertically down the plate. Antibody (Ab) titres were determined by calculating the reciprocal titre of the last well in which signal could be detected above background ($OD_{485-10nm} 0.3$).

6.2 IgG subclasses induced by Immunization with PspA fusion vaccines

Similarly to PATH 1 figure 6-1, intranasal immunization with PspA-PLY results in an IgG1/2b anti-PspA response (figure 6-3).

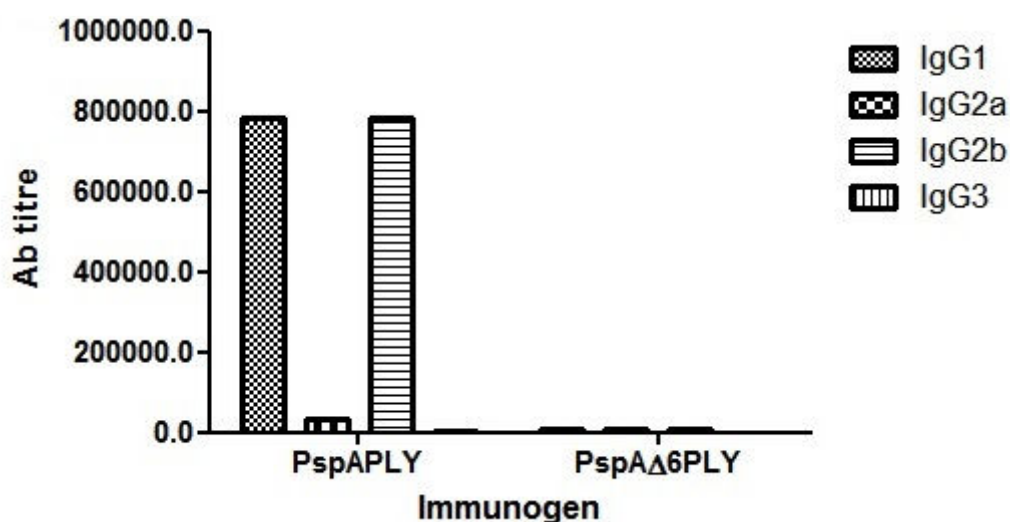


Figure 6-3 PATH 3.

IgG subsets were determined in terminal serum samples from MF1 mice immunized intranasally with either PspA-PLY or PspA-Δ6PLY (following schedule detailed in table 2-13). Anti-PspA antibodies were assessed by ELISA (Southern Biotech antibody clonotyping kit). Serum samples were pooled from 5 immunized mice, samples were added to the first well at 1:50 dilution and serially diluted 1:5 vertically down the plate. Antibody (Ab) titres were determined by calculating the reciprocal titre of the last well in which signal could be detected above background ($OD_{485-10nm} > 0.3$).

When administered subcutaneously the antibody response to PspA-Δ6PLY is restored, however, the response to PspA-PLY is diminished in comparison to intranasal immunization and is dominated by an IgG2b phenotype (figure 6-4). The IgG3 subset is produced with this administration route but only in response to PspA-PLY. In the PATH 3 and 4 studies the IgG1 subset is produced in response to PspA-PLY only when given intranasally, yet is produced in response to both vaccines when given subcutaneously (albeit at greatly reduced titres).

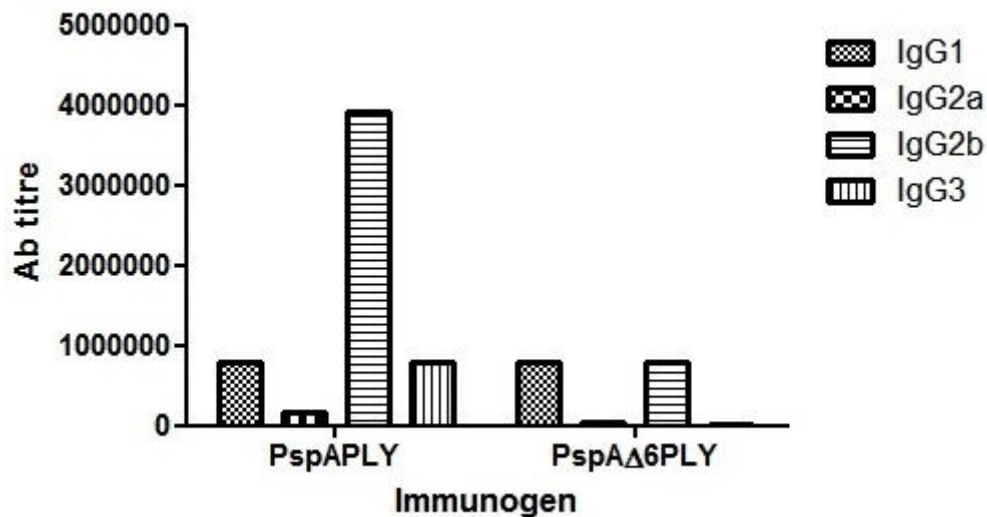


Figure 6-4 PATH 4.

IgG subsets were determined in terminal serum samples from MF1 mice immunized subcutaneously with either PspA-PLY or PspA-Δ6PLY (following protocol detailed in table 2-13). Anti-PspA antibodies were assessed by ELISA (Southern Biotech antibody clonotyping kit). Serum samples were pooled from 5 immunized mice, samples were added to the first well at 1:50 dilution and serially diluted 1:5 vertically down the plate. Antibody (Ab) titres were determined by calculating the reciprocal titre of the last well in which signal could be detected above background ($OD_{485-10nm} > 0.3$).

6.3 IgG subclasses induced by Immunization with PspC fusion vaccines

When PspC was used as a fusion antigen in PATH 5 anti-PspC IgG1, IgG2a and IgG2b titres were produced equally in response to PspC-PLY, there was no response to PspC-Δ6PLY (figure 6-5). There was a notable increase in anti-PLY antibodies in response to PspC-PLY and they were predominantly of the IgG2b subset, this could potentially indicate that PspC itself has some adjuvant activity.

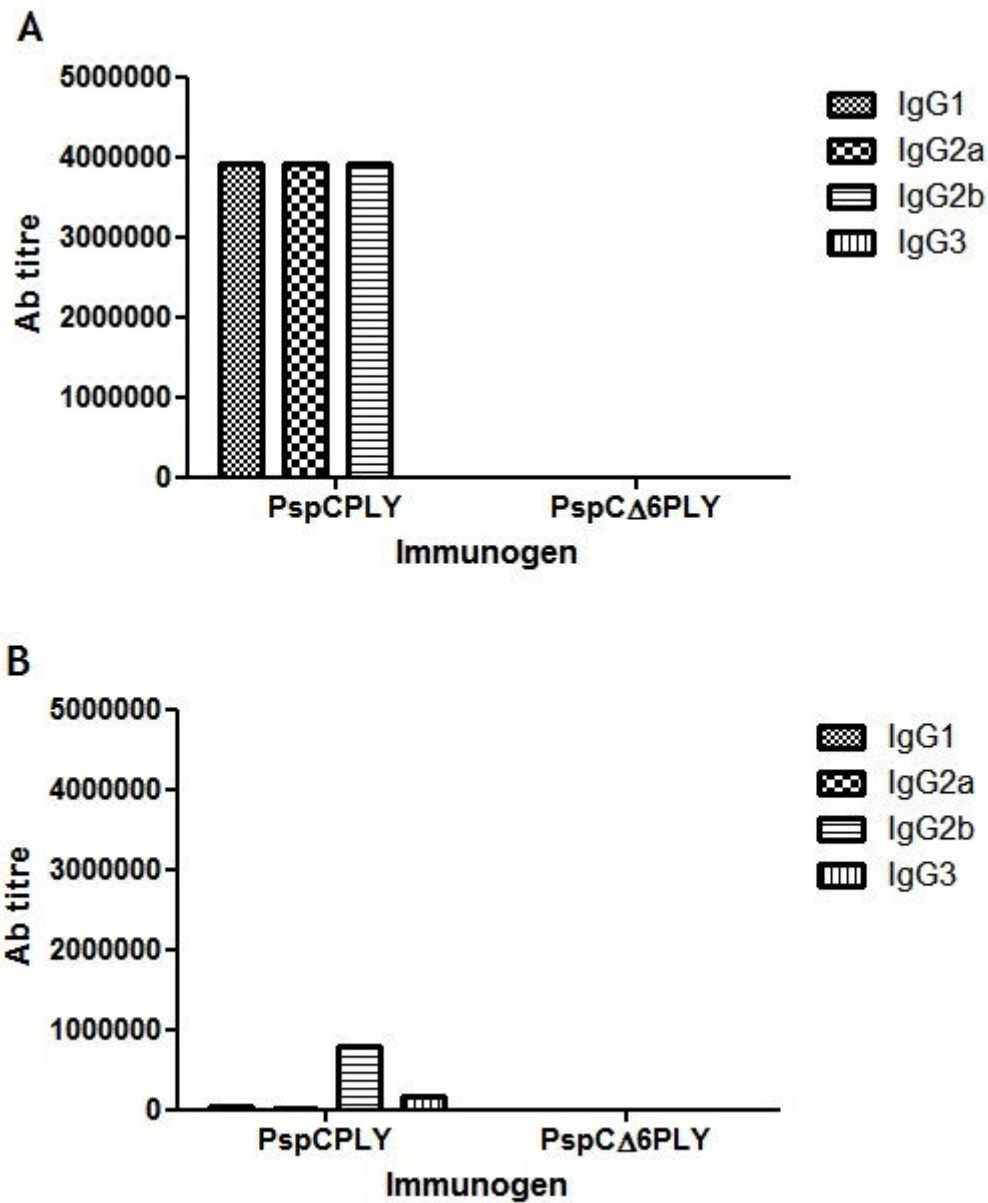


Figure 6-5 PATH 5.

IgG subsets were determined in terminal serum samples from MF1 mice immunized intranasally with either PspC-PLY or PspC- Δ 6PLY (following schedule detailed in table 2-13). Both anti-PspC (A) and anti-PLY (B) antibodies were assessed by ELISA (Southern Biotech antibody clonotyping kit). Serum samples were pooled from 5 immunized mice, samples were added to the first well at 1:50 dilution and serially diluted 1:5 vertically down the plate. Antibody (Ab) titres were determined by calculating the reciprocal titre of the last well in which signal could be detected above background ($OD_{485-10nm} > 0.3$).

In contrast to intranasal administration, when PspC-PLY is given subcutaneously the antibody response is predominantly composed of IgG1 (figure 6-6). The anti-PspC response to PspC- Δ 6PLY is absent when either administration route is used. Interestingly, an anti-PLY response is generated to both vaccines when given

subcutaneously; similarly to PATH 5 the response is predominantly composed of IgG2b, however, the response is around 25-fold lower when the subcutaneous route is used (titres of 30000 compared to 750,000 approx.)

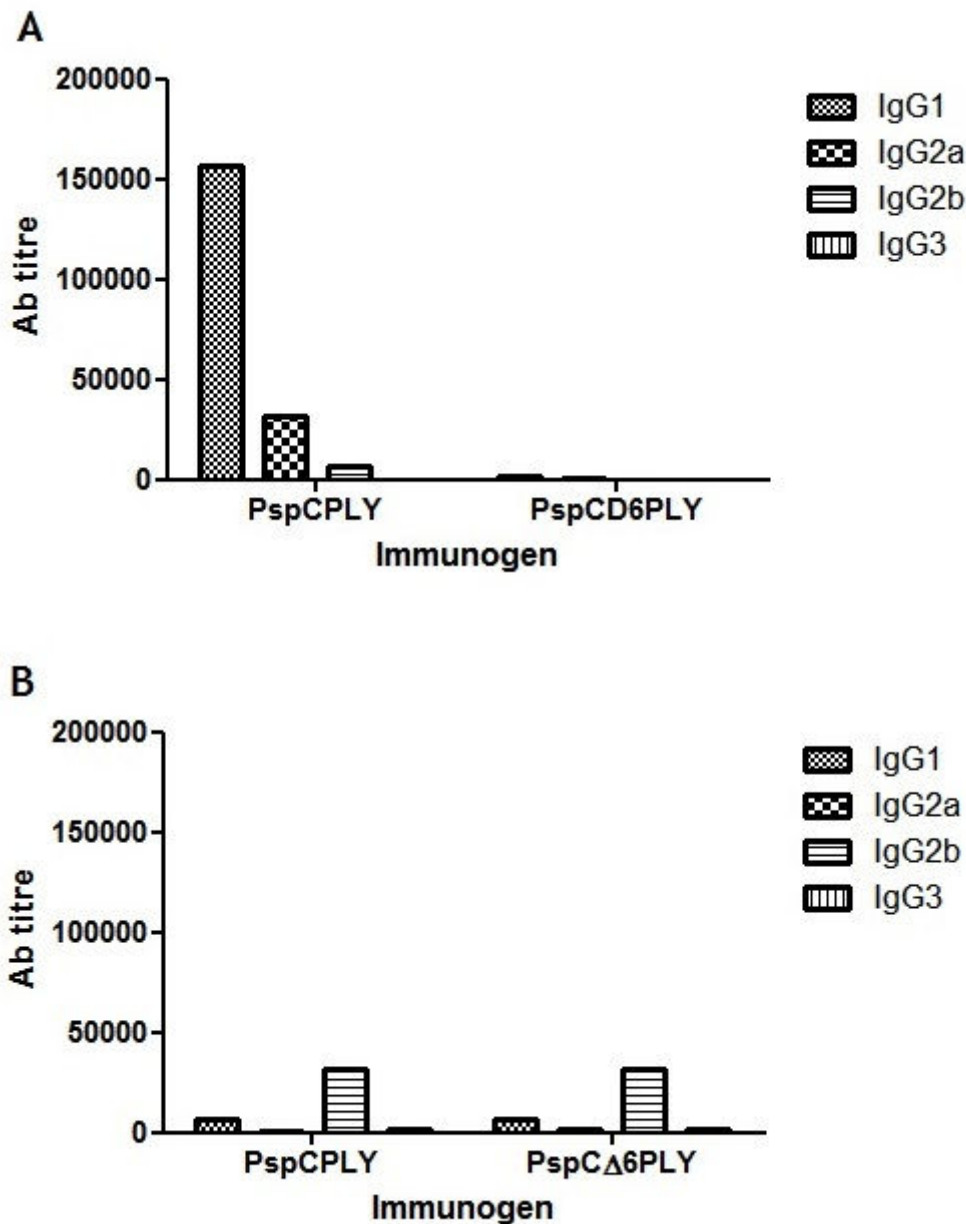


Figure 6-6 PATH 6.

IgG subsets were determined in terminal serum samples from MF1 mice immunized subcutaneously with either PspC-PLY or PspC- Δ 6PLY (following schedule detailed in table 2-13). Both anti-PspC (A) and anti-PLY (B) antibodies were assessed by ELISA (Southern Biotech antibody clonotyping kit). Serum samples were pooled from 5 immunized mice, samples were added to the first well at 1:50 dilution and serially diluted 1:5 vertically down the plate. Antibody (Ab) titres were determined by calculating the reciprocal titre of the last well in which signal could be detected above background ($OD_{485-10nm} 0.3$).

6.4 IgG subclasses induced by Immunization with PhtD fusion vaccines

Intranasal immunization with PhtD-PLY and PhtD- Δ 6PLY results in an antibody response composed of IgG1 and IgG2a (a subset not dominant in any other PATH group) (figure 6-7). In fact IgG2a is the dominant IgG subset in mice immunized intranasally with PhtD-PLY. There is no anti-PLY IgG response towards either vaccine when given intranasally.

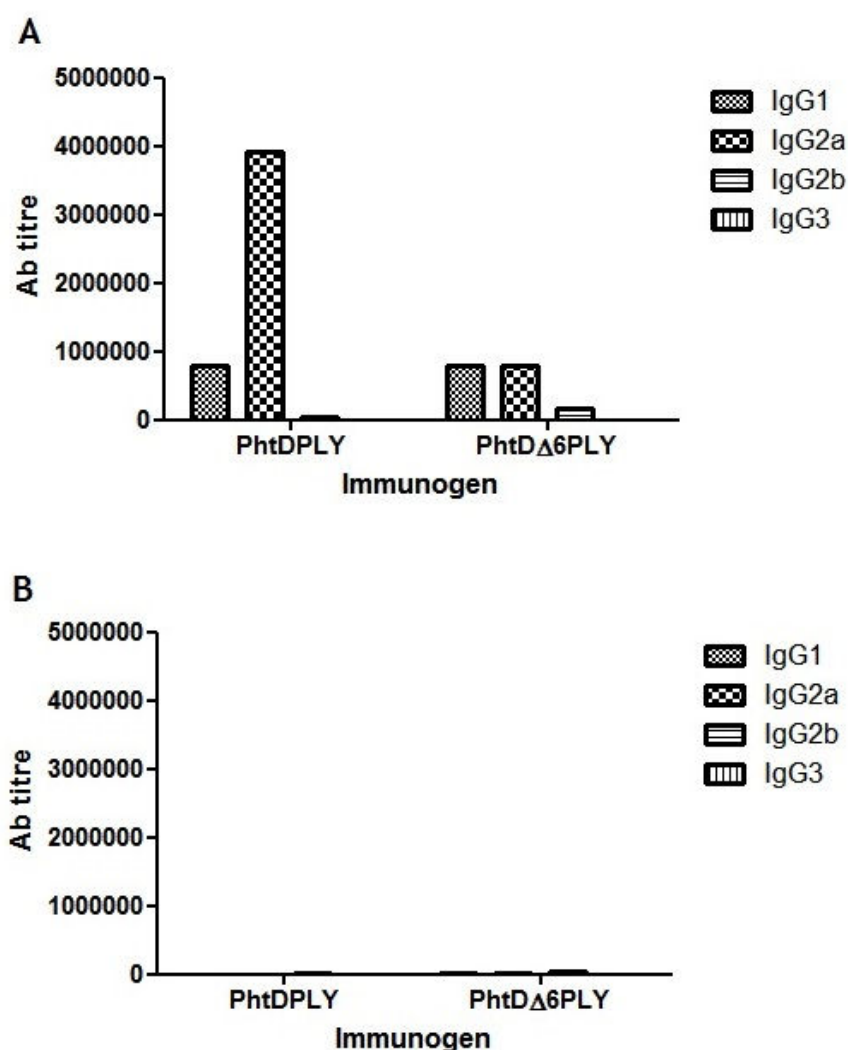


Figure 6-7 PATH 7.

IgG subsets were determined in terminal serum samples from MF1 mice immunized intranasally with either PhtD-PLY or PhtD- Δ 6PLY (following schedule detailed in table 2-13). Both anti-PhtD (A) and anti-PLY (B) antibodies were assessed by ELISA (Southern Biotech antibody clonotyping kit). Serum samples were pooled from 5 immunized mice, samples were added to the first well at 1:50 dilution and serially diluted 1:5 vertically down the plate. Antibody (Ab) titres were determined by calculating the reciprocal titre of the last well in which signal could be detected above background ($OD_{485-10nm}$ 0.3).

As previously seen subcutaneous immunization with PLY and $\Delta 6$ PLY fusions results in lower IgG titres compared to intranasal immunization, this is also true in PATH 8 (figure 6-8). Additionally the IgG subset profile is now predominantly composed of IgG1. Finally, subcutaneous immunization with PhtD- $\Delta 6$ PLY does generate anti-PLY antibodies, IgG2a is the least prevalent subset and IgG2b is the most prevalent, IgG1 and IgG3 are produced at similar concentrations.

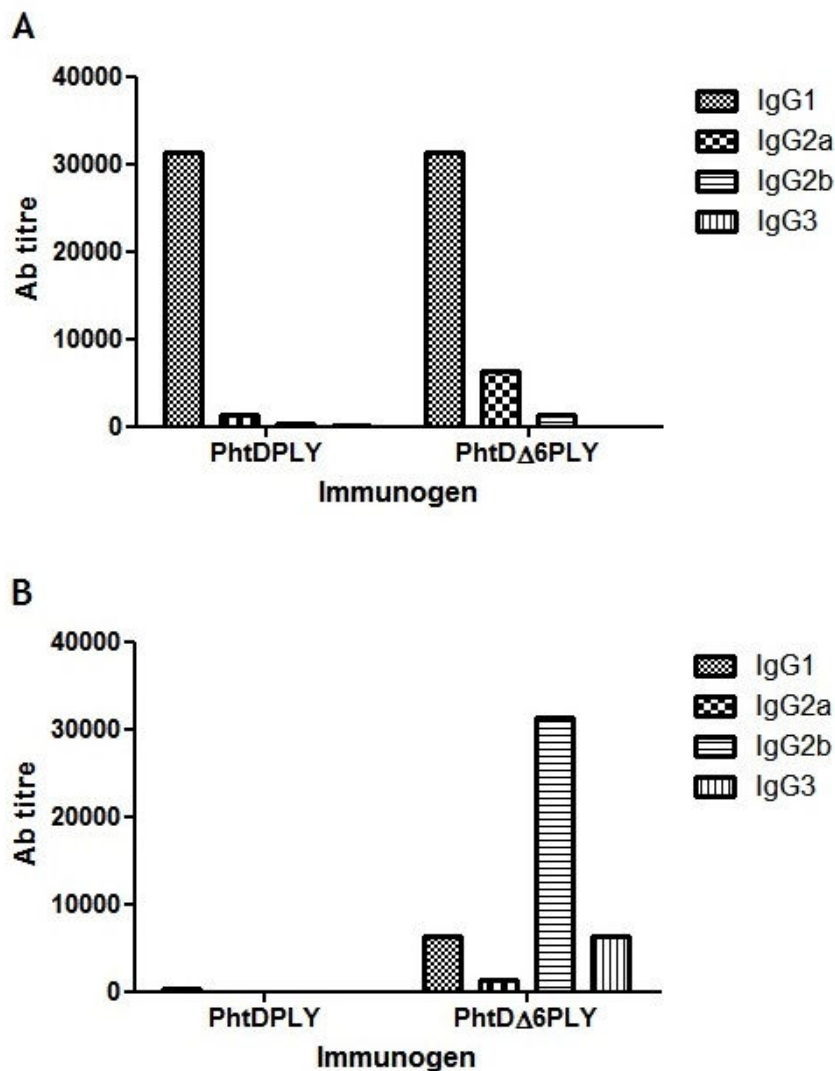


Figure 6-8 PATH 8.

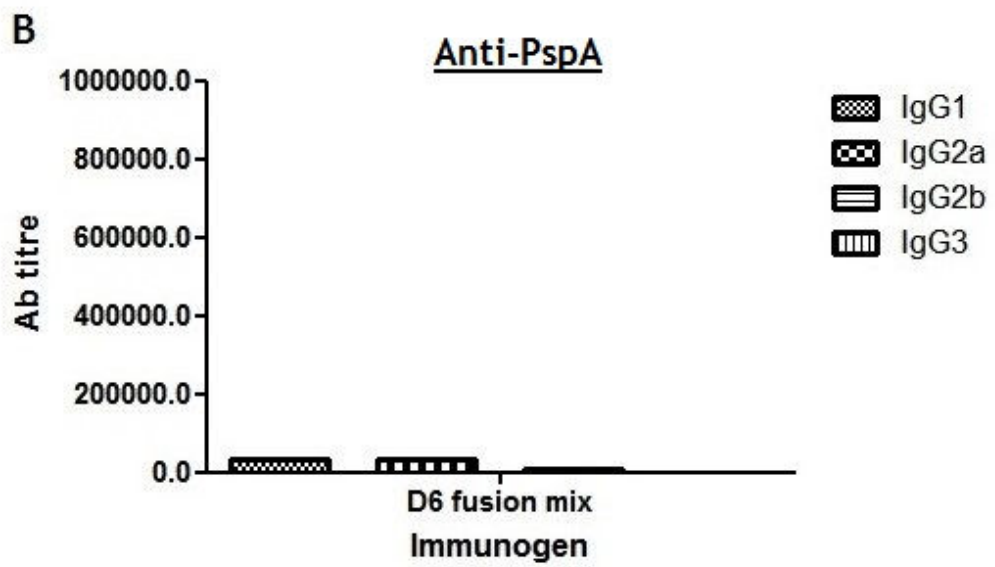
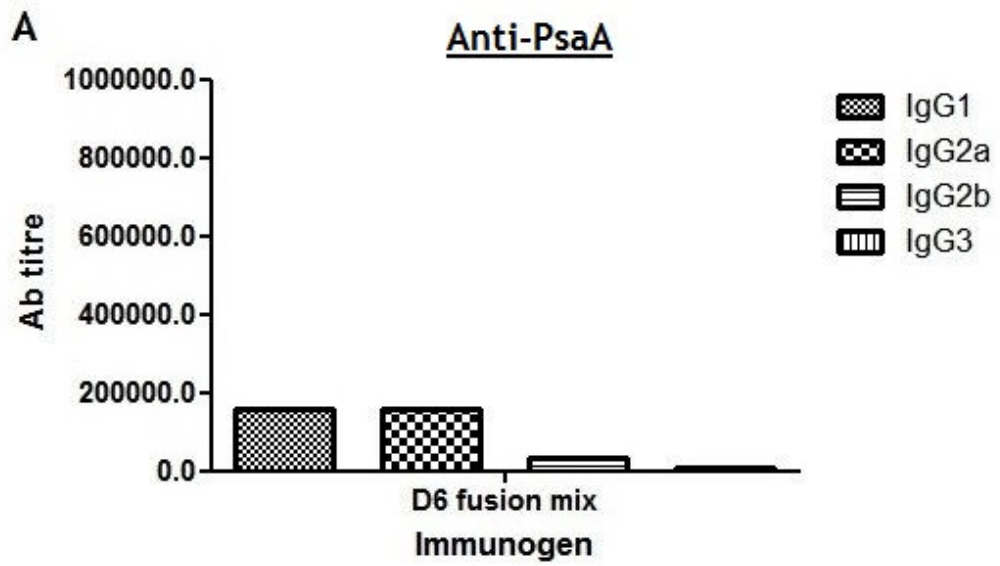
IgG subsets were determined in terminal serum samples from MF1 mice immunized subcutaneously with either PhtD-PLY or PhtD- $\Delta 6$ PLY (following schedule detailed in table 2-13). Both anti-PhtD (A) and anti-PLY (B) antibodies were assessed by ELISA (Southern Biotech antibody clonotyping kit). Serum samples were pooled from 5 immunized mice, samples were added to the first well at 1:50 dilution and serially diluted 1:5 vertically down the plate. Antibody (Ab) titres were determined by calculating the reciprocal titre of the last well in which signal could be detected above background ($OD_{485-10nm} > 0.3$).

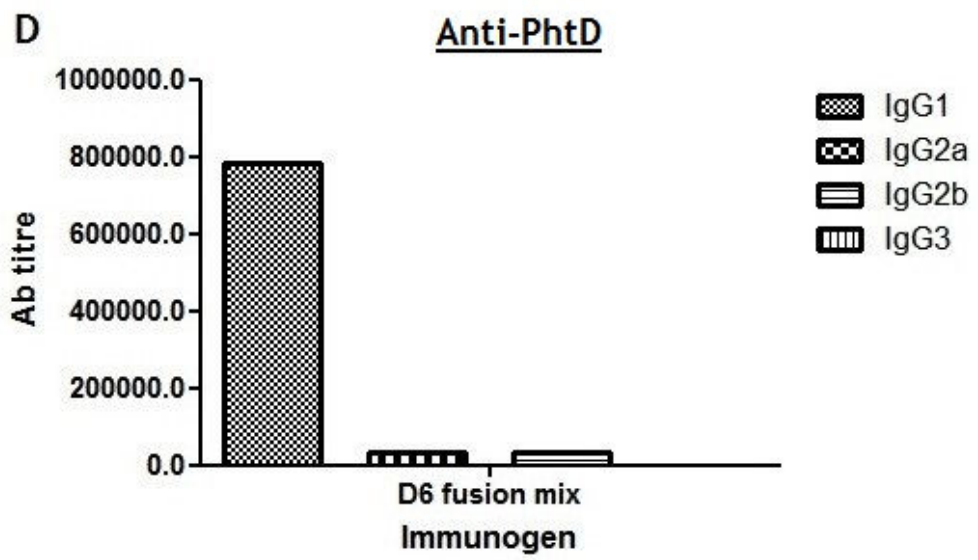
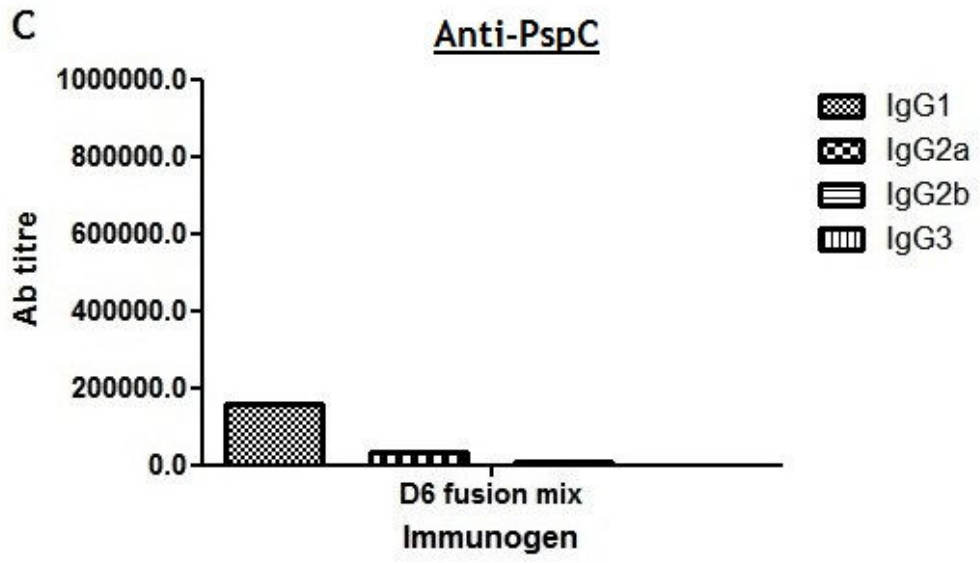
6.5 IgG subclasses induced by Immunization with a 10x mix of PsaA/PspA/PspC/PhtD - Δ 6PLY fusion vaccines

Following the assessment of single antigen fusion vaccines PATH 9 and 10 experiments were carried out to test the efficacy of the four fusion vaccines in combination using Δ 6PLY only as the adjuvant. The terminal immune sera from these experiments were tested for IgG subsets to determine how the antigen combinations influence immune phenotype. Additionally, the PLY only condition in both experimental groups gives insight into the baseline IgG subset response to PLY before the addition of other antigens.

The terminal immune sera was tested for antibody subsets directed against each individual fusion antigen and compared to the response generated against single antigen vaccines.

In PATH 9 (figure 6-9) the IgG response to PspA is unchanged compared to the single antigen vaccine, IgG1 antibody titres towards the other three antigens have all increased. The anti-PsaA IgG subset also has increased titres of IgG2a and greatly reduced IgG2b titres compared to the single antigen vaccine. In the case of PhtD the IgG subset pattern has reversed and IgG1 is now the dominant subset over IgG2a. Consistent with previous PATH studies there is little to no anti-PLY response generated following intranasal immunization with Δ 6PLY fusions; in contrast the response generated to PLY alone is strong and composed predominantly of IgG2b followed by IgG1.





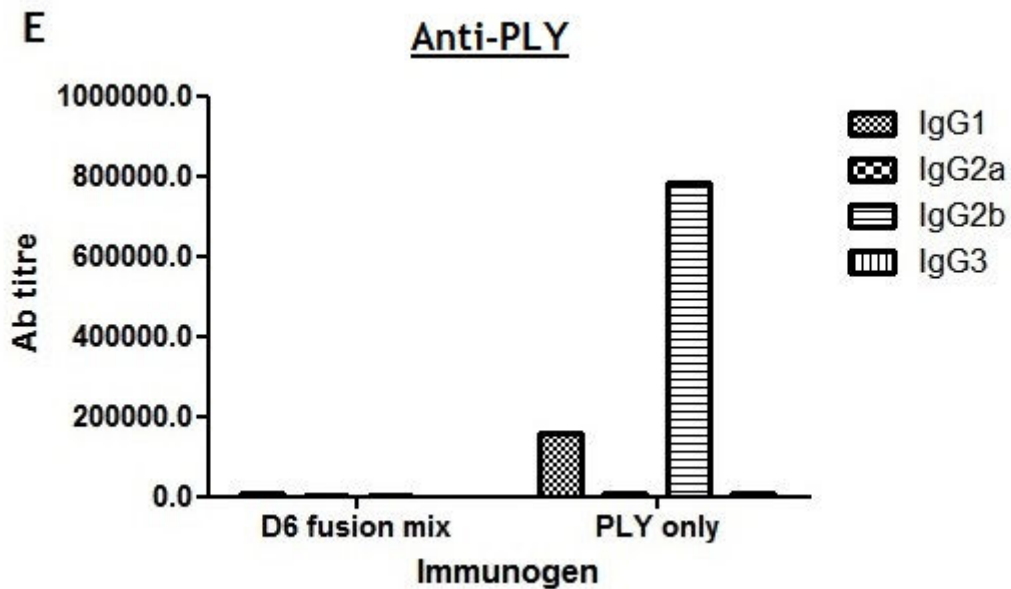
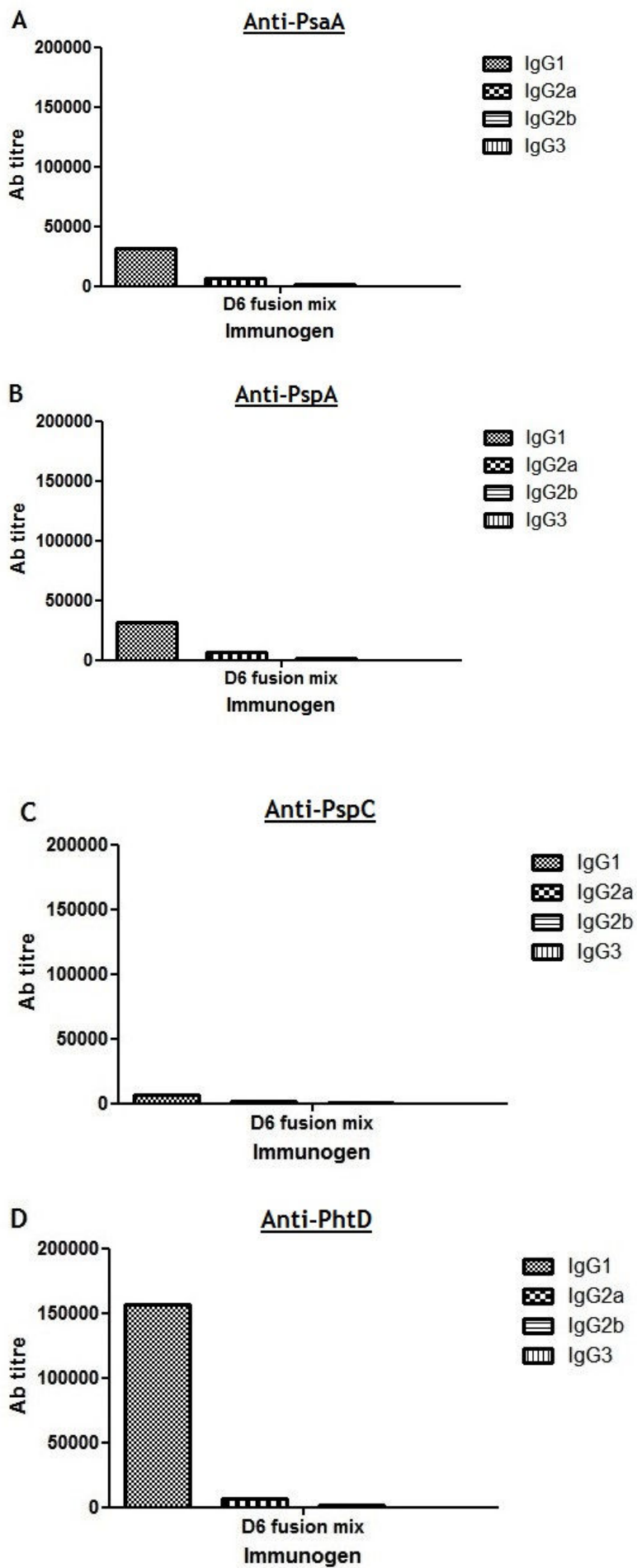


Figure 6-9 PATH 9.

IgG subsets were determined in terminal serum samples from MF1 mice immunized intranasally with a mix of PsaA- Δ 6PLY, PspA- Δ 6PLY, PspC- Δ 6PLY and PhtD- Δ 6PLY (following schedule detailed in table 2-13). Antibodies raised against PsaA (A), PspA (B), PspC (C), PhtD (D) PLY (E) antibodies were assessed. In addition, PATH 9 included MF1 mice immunized with PLY only, anti-PLY IgG subsets in this group were also assessed (E). Antibody titres were assessed by ELISA (Southern Biotech antibody clonotyping kit). Serum samples were pooled from 5 immunized mice, samples were added to the first well at 1:50 dilution and serially diluted 1:5 vertically down the plate. Antibody (Ab) titres were determined by calculating the reciprocal titre of the last well in which signal could be detected above background ($OD_{485-10nm}$ 0.3).

The antibody response generated towards fusion antigens in PATH 10 (figure 6-10) is greatly reduced compared to PATH 9 and IgG1 is the dominant IgG subset in all conditions. The antibody response to PLY only is now composed of IgG2a and IgG3 with a lower titre of IgG1.



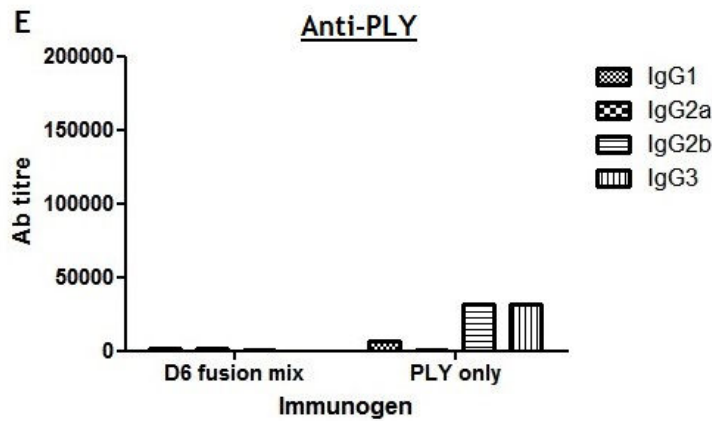


Figure 6-10 PATH 10.

IgG subsets were determined in terminal serum samples from MF1 mice immunized subcutaneously with a mix of PsaA- Δ 6PLY, PspA- Δ 6PLY, PspC- Δ 6PLY and PhtD- Δ 6PLY (following schedule detailed in table 2-13). Antibodies raised against PsaA (A), PspA (B), PspC (C), PhtD (D) PLY (E) antibodies were assessed. In addition, PATH 10 included 5 MF1 mice immunized with PLY only, anti-PLY IgG subsets in this group were also assessed (E). Antibody titres were assessed by ELISA (Southern Biotech antibody clonotyping kit). Serum samples were pooled from 5 immunized mice, samples were added to the first well at 1:50 dilution and serially diluted 1:5 vertically down the plate. Antibody (Ab) titres were determined by calculating the reciprocal titre of the last well in which signal could be detected above background ($OD_{485-10nm} > 0.3$).

6.6 Discussion

It appears that the fused antigen plays a significant role in determining the phenotype of the antibody response generated against PLY and Δ 6PLY fusion vaccines. Analysis of IgG subtypes in PATH serum samples has revealed that the magnitude of antibody response is not only determined by lytic activity (IL-1 β etc.) but also by administration route as subcutaneous immunization resulted in consistently lower antibody titres compared to intranasal immunization, this is fortuitous as the fusion vaccines are intended to be administered intranasally should they be deemed suitable and effective for human use. IgG3 appears to be more prevalent where vaccines are administered subcutaneously compared to intranasally, this trend may be a reflection of the resident cell types in both locales and therefore the cytokine milieu induced in response to PLY. The cytokines induced during initial, innate responses to fusion vaccines will ultimately instruct the phenotype of the adaptive response for example, as INF- γ induces the IgG3 subclass and is a signature cytokine of Th1-type response it is likely that subcutaneously immunization promotes a Th1 response more strongly compared to intranasal immunization. The comparison of immunization with PLY

only between subcutaneous and intranasal administration has revealed that while subcutaneous immunization results in predominant IgG3 (Th1 induced) and IgG2b (Th2 induced) subsets, immunization intranasally induced IgG1 and IgG2b (both Th2 induced) subsets. In a study of children with recurrent pneumococcal respiratory infections IgG2b was shown to be a protective subclass (Sorensen et al., 1996). A study of protection in immunized mice using various Fc receptor transgenic animals suggested a protective role for Ig1 but not IgG3 (Saeland et al., 2003). Taken together these studies suggest that the IgG3 subset is not essential for protection and that its absence following intranasal immunization is not detrimental.

Although there is a general trend towards IgG1 predominance and IgG2b production in most groups each PATH antigen has a unique IgG subset phenotype, this suggests that there is antigenic immunodominance within the fusion vaccines. This is best demonstrated in PATH 9 and PATH 10 (figures 6-9 and 6-10), in both groups the highest antibody titre is IgG1 directed against PhtD, and in addition specific IgG1 against the other antigens has increased suggesting that PhtD is influencing the IgG subset phenotype. There is evidence to suggest that PhtD in itself may be a potent adjuvant (Ma, 2012). The pneumococcal virulence factors all have their own immunogenic properties therefore it is not surprising that they influence the immune phenotype when used as vaccine antigens. Interestingly, as shown in figure 5-15 even an innocuous antigen such as eGFP has some influence over the IgG subset phenotype; given that eGFP is not immunogenic it would be expected that intranasal immunization with e-PLY would result in the same IgG subsets as PLY given intranasally (figure 6-9), however this is not the case, IgG2b is reduced in response to e-PLY and IgG2a is increased. Finally, anti-PLY antibodies are rarely generated against PLY/ Δ 6PLY fusion vaccines; this could indicate another virulence property of PLY. It is possible that the adjuvant activity of PLY has arisen and been conserved through an ability to promote adaptive immune responses to antigens other than itself.

7. Final Discussion

7.1 The Interaction of PLY with Toll-like Receptors

The work presented in this thesis has contributed to our understanding of interactions between PLY and the host immune response. In particular the interaction between TLR4 and PLY has been confirmed and attributed to a specific region of the toxin (domains 1-3). Previously, TLR4-dependent responses to PLY had been treated sceptically, a particular criticism being that purified PLY was likely contaminated by LPS. However, analysis of LPS content and the use of appropriate vehicle controls have bolstered the argument that the interaction between TLR4 and PLY is genuine.

In addition evidence has been presented that could suggest another TLR binding site. The THP-1 reporter cell line indicated TLR activity in response to treatment with both D123PLY and D4PLY (figures 3-9 and 3-11). There was no evidence of TLR4 binding in response to D4 suggesting that a different TLR could be involved (figure 3-10).

The importance of TLR4 in the adjuvant activity of PLY was explored primarily by assessing its role in cytokine and chemokine production (section 6.2). The role of TLR4 in PLY-based vaccines has previously been studied in a mouse model of immunization, however, there were no statistical differences between TLR4^{-/-} and genetic background control mice (Ma, 2012). This would suggest that TLR4 is not essential for the adjuvant activity of PLY, however, (as will be discussed in more detail) TLR4 though not essential for adjuvant activity may still play a role in the immune response to PLY-fusion vaccines.

7.2 The Production of KC, IL-6 and IL-1 β and Their Potential Role(s) in the Adjuvant Activity of PLY

The list of cytokines and chemokines that could potentially be involved in the adjuvant activity of PLY and therefore would be of interest to measure by ELISA is prohibitively long. Therefore, KC, IL-6 and IL-1 β were chosen as candidates

for initial assessment either because they had already been shown to be produced in response to PLY and/or had been shown to have a role in protection from pneumococcal infection or disease. Ideally, the production of additional cytokines/chemokines identified by gene expression analysis (noted in section 7.5) would have been explored; however there was not sufficient time to do this.

7.2.1 IL-1 beta

IL-1- β was chosen as a candidate cytokine because it has previously been shown to be involved in pneumococcal infection/protection (Shoma et al., 2008). Additionally its production is tightly regulated by a two-step process (1) TLR ligation resulting in pro-IL-1 β production, and (2) activation of the NLRP3 inflammasome, a platform for caspase-1 activation and subsequent cleavage of pro-IL-1 β into its active form; this made it an ideal candidate for examining the TLR4 binding capability of PLY.

The IL-1 β hypothesis was based on two observations about PLY - (1) PLY is thought to interact with TLR4 and (2) PLY forms pores in cell membranes causing ion flux (which in theory would activate the NLRP3 inflammasome). Therefore the initial IL-1 β hypothesis was simple, if PLY can provide both signal 1 and 2 in the same cell IL-1 β will be produced, $\Delta 6$ PLY (being non-lytic) would not activate the NLRP3 inflammasome, IL-1 β would not be produced, and that this could be the biological basis for reduced antibody titres in response to $\Delta 6$ PLY compared to PLY. However, while testing of this hypothesis has shown that although the theory is essentially correct, the mechanism of PLY-dependent IL-1 β production is far more complex than initially thought. The production of IL-1 β in response to PLY was completely dependent on NLRP3 activation (figure 5-1), however, the role of TLR4 was more complex. When BMDM from outbred MF1 mice were treated with PLY alone IL-1 β was not present in the supernatants (figure 3-13), however, when TLR4 was removed from the treatment model, either by blocking TLR4 signalling with VIPER or using TLR4 $^{-/-}$ BMDM IL-1 β was present in cell supernatants (figures 5-7 and 5-8). This suggest two new hypotheses -

- 1) TLR4 has a suppressive effect on IL-1 β production or secretion when PLY alone is used to treat BMDM.
- 2) In the absence of TLR4 the presence of IL-1 β in cell supernatants would suggest transcription of pro-IL-1 β is mediated by another, as yet unidentified TLR binding site in PLY.

Finally, an additional mechanism for IL-1 β production was observed, where TLR4 is present (MF1 mice) it is possible for PLY to induce IL-1 β production without the need for an exogenous TLR ligand if treatment is performed in the presence of complement sufficient sera (figures 5-2 and 5-3). Complement activation has been shown to synergize with TLR ligation to enhance or induce cytokine secretion, particularly IL-1 β (Fang et al., 2009; Zhang et al., 2007). If TLR4 is in some way suppressing IL-1 β production it is possible that simultaneous complement activation provides the inflammatory stimulus required to overcome this and induce IL-1 β production. It is unclear at this stage which complement components are involved in this mechanism, the anaphylotoxins C3a and C5a have been implicated in previous studies of complement - TLR synergy, however, as there is still residual IL-1 β produced in the absence of C3 it would seem that components that precede C3 in the classical complement cascade are involved.

It is not surprising that the relationship between PLY, TLR4 and IL-1 β has been difficult to elucidate in the past given this new model of activation. Proving that PLY was capable of inducing IL-1 β production without the need for exogenous TLR ligands was essential before investigating the role of IL1 β in adjuvant activity.

7.2.2 IL-6

As stated in chapter three, no IL-6 was found in the supernatants of PLY treated BMDM, it is possible that PLY-dependent IL-6 production is suppressed in a similar manner to IL-1 β , although the presence of complement had no effect on its production (data not shown). Additionally, in a previous study of cytokines

present in BALF following instillation of PLY into mouse lungs, IL-6 was present at significant concentrations (Kirkham, 2006). Clearly IL-6 is produced in response to PLY; it may be that IL-6 production is favoured under *in vivo* conditions and/or that it is a late response and was not observed at the time points analysed.

IL-6 has been shown to be induced by and have a protective effect during pneumococcal infection (Antunes et al., 2002; van der Poll et al., 1997). It is also required (in combination with TGF β) for induction of Th17 cells which are involved in protection from pneumococcal infection. Therefore it will be important to further investigate the production of IL-6 in response to PLY, particularly which cells under what circumstances produce IL-6 and what effect this has on adjuvant activity and final immune phenotype.

7.2.3 KC

KC is a potent neutrophil chemoattractant and has been shown to be present in high concentrations in BALF following instillation of PLY into mouse lungs (Kirkham, 2006). High concentrations of KC were also produced by BMDM treated with PLY (figure 3-15). When analysing the production of KC in response to PLY treatment D4PLY did not induce production of this chemokine; KC production was primarily mediated by D123PLY (although PLY and Δ 6PLY induced KC at greater concentrations) and was at least partially TLR4-dependent.

The attraction of neutrophils could be an important feature of PLY adjuvanticity; the role of neutrophils in antigen presentation is increasingly recognized as they have been shown to both influence the level of antigen presentation and in some circumstances present antigen themselves (Culshaw et al., 2008; Yang et al., 2010).

7.2.4 The Role of Complement in Cytokine Production and Adjuvant Activity

In vitro the presence of complement was found to be essential for IL-1 β production, however, it did not appear to have a role in adjuvant activity as

there was no difference in antibody response between C3^{-/-} and C57BL6 mice. The number of variables in this immunization study was limited by the number of available transgenic animals and so only e-Δ6PLY immunizations were performed. Therefore this was not a study of the role of complement-enhanced IL-1β in adjuvant activity but a study of the role of complement C3 itself in adjuvant activity. Further investigation of the role of complement activation should be pursued, particularly since complement C3 gene expression was upregulated in initial expression studies of PLY treated BMDM (appendix 5), this would provide a source of peripheral complement and could sustain and ‘inflammatory focus’ at the site of inoculation.

7.3 Binding of PLY Variants to Host Cells and Interactions with the Cell Cytoskeleton

The binding of PLY to host cells via cholesterol and subsequent formation of pores is well understood and is clearly an important feature of adjuvanticity. PLY has been shown to bind RAW 264.7 cells as rapidly as 5 seconds after introduction *in vitro*, however, there is a lag time of up to 30 minutes before signs of cell death (such as rounding) are obvious (figure 4-1). The sensitivity of different cell types to PLY-mediated lysis and death varied, in particular mature macrophages were highly resistant to PLY-mediated lysis compared to cell lines of a monocytic lineage (table 3-2), potentially due to active membrane repair through endocytosis of pores. This highlighted the need to be aware of differences in lytic activity in different cells when creating new models, particularly if the BMDM model is repeated in bone marrow derived dendritic cells (BMDC). As described in section 2.9.2 it was decided that consistency in the number of PLY monomers would be adhered to (rather than percentage lysis), this will be more useful if these studies are repeated in other cell types as it will allow direct comparison of responses to non-lytic and truncation mutants between cell types.

The HaloTag® system was a useful platform for analysis of both binding to host cells using microscopy and analysis of subsequent interactions with host proteins by pull-down. Unexpectedly, all PLY variants were found to bind to host cells and each had a unique binding pattern; D123PLY had a striking binding pattern

and was observed in aggregates covering large areas of the cell surface (figures 4-6 and 4-21). This was a previously unknown feature of D123PLY, although binding of domains 1-3 of LLO has previously been reported (Dubail et al., 2001). Both PLY and $\Delta 6$ PLY were observed inside the cells indicating a specific uptake mechanism (figures 4-3 and 4-5); this is unsurprising as the proteins must enter the cell at some point in order for antigen processing and presentation to occur. There was some evidence that D123PLY could be mediating antigen uptake, however this will need further confirmation.

Finally, D123PLY and D4PLY had dramatically different binding patterns to full-length PLY and $\Delta 6$ PLY. In a previous study using the *in vivo* model described in this thesis, the truncation mutants e-D123PLY and e-D4PLY did not possess adjuvant activity (Ma, 2012). This suggests that the truncation mutants behave very differently to the full-length proteins and that adjuvant activity must derive from a combination of attributes from both domains. While the truncations mutants were useful for identifying TLR binding sites and other biological responses (such as KC production) they may not be reflective of the behaviour of the whole molecule.

7.4 Characteristics of Final Immune Phenotype following Immunization with PLY/ $\Delta 6$ PLY Fusion Vaccines

The difference in magnitude of antibody response between PLY and $\Delta 6$ PLY based fusion vaccines has been demonstrated to be due to differential IL-1 β production, caused by lack of NLRP3 activation by $\Delta 6$ PLY (figures 5-12 and 5-13). This was found to affect antibody magnitude alone, the IgG subclasses present following immunization with either e-PLY or e- $\Delta 6$ PLY were identical (figure 5-15) indicating that lytic activity (and IL-1 β) did not influence antibody phenotype (IgG1<IgG2a<IgG2b). Data collected thus far from the PATH project show that protection is still observed using $\Delta 6$ PLY-based fusion vaccines (unpublished data) therefore while IL-1 β induces increased antibody production this may not be an important indicator of protection. As mentioned in chapter 1 Th17 based immunity is thought to be essential for preventing pneumococcal colonization, whereas humoral immunity is required for protection from invasive disease. In

future phenotyping of antigen specific T-cells following immunization with e-PLY or e- Δ 6PLY should be performed to discover whether Th17 cells are induced and if so are they equally induced by PLY and Δ 6PLY based vaccines.

The use of PATH proteins demonstrated that IgG subclass is influenced by fusion antigens (chapter 6). Since IgG1 and IgG2b are known to be protective subclasses it may be important to modify fusion mix vaccines to preferentially induce this IgG phenotype. Interestingly, even eGFP had a modest effect on antibody phenotype compared to PLY alone (IgG2b decreased IgG2a increased). The cytokines thought to influence this type antibody subclass pattern are in fact in competition, for instance IL-4 induces IgG1 but inhibits IgG2a and IFN γ induces IgG2a but inhibits IgG1, IgG2b is induced by TGF β and this also induces IgA production (a key feature of PLY/ Δ 6PLY-based vaccines). So the final antibody phenotype is probably influenced by a delicate balance of these three cytokines and this could explain why the antibody phenotype differs based on the fusion antigen.

7.5 Gene expression analysis

An analysis of gene expression in BMDM treated with PLY and its derivatives was undertaken using gene profiler arrays (SABiosciences), unfortunately it was not possible to perform biological replicates before submission of this thesis and so there are substantial limitations in the interpretation of this data. However, the data may be of future use for informing hypotheses and some of the data corroborates with both data presented in this thesis and in the literature, as such the data have been included as an appendix (appendix 5). Analysis of gene expression in response to vaccine adjuvants CpG, PCEP, Alum and MF59 has identified a cluster of genes that are differentially regulated and are referred to as 'core response genes' (Awate et al., 2012; Mosca et al., 2008). This study has identified upregulation of these core genes in response to PLY and Δ 6PLY, although few were upregulated in response to the truncation mutants D123PLY and D4PLY (tables 7-1 and 7-2), this is consistent with previous work that demonstrates adjuvant activity in full-length PLY derivatives only (Ma, 2012).

Tables 7-1 and 7-2 show the regulation of gene expression of cytokines and chemokines by PLY and its derivatives that are thought to be part of a 'core

response' to adjuvants. The cytokines and chemokine upregulated in response to PLY are all involved at some stage in early immune responses. In combination the cytokine and chemokines induced by PLY would induce an early pro-inflammatory response, inducing migration and activation of cytokine milieu mediating cells such as macrophages, sustaining this response by inducing monocyte migration and attracting key antigen presenting cells such as DC. One chemokine that was not included in the RT² PCR panels is KC, as shown previously (chapter 3) KC is produced in large concentrations in response to PLY treatment and so it is likely that there is an influx of neutrophils to the site of PLY administration, there is also up-regulation of CXCL-3 (MIP-2 β) (appendix 5, table 2) in response to all PLY variants, this is a potent neutrophil chemoattractant (Nakagawa et al., 1994) and possibly also involved in PLY-mediated neutrophil recruitment.

Table 7-1 Regulation of adjuvant core response genes following PLY treatment
Cytokine | **Function** | **Is Gene Upregulated in Response to PLY Derivative?**

Cytokine	Function	Is Gene Upregulated in Response to PLY Derivative?			
		PLY	Δ 6PLY	D123PLY	D4PLY
IL-6	Induction of acute phase proteins, stimulates T- and B-cell growth.	Y	Y	Y	N
IL-12a (p35)	Both components form the IL-12 heterodimer responsible for inducing IFN gamma and promoting Th-1 type responses.	Y	Y	N	N
IL-12 b (p40)		Y	Y	Y	Y
IL-1 beta		Y	Y	Y	Y
TNF	Induces local inflammatory response.	Y	Y	N	N

Table 7-2 Regulation of Adjuvant Core Response genes Following PLY treatment.

Chemokine	Function/Cells Attracted	Is Gene Upregulated in Response to PLY Derivative?			
		PLY	Δ 6PLY	D123PLY	D4PLY
CCL2 (MCP-1)	Monocytes, memory T-cells and DCs.	Y	N	N	N
CCL5 (RANTES)	Eosinophils, monocytes, NK and T cells and DCs.	Y	Y	N	N
CCL12	Attracts eosinophils, monocytes and lymphocytes.	Y	Y	Y	Y

As previously mentioned, D123PLY and D4PLY have been investigated as adjuvants but did not possess notable adjuvant activity, it was thought that this study could isolate and assign properties from the separate domains to the adjuvant activity of the full-length protein. However, the gene expression profiles of D123PLY and D4PLY were broadly similar with some exceptions such as IL-6 (a core response gene) which is upregulated in response to D123PLY but not D4PLY.

The profile of gene expression in response to LPS did differ in some respects to the profiles of BMDM treated with PLY or its derivatives; of the 58 genes described in appendix 5, the fold-regulation of 17 genes was different in LPS treated BMDM compared to PLY treated BMDM. It is unlikely that the gene expression profiles seen in response to PLY and its derivatives are influenced by LPS contamination as the similarities in profiles would be more extensive. The similarities that are seen between the expression profiles could be an indication of a common interaction(s) with the host, for example TLR4 ligation, thought to be responsible for LPS-induced production of IL-12, IFN γ , TNF- α and IL-1 β .

This study has highlighted genes that could be essential to adjuvant activity in PLY-based vaccines and forms a basis for further study. Importantly, the

changes in gene expression in BMDM treated with PLY and its derivatives should be verified by individual RT-PCR of biological replicates.

7.6 Future work

The data presented in this thesis have elaborated on our understanding of interactions between PLY and host cells, in particular the relationship between TLR4 and PLY has been confirmed and has revealed a complex mechanism of PLY-dependent IL-1 β production. This in turn has explained why Δ 6PLY-based vaccines induce a lower magnitude of antibody response than PLY-based vaccines. However, this work does not put forward a conclusive mechanism of adjuvant activity. Given the breadth of immune responses shown to be induced by PLY and its derivatives it is unlikely that one single mechanism is responsible for adjuvant activity. This thesis has however highlighted several avenues of investigation and should this work be continued it should include the following studies:

- The gene expression analysis presented in appendix 5 must be validated by individual RT-PCR of selected genes.
- Determine whether there are additional TLR binding sites within PLY. The HEK293/SEAP reporter cells could be used to screen for TLR activity, if additional TLR binding sites are discovered what role do they play in cytokine/chemokine production and subsequent adjuvant activity?
- The final immune phenotype following immunization with PLY/ Δ 6PLY-based vaccines must be fully characterized, not only will this be useful in understanding the optimum immune phenotype for pneumococcal protection but will also shed light on the conditions present at the site of inoculation (cytokine milieu, chemoattraction etc.) that are conducive to adjuvant activity.
- Further analysis of the role of complement in the immune response to PLY. Particularly, which components of the classical activation pathway are involved in licensing IL-1 β production, this could be tested using Quidel's depleted sera in the BMDM treatment model. Also, is complement required *in vivo* for an increased response to PLY based vaccines over Δ 6-PLY based vaccines?

- Characterize gene expression and cytokine/chemokine production in a TLR4-/- BMDM and BMDC PLY treatment model, there is some evidence to suggest that DC respond differently to PLY compared to macrophages. Additionally, as DC are the most efficient APC studies of antigen uptake and processing would be more appropriate in this cell type.
- *In vivo* tracking of PLY following immunization could be useful in determining if there is a depot-effect following PLY immunization, this could also help to establish a time line and identify the cells that initially come into contact with PLY-based vaccines.
- Determine why PLY variants have such different binding patterns. Discover whether D123PLY binds to a specific receptor that causes aggregation on the cell surface, additionally, use cholesterol-depletion to determine whether the binding pattern observed for D4PLY is due to cholesterol distribution or is caused by D4PLY binding a specific receptor/host protein.
- Visualise the interaction between PLY/ Δ 6PLY/D123PLY and TLR4, could analyse colocalization using eGFP tagged version of PLY and its derivatives and staining TLR4 using fluorescent conjugate antibodies. This would however depend on levels of TLR4 expression, if expression is low it could be difficult to visualise.

7.7 Conferences/presentations

Some of the work presented in this thesis has also been presented at national and international conferences as follows:

- SULSA symposium - St. Andrews University 2010 - presented poster “Investigating the Adjuvant Activity of Pneumolysin.”
- SGM Nottingham - University of Nottingham 2010 - presented poster “Investigating the Adjuvant Activity of Pneumolysin.” Same title as above but different poster.

- SULSA symposium - University of Glasgow 2011 - presented poster and oral presentation both titled “Pneumolysin: Host Responses and Adjuvant Activity.”
- SULSA symposium - University of Edinburgh 2012 - presented poster “Investigating Interactions between Pneumolysin and Host cells using HaloTag® technology.”
- SGM Warwick - University of Warwick 2012 - presented poster “Investigating Protein: Protein Interactions between Pneumolysin and Mammalian Cells.”
- Europneumo - Instituto de Salud Carlos II, Madrid 2013 - oral presentation “The Role of Complement in the Adjuvant Activity of Pneumolysin.”

Appendices

Appendix 1 - Buffer recipes

	1 X PBS	10 x PBS
NaCl	8g	80g
KCL	0.2g	2g
NaH ₂ PO ₄	1.82g	18.2g
KH ₂ PO ₄	0.24g	2.4g
Make up to 1L with sterile dH ₂ O, pH 7.2-7.4		

Mammalian cell lysis buffer	
50mM Tris-HCL	0.6g
5mM EDTA	0.19g
150mM NaCl	0.87g
1% IGEPAL-CA630	1ml
EDTA-free Protease inhibitor cocktail (Roche)	1 tablet per 100ml
Make up to 100ml in sterile dH ₂ O, pH7.4. Autoclave.	

	Resolving Gel (10mls, 10%)	Stacking Gel (10mls, 4%)
Acrylamide/bis-acrylamide (30% solution)	3.3mls	1.33mls
1.5M Tris-HCL, pH 8.8	2.5mls	-
0.5M Tris-HCL, pH 6.8	-	2.5mls
10% (w/v) SDS	100µl	100µl
dH ₂ O	4.05mls	6.05mls
Ammonium persulphate 10% (w/v)	100µl	100µl
TEMED	10µl	10µl

Sample buffer (5x)	Running Buffer (10x)	Destain	Coomassie Stain
0.6ml 0.5M Tris, pH 6.8	30g Tris-base	500ml dH ₂ O	0.5g Coomassie Blue R-250
5mls 50% glycerol	144g glycine	400ml methanol	500ml destain
2.0mls 10% SDS	10g SDS	100ml Acetic acid	
1ml 1% Bromophenol blue	Make up to 1L using sterile water		
0.9mls H ₂ O			

Transfer buffer	Tris NaCl pH 7.4	Developer
25mM Tris base (3.03g)	Tris base (1.2g)	30mg 4-chloro-1-naphthol
192mM Glycine (14.4g)	NaCl (8.7g)	10ml methanol
20% Methanol (200ml)	Make up to 1L with dH ₂ O	40ml Tris NaCl pH 7.4
Make up to 1L with dH ₂ O	Adjust pH with conc. HCL	30µl H ₂ O ₂
Chilled to 4 °C	-	-

Nickel Solution	NAC Elution Buffer pH 7.4	AEC Start Buffer pH 8.0	AEC Elution Buffer pH 8.0
0.2M Nickel	0.5M NaCl	20mM Tris base	20mM Tris base
500ml dH ₂ O	0.5M Imadizole	Make up to 1L in sterile dH ₂ O	1.0M NaCl
-	Make up to 1L in sterile PBS	-	Make up to 1L in sterile dH ₂ O

General Actin Buffer (A-buffer) pH 8.0	Actin Polymerization Buffer (APB) (10X)	General F-actin Buffer (F-buffer)
5mM Tris-HCL	500mM KCL	APB diluted 1/10 in GAB
0.2mM CaCl ₂	20mM MgCl ₂	
0.2mM ATP*	10mM ATP*	
0.5mM DTT*	-	
*Add immediately before use	*add 1mM before use or freeze aliquots at -70 °C	

Appendix 2 - Table of Properties of PLY and its Derivatives (mol. weight etc.)

	PLY	$\Delta 6$ PLY	D123PLY	D4PLY
length (aa)	509	507	306	115
Molecular weight (kDa)	57	57	40	13.5
Molar extinction CoEfficient	69910	69960	44120	8370
Molecular extinction CoEfficient	0.8142	0.810726	0.94377	1.5535
1 μ g=?nMol	17.561	17.563	25.02	74.24

Appendix 3 - Concentration of HaloTagged proteins in Halo lysates

Protein	Approximate Concentration (μ g/ml)
Halo-PLY	1321
Halo- $\Delta 6$ PLY	1448
Halo-D123PLY	2099
Halo- $\Delta 6$ D123PLY	2079
Halo-D4PLY	2487
Halo-eGFP	1538

Appendix 4 - Sequence alignment of Tubulin β -5 chain from *Bos taurus* and *Mus musculus*

```

1 MREIVHIQAGQCGNQIGAKFWEVISDEHGIDPTGTYHGSDSLQLDRISVYYNEATGGKYV 60 Q2KJD0 TBB5_BOVIN
1 MREIVHIQAGQCGNQIGAKFWEVISDEHGIDPTGTYHGSDSLQLDRISVYYNEATGGKYV 60 P99024 TBB5_MOUSE
*****
61 PRAILVDLEPGTMDSVRSRGPFGQIFRPDNFVFGQSGAGNNWAKGHYTEGAELVDSVLDV 120 Q2KJD0 TBB5_BOVIN
61 PRAILVDLEPGTMDSVRSRGPFGQIFRPDNFVFGQSGAGNNWAKGHYTEGAELVDSVLDV 120 P99024 TBB5_MOUSE
*****
121 RKEAESCDCLOQGFQLTHSLGGGTGSGMGTLLISKIREEYPDRIMNTFSVVPSPKVS 180 Q2KJD0 TBB5_BOVIN
121 RKEAESCDCLOQGFQLTHSLGGGTGSGMGTLLISKIREEYPDRIMNTFSVVPSPKVS 180 P99024 TBB5_MOUSE
*****
181 EPYNATLSVHQLVENTDETYCIDNEALYDICFRTLKLTPTTYGDLNHLVSATMSGVT 240 Q2KJD0 TBB5_BOVIN
181 EPYNATLSVHQLVENTDETYCIDNEALYDICFRTLKLTPTTYGDLNHLVSATMSGVT 240 P99024 TBB5_MOUSE
*****
241 RFPGQLNADLRKLANVMVFPRLHFFMPGFAPLTSRGSQQYRALTVPELTQQVFD 300 Q2KJD0 TBB5_BOVIN
241 RFPGQLNADLRKLANVMVFPRLHFFMPGFAPLTSRGSQQYRALTVPELTQQVFD 300 P99024 TBB5_MOUSE
*****
301 AACDPRHGRYLTVAAVFRGRMSMKEVDEQMLNVQNKNSYFVEWIPNNVKTAVCD 360 Q2KJD0 TBB5_BOVIN
301 AACDPRHGRYLTVAAVFRGRMSMKEVDEQMLNVQNKNSYFVEWIPNNVKTAVCD 360 P99024 TBB5_MOUSE
*****
361 LKMAVTFIGNSTAIQELFKRISEQFTAMFRRKAFLHWYTGEGMDEMEFTEAESNM 420 Q2KJD0 TBB5_BOVIN
361 LKMAVTFIGNSTAIQELFKRISEQFTAMFRRKAFLHWYTGEGMDEMEFTEAESNM 420 P99024 TBB5_MOUSE
*****
421 EYQQYQDATAEEEEDFGEEAEAAA 444 Q2KJD0 TBB5_BOVIN
421 EYQQYQDATAEEEEDFGEEAEAAA 444 P99024 TBB5_MOUSE

```

Appendix 5 - Analysis of BMDM Gene Expression in Response to Treatment with PLY and its Derivatives

To identify host responses that are involved in the adjuvant activity of PLY an analysis of gene expression using RT² PCR profiler arrays (SABiosciences) was performed. Using RNA obtained from BMDM treated with LPS, PLY or its derivatives the expression of genes involved in inflammatory and antibacterial responses was measured compared to RNA from untreated BMDM. The profiler arrays used were - PAMM-011 (inflammatory cytokine and chemokine response genes) and PAMM-148 (antibacterial response genes). Previously, PLY-dependent gene expression has been analysed in the THP-1 cell line using PLY-/- pneumococci and isogenic controls (Rogers et al., 2003). However, expression in response to purified proteins has not previously been performed; in addition this study included the non-lytic and truncation derivatives Δ 6PLY, D123PLY and D4PLY and used primary cells rather than cell lines to create a less artificial model. Unfortunately, it was not possible to verify the gene expression analysis by individual RT-PCR. RT-PCR primers had been selected to verify the expression of IL-10, C3, IL-1 β , TNF-alpha and GAPDH, however, at the time of submitting this thesis the order had not been fulfilled.

Below tables show fold regulation of genes considered to be statistically significant compared to internal controls.

Table 1 Regulation of Cytokine Genes in BMDM treated with LPS or PLY and its Derivatives.
Symbol Description Fold-change Up, Down (-) or Unchanged (X) Compared to Untreated BMDM

		LPS	PLY	Δ 6PLY	D123PLY	D4PLY
IL10	Interleukin 10	24	8.5	X	4.7	4.1
IL12a	Interleukin 12 alpha	105.4	18	2	X	X
IL12b	Interleukin 12 beta	885.3	77.7	10	3.3	3.6
IL13ra1	Interleukin 13 receptor, alpha 1	6.5	2.4	3.2	X	X
IL15	Interleukin 15	10.7	X	X	X	X
IL16	Interleukin 16	-5	-4	X	X	X
IL18	Interleukin 18	15.5	X	X	X	X
IL1a	Interleukin 1 alpha	1640.3	3061.4	77.7	12.8	16.6
IL1b	Interleukin 1 beta	1112.6	604	26	4.4	3.8
IL1R2	Interleukin 1 receptor type 2	-1.0	1.0	1.2	4.6	4.5
IL1f6	Interleukin 1 family, member 6	3	X	X	17	14
IL1f8	Interleukin 1 family, member 8	X	X	X	6.8	6.5
IL2rg	Interleukin 2 receptor, gamma chain	3.4	2.1	2	X	X
IL6	Interleukin 6	1082.3	98.4	7.6	2.6	X
IL6ra	Interleukin receptor alpha	-6	-3.7	X	X	X
IL6st	Interleukin signal transducer	-4	X	X	5.5	5.6

Tnf	Tumour necrosis factor	32	14.8	5.5	X	X
Tnfrsf1b	TNF receptor superfamily, member 1 beta	5.5	3.1	X	-2.2	-2.5

Table 2 Regulation of Chemokine Genes in BMDM treated with LPS or PLY and its Derivatives.

Symbol	Description	Fold-change Up, Down (-) or Unchanged (X) Compared to Untreated BMDM				
		LPS	PLY	Δ 6PLY	D123PLY	D4PLY
CCL12	Chemokine (C-C motif) ligand 12	369.6	10.5	4.5	3.5	2.7
CCL17	Chemokine (C-C motif) ligand 17	11.5	12.6	x	4.6	5.2
CCL2	Chemokine (C-C motif) ligand 2	27.9	5	x	x	x
CCL22	Chemokine (C-C motif) ligand 22	39	13.5	x	x	x
CCL3	Chemokine (C-C motif) ligand 3	113	78	4.5	x	x
CCL4	Chemokine (C-C motif) ligand 4	250.7	118.6	7.5	3.8	3.6
CCL5	Chemokine (C-C motif) ligand 7	1105	83.8	10	x	x
CCL7	Chemokine (C-C motif) ligand 5	101	5.2	x	x	x
CCL8	Chemokine (C-C motif) ligand 8	42	x	x	x	x
CCL9	Chemokine (C-C motif) ligand 9	6.1	10.3	x	x	x
CCR1	Chemokine (C-C motif) receptor 1	2.5	3.5	x	x	x
CCR2	Chemokine (C-C motif) receptor 2	-10.2	-8.7	x	x	x

CCR9	Chemokine (C-C motif) receptor 9	5	3.5	x	2.9	2.2
CX3CL1	Chemokine (C-X3-C motif) ligand 1	2.2	x	x	22.8	21.4
CXCL1	Chemokine (C-X-C motif) ligand 1	96.3	144	11.9	4.9	4.7
		LPS	PLY	Δ 6PLY	D123PLY	D4PLY
CXCL3	Chemokine (C-X-C motif) ligand 3	270.6	2778	21.4	4.5	2.5
CXCL10	Chemokine (C-X-C motif) ligand 10	814.6	28.2	18.6	3	2.2
CXCL11	Chemokine (C-X-C motif) ligand 11	47.5	x	x	x	x
CXCL5	Chemokine (C-X-C motif) ligand 5	3.2	61.8	x	2.9	2.5
CXCL9	Chemokine (C-X-C motif) ligand 9	474.4	2.9	4.3	7.5	8

Table 3 Regulation of Inflammatory Receptor Genes in BMDM treated with LPS or PLY and its Derivatives.

Symbol	Description	Fold-change Up, Down (-) or Unchanged (X) Compared to Untreated BMDM				
		LPS	PLY	Δ 6PLY	D123PLY	D4PLY
Cd14	CD14 antigen	5	7.6	2	x	x
Nod1	Nucleotide-binding oligomerization domain containing 1	2.6	x	x	2.6	2.9
Nod2	Nucleotide-binding oligomerization domain containing 2	4.1	3.1	x	2.4	2.9

Ticam1	Toll-like receptor adaptor molecule 1	-5.4	x	-15	-8	-9.6
Tlr1	Toll-like receptor 1	3.4	x	x	x	x
Tlr2	Toll-like receptor 2	3.2	4.9	x	x	x
Tlr4	Toll-like receptor 4	-4.3	x	x	x	x

Table 4 Regulation of Genes responsible for signal transduction and cytokine production in BMDM treated with LPS or PLY and its Derivatives.

Symbol	Description	Fold-change Up, Down (-) or Unchanged (X) Compared to Untreated BMDM				
		LPS	PLY	Δ 6PLY	D123PLY	D4PLY
Casp1	Caspase-1	5	x	x	x	x
Irak1	Interleukin-1 receptor-associated kinase 1	-5.1	-2.2	x	x	x
Irak3	Interleukin-1 receptor-associated kinase 3	6	4.7	x	x	x
Irf5	Interferon regulatory factor 5	-3.2	x	-3.4	-2.6	-2.9
Irf7	Interferon regulatory factor 7	20.3	2.7	x	-2.4	-3.2
Mapk3	Mitogen-activated protein kinase 3	-4.9	-2.7	-2.0	x	-2.1

Nfkb1	Nuclear factor of kappa light polypeptide gene enhancer in B-cells 1, p105	3	3.7	x	x	x
Nfkbia	Nuclear factor of kappa light polypeptide gene enhancer in B-cells inhibitor, alpha	7.2	4.3	3.5	2	2

Table 5 Regulation of Genes encoding Proinflammatory Mediators in BMDM treated with LPS or PLY and its Derivatives.

Symbol	Description	Fold-change Up, Down (-) or Unchanged (X) Compared to Untreated BMDM				
		LPS	PLY	Δ 6PLY	D123PLY	D4PLY
C3	Complement component C3	31.5	4.6	4	x	x
Ltb	Lymphotoxin b	2	x	x	5.5	5.1
Ctsg	Cathepsin G	-16.7	x	-9.1	-2.9	-6.6
Lcn2	Lipocalin 2	39.7	5	-2.2	-2.6	-3.1
Lyz2	Lysozyme 2	-4	-2	-3.2	x	x
Zbp1	Z-DNA binding protein 1	36.5	6.6	4.4	x	x

List of References

- Alcantara, R. B., Preheim, L. C., & Martha, J. (2001). Pneumolysin-Induced Complement Depletion during Experimental Pneumococcal Bacteremia. *Infection and Immunity*, 69(6), 3569-75.
- Alexander, J. E., Lock, R. A., Peeters, C. C., Poolman, J. T., Andrew, P. W., Mitchell, T. J., Paton, J. C. (1994). Immunization of mice with pneumolysin toxoid confers a significant degree of protection against at least nine serotypes of *Streptococcus pneumoniae*. *Infection and immunity*, 62(12), 5683-8.
- AlonsoDeVelasco, E., Verheul, A. F., Verhoef, J., & Snippe, H. (1995). *Streptococcus pneumoniae*: virulence factors, pathogenesis, and vaccines. *Microbiological reviews*, 59(4), 591-603.
- Antunes, G., Evans, S. A., Lordan, J. L., & Frew, A. J. (2002). Systemic cytokine levels in community-acquired pneumonia and their association with disease severity. *European Respiratory Journal*, 20(4), 990-995.
- Awate, S., Wilson, H. L., Lai, K., Babiuk, L. A, & Mutwiri, G. (2012). Activation of adjuvant core response genes by the novel adjuvant PCEP. *Molecular immunology*, 51(3-4), 292-303.
- Baba, H., Kawamura, I., Kohda, C., Nomura, T., Ito, Y., Kimoto, T., ... Mitsuyama, M. (2001). Essential role of domain 4 of pneumolysin from *Streptococcus pneumoniae* in cytolytic activity as determined by truncated proteins. *Biochemical and biophysical research communications*, 281(1), 37-44.
- Baldwin, S. L., Bertholet, S., Reese, V. a, Ching, L. K., Reed, S. G., & Coler, R. N. (2012). The importance of adjuvant formulation in the development of a tuberculosis vaccine. *Journal of immunology*, 188(5), 2189-97.
- Basset, A., Thompson, C. M., Hollingshead, S. K., Briles, D. E., Ades, E. W., Lipsitch, M., & Malley, R. (2007). Antibody-independent, CD4+ T-cell-dependent protection against pneumococcal colonization elicited by intranasal immunization with purified pneumococcal proteins. *Infection and immunity*, 75(11), 5460-4.
- Baumgarth, N., Tung, J. W., & Herzenberg, L. A. (2005). Inherent specificities in natural antibodies: a key to immune defense against pathogen invasion. *Springer Semin Immunopathol.*, 26(4347-62).
- Bernatoniene, J., Zhang, Q., Dogan, S., Mitchell, T. J., Paton, J. C., & Finn, A. (2008). Induction of CC and CXC chemokines in human antigen-presenting dendritic cells by the pneumococcal proteins pneumolysin and CbpA, and the role played by toll-like receptor 4, NF-kappaB, and mitogen-activated protein kinases. *The Journal of infectious diseases*, 198(12), 1823-33.

- Beurg, M., Hafidi, A., Skinner, L., Cowan, G., Hondarrague, Y., Mitchell, T. J., & Dulon, D. (2005). The mechanism of pneumolysin-induced cochlear hair cell death in the rat. *The Journal of physiology*, 568(Pt 1), 211-27.
- Braun, J. S., Novak, R., Gao, G., Murray, P. J., & Shenep, J. L. (1999). Pneumolysin, a protein toxin of *Streptococcus pneumoniae*, induces nitric oxide production from macrophages. *Infection and immunity*, 67(8), 3750-6.
- Brooks-Walter, A., Briles, D. E., & Hollingshead, S. K. (1999). The *pspC* gene of *Streptococcus pneumoniae* encodes a polymorphic protein, PspC, which elicits cross-reactive antibodies to PspA and provides immunity to pneumococcal bacteremia. *Infection and immunity*, 67(12), 6533-42.
- Carvalho, M. G. S., Steigerwalt, A. G., Jackson, D., Facklam, R. R., & Thompson, T. (2003). Confirmation of Nontypeable *Streptococcus pneumoniae*- Like Organisms Isolated from Outbreaks of Epidemic Conjunctivitis as *Streptococcus pneumoniae*. *Journal of Clinical Microbiology*, 41(9), 4415-7.
- Casadevall, A., & Pirofski, L.-A. (2003). Exploiting the redundancy in the immune system: vaccines can mediate protection by eliciting “unnatural” immunity. *The Journal of experimental medicine*, 197(11), 1401-4.
- Cassidy, S. K., & O’Riordan, M. X. (2013). More than a pore: the cellular response to cholesterol-dependent cytolysins. *Toxins*, 5(4), 618-36.
- Chu, J., Thomas, L. M., Watkins, S. C., Franchi, L., Núñez, G., & Salter, R. D. (2009). Cholesterol-dependent cytolysins induce rapid release of mature IL-1 β from murine macrophages in a NLRP3 inflammasome and cathepsin B-dependent manner. *Journal of leukocyte biology*, 86(5), 1227-38.
- Clark, M. R. (1997). Antibody engineering IgG effector mechanisms. *Chemical Immunology* 65, 88-110.
- Cockran, R., Theron, A. J., Steel, H. C., Matlola, N. M., Mitchell, T. J., Feldman, C. & Anderson, R. (2001). Proinflammatory interactions of pneumolysin with human neutrophils. *The Journal of infectious diseases*, 183(4), 604-11.
- Cockran, R., Durandt, C., Feldman, C., Mitchell, T. J. & Anderson, R. (2002). Pneumolysin activates the synthesis and release of interleukin-8 by human neutrophils in vitro. *The Journal of infectious diseases*, 186(4), 562-5.
- Cockran, R., Steel, H. C., Mitchell, T. J., Anderson, R. & Feldman, C. (2001). Pneumolysin Potentiates Production of Prostaglandin E₂ and Leukotriene B₄ by Human Neutrophils Pneumolysin Potentiates Production of Prostaglandin E₂ and Leukotriene B₄ by Human Neutrophils. *Infection and immunity*, 69(5), 3494-6.
- Cohen, J. M., Khandavilli, S., Camberlein, E., Hyams, C., Baxendale, H. E., & Brown, J. S. (2011). Protective contributions against invasive *Streptococcus pneumoniae* pneumonia of antibody and Th17-cell responses to nasopharyngeal colonisation. *PloS one*, 6(10), e25558.

- Craig, A., Mai, J., Cai, S., & Jeyaseelan, S. (2009). Neutrophil recruitment to the lungs during bacterial pneumonia. *Infection and immunity*, 77(2), 568-75.
- Culshaw, S., Millington, O. R., Brewer, J. M., & McInnes, I. B. (2008). Murine neutrophils present Class II restricted antigen. *Immunology letters*, 118(1), 49-54.
- Dave, S., Brooks-Walter, A., & Pangburn, M. K. (2001). PspC , a Pneumococcal Surface Protein , Binds Human Factor H. *Infection and Immunity*, 69(5), 3435-3437.
- Dave, S., Carmicle, S., Hammerschmidt, S., Pangburn, M. K., & McDaniel, L. S. (2004). Dual roles of PspC, a surface protein of *Streptococcus pneumoniae*, in binding human secretory IgA and factor H. *Journal of immunology*, 173(1), 471-7.
- De Gregorio, E., Tritto, E., & Rappuoli, R. (2008). Alum adjuvanticity: unraveling a century old mystery. *European journal of immunology*, 38(8), 2068-71.
- Didierlaurent, A. M., Morel, S., Lockman, L., Giannini, S. L., Bisteau, M., Carlsen, H., & Garçon, N. (2009). AS04, an aluminum salt- and TLR4 agonist-based adjuvant system, induces a transient localized innate immune response leading to enhanced adaptive immunity. *Journal of immunology*, 183(10), 6186-97.
- Doern, G. V. (2001). Antimicrobial use and the emergence of antimicrobial resistance with *Streptococcus pneumoniae* in the United States. *Clinical infectious diseases: an official publication of the Infectious Diseases Society of America*, 33(Suppl 3), S187-92.
- Dogan, S., Zhang, Q., Pridmore, A. C., Mitchell, T. J., Finn, A., & Murdoch, C. (2011). Pneumolysin-induced CXCL8 production by nasopharyngeal epithelial cells is dependent on calcium flux and MAPK activation via Toll-like receptor 4. *Microbes and infection / Institute Pasteur*, 13(1), 65-75.
- Douce, G., Ross, K., Cowan, G., Ma, J., & Mitchell, T. J. (2010). Novel mucosal vaccines generated by genetic conjugation of heterologous proteins to pneumolysin (PLY) from *Streptococcus pneumoniae*. *Vaccine*, 28(18), 3231-7.
- Dowd, K. J., & Tweten, R. K. (2012). The cholesterol-dependent cytolysin signature motif: a critical element in the allosteric pathway that couples membrane binding to pore assembly. *PLoS pathogens*, 8(7), e1002787.
- Dubail, I., Autret, N., Beretti, J. L., Kayal, S., Berche, P., & Charbit, A. (2001). Functional assembly of two membrane-binding domains in listeriolysin O, the cytolysin of *Listeria monocytogenes*. *Microbiology*, 147(Pt 10), 2679-88.
- Facklam, R. R., Ph, D., Sodha, S., Elliott, J. A., Pryor, J. H., Beall, B., ... Whitney, C. G. (2003). An Outbreak of Conjunctivitis Due to Atypical *Streptococcus pneumoniae*. *New England Journal of Medicine*, 348(12), 1112-21.

- Fang, C., Zhang, X., Miwa, T., & Song, W.-C. (2009). Complement promotes the development of inflammatory T-helper 17 cells through synergistic interaction with Toll-like receptor signaling and interleukin-6 production. *Blood*, *114*(5), 1005-15.
- Farrand, A. J., LaChapelle, S., Hotze, E. M., Johnson, A. E., & Tweten, R. K. (2010). Only two amino acids are essential for cytolytic toxin recognition of cholesterol at the membrane surface. *Proceedings of the National Academy of Sciences of the United States of America*, *107*(9), 4341-6.
- Feature, T. (2006). Helping cells to tell a colorful tale. *Nature Methods*, *3*(8).
- Ferreira, D. M., Darrieux, M., Silva, D. A., Leite, L. C. C., Ferreira, J. M. C., Ho, P. L., ... Oliveira, M. L. S. (2009). Characterization of protective mucosal and systemic immune responses elicited by pneumococcal surface protein PspA and PspC nasal vaccines against a respiratory pneumococcal challenge in mice. *Clinical and vaccine immunology: CVI*, *16*(5), 636-45.
- Fickl, H., Cockeran, R., Steel, H. C., Feldman, C., Cowan, G., Mitchell, T. J., & Anderson, R. (2005). Pneumolysin-mediated activation of NFkappaB in human neutrophils is antagonized by docosahexaenoic acid. *Clinical and experimental immunology*, *140*(2), 274-81.
- Filippo, K. De, Henderson, R. B., Laschinger, M., & Hogg, N. (2013). Neutrophil Chemokines KC and Macrophage-Inflammatory Protein-2 are Newly Synthesized by Tissue Macrophages using Distinct TLR Signaling Pathways. *The Journal of Clinical Immunology*, *180*, 4308-4315.
- Fleck, R. A., & Nahm, M. H. (2005). MINIREVIEWS Use of HL-60 Cell Line To Measure Opsonic Capacity of Pneumococcal Antibodies. *Infection and Immunity*, *12*(1), 19-27.
- Förtsch, C., Hupp, S., Ma, J., Mitchell, T. J., Maier, E., Benz, R., & Iliev, A. I. (2011). Changes in astrocyte shape induced by sublytic concentrations of the cholesterol-dependent cytolysin pneumolysin still require pore-forming capacity. *Toxins*, *3*(1), 43-62.
- Franchi, L., Eigenbrod, T., Muñoz-Planillo, R., & Núñez, G. (2009). The inflammasome: a caspase-1-activation platform that regulates immune responses and disease pathogenesis. *Nature immunology*, *10*(3), 241-7.
- Franchi, L., & Núñez, G. (2008). The Nlrp3 inflammasome is critical for aluminium hydroxide-mediated IL-1beta secretion but dispensable for adjuvant activity. *European journal of immunology*, *38*(8), 2085-9.
- Giebink, G. S., Dee, T. H., Kim, Y., & Quie, P. G. (1980). Alterations in serum opsonic activity and complement levels in pneumococcal disease. *Infection and immunity*, *29*(3), 1062-6.
- Goldblatt, D., Hussain, M., Andrews, N., Ashton, L., Virta, C., Melegaro, A., ... Miller, E. (2005). Antibody responses to nasopharyngeal carriage of *Streptococcus pneumoniae* in adults: a longitudinal household study. *The Journal of infectious diseases*, *192*(3), 387-93.

- Goulart, C., da Silva, T. R., Rodriguez, D., Politano, W. R., Leite, L. C. C., & Darrieux, M. (2013). Characterization of protective immune responses induced by pneumococcal surface protein A in fusion with pneumolysin derivatives. *PloS one*, 8(3), e59605.
- Gouveia, E. L., Reis, J. N., Flannery, B., Cordeiro, S. M., Lima, J. B. T., Pinheiro, R. M., ... Ko, A. I. (2011). Clinical outcome of pneumococcal meningitis during the emergence of penicillin-resistant *Streptococcus pneumoniae*: an observational study. *BMC infectious diseases*, 11(1), 323.
- Gray, B. M., Converse, G. M., & Dillon, H. C. (1980). Epidemiologic studies of *Streptococcus pneumoniae* in infants: acquisition, carriage, and infection during the first 24 months of life. *The Journal of infectious diseases*, 142(6), 923-33.
- Gupta, R. K., Relyveldt, E. H., Lindblad, E. B., & Bizzini, B. (1993). Review. Adjuvants a balance between toxicity and adjuvanticity. *Vaccine*, 11(3), 293-306.
- Güven, E., Duus, K., Laursen, I., Højrup, P., & Houen, G. (2013). Aluminum hydroxide adjuvant differentially activates the three complement pathways with major involvement of the alternative pathway. *PloS one*, 8(9), e74445.
- Haas, K. M., Poe, J. C., Steeber, D. A., Tedder, T. F., & Carolina, N. (2005). B-1a and B-1b Cells Exhibit Distinct Developmental Requirements and Have Unique Functional Roles in Innate and Adaptive Immunity to *S. pneumoniae*. *Immunity*, 23, 7-18.
- Herbold, W., Maus, R., Hahn, I., Ding, N., Srivastava, M., Christman, J. W., ... Maus, U. A. (2010). Importance of CXC chemokine receptor 2 in alveolar neutrophil and exudate macrophage recruitment in response to pneumococcal lung infection. *Infection and immunity*, 78(6), 2620-30.
- Hicks, L. A., Harrison, L. H., Flannery, B., Hadler, J. L., Schaffner, W., Craig, A. S., ... Whitney, C. G. (2007). Incidence of pneumococcal disease due to non-pneumococcal conjugate vaccine (PCV7) serotypes in the United States during the era of widespread PCV7 vaccination, 1998-2004. *The Journal of infectious diseases*, 196(9), 1346-54.
- Hirst, R. A., Mohammed, B. J., Mitchell, T. J., Andrew, P. W., & Callaghan, C. O. (2004). *Streptococcus pneumoniae*-Induced Inhibition of Rat Ependymal Cilia Is Attenuated by Antipneumolysin Antibody. *Infection and immunity*, 72(11), 6694-6698.
- Hirst, R. A., Yesilkaya, H., Clitheroe, E., Rutman, A., Dufty, N., Mitchell, T. J., ... Andrew, P. W. (2002). Sensitivities of Human Monocytes and Epithelial Cells to Pneumolysin Are Different. *Infection and Immunity*, 70(2), 1017-1022.
- Houldsworth, S., Andrew, P. W., & Mitchell, T. J. (1994). Pneumolysin Stimulates Production of Tumor Necrosis Factor Alpha and Interleukin-13 by Human Mononuclear Phagocytes. *Infection and immunity*, 62(4), 1501-1503.

- Hupp, S., Fortsch, C., Wippel, C., Ma, J., Mitchell, T. J., & Iliev, A. I. (2013). Direct Transmembrane Interaction between Actin and Pneumolysin. *Journal of molecular biology*, 425(3), 636-646.
- Huss, A., Scott, P., Stuck, A. E., Trotter, C., & Egger, M. (2009). Efficacy of pneumococcal vaccination in adults: a meta-analysis. *CMAJ : Canadian Medical Association journal*, 180(1), 48-58.
- Hutchison, S., Benson, R. A, Gibson, V. B., Pollock, A. H., Garside, P., & Brewer, J. M. (2012). Antigen depot is not required for alum adjuvanticity. *FASEB journal : official publication of the Federation of American Societies for Experimental Biology*, 26(3), 1272-9.
- Hyams, C., Camberlein, E., Cohen, J. M., Bax, K., & Brown, J. S. (2010). The Streptococcus pneumoniae capsule inhibits complement activity and neutrophil phagocytosis by multiple mechanisms. *Infection and immunity*, 78(2), 704-15.
- Iliev, A. I., Djannatian, J. R., Opazo, F., Gerber, J., Nau, R., Mitchell, T. J., & Wouters, F. S. (2009). Rapid microtubule bundling and stabilization by the Streptococcus pneumoniae neurotoxin pneumolysin in a cholesterol-dependent, non-lytic and Src-kinase dependent manner inhibits intracellular trafficking. *Molecular microbiology*, 71(2), 461-77.
- Iwasaki, A., & Medzhitov, R. (2010). Regulation of adaptive immunity by the innate immune system. *Science (New York, N.Y.)*, 327(5963), 291-5.
- Jacobs, T., Cima-Cabal, M. D., Darji, a, Méndez, F. J., Vázquez, F., Jacobs, A. A., ... de los Toyos, J. R. (1999). The conserved undecapeptide shared by thiol-activated cytolysins is involved in membrane binding. *FEBS letters*, 459(3), 463-6.
- Jarva, H. (2003). Complement resistance mechanisms of streptococci. *Molecular Immunology*, 40(2-4), 95-107.
- JCVI - Joint committee on vaccination and immunisation, (2011). JCVI statement on the routine pneumococcal vaccination programme for adults aged 65 years and older. <https://www.gov.uk/government/publications/joint-committee-on-vaccination-and-immunisation-advice-on-the-pneumococcal-vaccination-programme-for-people-aged-65-years-and-older>
- Jefferies, J. M. C., Johnston, C. H. G., Kirkham, L.-A. S., Cowan, G. J. M., Ross, K. S., Smith, A., ... Mitchell, T. J. (2007). Presence of nonhemolytic pneumolysin in serotypes of Streptococcus pneumoniae associated with disease outbreaks. *The Journal of infectious diseases*, 196(6), 936-44.
- Johnston, J. W., Myers, L. E., Ochs, M. M., Benjamin, W. H., Briles, D. E., & Hollingshead, S. K. (2004). Lipoprotein PsaA in Virulence of Streptococcus pneumoniae : Surface Accessibility and Role in Protection from Superoxide. *Infection and immunity*, 72(10), 5858-5867.
- Kadioglu, A., Coward, W., Colston, M. J., Hewitt, C. R. A., & Andrew, P. W. (2004). CD4-T-Lymphocyte Interactions with Pneumolysin and Pneumococci

Suggest a Crucial Protective Role in the Host Response to Pneumococcal Infection. *Infection and Immunity*, 72(5), 2689-2697.

- Kamtchoua, T., Bologa, M., Hopfer, R., Neveu, D., Hu, B., Sheng, X., ... Gurunathan, S. (2013). Safety and immunogenicity of the pneumococcal pneumolysin derivative PlyD1 in a single-antigen protein vaccine candidate in adults. *Vaccine*, 31(2), 327-33.
- Kataoka, K., Fujihashi, K., Oma, K., Fukuyama, Y., Hollingshead, S. K., Sekine, S., ... Oishi, K. (2011). The nasal dendritic cell-targeting Flt3 ligand as a safe adjuvant elicits effective protection against fatal pneumococcal pneumonia. *Infection and immunity*, 79(7), 2819-28.
- Kerr, A. R., Paterson, G. K., McCluskey, J., Iannelli, F., Oggioni, M. R., Pozzi, G., & Mitchell, T. J. (2006). The contribution of PspC to pneumococcal virulence varies between strains and is accomplished by both complement evasion and complement-independent mechanisms. *Infection and immunity*, 74(9), 5319-24.
- Kerr, A. R., Paterson, G. K., Riboldi-Tunncliffe, A., & Mitchell, T. J. (2005). Innate Immune Defense against Pneumococcal Pneumonia Requires Pulmonary Complement Component C3. *Infection and immunity*, 73(7), 4245-4252.
- Khan, M. N., & Pichichero, M. E. (2012). Vaccine candidates PhtD and PhtE of *Streptococcus pneumoniae* are adhesins that elicit functional antibodies in humans. *Vaccine*, 30(18), 2900-2907.
- Kirkham, L. S. (2006). *Construction and immunological characterisation of a non-toxic form of pneumolysin for use in pneumococcal vaccines*. University of Glasgow.
- Kirkham, L. S., Kerr, A. R., Douce, G. R., Paterson, G. K., Dilts, D. A., Liu, D., & Mitchell, T. J. (2006). Construction and Immunological Characterization of a Novel Nontoxic Protective Pneumolysin Mutant for Use in Future Pneumococcal Vaccines. *Infection and immunity*, 74(1), 586-593.
- Koppe, U., Suttorp, N., & Opitz, B. (2011). Recognition of *Streptococcus pneumoniae* by the innate immune system. *Cellular microbiology*, 14, 460-466.
- Kuroda, E., Ishii, K. J., Uematsu, S., Ohata, K., Coban, C., Akira, S., ... Morimoto, Y. (2011). Silica crystals and aluminum salts regulate the production of prostaglandin in macrophages via NALP3 inflammasome-independent mechanisms. *Immunity*, 34(4), 514-26.
- Lamaze, C. (1997). The Actin Cytoskeleton Is Required for Receptor-mediated Endocytosis in Mammalian Cells. *Journal of Biological Chemistry*, 272(33), 20332-20335.
- Lane, P. (1996). Are polysaccharide antibody responses independent: the T cell enigma? *Clinical and experimental immunology*, 105(1), 10-1.

- Lebon, A., Verkaik, N. J., Labout, J. A. M., Vogel, C. P. De, Hooijkaas, H., Verbrugh, H. A., ... Hofman, A. (2011). Natural Antibodies against Several Pneumococcal Virulence Proteins in Children during the Pre-Pneumococcal-Vaccine Era : the Generation R Study. *Infection and immunity*, 79(4), 1680-7
- Lefeber, D. J., Benaissa-Trouw, B., Vliegenthart, J. F. G., Kamerling, J. P., Jansen, W. T, J., Kraaijeveld, K. & Snippe, H. (2003). Th1-Directing Adjuvants Increase the Immunogenicity of Oligosaccharide-Protein Conjugate Vaccines Related to Streptococcus pneumoniae Type 3. *Infection and immunity*, 7(12), 6912-20.
- Liñares, J., Ardanuy, C., Pallares, R., & Fenoll, A. (2010). Changes in antimicrobial resistance, serotypes and genotypes in Streptococcus pneumoniae over a 30-year period. *Clinical microbiology and infection : the official publication of the European Society of Clinical Microbiology and Infectious Diseases*, 16(5), 402-10.
- Linder, S., Hüfner, K., Wintergerst, U., & Aepfelbacher, M. (2000). Microtubule-dependent formation of podosomal adhesion structures in primary human macrophages. *Journal of cell science*, 113 Pt 23, 4165-76.
- Littmann, M., Albiger, B., Frentzen, A., Normark, S., Henriques-Normark, B., & Plant, L. (2009). Streptococcus pneumoniae evades human dendritic cell surveillance by pneumolysin expression. *EMBO molecular medicine*, 1(4), 211-22.
- Los, G. V, Encell, L. P., Mcdougall, M. G., Hartzell, D. D., Karassina, N., Zimprich, C., ... Wood, K. V. (2008). HaloTag: A novel protein labelling technology for cell imaging and protein analysis. *ACS Chemical Biology*, 3(6), 373-382.
- Lu, Y.-C., Yeh, W.-C., & Ohashi, P. S. (2008). LPS/TLR4 signal transduction pathway. *Cytokine*, 42(2), 145-51.
- Lu, Y.-J., Forte, S., Thompson, C. M., Anderson, P. W., & Malley, R. (2009). Protection against Pneumococcal colonization and fatal pneumonia by a trivalent conjugate of a fusion protein with the cell wall polysaccharide. *Infection and immunity*, 77(5), 2076-83. doi:10.1128/IAI.01554-08
- Lu, Y.-J., Gross, J., Bogaert, D., Finn, A., Bagrade, L., Zhang, Q., ... Malley, R. (2008). Interleukin-17A mediates acquired immunity to pneumococcal colonization. *PLoS pathogens*, 4(9), e1000159.
- Ma, J. (2012). *A Fusion Protein Based Vaccine*. University of Glasgow.
- Mackenzie, G. A., Carapetis, J. R., Leach, A. J., & Morris, P. S. (2009). Pneumococcal vaccination and otitis media in Australian Aboriginal infants: comparison of two birth cohorts before and after introduction of vaccination. *BMC pediatrics*, 9, 14.
- Malley, R., Henneke, P., Morse, S. C., Cieslewicz, M. J., Lipsitch, M., Thompson, C. M., ... Golenbock, D. T. (2003). Recognition of pneumolysin by Toll-like

receptor 4 confers resistance to pneumococcal infection. *Proceedings of the National Academy of Sciences of the United States of America*, 100(4), 1966-71.

- Malley, R., Srivastava, A., Lipsitch, M., Thompson, M., Watkins, C., Tzianabos, A., ... Anderson, P. W. (2006). Immunity to Pneumococci in Mice Immunized Intranasally with the Cell Wall Polysaccharide Immunity to Pneumococci in Mice Immunized Intranasally with the Cell Wall Polysaccharide. *Infection and immunity*, 74(4), 2187-95.
- Marimon, J. M., Ercibengoa, M., García-Arenzana, J. M., Alonso, M., & Pérez-Trallero, E. (2013). Streptococcus pneumoniae ocular infections, prominent role of unencapsulated isolates in conjunctivitis. *Clinical microbiology and infection: the official publication of the European Society of Clinical Microbiology and Infectious Diseases*, 19(7), E298-305.
- Marriott, H. M., Mitchell, T. J., & Dockrell, D. H. (2008). Pneumolysin: a double-edged sword during the host-pathogen interaction. *Current molecular medicine*, 8(6), 497-509.
- Martin, R. L., Brady, J. L. (1998). The need for IgG2c specific antiserum when isotyping antibodies from C57BL/6 and NOD mice. *Journal of Immunological Methods*, 212, 187-192.
- Matthias, K. A., Roche, A. M., Standish, A. J., Shchepetov, M., & Weiser, J. N. (2013). Neutrophil-toxin interactions promote antigen delivery and mucosal clearance of Streptococcus pneumoniae. *Journal of immunology*, 180, 6246-54.
- Mattsson, J., Yrlid, U., Stensson, A., Schon, K., Karlsson, M. C. I., Ravetch, J. V., & Lycke, N. Y. (2011). Complement Activation and Complement Receptors on Follicular Dendritic Cells Are Critical for the Function of a Targeted Adjuvant. *Journal of Immunology*, 187(7), 3641-3652.
- Mccool, T. L., & Weiser, J. N. (2004). Limited Role of Antibody in Clearance of Streptococcus pneumoniae in a Murine Model of Colonization. *Infection and immunity*, 72(10), 5807-5813.
- McDaniel, L. S., Sheffield, J. S., Delucchi, P., & Briles, D. E. (1991). PspA, a surface protein of Streptococcus pneumoniae, is capable of eliciting protection against pneumococci of more than one capsular type. *Infection and immunity*, 59(1), 222-8.
- McDermott, M. R., & Bienenstock, J. (1979). Evidence for a common mucosal immunologic system. I. Migration of B immunoblasts into intestinal, respiratory, and genital tissues. *Journal of immunology*, 122(5), 1892-8.
- McNeela, E. A., Burke, A., Neill, D. R., Baxter, C., Fernandes, V. E., Ferreira, D., ... Lavelle, E. C. (2010). Pneumolysin activates the NLRP3 inflammasome and promotes proinflammatory cytokines independently of TLR4. *PLoS pathogens*, 6(11), e1001191.

- Mestas, J., & Hughes, C. (2012). Of Mice and Not Men: Differences between Mouse and Human Immunology. *The journal of immunology*, 172(5), 2781-88.
- Mina, M. J., Klugman, K. P., & McCullers, J. A. (2013). Live attenuated influenza vaccine, but not pneumococcal conjugate vaccine, protects against increased density and duration of pneumococcal carriage after influenza infection in pneumococcal colonized mice. *The Journal of infectious diseases*, 208(8), 1281-5.
- Mitchell, A. M., & Mitchell, T. J. (2010). Streptococcus pneumoniae: virulence factors and variation. *Clinical microbiology and infection: the official publication of the European Society of Clinical Microbiology and Infectious Diseases*, 16(5), 411-8.
- Mitchell, T. J., Andrew, P. W., Saunders, F. K., Smith, A. N., & Boulnois, G. J. (1991). Complement activation and antibody binding by pneumolysin via a region of the toxin homologous to a human acute-phase protein. *Molecular microbiology*, 5(8), 1883-8.
- Moffitt, K. L., Gierahn, T. M., Lu, Y., Gouveia, P., Alderson, M., Flechtner, J. B., ... Malley, R. (2012). Th17-based vaccine design for prevention of Streptococcus pneumoniae colonization. *Cell*, 9(2), 158-165.
- Moreland, J. G., & Bailey, G. (2006). Neutrophil transendothelial migration in vitro to Streptococcus pneumoniae is pneumolysin dependent. *American journal of physiology. Lung cellular and molecular physiology*, 290(5), L833-40.
- Morgado, M. G., Cam, P., Gris-Liebe, C., Cazenave, P. A, & Jouvin-Marche, E. (1989). Further evidence that BALB/c and C57BL/6 gamma 2a genes originate from two distinct isotypes. *The EMBO journal*, 8(11), 3245-51.
- Mosca, F., Tritto, E., Muzzi, a, Monaci, E., Bagnoli, F., Iavarone, C., ... De Gregorio, E. (2008). Molecular and cellular signatures of human vaccine adjuvants. *Proceedings of the National Academy of Sciences of the United States of America*, 105(30), 10501-6.
- Musher, D M, Groover, J. E., Reichler, M. R., Riedo, F. X., Schwartz, B., Watson, D. A, ... Breiman, R. F. (1997). Emergence of antibody to capsular polysaccharides of Streptococcus pneumoniae during outbreaks of pneumonia: association with nasopharyngeal colonization. *Clinical infectious diseases: an official publication of the Infectious Diseases Society of America*, 24(3), 441-6.
- Musher, D.M. (1992). Infectious disease caused by Streptococcus pneumoniae: Clinical Spectrum, Immunity and Treatment. *Clinical infectious diseases: an official publication of the Infectious Diseases Society of America*, 14, 801-9.
- Nakagawa, H., Komorita, N., Shibata, F., Ikesue, A., Konishi, K., Fujioka, M., & Kato, H. (1994). Identification of cytokine-induced neutrophil chemoattractants (CINC), rat GRO/CINC-2 alpha and CINC-2 beta, produced by granulation tissue in culture: purification, complete amino acid

- sequences and characterization. *The Biochemical journal*, 301 (Pt 2), 545-50.
- Nelson, A. L., Roche, A. M., Gould, J. M., Chim, K., Ratner, A. J., & Weiser, J. N. (2007). Capsule enhances pneumococcal colonization by limiting mucus-mediated clearance. *Infection and immunity*, 75(1), 83-90.
- Netea, M. G., Nold-Petry, C. A., Nold, M. F., Joosten, L. A. B., Opitz, B., Van der Meer, J. H. M., ... Dinarello, C. A. (2009). Differential requirement for the activation of the inflammasome for processing and release of IL-1beta in monocytes and macrophages. *Blood*, 113(10), 2324-35.
- Neutra, M. R., & Kozlowski, P. A. (2006). Mucosal vaccines: the promise and the challenge. *Nature reviews. Immunology*, 6(2), 148-58.
- Nimmerjahn, F., & Ravetch, J. V. (2005). Divergent immunoglobulin g subclass activity through selective Fc receptor binding. *Science (New York, N.Y.)*, 310(5753), 1510-2.
- Nöllmann, M., Gilbert, R., Mitchell, T., Sferrazza, M., & Byron, O. (2004). The role of cholesterol in the activity of pneumolysin, a bacterial protein toxin. *Biophysical journal*, 86(5), 3141-51.
- O'Brien, K. L., Millar, E. V., Zell, E. R., Bronsdon, M., Weatherholtz, R., Reid, R., ... Santosham, M. (2007). Effect of pneumococcal conjugate vaccine on nasopharyngeal colonization among immunized and unimmunized children in a community-randomized trial. *The Journal of infectious diseases*, 196(8), 1211-20.
- O'Brien, K. L., Wolfson, L. J., Watt, J. P., Henkle, E., Deloria-Knoll, M., McCall, N., ... Cherian, T. (2009). Burden of disease caused by *Streptococcus pneumoniae* in children younger than 5 years: global estimates. *Lancet*, 374(9693), 893-902.
- O'Hagan, D. T., Ott, G. S., De Gregorio, E., & Seubert, A. (2012). The mechanism of action of MF59 - An innately attractive adjuvant formulation. *Vaccine*, 30(29), 4341-8.
- Olafsdottir, T. A., Lingnau, K., Nagy, E., & Jonsdottir, I. (2012). Novel protein-based pneumococcal vaccines administered with the Th1-promoting adjuvant IC31 induce protective immunity against pneumococcal disease in neonatal mice. *Infection and immunity*, 80(1), 461-8.
- Opitz, B., Püschel, A., Schmeck, B., Hocke, A. C., Rosseau, S., Hammerschmidt, S., ... Hippenstiel, S. (2004). Nucleotide-binding oligomerization domain proteins are innate immune receptors for internalized *Streptococcus pneumoniae*. *The Journal of biological chemistry*, 279(35), 36426-32.
- Park, J. M., Ng, V. H., Maeda, S., Rest, R. F., & Karin, M. (2004). Anthrolysin O and other gram-positive cytolysins are toll-like receptor 4 agonists. *The Journal of experimental medicine*, 200(12), 1647-55.

- Pasteur, L. (1881). Sur une maladie nouvelle provoquée par la salive d'un enfant mort de rage. *Academie de Sciences, Paris*, 92, 159.
- Paterson, G. K., & Mitchell, T. J. (2006). Innate immunity and the pneumococcus. *Microbiology*, 152(Pt 2), 285-93.
- Paton, J. C., & Ferrante, A. (1984). pneumococcal toxin pneumolysin . Activation of Human Complement by the Pneumococcal Toxin Pneumolysin. *Microbiology*, 43(3).
- Pavia, M., Bianco, A., Nobile, C. G. A., Marinelli, P., & Angelillo, I. F. (2009). Efficacy of pneumococcal vaccination in children younger than 24 months: a meta-analysis. *Pediatrics*, 123(6), e1103-10.
- Pelletier, M., Maggi, L., Micheletti, A., Lazzeri, E., Tamassia, N., Costantini, C., ... Cassatella, M. a. (2010). Evidence for a cross-talk between human neutrophils and Th17 cells. *Blood*, 115(2), 335-43.
- Pestka, J., & Zhou, H.-R. (2006). Toll-like receptor priming sensitizes macrophages to proinflammatory cytokine gene induction by deoxynivalenol and other toxicants. *Toxicological sciences: an official journal of the Society of Toxicology*, 92(2), 445-55.
- Plumptre, C. D., Ogunniyi, A. D., & Paton, J. C. (2013). Surface Association of Pht Proteins of *Streptococcus pneumoniae*. *Infection and immunity*, 81(10), 3644-51.
- Pollard, A. J., Perrett, K. P., & Beverley, P. C. (2009). Maintaining protection against invasive bacteria with protein-polysaccharide conjugate vaccines. *Nature reviews. Immunology*, 9(3), 213-20.
- Price, K. E., Greene, N. G., & Camilli, A. (2012). Export requirements of pneumolysin in *Streptococcus pneumoniae*. *Journal of bacteriology*, 194(14), 3651-60.
- Ram, S., Lewis, L. A., & Rice, P. A. (2010). Infections of people with complement deficiencies and patients who have undergone splenectomy. *Clinical microbiology reviews*, 23(4), 740-80.
- Rayner, C. F., Jackson, A. D., Rutman, A., Dewar, A., Mitchell, T. J., Andrew, P. W., ... Wilson, R. (1995). Interaction of pneumolysin-sufficient and -deficient isogenic variants of *Streptococcus pneumoniae* with human respiratory mucosa. *Infection and immunity*, 63(2), 442-7.
- Rijneveld, A. W., van den Dobbelsteen, G. P., Florquin, S., Standiford, T. J., Speelman, P., van Alphen, L., & van der Poll, T. (2002). Roles of interleukin-6 and macrophage inflammatory protein-2 in pneumolysin-induced lung inflammation in mice. *The Journal of infectious diseases*, 185(1), 123-6.
- Rogers, P. D., Thornton, J., Barker, K. S., Mcdaniel, D. O., Sacks, G. S., Swiatlo, E., ... Mcdaniel, L. S. (2003). Pneumolysin-Dependent and -Independent Gene Expression Identified by cDNA Microarray Analysis of THP-1 Human

Mononuclear Cells Stimulated by *Streptococcus pneumoniae*. *Infection and immunity*, 71(4), 2087-2094.

Romero-steiner, S., Frasch, C. E., Carlone, G., Fleck, R. A., Goldblatt, D., & Nahm, M. H. (2006). MINIREVIEWS Use of Opsonophagocytosis for Serological Evaluation of Pneumococcal Vaccines. *Infection and immunity*, 13(2), 165-169.

Romero-Steiner, S., Libutti, D., Pais, L. B., Dykes, J., Anderson, P., Whitin, J. C., ... Carlone, G. M. (1997). Standardization of an opsonophagocytic assay for the measurement of functional antibody activity against *Streptococcus pneumoniae* using differentiated HL-60 cells. *Clinical and diagnostic laboratory immunology*, 4(4), 415-22.

Rubins, J. B., Duane, P. G., & Charboneau, D. (1992). endothelial cells in vitro . Toxicity of Pneumolysin to Pulmonary Endothelial Cells In Vitro. *Infection and immunity*, 60(5), 1740-6.

Saeland, E., Leusen, J. H. W., Vidarsson, G., Kuis, W., Sanders, E. A. M., Jonsdottir, I., & van de Winkel, J. G. J. (2003). Role of Leukocyte Immunoglobulin G Receptors in Vaccine-Induced Immunity to *Streptococcus pneumoniae*. *The journal of infectious disease*, 187, 1686-93.

Scott, J. A. G. (2007). The preventable burden of pneumococcal disease in the developing world. *Vaccine*, 25(13), 2398-405.

Shoma, S., Tsuchiya, K., Kawamura, I., Nomura, T., Hara, H., Uchiyama, R., ... Mitsuyama, M. (2008). Critical involvement of pneumolysin in production of interleukin-1alpha and caspase-1-dependent cytokines in infection with *Streptococcus pneumoniae* in vitro: a novel function of pneumolysin in caspase-1 activation. *Infection and immunity*, 76(4), 1547-57.

Sorensen RU, Hidalgo H, Moore C, L. L. (1996). Post-immunization pneumococcal antibody titers and IgG subclasses. *Pediatr Pulmonol.*, 22(3), 167-73.

Srivastava, A., Henneke, P., Visintin, A., Morse, S. C., Martin, V., Watkins, C., ... Malley, R. (2005). The Apoptotic Response to Pneumolysin Is Toll-Like Receptor 4 Dependent and Protects against Pneumococcal Disease. *Infection and immunity*, 73(10), 6479-6487.

Sternberg, G. M. (1881). A fatal form of septicaemia in the rabbit produced by the subcutaneous injection of human saliva. *Bull. Nat.Bd. Health*, 2(44), 781.

Strunk, R. C., Kunke, K. S., & Giclas, P. C. (1983). Human peripheral blood monocyte-derived macrophages produce haemolytically active C3 in vitro. *Immunology*, 49(1), 169-74.

Sun, K., Gan, Y., & Metzger, D. W. (2011). Analysis of murine genetic predisposition to pneumococcal infection reveals a critical role of alveolar macrophages in maintaining the sterility of the lower respiratory tract. *Infection and immunity*, 79(5), 1842-7.

- Symons, J. A., Young, P. R., & Duff, G. W. (1995). Soluble type II interleukin 1 (IL-1) receptor binds and blocks processing of IL-1 beta precursor and loses affinity for IL-1 receptor antagonist. *Proceedings of the National Academy of Sciences of the United States of America*, 92(5), 1714-8.
- Tanigawa, T., Susuki, J., Ueta, T., Katsumoto, T., & Tanaka, Y. (1996). Different sensitivity to Streptolysin-O of cells in macrophage lineage. *Microbiology and Immunology*, 40(1), 81-84.
- Tilley, S. J., Orlova, E. V, Gilbert, R. J. C., Andrew, P. W., & Saibil, H. R. (2005). Structural basis of pore formation by the bacterial toxin pneumolysin. *Cell*, 121(2), 247-56.
- Tseng, H., Mcewan, A. G., Paton, J. C., & Jennings, M. P. (2002). Virulence of Streptococcus pneumoniae : PsaA Mutants Are Hypersensitive to Oxidative Stress Virulence of Streptococcus pneumoniae : PsaA Mutants Are Hypersensitive to Oxidative Stress. *Infection and immunity*, 70(3), 1635-9.
- Tu, A. T., Fulgham, R. L., Mccrory, M. A., Briles, E., Szalai, A. J., Crory, M. A. M. C., & Briles, D. E. (1999). Pneumococcal Surface Protein A Inhibits Complement Activation by Streptococcus pneumoniae. *Infection and immunity*, 67(9), 4720-4.
- Tweten, R. K. (2005). MINIREVIEW Cholesterol-Dependent Cytolysins , a Family of Versatile Pore-Forming Toxins. *Infection and immunity*, 73(10), 6199-6209.
- Van der Poll, T., Keogh, C. V, Guirao, X., Buurman, W. A., Kopf, M., & Lowry, S. F. (1997). Interleukin-6 gene-deficient mice show impaired defense against pneumococcal pneumonia. *The Journal of infectious diseases*, 176(2), 439-44.
- Vogel, F. R., Powell, M. F., & Alving, C. R. (1926). *A Compendium of Vaccine Adjuvants and Excipients (2nd Edition)* . *Pharmaceutical Biotechnology*.
- Waley, I., Palmer, M., Martin, E., Jonas, D., Weller, U., Höhn-Bentz, H., Husmann, M. B. S. (1994). Recovery of human fibroblasts from attack by the pore-forming alpha-toxin of Staphylococcus aureus. *Microbial pathogenesis*, 17(3), 187-201.
- Wang, Y. L., Geer, L. Y., Chappay, C., Kans, J. A., & Bryant, S. H. (2000). Cn3D : sequence and structure views for Entrez. *Trends in Biochemical Science*, 25(00), 300-302.
- Weinberger, D. M., Malley, R., & Lipsitch, M. (2011). Serotype replacement in disease following pneumococcal vaccination: A discussion of the evidence. *Lancet*, 378(9807), 1962-73.
- Wenger, J. D., Zulz, T., Bruden, D., Singleton, R., Bruce, M. G., Bulkow, L., Parks, D., Rudolph, K., Hurlburt, D., Ritter, T., Klejka, J. (2010). Invasive pneumococcal disease in Alaskan children: impact of the seven-valent pneumococcal conjugate vaccine and the role of water supply. *Pediatric Infectious Disease*, 29(3), 251-6.

- Witzenrath, M., Pache, F., Lorenz, D., Koppe, U., Gutbier, B., Tabeling, C., ... Opitz, B. (2011). The NLRP3 inflammasome is differentially activated by pneumolysin variants and contributes to host defense in pneumococcal pneumonia. *Journal of immunology*, 187(1), 434-40.
- Xu, B., Zhang, Y., Zhao, Z., Yoshida, Y., Magdeldin, S., Fujinaka, H., ... Yamamoto, T. (2011). Usage of electrostatic eliminator reduces human keratin contamination significantly in gel-based proteomics analysis. *Journal of proteomics*, 74(7), 1022-9.
- Yang, C.-W., Strong, B. S. I., Miller, M. J., & Unanue, E. R. (2010). Neutrophils influence the level of antigen presentation during the immune response to protein antigens in adjuvants. *Journal of immunology*, 185(5), 2927-34.
- Yano, M., Gohil, S., Coleman, J. R., Manix, C., & Pirofski, L. (2011). Antibodies to Streptococcus pneumoniae Capsular Polysaccharide. *Mbio*, 2(5), 1-10.
- Yuste, J., Botto, M., Paton, J. C., Holden, D. W., & Brown, J. S. (2005). Additive inhibition of complement deposition by pneumolysin and PspA facilitates Streptococcus pneumoniae septicemia. *Journal of immunology*, 175(3), 1813-9.
- Zhang, X., & Morrison, D. C. (1993). Lipopolysaccharide structure-function relationship in activation versus reprogramming of mouse peritoneal macrophages. *Journal of leukocyte biology*, 54(5), 444-50.
- Zhang, Xinhua, Kimura, Y., Fang, C., Zhou, L., Sfyroera, G., Lambris, J. D., ... Song, W.-C. (2007). Regulation of Toll-like receptor-mediated inflammatory response by complement in vivo. *Blood*, 110(1), 228-36.
- Zhang, Z., Clarke, T. B., & Weiser, J. N. (2009). Cellular effectors mediating Th17-dependent clearance of pneumococcal colonization in mice. *The journal of clinical investigation*, 119(7), 1899-1909.
- Zysk, G., Schneider-wald, B. K., Hwang, J., Bejo, L., Kim, K., Mitchell, T. J., ... Heinz, H. (2001). Pneumolysin Is the Main Inducer of Cytotoxicity to Brain Microvascular Endothelial Cells Caused by Streptococcus pneumoniae. *Infection and immunity*, 69(2), 845-852.